Technical Data Report

Marine Physical Environment

ENBRIDGE NORTHERN GATEWAY PROJECT

ASL Environmental Sciences
Sidney, British Columbia

D. B. Fissel, M.Sc., Oceanographer
K. Borg, M. Sc., Oceanographer
D. D. Lemon, M. Sc., Oceanographer
J. R Birch, M. Sc., Oceanographer

2010

Table of Contents

List of Tables

List of Figures

Abbreviations

µPa ..... micropascals
ADCP ..... acoustic doppler current profiler
CCAA ..... confined channel assessment area
CHS ..... Canadian Hydrographic Service
CM ..... current meter
CO_2 ..... carbon dioxide
CTD ..... conductivity and temperature at various depths
DFO ..... Fisheries and Oceans Canada
DO ..... dissolved oxygen
ENSO ..... El Niño Southern Oscillation
ESA ..... environmental and socio-economic assessment
Fe ..... iron
IOS ..... Institute of Ocean Sciences
IPCC ..... International Panel on Climate Change
KPOS ..... Kitimat Physical Oceanographic Study
NH_4 ..... ammonia
NO_3 ..... nitrate
OBH ..... on-bottom-hydrophone
PDT ..... Pacific Daylight Time
ppt ..... parts per thousand
psu ..... practical salinity unit
the Project ..... Enbridge Northern Gateway Project
WGS84 ..... World Geodetic System 1984
WL ..... water level measurement

Glossary of Oceanographic Terms

advection	Transportation of a water property such as heat, salt or nutrients by currents.
anticyclonic	Rotation opposite to the sense of the earth's rotation (clockwise in the northern hemisphere).
barotropic	The portion of an ocean current that is uniform with depth.
baroclinic	The portion of an ocean current that varies with depth.
benthic	Related to the ocean bottom.
buoyancy	The force exerted on an object immersed in a fluid by the difference between its density and the density of the fluid around it. Object or fluid parcels less dense than their surroundings experience an upward force (positive buoyancy); those that are more dense experience a downward force (negative buoyancy).
constituent (tidal)	One of the sinusoidal (also called harmonic) components of fixed frequency into which the tide can be decomposed. The amplitude and phase of the components at any location are determined from observations. Once determined, the constituents can be used to predict the tide for many years into the future.
cyclonic	Rotation in the same sense as the earth (counterclockwise in the northern hemisphere).
density	The mass of a substance divided by its volume.
detided	A time series of ocean current or water level data that has had the tidal portion removed.
diurnal	Recurring with a period of one day.
entrainment	The incorporation of water into a less dense layer flowing over it by turbulence at the boundary.
estuary	The region where a river glows into the sea.
euphotic zone	Upper water strata with enough sunlight penetration to support photosynthesis by phytoplankton or other plant life. Also known as photic zone.
fetch	The extent of the ocean surface over which a wind of constant direction blows to generate waves.
frequency	Number of oscillations per unit time; 1 hertz denotes 1 cycle per second.
halocline	A layer of water in which the salinity changes rapidly with depth.
internal tide	A subsurface wave of tidal frequency in stratified water generated by the interaction of the astronomical tide with bottom topography.

isopycnal	A surface of constant density.
katabatic	Wind flowing down slope, on British Columbia coast, usually cold air from mountain snow and ice fields.
knot	A measure of speed equal to 1 nautical mile per hour.
mixed layer	A surface layer of water of near-uniform properties produced by surface wave action or convection.
nautical mile	6082.6 feet (1 second of latitude).
non-tidal current	See residual current.
pycnocline	A layer of water in which the density changes rapidly with depth.
residual current	The portion of the current at a location that is not directly driven by the tidal forces.
Rossby Radius	Length scale at which rotational effects become as important as buoyancy or gravity wave effects in the evolution of water flow around a disturbance.
salinity	The amount of salts dissolved in seawater, measured in practical salinity units, very nearly equivalent to parts per thousand by weight.
semidiurnal	Recurring with a period of half a day.
significant wave height	The average of the largest one-third of all waves present.
stratification	The layering, either continuously or in steps, of a column of water by density, with lighter water above heavier.
swell	Waves of nearly uniform wavelength, which have usually travelled a great distance from their origin.
thermocline	A layer of water in which the temperature changes rapidly with depth.
water mass	A body of water with a particular combination of temperature and salinity range that allows it to be uniquely identified.

1 Introduction

This technical data report reviews the existing marine physical environment of Douglas Channel, from the Port of Kitimat out to and including Caamaño Sound and Principe Channel, known as the CCAA (Figure 1-1). Available oceanographic literature and databases were reviewed and a summary of the existing knowledge of the marine physical environment of the CCAA was prepared. Information was assembled on the circulation, waves, water levels, physical water properties, underwater sound environment and the meteorology. An oceanographic measurement program was also carried out to collect new data on ocean currents and water levels at four sites and waves at an outermost site. Physical water property data were also collected during the deployment and recovery operations. The measurement locations provide representative data in the inland portions of the CCAA for input to numerical modelling described in the Wind Observations in Douglas Channel, Squally Channel and Caamaño Sound Technical Data Report (TDR) (Hayco 2010). Current and water level data were also collected over many months at the marine teminal. The new data have been added to the results of the existing data synthesis to provide a more complete description of the marine physical environment.

The length of time required to collect the data under the measurement program, and the overall project schedule, meant that the historical data assembly and synthesis was completed while the measurement program was still under way. As a result, the marine physical environment is first described using the existing historical data; the results of the measurement program are then presented separately and used to augment the description of the marine physical environment.

Data were gathered for key subject areas through literature review and field surveys. The body of this report contains a summary of the findings for each subject area and detailed results are presented in the appendices:

- Meteorology Review from Historical Data (Appendix A):
  - surface winds
  - atmospheric pressure systems
  - air temperature and precipitation
  - climate variability and climate change
- Ocean Currents (Appendix B):
  - surface currents
  - subsurface currents
  - in relation to:
    - water depths
    - wind forcing
    - tidal forcing
    - estuarine circulation (caused by freshwater runoff)
- Freshwater Discharges and Temperature-Salinity Distributions (Appendix C):
  - estuarine water properties
  - temperatures, salinities and densities
  - river runoff

    - drainage basins
    - precipitation
- Water Levels and Waves (Appendix D):
    - tides
    - waves
    - storm surges and inverted barometer effect
    - tsunamis
    - seasonal and long-term sea level changes
- Underwater Acoustics (Appendix E):
    - fundamental concepts: frequency, intensity, measurement units and references
    - underwater ambient noise
    - underwater sound propagation characteristics and acoustic modeling
- Other Water Properties (Appendix F):
    - dissolved oxygen
    - nutrients (dissolved phosphate, silicate and nitrate)
    - pH and turbidity
- GEM (refers to data collected specifically for the Project) measurement program, September 2005 to January 2006 (Appendix G):
    - subsurface currents
    - waves
    - water levels
    - CTD profiles
- GEM measurement program, January to April 2006 (Appendix H), April to December 2006 (Appendix I), December 2006 to July 2007 (Appendix J):
    - subsurface currents
    - water levels
    - CTD profiles

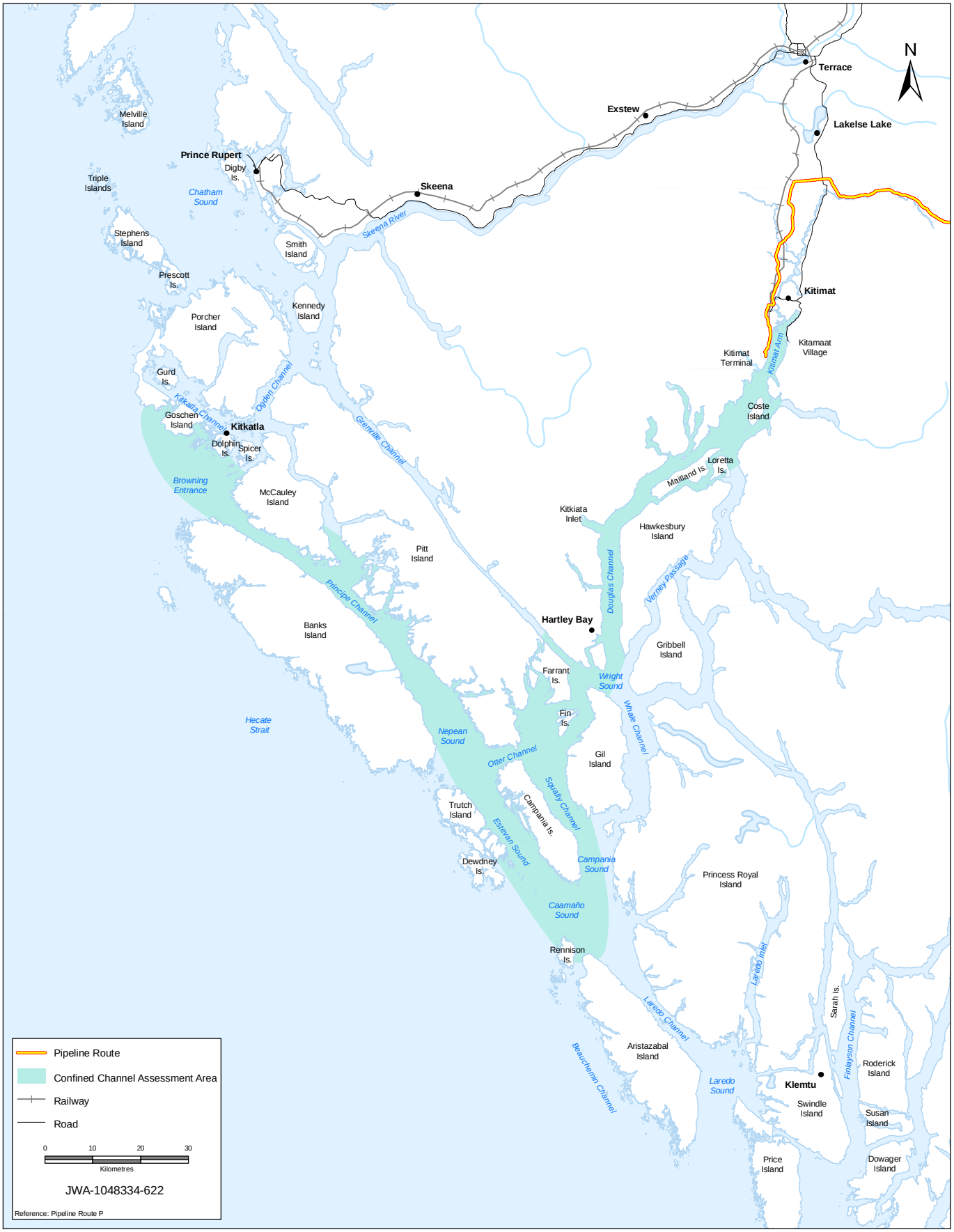

CONTRACTOR: Jacques Whitford AXYS Ltd.	ENBRIDGE NORTHERN GATEWAY PROJECT	FIGURE NUMBER: 1-1	DATE: 20090728
PREPARED BY: gem	Confined Channel Assessment Area	SCALE: 1:1,100,000	AUTHOR: NP / APPROVED BY: CM
PREPARED FOR: ENBRIDGE NORTHERN GATEWAY PIPELINES		PROJECTION: UTM 9	DATUM: NAD 83

R:\2009Fiscal\1048334_NorthernGateway_TDR\MXDs\1048334-622 Fig 2-1_ConfinedChannelAssessmentArea.mxd

2 Methods

2.1 Field Surveys

In September 2005, current meters were deployed at four locations in the CCAA (see Figure 2-2). Ocean currents and water levels were measured at each of the sites; wave heights were also measured at the site in Caamaño Sound. The instruments were operated until January 2006. During September 2005 and January 2006 oceanographic cruises, profiles of temperature and salinity were undertaken at 15 locations in the CCAA.

During the fall and winter of 2005 to 2006, coastal weather stations were operated at several coastal locations in the CCAA including Ashton Rock and Kersey Island in Douglas Channel, Dorothy Island in Devastation Channel and Wall Island in Caamaño Sound. The results of that program are presented in the Weather and Oceanographic Conditions in the CCAA TDR (ASL 2010).

Underwater acoustic measurements were carried out by JASCO Research Ltd. at four locations in the CCAA: Principe Channel, Caamaño Sound, Wright Sound and the Emsley Creek estuary (see the Marine Acoustics (2006) TDR, JASCO 2006).

2.2 Instrumentation

Acoustic Doppler Current Meters

The sites in the Douglas Channel and Principe Channel were too deep to allow a single profiling instrument to sample the entire water column; therefore, multiple instruments were used at these sites (see Table 2-1). The single point current meters were used to measure near-bottom currents.

Nine acoustic Doppler current meters were deployed at the four locations (see Figure 2-2 and Table 2-1 for deployment details). Of the nine instruments, five were Acoustic Doppler Current Profilers (ADCPs). Four of these ADCPs were 300-kHz instruments operated on taut line mooring systems in the water column, whereas at Site CM4, a 600-kHz instrument was operated from a bottom frame to allow the measurement of directional waves and ocean current profiles. At Site CM3 (in Principe Channel), the 300-kHz ADCP broke free of its mooring on November 25, 2006 and floated away. It was, however, later recovered from a beach and found to contain valid data up to the time the mooring broke. The ADCPs also measured water temperature and acoustic backscatter return values as well as internal instrument functional parameters. The 600-kHz ADCP, operated at Site CM4, also measured hydrostatic pressure, which can be used to compute water levels.

The four other Doppler current meters were a type that uses the Doppler measurement principle to measure ocean currents at a single level. These current meters also measured pressure (for water level computations), temperature and internal instrument functional parameters.

The ADCPs use inclined sonar beams. When deployed in upward-looking configurations, interference caused by sidelobe reflections from the water surface prevents the collection of useful data in a region

below the surface equal to approximately 6% of the instrument depth for the usual 20-degree beam inclination.

During the deployment cruise to the CCAA in September 2005 and again in January 2006, as part of the recovery cruise, conductivity and temperature at various depths (CTD) profile data were obtained at 15 locations within the CCAA. For the locations of the CTD stations, see Figure 2-1.

One current meter was redeployed in January 2006 for ongoing data collection near the marine terminal location. The instrument was recovered and redeployed on April 22, 2006, again on December 13, 2006 and finally recovered July 10, 2007. CTD profiles were collected at the site during the initial deployment and again during the redeployments.

For the detailed location maps for each mooring site and tabulated positions for the CTD stations, see Appendices G through J.

2.3 Review of Existing Data Sources

Meteorological data for past and current stations were obtained mainly from Environment Canada, in the form of records from coastal weather stations and ocean buoys located in or close to the CCAA. Published climatology summaries and reports from the International Panel on Climate Change (IPCC) and other research organizations were also referenced. For a summary of the data sources, see Appendix A.

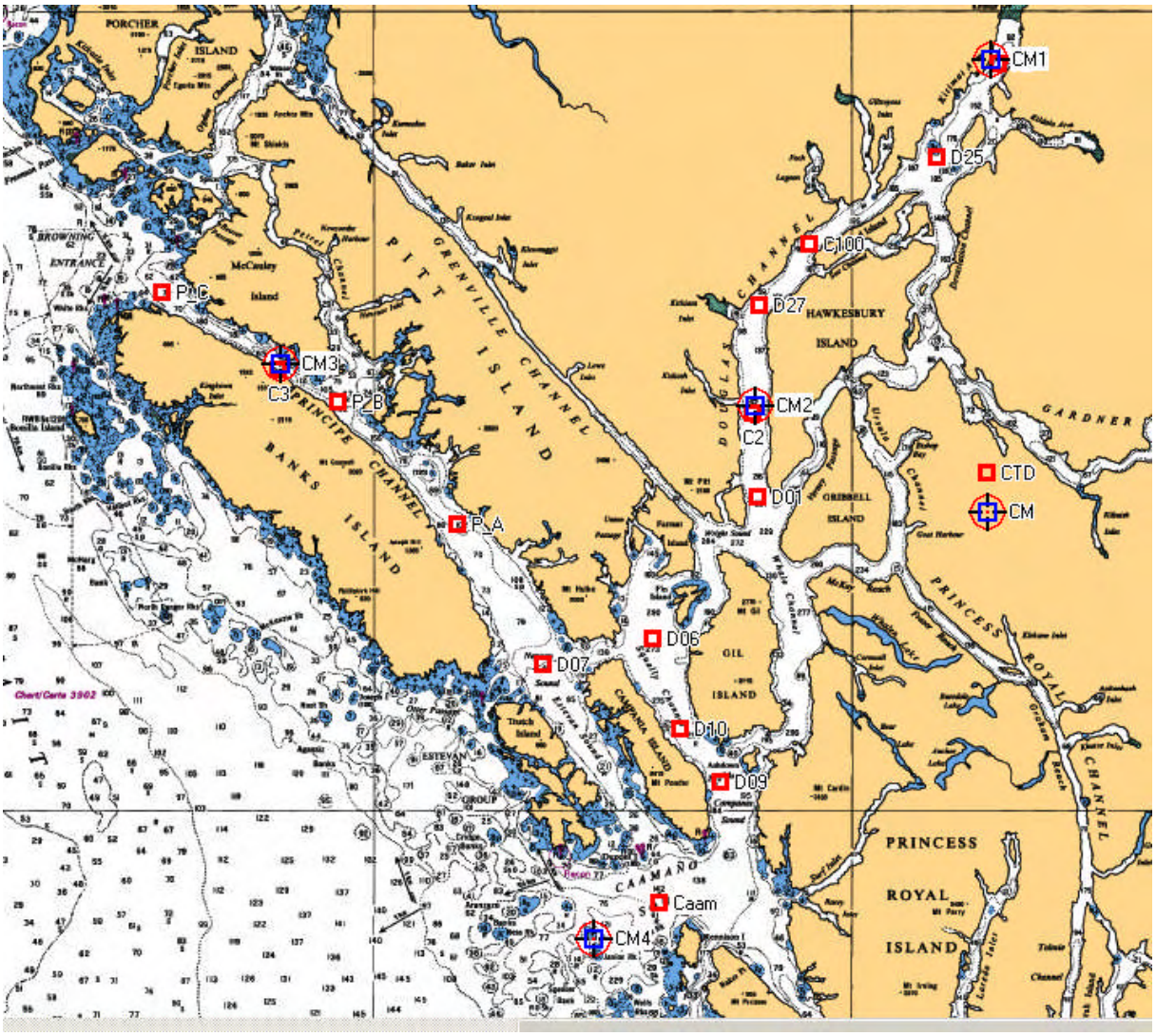

NOTES:
Blue squares: Current meter sites September 2005 to January 2006.
Red squares: CTD sites September 2005 and January 2006.

Figure 2-1 Locations of Current Meter Measurement and Conductivity, Temperature and Depth Profiling Sites

Table 2-1 Location, Deployment Time and Water Depth for Current Measurement Sites

Site	Area	Deployment Time Date (PDT)	Lat, Long (WGS84)	Water Depth to Sea Floor (m)	Recovery Time Date (PDT)	Instrument Depth or Depth Range
1	Kitimat Arm, Offshore of Bish Creek Terminal	14 Sept 2005 10:02	53 56.468 128 42.461	179	17 Jan 2006 10:40	1. ADCP 300 kHz: 9-97 m @ 2 m bins. Battery dead at recovery. Last good data 01 Jan 2006. 2. Single Level CM: 165 m + WL
2	Douglas Channel	13 Sept 2005 16:00	53 30.574 129 12.150	380	15 Jan 2006 16:02	3. ADCP 300 kHz: 7-57 m @ 2 m bins, (upward looking) 4. ADCP 300 kHz: 67-151 m @ 2 m bins, (downward looking) 5. Single Level CM: 212 m + WL 6. Single Level CM: 312 m + WL
3	Principe Channel	12 Sept 2005 10:15	53 33.772 130 11.834	135	06 Nov 2005 20:00 _____ 13 Jan 2006 15:15	7. 300 kHz ADCP: 10-80 m @ 2 m bins (upward looking); broke free of mooring on 06 Nov 2005. 8. Single Level CM: 123 m + WL, direction data on this instrument was adjusted to align with channel.
4	West Approach to Caamaño Sound, Yates Shoal (Aranzazu Banks)	12 Sept 2005 17:30	53 50.235 129 32.555	34	12 Jan 2006 12:40	9. ADCP 600 kHz: 10-33 m @ 1 m bins With directional wave measurements Acoustic release on pop-up canister was not recovered.

NOTES:
CM = current meter
PDT = Pacific Daylight Time
WL = Water Level Measurement
WGS84 = World Geodetic System 1984

The bulk of physical oceanographic data pertaining to the CCAA is contained in a six-volume series of reports published by the Institute of Ocean Sciences (IOS) in Sidney, British Columbia (Webster 1980) and the proceedings of a workshop on the Kitimat marine environment (Macdonald 1983). Subsurface and surface current data sets were also obtained from the data archive service at IOS and from the Canadian Hydrographic Service (CHS). Other oceanographic and related data (temperature and salinity profiles, tidal data and river discharge) were obtained from databases maintained by Fisheries and Oceans Canada (IOS, Marine Environmental Data Service and CHS) and Environment Canada (Meteorological Service Branch and Inland Waters Directorate). For details regarding these sources, see Appendices B, C, D and F.

Information for the review of existing underwater acoustic data was drawn from general sources and the limited published data for the region (see Appendix E).

3 Results of Baseline Investigations

The results of the baseline investigations for each marine physical environment subject area are summarized below. For the detailed reports, see Appendices A through H.

3.1 Meteorology

The climate and weather conditions of the CCAA are a direct result of its location in an extensive network of mountainous islands between the major inland waters of the Pacific Ocean (Hecate Strait) and the British Columbia mainland. At its seaward limit, the CCAA is dominated by the Pacific marine climate characterized by moderate air temperatures and intense storms in fall and winter. At its landward limit, the temperatures exhibit a greater range, reflecting the increased influence of a continental climate. Here, the marine storm winds are generally abated by the mountainous terrain. In winter, strong Arctic outflow winds occur because of the presence of a cold and dry continental Arctic high-pressure system that episodically extends into the interior of British Columbia. The high atmospheric pressures in the interior can result in strong, low-temperature winds that flow into the inland fjords. Arctic outflows are associated with strong winds from the northeast, moderate to heavy snowfalls and squalls, and the potential for large waves, reduced visibility and icing of structures because of freezing spray.

3.1.1 Wind Speed and Direction

The wind speeds on the open coast of eastern Hecate Strait are considerably greater than those over the inland waters. The yearly average wind speed at Nanakwa Shoal (4.5 m/s) is reduced by 38.0% from that at Bonilla Island (7.3 m/s), while the reduction at Kitimat Eurocan (5.1 m/s) is about 30.0%. In terms of maximum observed wind speeds over 20 years or longer, the reduction in wind speeds at inland locations is even larger. For the maximum observed wind speeds, the reduction from the eastern coast of Hecate Strait to the inland waters of the CCAA is more than 50.0%. Consistent with the differences in the average and maximum wind speed statistics, the distribution of the wind speeds exhibits major changes between the offshore (Bonilla Island) and inshore areas (Nanakwa Shoal and Kitimat Eurocan; see Figure A-5 in Appendix A). Only 4.8% and 6.3% of all winds at Kitimat Eurocan and Nanakwa Shoal, respectively, exceed 10 m/s (18 knots), in sharp contrast to 23.1% of winds exceeding 10 m/s at Bonilla Island.

Wind speeds exhibit a distinct seasonal pattern, with the highest wind speeds occurring in fall and winter, and the lowest wind speeds in spring and summer. The seasonal cycle in wind speeds is most pronounced in eastern Hecate Strait at Bonilla Island and Ethelda Bay and is less apparent in the inland waters, especially at Kitimat Eurocan where average wind speeds exhibit little change with the seasons, while the maximum wind speeds are reduced by 10% to 20% from winter to summer.

In addition to higher wind speeds occurring in winter, wind directions also change with the season at inland locations. From October to April, the prevailing wind direction at Nanakwa Shoal is from the north whereas the dominant wind directions from May to September are from the south to southwest. At Kitimat Eurocan, northerly winds prevail from November to March and southerly winds are most common from April to October. The predominance of northerly winds in fall and winter is associated

with the Arctic outflow conditions, especially for the strongest winds in these seasons. These Arctic outflow winds reach maximum hourly values of up to 18.4 m/s (36 knots) at Nanakwa Shoal and approximately 17 m/s (33 knots) at Kitimat Eurocan.

3.1.2 Air Temperature

The air temperatures in the CCAA reflect a transition from the Pacific Ocean air masses of the Hecate Strait marine climate region through the inland waters that traverse the Coast Mountains zone. In winter, the warm, moist marine conditions to the west are paralleled by very wet and mild conditions in the inland waters, accompanied by increased snowfall amounts at higher elevations and with distance to the east. The increased precipitation results from the moist marine air encountering the hills and mountains that border the inland waterways. In summer, the mild marine conditions to the west over Hecate Strait are accompanied by mild scattered showers, again associated with the moist marine air encountering the mountainous terrain.

The change in air temperatures from Hecate Strait (Bonilla Island and Ethelda Bay) to the inland locations (Hartley Bay, Kitimat and Kildala) is evident in the statistics derived from long-term measurements of temperature. From October to March, monthly average air temperatures are reduced by as much as 2.5°C and 6°C at Hartley Bay and Kitimat, respectively, from those at Bonilla Island. In summer, the temperature gradient reverses, with warmer temperatures at inland locations, by 2.2°C and 3.7°C at Hartley Bay and Kitimat, respectively, from those at Bonilla Island.

3.1.3 Precipitation

Large amounts of precipitation occur in the CCAA because of the mild, moist marine climate. Precipitation occurs mostly in the form of rainfall, with snowfall amounts being very low at the seaward edge of the CCAA (i.e., 520 mm average total annual snowfall at Bonilla Island [2,077 mm average annual rain]). However, at inland locations, where the air temperatures are consistently cooler in fall and winter, the amount of snowfall increases considerably (i.e., 2,380 mm average total annual snowfall at Hartley Bay [4,244 mm average annual rain], 3,380 mm at Kitimat 2 [2,398 mm average annual rain], and 4,600 mm at Kitimat Township [1,769 mm average annual rain]). Kitimat holds the Canadian record for the most snowfall in a five-day period (i.e., 2,462 mm from 14 to 18 January 1974 [Heidorn 2004]). Nevertheless, even in Kitimat, the amount of precipitation due to rainfall exceeds that of snowfall in all months, on average.

Total precipitation has a very marked seasonal cycle and peaks in October and November as more frequent and intense Pacific storms approach the area. Gradually through the remainder of the fall and the winter, average monthly precipitation decreases, reaching the lowest annual levels in June through August. Monthly precipitation in autumn is typically more than twice that which occurs in summer.

3.1.4 Climate Variability and Trends

The climate of the CCAA as described above is based on averages of data collected over long periods (generally 30 years or more). However, significant variability exists within that data on a number of time scales. The shortest scale generally discussed is seasonal variability, which refers to changes in the

climate from season to season. This seasonal variability is the highest in magnitude because the seasons differ from one another so greatly (winter weather versus summer weather). Longer scales of variability compare the same months or seasons between different years or decades, or compare annual averages over decades or centuries.

The availability of weather data is limited to between 25 and 45 years at the major meteorological measurement sites. A trend analysis comparing average annual air temperature and total precipitation to averages for winter and summer, respectively, was carried out for measurement sites with 30 or more years of available data.

The results show that most of the interannual variability in temperatures occurs over periods of one to seven years, possibly related to El Niño or La Niña, or similar effects. However, a small increase in air temperatures (approximately 1°C) was indicated at most locations over a period of 35 to 40 years, from the 1960s to 2002. This change is relatively small by comparison to changes that occur over time scales of one to eight years, as can be seen in the Bonilla Island and Kitimat 2 weather observations. The trend is more consistent in the full year average values than in either summer or winter seasons. Even in the full year average values, the correlation statistic (R^2) is only about 0.25, indicating that only 25% of the total variance is actually due to the linear increase in temperature. At the other air temperature measurement sites (Ethelda Bay, Kitimat Township and Kildala), the increase in air temperature is smaller and the correlation statistic is even lower (0.18, 0.11 and 0.13, respectively).

For a detailed review of the meteorological data and the analysis results, see Appendix A.

3.2 Ocean Currents

The currents in the CCAA have typical flow speeds of about 15 to 30 cm/s at the surface. The highest surface currents were measured in the outer seaward portions of the CCAA including Campania Sound, Caamaño Sound and Principe Channel, while Kitimat Arm has lower surface currents. Maximum surface currents range from 50 to 60 cm/s in Kitimat Arm, to 90 to 100 cm/s in southern Douglas Channel, to well over 100 cm/s in the seaward portions of the CCAA and in Principe Channel.

The subsurface currents below the main halocline at water depths exceeding 75 to 100 m typically average between 3 and 20 cm/s with maximum speeds of 10 to 60 cm/s in the deep inland water basins of Squally Channel, Wright Sound, Douglas Channel and Kitimat Arm. For these inland waterways, subsurface current speeds generally decrease with increased distance from Hecate Strait. In the shallower approach waters to the Kitimat system, subsurface current speeds are generally higher, with typical values of 10 to 25 cm/s and maximum values of 40 to 100 cm/s. Principe Channel has the highest near-bottom (100-m water depth) current speeds, with typical speeds of 25 cm/s and maximum speeds of 110 cm/s.

In the confined inland waterways and in some of the narrow passages (e.g., Otter Channel), current directions are aligned with the axes of the channels themselves, and cross-channel current speeds are much slower than such along-channel currents. In the more open waters of Caamaño Sound and Browning Entrance, the currents encompass a much greater range of directions.

Average net flows are generally seaward near the surface and landward at depth, consistent with the highly estuarine nature of the Kitimat system. The typical net surface current speeds are 10 to 15 cm/s to the south in Douglas Channel with a deeper net return flow to the north of 1 to 3 cm/s.

The currents in the CCAA are highly variable because of a combination of wind, tidal and estuarine forcing. The wind forcing is highly episodic and particularly important in the fall and winter under the combined influence of frequent Pacific storms and Arctic outflow winds. Pacific storms result in very strong winds in the outer seaward portions of the CCAA, which, while reduced in speed, are still as important as strong winds from the south in the inland waterways. The Arctic outflow winds from the north are strongest in the northern portions of the inland waterways. The response of the surface layer to wind forcing, in terms of the magnitude of the resulting current, can be highly variable because of the variable degree of stratification of the water column, which depends on the freshwater runoff and precipitation.

The tidal currents exhibit a considerable degree of variability with location and with measurement depth because of the underlying effects of water column strata variability. The astronomical tide is highly predictable and uniform with depth and changes little over the length of the system. However, the astronomical tide is often smaller than the internal tide in the upper portions of the water column. The internal tide is much less predictable because it varies in amplitude and phase over periods as short as a few days or less. It also exhibits a high degree of depth dependence, and the horizontal scale of the internal tide is of the order of tens of kilometres rather than many hundreds of kilometres for the astronomical tide. Internal waves generated by the flow of stratified fluid over topographic features are also of relevance to the CCAA; in addition to internal tides, phenomena such as internal hydraulic jumps and lee waves can also occur.

River plumes are formed by river outflows discharging into coastal seas or fjords. They occur wherever buoyant river fresh water encounters more dense seawater. River plumes typically form narrow coastal currents; under the influence of the Earth's rotation, the fresher river waters in the Northern Hemisphere tend to turn to the right on leaving the river mouth. Numerous rivers discharge into the CCAA, and it is likely that they form plumes, but because the widths of the inlets are subject to the internal Rossby Radius of deformation, it is likely that inertial effects are also important. Apart from a few photographs, no other direct evidence verifies their existence in the CCAA. The numerical model results for the CCAA indicate the presence of tidally pulsed river plumes.

For a detailed review of the ocean current data and the analysis results, see Appendix B.

3.3 Freshwater Discharges and Temperature-Salinity Distributions

The major rivers in the CCAA are the Kitimat and Kemano Rivers, which are gauged and discharge directly into Kitimat Arm of Douglas Channel and Gardner Canal. Also important are the two major rivers draining into northern British Columbia waters, the Skeena and the Nass.

3.3.1 Freshwater Budget of the CCAA

Freshwater input to the ocean has two major components:

- land runoff from rivers, creeks and other drainage features
- direct total precipitation (rainfall and snowfall) that enters the ocean directly from the atmosphere or through small, low-elevation islands

Rivers with large watersheds, such as the Skeena and Nass, have high overall discharge and their broad peak is in the spring and early summer because of snowmelt. At the opposite extreme are the small watershed rivers, often found on islands that have low annual flows and are dominated by rainfall. Between these extremes are the small- to medium-sized rivers along the mainland coast, including the Kitimat River. Many of these watersheds include snowfields and glaciers providing high summer flows. However, these rivers are also highly affected by rainfall and their winter storm-related flow peaks can rival their summer flow levels.

Considerable year-to-year variability is present in the river discharges as is shown by the Kitimat River annual average discharge rate. In any given year, the actual discharge for this river can differ by up to 20% from the long-term annual average value. The river discharges were unusually low in the mid-1980s and reached a record high value in 1991.

An analysis of NTS 1:50,000 topographic maps issued by Natural Resources Canada was carried out to divide the full area of interest into major discharge basins. A total of 29 drainage basins were identified, including the gauged Kitimat and Kemano River basins. The 29 drainage basins were grouped according to distinct portions of the waterways receiving the land-based discharges. A total of seven major waterways zones were defined within the CCAA (see Figure C-6 in Appendix C):

1. Principe Channel
2. Southern waterways: Campania Sound, Caamaño Sound, Squally Channel, Otter Channel, Estevan Sound and southern Principe Channel
3. Southern Douglas Channel, Whale Channel, Verney Channel, Ursula Reach and Mackay Reach
4. Central Douglas Channel including Devastation Channel
5. Kitimat Arm, including northern Douglas Channel
6. Kildala Arm
7. Gardner Canal

The freshwater discharge from river runoff was computed for each waterway zone. The freshwater discharge directly from precipitation (on land areas without well-developed drainage channels and creeks) is calculated from monthly precipitation measurements at the nearest or a combination of the nearest weather stations. The relative importance of land-derived freshwater runoff to direct precipitation varies considerably among the seven major waterways. In the seaward Zones 1 to 3, consisting of Principe Channel, the outer southern waterways and southern Douglas Channel, the freshwater contribution from direct precipitation is comparable to or even greater than the river discharge values. For the more inland waterways, the river discharge contribution is much greater than direct precipitation because of the larger

drainage basins and the smaller size of the receiving waterways. The combined total river runoff for Kitimat Arm (Zone 5) and Kildala Arm (Zone 6) has an average monthly volume of 0.49 km^3, about 24 times more than direct precipitation. Gardner Canal receives an average total river discharge of 1.71 km^3, nearly 60 times more than the amount of direct precipitation. About 18% of the total river discharge in Gardner Canal, or 3.1 km^3, is due to water diverted from the Nechako River basin through the Kemano powerhouse into the Gardner Canal.

Year-to-year variations in total freshwater discharge are considerable, with differences of up to 50%, as seen in the low levels of the mid-1980s compared with the high total discharges of the early 1990s. The total monthly freshwater discharge within each zone can be represented as an equivalent water depth computed as total discharge divided by the surface area of the zone. In the outer southern zones, the equivalent monthly depth of freshwater is less than 1 m. In the more inland zones (Zones 4 to 7), the equivalent monthly freshwater depth exhibits a pronounced increase to 1.2 m in Zone 4 (central Douglas Channel), to 3.6 m in Zone 5 (northern Douglas Channel and Kitimat Arm) and to very large values of 9.6 m and 8.1 m in Kildala Arm and Gardner Canal, respectively.

3.3.2 Temperature-Salinity Distributions

The temperature and salinity profiles in the CCAA consistently reveal distinct upper layers ranging from a few metres to 10 to 15 m depth, characterized by much-reduced salinities compared to the underlying deeper waters. From late spring through the fall months, the salinities are much lower than those at depth, resulting in a large density gradient between the upper layers and the remainder of the water columns. These lower salinities result from the large amounts of freshwater land runoff and direct precipitation. The upper layers also have higher water temperatures in spring, summer and fall.

In addition to the pronounced seasonal changes in the shallow upper layer salinity and temperature properties, most of the temperature-salinity profiles reveal a mid-water feature from 5 to 10 m depth to between 50 and 100 m (where a gradual increase in salinity and density occurs, as well as a temperature minimum [Pickard 1961] often present from winter through spring). The temperature minimum results from fall and winter cooling through heat loss to the surface, followed by local warming of the upper layer due to seasonal changes or individual weather events.

Long-term continuous measurements of surface temperature and salinity in the CCAA are limited to two data sources: daily temperature and salinity measurements at the Bonilla Island light station at the eastern side of N. Hecate Strait (1960 to 2005) and surface temperature measurements made at the Nanakwa Shoal weather buoy in northern Douglas Channel.

The Bonilla Island results show that average monthly surface salinities at this exposed oceanic location have a very small or negligible seasonal cycle, with values ranging from 31.0 to 31.4 psu, compared to river runoff-influenced cycles in the adjoining inland waters. The seasonal temperature variations appear to correspond to seasonal air temperatures, with average surface sea temperatures ranging from 6.5°C in February to 12.5°C in August.

Surface temperatures have been measured at the Nanakwa Shoal buoy since 1988. These data show that the annual range in monthly average temperatures is much greater than at Bonilla Island, with a minimum

value of 5.2°C in January and a maximum value of 16.1°C in August. The range from highest to lowest measured temperature is greater still, at –0.4°C to 22.3°C.

Salinity and temperature distributions at select locations in the CCAA were analyzed using historic data for four different months (July 1977, September/October 1977, December 1977 and March 1978), and for three different years (1951, 1972 and 1977) in the month of July. The distributions for July in three different years showed a distinct but shallow upper layer extending the full length of Douglas Channel, with salinities of less than 20 psu and temperatures exceeding 10°C. In contrast, the upper layer in the seaward portions of the waterway, from Wright Sound through Caamaño Sound, had increased salinities of between 20 and 25 psu, while its temperatures showed less change than the salinity, remaining greater than 10°C. The salinities in the deeper waters exhibited a modest gradient from those in the upper layer to values of about 32.5 psu at depths of 60 to 100 m, depending on the year. At greater depths, the salinities had a narrower range of values from 32.5 to about 33.0 psu. The water temperatures at depth (deeper than 200 m) in Douglas Channel were generally in the range of 6°C to 8°C, except when a temperature minimum was present (observed in 1951 and 1972) with values less than 6 °C. Cold temperatures of less than 6°C also occurred in the deeper waters (greater than 200 to 250 m) of Campania Sound to Wright Sound in July 1977.

The temperature-salinity distributions with depth in the CCAA (recorded from July 1977 to March 1978 at approximately three-month intervals) follow the expected cooling of the upper layer and a reduction in salinity, along with a retreat in the extent of well-defined, pronounced low salinity values. In the deeper waters of Douglas Channel, temperatures had increased to over 8°C at depths of 40 m in September and October 1977 and at depths of 70 to 160 m in December. This deep-water temperature maximum may have been caused by residual heat from the previous summer and fall or by advection of warmer water into the area from seasonally warmed waters in Hecate Strait. The deep water remains at low temperatures of less than 7°C.

The deeper waters show a consistent increase in salinities at depth from May to July to October, increasing more than 0.5 psu below 200 m, and accompanied by lower temperatures and lower oxygen concentrations. In summer, deep water in the inland waterways is displaced and renewed by the upwelling and intrusion of colder, denser, more saline water from the British Columbia shelf.

Overall, the long-term variations in temperature and salinity properties are not large, making it difficult to detect these with the sporadic observations that are available. It should be noted that this long-term trend analysis, when applied to meteorological time series data sets available for durations of up to 40 years, indicated that surface air temperatures exhibited a small increasing trend in the annual average values at some measurement sites (see Appendix A).

The high levels of freshwater discharge into the CCAA represent a central defining characteristic of the oceanography of the system. The highly stratified upper water layer generates its own estuarine circulation in addition to significant current changes caused by tidal forcing and wind forcing (see Appendix B).

For a detailed review of the data and analysis results for freshwater discharges and temperature-salinity distributions, see Appendix C.

3.4 Water Levels and Waves

Changes in sea level along the British Columbia coast are primarily caused by tides; however, other episodic and seasonal factors can also affect the water levels. Ocean waves are the result of wind energy in regional and local waters, as well as occasional occurrences of very long-period swell waves in Hecate Strait that can originate elsewhere in the Pacific Ocean. Storm surges are caused by wind stress acting on the water surface causing a direct set-up of the sea level and have the greatest effect in shallow water and low-lying coastal areas. Surge levels are usually greater along the eastern side of Hecate Strait than on the western side. The inverted barometric effect (higher atmospheric pressure depresses the sea surface; low atmospheric pressure raises the sea surface) can change the water level by about 1 cm for every 100 Pa change in air pressure. This is particularly noticeable during winter, with typical sea level changes on the order of 30 cm.

Tides along the British Columbia central coast are classified as mixed, mainly semi-diurnal (two highs and two lows for each 24.75 hour day, with successive highs or lows of unequal height). A spring-neap cycle of about 14 days occurs as the gravitational forces of the sun and moon reinforce each other at full and new moons. Tidal ranges during these spring tides are about twice those that occur during the weaker neap tides. The spring tide range at Kitimat is 6.5 m, reducing to about 3 m during neap tides. The tide in the CCAA is driven by the tide in Hecate Strait, but is modified by the network of channels and inlets. The tidal range increases with northward distance along the coast of the region, by about 25% from Beauchemin Channel in the southeast (3.9 m at mean tides, 5.9 m at large tides) to Welcome Harbour in the northwest (4.9 m mean, 7.5 m large). Tidal range also increases from the mouth to the head of the inlet system, but by a much smaller amount (approximately 6% between Caamaño Sound and Kitimat). The tide at Kitimat lags that in Caamaño Sound by approximately 10 minutes. The greatest range occurs at Site CM3 in Principe Channel (7.8 m at large tides). Evidence suggests some seasonal dependence in the diurnal portion of the tide, which could lead to some deviations from the predicted tide, but of sufficiently small magnitude (less than 25 cm) as to be similar to other non-tidal water level changes.

The waters of Hecate Strait and Queen Charlotte Sound are open to large fetches, particularly from the southwest, and can receive long-period swells (16 to 22 second period) although average wave periods are generally about 5 to 10 seconds for most months. During winter, significant wave heights (defined as the average of the heights of the largest one-third of all waves present) in excess of 3.5 m occur 20% to 30% of the time offshore, reducing to 10% along the coast. Cycles of large waves during winter have a 2- to 3-day periodicity, consistent with intervals between the passages of frontal systems. Storm-force winds (sustained wind speeds up to 40 to 50 knots), accompanied by significant wave heights of 6 to 8 m, occur several times each winter. The increase in winter wind speeds generally occurs quickly in early fall. In Hecate Strait, the 100-year return period wave is estimated to have a significant wave height of nearly 14 m and a maximum wave height of nearly 25 m.

The coastal waterways, including inlets and fjords, are generally more sheltered with weaker winds and reduced fetch. However, strong winds, particularly when combined with an opposing tide, can generate steep, choppy wave conditions of up to 1 to 2 m height. Arctic outflow winds during fall and winter can produce rough seas even in the inlets. The waves in the enclosed inland waters that make up most of the CCAA are much smaller than those of the exposed waters of Hecate Strait. At Nanakwa Shoal, less than 5% of all observations exceed 0.5 m in significant wave height, while in northern Hecate Strait, 80% of

all such observations exceed 0.5 m. The maximum recorded significant wave height in Kitimat Arm was 2.0 m, measured at Nanakwa Shoal.

In addition to their much lower wave heights, the periods and wavelengths of the waves in the inland waters are also considerably reduced. At Nanakwa Shoal, most wave periods are 2.5 to 5 s, with a few at 7 s. The wave heights are strongly related to wind direction, which reflects the importance of the wind fetch (distance that the wind blows over open water). This influence is particularly apparent at Nanakwa Shoal, where the largest waves are clearly due to the strong (winter) outflow winds from the north-northeast, while a secondary peak in wave height is evident for winds from the south-southwest, blowing up Douglas Channel towards Kitimat.

Tsunamis are ocean waves that can be destructive and endanger human lives where they strike populated coastlines. Tsunamis are very long-period waves (15 to 90 minutes) that travel rapidly from the source. Generally, they are the result of an earthquake and, less commonly, a result of an underwater landslide or a surface landslide that enters the water. The British Columbia coast is susceptible to submarine earthquakes, and submarine landslides and related tsunamis have been recorded along this coast. Funnelling effects can increase wave height as a tsunami penetrates up the inlet. The extent of flooding and damage to affected coastal areas depends on factors such as the bathymetry and distance from the source. A submarine slide in Kitimat Inlet in April 1975 resulted in a wave estimated at 8.2 m height.

For the detailed data review and analysis results for this topic, see Appendix D.

3.5 Underwater Acoustics

The relevant aspects of the underwater acoustic environment are the ambient noise background and the propagation characteristics of the area, which determine how sound from a source will travel. Sound is characterized by its frequency content and its pressure or intensity (equivalent to the human concepts of pitch and loudness, respectively).

The ocean has an ambient noise background produced by natural processes (physical and biological) and human activities. Little specific information exists regarding the ambient noise environment of the CCAA; some previous measurements made in Queen Charlotte Sound showed ambient noise levels to be mainly dependent on wind speed at the ocean surface. At present, vessel traffic is the main anthropogenic contributor to the ambient noise environment in the CCAA and is highest in summer. Underwater ambient noise measurements made at four locations in the CCAA in the fall of 2005 (Marine Acoustics [2006] TDR) produced results consistent with the previous observations, with minimum ambient levels of 82 to 84 dB found in the frequency band between 10 Hz and 20 kHz in the absence of vessel traffic. Levels in Caamaño Sound were about 10 dB higher, an effect attributed to the proximity of the open waters of Hecate Strait where higher levels of wind and wave energy are prevalent.

The propagation speed of sound in the ocean is a function of the temperature, salinity and pressure of the water, as well as the properties of the seafloor. Because of the complexity of sound propagation in the ocean, numerical propagation modelling is required to predict the effects of an acoustic source. Transmission loss measurements were made at the same four locations at which noise data were collected in the fall of 2005. The loss as a function of distance can be used to predict the sound intensity from a

source, such as a vessel, at various distances. Those data, and existing data on the characteristics of the seafloor, are used as input for acoustic propagation modelling.

For the detailed data review and analysis results from which the above summary was derived, see Appendix E.

3.6 Other Water Properties

This section deals with water properties other than temperature and salinity: dissolved oxygen, nutrients, pH and turbidity. The properties of the central British Columbia coast waters are variable both spatially and temporally, influenced by oceanic as well as coastal processes. The offshore oceanic waters are generally more saline than those of inland waterways. The properties of the coastal inlet waters are influenced by the amount of runoff and exchange with the offshore waters. Shallow sills, if present, restrict the exchange and flushing of the deeper inlet waters and can result in oxygen depletion. The water properties of the area vary seasonally, with winter and summer extremes. The associated large-scale wind shifts between winter and summer, and the resulting changes in overall current patterns, control the make-up of the water masses.

The inlet system comprising Kitimat Arm and Douglas Channel is a class of coastal fjords (Pickard 1961), those that have a relatively high runoff resulting in low (less than 3 psu) surface salinity at the head and surface salinities between 5 and 20 psu at the mouth. Such inlets are characterized by an estuarine circulation with fresher water flowing seaward at the surface and a deeper return flow of oceanic water. Sills separating the deep inner basins of these inlets from the outside usually limit the replacement of the bottom water to periodic episodes.

The amount of dissolved oxygen (DO) in the water is critical to the ocean's ability to support life. Oxygen is added to the water by surface mixing and photosynthesis; it is consumed (subtracted) by animals, fish, bacteria and decomposition. The less dense surface waters are generally higher in DO than the more dense deeper waters, and runoff tends to increase DO levels near shore. Without replenishment, waters become oxygen-depleted and anoxic. This can occur in the bottom waters of coastal inlets where a shallow sill often limits flushing of the deep water.

Dissolved oxygen concentrations in coastal inlets such as the Kitimat system depend in a complex manner on the circulation in the inlet and on biological processes taking place in it. Generally, near-surface oxygen concentrations are at or above saturation, and deep-water concentrations are below saturation. Anoxic conditions are rare, but have been observed in the deeper water of Minette Bay, at the head of Kitimat Arm because it has only a very shallow connection to Kitimat Arm. Oxygen concentration maxima, with supersaturated values, have been observed beneath the halocline in Douglas Channel and are attributed to production by phytoplankton. The deep water in the basins is renewed regularly, and two different processes appear to be involved. The first is the usual deep-water renewal process, in which cold, dense, low-oxygen water produced by upwelling on the shelf flows over the sill and replaces the bottom water in the basins in the spring and summer. In the second process, strong winter outflow winds drive the inlet surface waters seaward to produce a rapid counter-directional influx of water from 30 to 150 m depth in Hecate Strait into Douglas Channel.

Phytoplankton, the small plants that form the base of the oceanic food chain, require nutrients for growth and reproduction. Phytoplankton also require adequate light for photosynthesis and this occurs only in the upper layer, the euphotic zone. On relatively shallow continental shelves such as those off the British Columbia coast, nutrients levels are high, making these areas some of the most productive in the world. The main nutrients include nitrogen (NO_3), phosphorus (PO_4), silica (SiO_2) and ammonia (NH_4), as well as carbon from carbon dioxide (CO_2). Nutrients enter the Kitimat inlet system through river runoff and through intrusions of oceanic water from Hecate Strait. Kitimat River water, observed in the surface layer in the summer, is characterized by high silicate concentrations (30 to 40 mmol/m^3) and low phosphates and nitrates. In the winter, less upper-layer nitrate depletion occurs, because of reduced phytoplankton growth, and surface layer silicate is reduced in the upper reaches of the inlet because of lower river flows.

The pH value is a measure of the acidity of the water. Pure water at pH 7 is neutral, whereas lower numbers are acidic and higher are basic (alkaline). Within the inlets and fjords, surface pH is usually high, except in the presence of low pH (acidic) runoff.

Turbidity is a measure of the cloudiness or opacity of water caused by suspended particles and dissolved material. Turbidity levels within the fjords are generally higher in summer because of suspended particles in the fresh water input, sometimes called rock flour. For photosynthetic plankton, turbidity reduces the depth of the euphotic zone and requires mixing of nutrients higher up above the halocline. Whether natural (rock flour) or anthropogenic (e.g., logging debris), turbid waters result in reduced primary productivity. As is visible in aerial photographs of the Bish Creek region, there can be considerable variance in surface turbidity.

Dissolved oxygen and turbidity levels are important parameters for assessment of water quality. These parameters, along with nutrients, influence productivity levels on which the marine food chain depends.

For a detailed data review and the analysis results, see Appendix F.

4 Project Physical Oceanography Program

4.1 September 2005 to January 2006

As was found in the historical data reviewed in Appendix B of this TDR, water currents were fastest in Douglas Channel and the approaches, and slowest within Kitimat Arm itself. Mean current speeds were 20 to 30 cm/s at the near-surface, except for Kitimat Arm where mean surface speeds reached only 5 to 10 cm/s. Maximum near-surface current speeds were near 100 cm/s in the approaches and Douglas Channel, reaching 110 cm/s in Principe Channel. The current speeds tend to decrease with depth, except in Principe Channel, where there is less variation with depth and where the maximum observed speed (for all sites) of 113 cm/s occurred.

In the inner passages of the Kitimat system, the currents tend to be aligned along the channel. The net flow tends to be seaward movement of fresher water at the surface and inland movement of denser seawater at depth.

Along with wind forcing, these freshwater inputs, which cause stratification of the water, can be as or more important than tidal forcing in Kitimat Arm and Douglas Channel. As was found in the historical data review, the relative importance of tidal currents tends to increase with depth and with proximity to the open ocean.

Water level measurements were also made. The largest tidal ranges, up to 8 m for the largest tides, were measured in Principe Channel. The smallest tidal ranges in the CCAA were measured at Caamaño Sound, where the maximum tidal ranges were 5.5 m. Kitimat Arm and Douglas Channel had similar tidal ranges, considered intermediate with maximum ranges of 6 m. The ranking and size of the tidal ranges is consistent with the historical results described in Appendix D.

Wave measurements were made at the west approach to Caamaño Sound (Yates Shoal on the Aranzazu Banks). The largest wave event had a significant wave height of 6.3 m and occurred on January 5, 2006 (period of 18 s and direction from 153° south-southeast). Waves usually arrive from the south to southwest, though an important component arrives from the southeast. Waves generated from the south and southeast sectors have the maximum fetch over which to develop and may then undergo refraction to arrive from the south to southwest. The largest waves (with a significant wave height greater than 4 m) tended to have peak interval periods between 10 and 20 s. On September 16, peak periods of 25.6 s were also measured. Most wave events had an important low-frequency contribution. Even on days when the local seas are calm, there may still be swell activity that has propagated from a distant storm in the northeast Pacific Ocean in the form of forerunners.

Cruises in September 2005 and January 2006 yielded 15 CTD profile measurements from which spatial and temporal patterns in the salinity and temperature could be obtained. The fresher and warmer surface water measurements were confined to depths of 10 m or less at all locations along the CCAA. As was found in the historical data presented in Appendix C, the upper layer was fresher farther inland, in accordance with the increased influence of freshwater discharge in the region. Gradients in temperature and salinity were likewise reduced in the approaches to the Kitimat system.

Between the two cruises, the surface temperatures cooled significantly, while at depth, small temperature increases of about one degree occurred. Wind events through the fall allowed vertical mixing and the surface salinities showed a large increase, with a small decrease in salinity at depth, consistent with the historical data examined in Appendix C.

Salinities were found to increase along Principe Channel toward Browning Entrance to the west, farther from the fresh water inputs of the Kitimat system. The September measurements indicate particularly fresh water at Site CM3 in the Principe Channel compared to other sampling locations in the channel. This may have been caused by an event that occurred earlier in the season, or possibly by inputs from Petrel Channel to the north. Variations in the effects of vertical mixing and cooling observed in the Kitimat waterway were also observed in Principe Channel between the two cruises.

For the detailed data collection methods and analysis results, see Appendix G.

4.2 January to April, 2006

Additional measurements were carried out in Kitimat Arm from January to April 2006, closer to shore than the September 2005 to January 2006 measurements. The current speeds were similar in magnitude, and the shallower deployment depth allowed measurements even closer to the surface. These measurements detected somewhat faster currents than were measured in the fall, when the mean (maximum) current speeds were 7.5 cm/s (50.8 cm/s) at the near-surface and 5.3 cm/s (39.9 cm/s) at mid-depth. At the new, near-shore location, the mean (maximum) current speeds were 8.9 cm/s (49.9 cm/s) at the near-surface and 6.6 cm/s (33.7 cm/s) at mid-depth. The fastest currents were at 5 m depth where the mean (max) speeds were 10.4 cm/s (65.6 cm/s). These higher values were likely caused by measuring 4 m closer to the surface than all previous measurements at this site.

The net flow over the measurement period was about 5 cm/s near-surface, decreasing to 1 cm/s at 29 m, with the direction to the south at all depths. These net flow rates were considerably larger than the near-surface flow rates of 1.6 cm/s measured in the fall.

Currents were found to be aligned more along the north-south axis than the NNE-SSW axis found in the fall. This rotation is consistent with the change in the direction of the bathymetry between the two sites. In the spring, the measurements also indicated a bias toward down-channel flow, which was not observed in the fall measurements.

Water levels were found to have a maximum tidal range of 6.2 m, with a range of 4.3 m from the 5% exceedance level to the 95% exceedance level. These values are the same as those found in the fall.

Both freshwater inputs, which cause stratification of the water column, and wind forcing are likely more important than the tidal forcing at Site CM1. As might be expected, CTD profiles indicate an intermediate spread in near-surface temperatures between the warm September 2005 values and the cold January 2006 values. However, at the mid-depth interval between 20 and 90 m, the water was cooler than in January, but below interval it was warmer than in January.

Near-surface salinities were strongest in January, likely due to mixing of the water column, though at depth this mixing has an opposite effect, with the least saline measurements of all. In April, when the least mixing occurred, the 10 to 60 m salinity values were the highest of any set of measurements. The

secondary peak in freshwater discharge in fall makes September the least saline at the near-surface. Over-all, the density profiles are very similar between measurements.

For the detailed data collection methods and analysis results for this period, see Appendix H.

4.3 April to December, 2006

Ocean current measurements were carried out from April to December 2006 as a continuation of measurements from January to April 2006 near the marine terminal. Earlier measurements from September 2005 to January 2006 were made at nearby sites in deeper waters, where maximum current speeds of 61.6 cm/s were measured in November. Net seaward drift was measured at all depths during the deployment. Mean current speeds varied from 9 cm/s at the near-surface to 2 cm/s at the near-bottom.

The CTD profile indicated the coldest water column measurements to date in the program. The near-surface salinity and density profiles were the second highest after the January measurements.

The measured water levels range is about 6.3 m from maximum to minimum and 4.2 m from the 5% exceedance level to the 95% exceedance level.

For the detailed data collection methods and analysis results for this period, see Appendix I.

4.4 December 2006 to July 2007

The 2006 program of ocean current measurements was extended to July 2007. Maximum current speeds of 81.6 cm/s were measured in January 2007. Net seaward drift was measured at all depths during the deployment. Mean current speeds varied from 14 cm/s at the near-surface to 4 cm/s at the near-bottom.

The CTD profile indicated a warming near-surface, but not as much as the September 2005 measurements. Near-surface salinities were the lowest measured in the program, at 1.3 to 2.0 psu.

The range between minimum and maximum water levels was 6.3 m, with a range of 4.2 m from the 5% exceedance level to the 95% exceedance level over the entire period.

For the detailed data collection methods and analysis results for this period, see Appendix J.

5 References

5.1 Literature Cited

ASL Environmental Sciences Inc. 2009. *Weather and Oceanographic Conditions in the CCAA Technical Data Report.* Prepared for: Northern Gateway Pipelines Inc. Calgary, AB.

Heidorn, K. 2004. *BC Weather Book: From the Sunshine Coast to Storm Mountain*. Fifth House. Calgary, AB.

JASCO Research Ltd. 2006. *Marine Acoustics (2006) Technical Data Report*. Prepared for Enbridge Northern Gateway Pipelines Inc. Calgary, AB.

Macdonald, R.W. 1983. *Proceedings of a Workshop on the Kitimat Marine Environment*. Canadian Technical Report of Hydrography and Ocean Sciences 18. Department of Fisheries and Oceans. Institute of Ocean Sciences. Sidney, BC.

Pickard, G.L 1961. Oceanographic features of inlets in the British Columbia mainland coast. *Journal of Fisheries Research Board of Canada* 18: 907-982.

Webster, I. 1980. *Kitimat Physical Oceanographic Study 1977-1978, Part 3, Estuarine Circulation*. Contract Report Series 80-3 (part 3). Department of Fisheries and Oceans. Institute of Ocean Sciences. Patricia Bay, BC.

Appendix A Meteorology Review from Historical Data

A.1 Introduction

A.1.1 Objectives

The purpose of this appendix is to describe baseline meteorological conditions within the CCAA to support the environmental assessment for the Project.

Information was sourced and summarized from existing literature and field surveys for the following key data categories:

- surface winds
- atmospheric pressure systems
- air temperature and precipitation
- climate variability and climate change

A.2 Methods

A.2.1 Spatial Boundaries

For the purposes of this report, meteorological data from Environment Canada coastal weather stations in the CCAA were reviewed (for the boundaries of the CCAA, see Figure 1-1). In addition, field surveys were conducted (Fall 2005 and Winter 2006) at the following coastal weather stations within the CCAA:

- Ashton Rock and Kersey Point in Douglas Channel
- Dorothy Island in Devastation Channel
- Wall Island in Caamaño Sound

The results from the field survey are documented in the Wind Observations in Douglas Channel, Squally Channel and Caamaño Sound TDR (Hayco 2010).

A.2.2 Review of Existing Data Sources

The existing data sources were obtained in large part from Environment Canada. The Meteorological Service of Canada (a division of Environment Canada) collects and archives all meteorological information for Canada and provides weather forecasts and reports. Within or near the project area Environment Canada has operated coastal weather stations at several locations (see Table A-1 and Figure A-1). Two of these sites are in the vicinity of the City of Kitimat, two sites are on the eastern side of Hecate Strait (Bonilla Island and Ethelda Bay), one (Hartley Bay) is in the southern Douglas Channel and two (Kildala and Kemano) are in nearby ocean channels.

In addition to the coastal Environment Canada weather stations, wind measurements were also obtained for the Nanakwa Shoal buoy in southern Kitimat Arm (also operated by Environment Canada) and at the Eurocan pulp mill in Kitimat. Summary statistics available for two historical weather stations in Kitimat were also obtained.

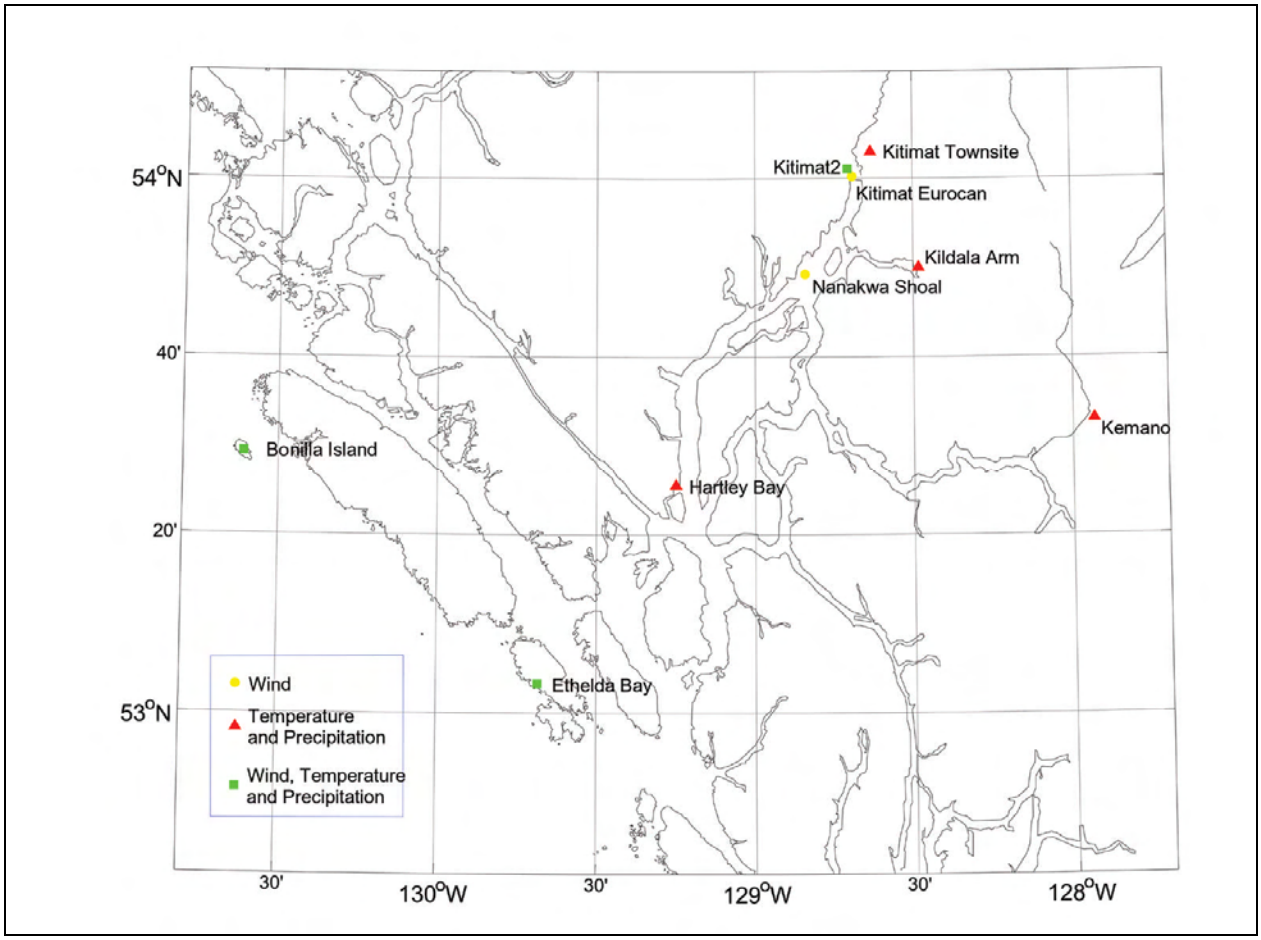

Figure A-1 Weather Stations used in Historical Data Review

Table A-1 Historical Weather Station Data Sets

Weather Station	Years of Data	Latitude	Longitude	Data Collected
Bonilla Island	1960 - 2002	53° 30' N	130° 38' W	Wind, temperature and precipitation
Ethelda Bay	1957 - 1991	53° 3' N	129° 41' W	Wind, temperature and precipitation
Hartley Bay	1973 - 1996	53° 25' N	129° 15' W	Temperature and precipitation
Nanakwa Shoal	1988 - 2005	53° 49' N	128° 50' W	Wind
Kitimat Eurocan	1996 - 2005	54° 0' N	128° 41' W	Wind
Kitimat 2	1966 - 2002	54° 1' N	128° 42' W	Wind, temperature and precipitation
Kitimat Townsite	1954 - 2002	54° 3' N	128° 38' W	Temperature and precipitation
Kildala	1966 - 2000	53° 50' N	128° 29' W	Temperature and precipitation
Kemano	1951 - 2002	53° 33' N	127° 56' W	Temperature and precipitation

The type of measured meteorological parameters varies among the weather stations. All of the coastal Environment Canada weather stations include measurements of air temperature, humidity, pressure and precipitation. Wind data are available from Bonilla Island, Kitimat Eurocan and the Nanakwa Shoal buoy.

The following information was also used in this report:

- The IPCC has produced a number of reports relating to the evidence for, potential effects of and possible reaction to climate change (IPCC 2006, Internet site). Reports on more local effects and adaptations include work by the Canadian Climate Impacts and Adaptation Research Network (C-CIARN 2006, Internet site) as well as work by individual agencies (British Columbia Ministry of Land, Water and Air Protection 2002).
- A detailed summary of British Columbia climatology can be found in The Climate of Canada and Alaska (Hare and Hay 1974) and the B.C. Weather Book (Heidorn 2004). Brief summaries are found in a number of broad topic reports (Chevron Canada Resources Ltd. 1982; Petro-Canada 1983; Hood and Zimmerman 1986; Scudder and Gessler 1989; Ricker and McDonald 1992; Ricker and McDonald 1995; Jacques Whitford Environment Limited 2001; Hall et al. 2004).

A.2.3 Field Surveys

Meteorological data was collected from the project area, as documented in ASL (2010).

A.3 Results of Baseline Investigations

A.3.1 Synopsis

The climate and weather conditions of the CCAA are a direct result of its location in an extensive network of mountainous islands between the major inland waters of the Pacific Ocean (Hecate Strait) and the British Columbia mainland. At the seaward limit of the CCAA, it is dominated by the Pacific marine climate characterized by moderate air temperatures and intense storms in fall and winter.

At the landward limit of the CCAA, the temperatures exhibit a greater range, reflecting the greater influence of a continental climate. Here, the marine storm winds are generally abated by the mountainous terrain. In winter, strong Arctic outflow winds occur because of the presence of a cold and dry Continental Arctic high-pressure system that episodically extends into the interior of British Columbia. The high surface pressures in the interior can result in strong, low-temperature winds that flow into the inland fjords. Arctic outflows are associated with strong winds from the northeast, moderate to heavy snowfalls and squalls, and the potential for large waves (due to the strong winds over large fetches), reduced visibility and icing of structures due to freezing spray.

The presence of the Coast Mountains, including the islands along the CCAA, results in very high rainfall as moist Pacific air encounters the rugged coastal terrain. The rainfall is greatest in the more exposed seaward part of the CCAA and is gradually reduced, with a greater proportion of snowfall, as one proceeds inland.

A.3.2 Winds and Pressure Systems

Pacific North Coast Region

The climate and weather conditions of British Columbia's coastal regions are largely governed by two Pacific Ocean air masses, as well as by the frequent west-to-east passage of cyclonic weather systems (most frequent from October through May) and the presence of large mountain belts parallel to the coast. It is one of the windiest areas of Canada. The strongest hourly winds measured in British Columbia were recorded at Cape St. James in 1963 at the southern tip of Haida Gwaii (i.e., 49.2 m/s or 177 km/h on October 31, 1963).

The two Pacific Ocean air masses in the region are the Aleutian Low and the North Pacific High (Thomson 1989) (see Figure A-2). They not only influence the winds, air temperature, air moisture and storm tracks in the region as a whole, but also drive surface currents within the CCAA. These pressure systems vary seasonally (as described below) and vary in intensity from year to year (Hamilton 1984), often making them the root cause of interannual wind fluctuations, forcing corresponding variations in the North Pacific wind-driven surface currents and associated climatic and oceanographic parameters.

During winter, a quasi-permanent low-pressure system, the Aleutian Low, dominates North Pacific weather patterns. The average counter-clockwise flow about the Aleutian Low and the presence of the Coast Mountains results in prevailing southeasterly winds along the British Columbia coast. The Aleutian Low reflects the frequent passage of extra-tropical storms into the Gulf of Alaska.

Rapidly developing extra-tropical cyclones are more likely to affect the British Columbia coast than in other areas in Canada, with the exception of the Canadian Atlantic coast. These coastal low weather systems are characterized by a rapid and sustained decrease in central air pressure and intensified wind speeds and are often accompanied by increased precipitation. These storms can travel quickly. Winds up to 70 knots (with gusts to 100 knots) are generated to the east and southeast of the low. Over a typical winter, about 17 such storms develop and affect the British Columbia coastal area (Stewart et al. 1995). Gale force winds at Cape St. James are usually a precursor to the arrival of similar winds along the north and central mainland coast about 24 hours later. The chart below (see Figure A-3) shows a pressure pattern typical of a coastal low.

In summer, the mean monthly weather patterns change with the North Pacific High moving northward and displacing the Aleutian Low (see Figure A-2, bottom left). This pressure pattern tends to deflect most storms to the north. The clockwise airflow around this high results in weaker, primarily northwesterly winds along the central coast.

The strong winds of the offshore Pacific, Queen Charlotte Sound and Hecate Strait decrease markedly within the inland waters of the CCAA throughout the year (see Figure A-4).

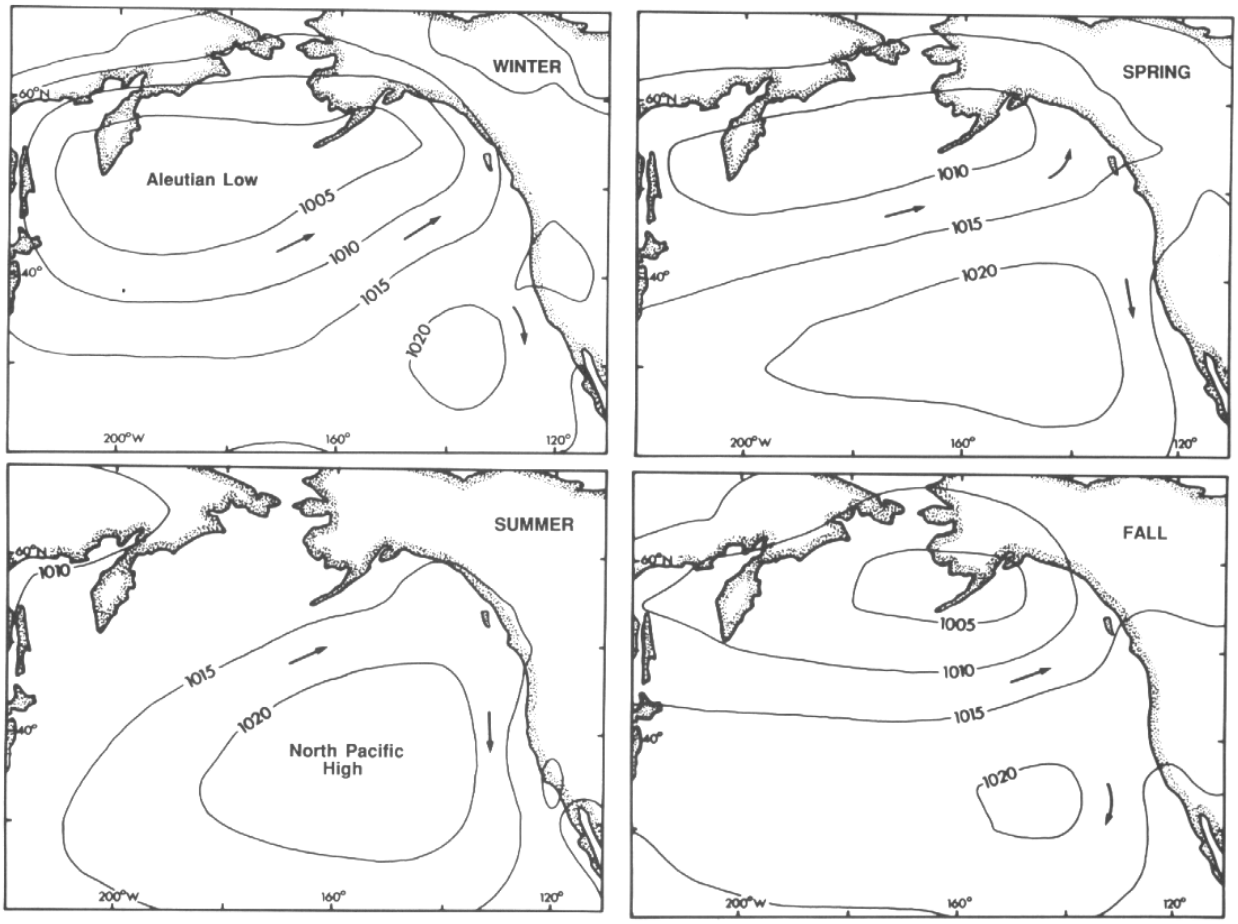

SOURCE: Thomson 1989

Figure A-2 Seasonal Mean Surface Atmospheric Pressure Maps, 1947 to 1982

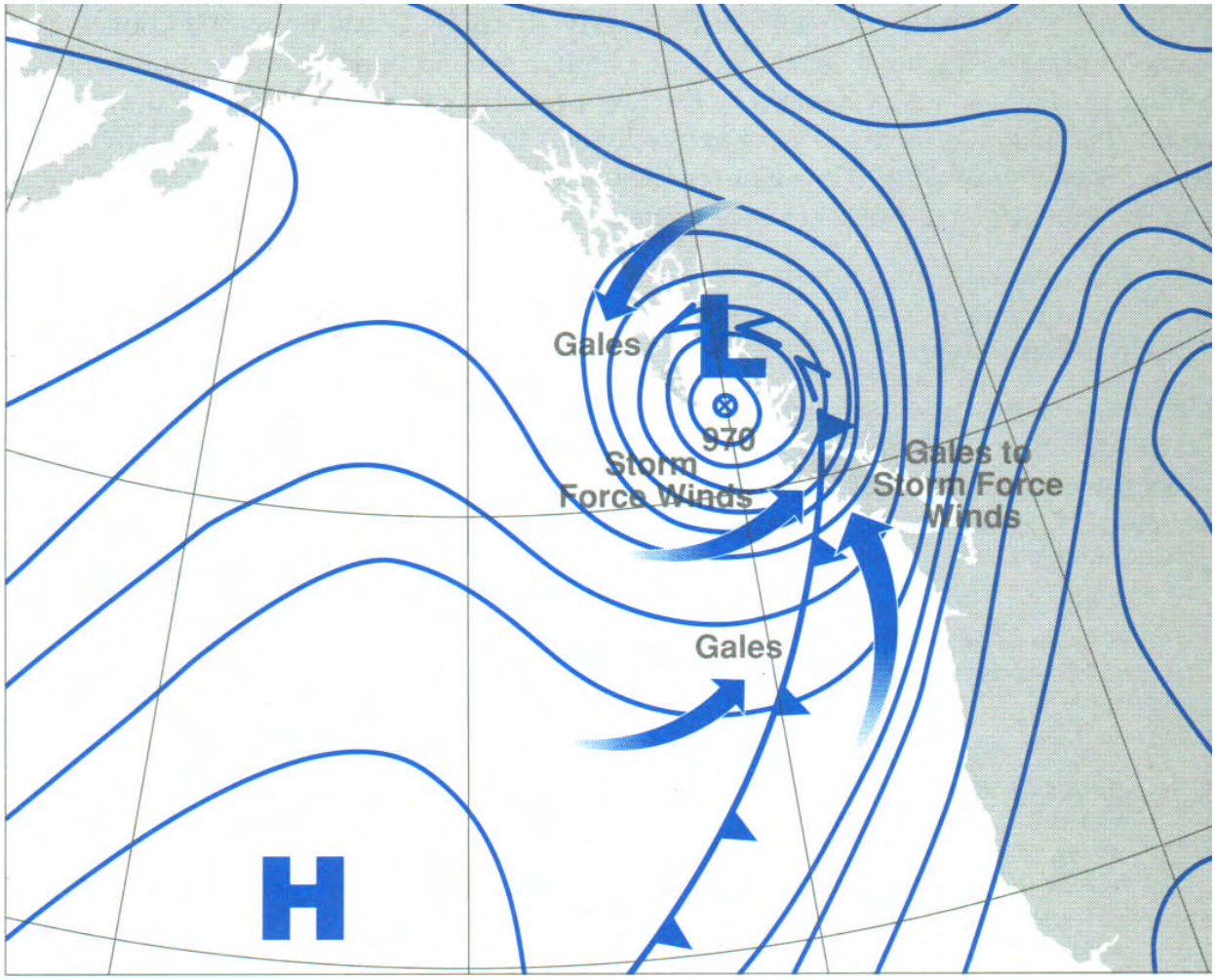

SOURCE: Environment Canada 1992

Figure A-3 Winter Pressure Pattern Typical of a Coastal Low

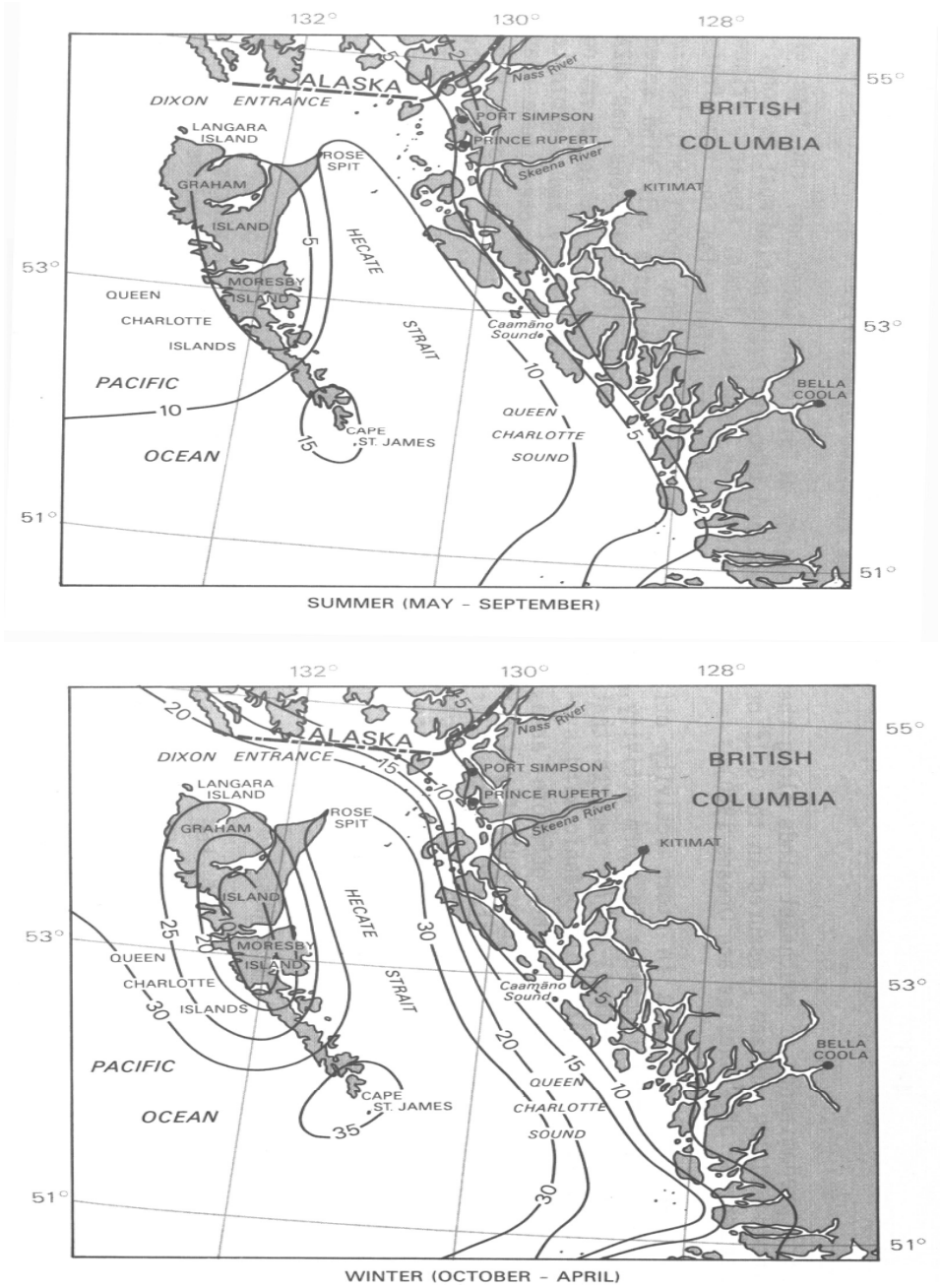

SOURCE: Petro-Canada 1983

Figure A-4 Frequency (Percentage) of Winds exceeding 40 km/h – Summer and Winter

During winter, when cold arctic air extends southward over the continent into northern British Columbia, arctic outflow winds can occur with cold dense air funnelling down the coastal inlets (Kendrew and Kerr 1955; see Figure A-5). The winds can be very strong, often up to 60 knots and occasionally to 100 knots. Sustained northeasterly outflow winds have been observed to remain above 60 knots for over 24 hours. The combination of strong winds and frigid temperatures can result in heavy freezing spray within and at the entrances to mainland inlets (Stewart et al. 1995). The alignment of the inlet with the cold arctic outflow wind directions has an effect on the severity of the cold outflow winds.

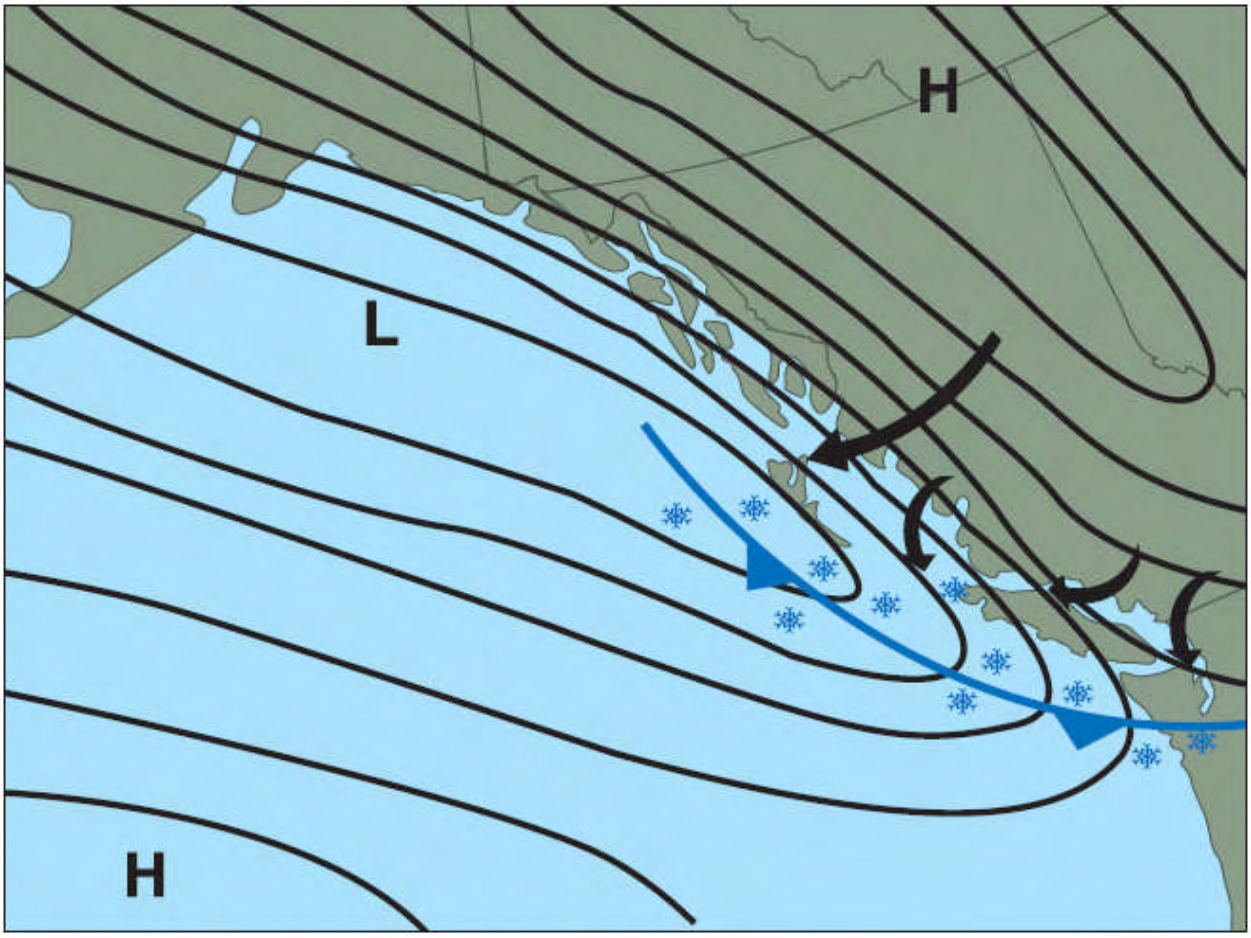

Figure A-5 Effect of a Continental Arctic High Pressure Ridge over the British Columbia Interior

Confined Channel Assessment Area

For characterizing the winds in the CCAA, historical wind data sets from the following three primary locations were used:

- Bonilla Island in eastern Hecate Strait
- Nanakwa Shoal, located at the north end of Douglas Channel about 23 km from Kitimat Harbour
- Kitimat Eurocan, situated at tidewater in Kitimat Harbour

The Bonilla Island data, available since 1960, are representative of the winds of eastern Hecate Strait that would be encountered by ships approaching Caamaño Sound or passing through Browning Entrance into Principe Channel. As supplemental information, statistical summaries of the occasional wind observations at the Ethelda Bay lighthouse (eastern Hecate Strait) and the extended measurements of winds at the Kitimat 2 site are also used.

For a summary of monthly wind statistics for the primary wind measurement sites in more recent years (1994 to 2005), see Table A-2. For the statistics for monthly maximum winds available from historical measurement sites with 20 years or more of data available, see Table A-3.

The monthly wind statistics reveal pronounced spatial and seasonal patterns. The wind speeds on the open coast of eastern Hecate Strait are considerably greater than those in the inland waters. The yearly average wind speed at Nanakwa Shoal (4.5 m/s) is reduced by 38% from that of Bonilla Island (7.3 m/s), whereas the reduction at Kitimat Eurocan (5.1 m/s) is about 30% (see Figure A-6). In terms of maximum observed wind speeds over 20 years or longer, the reduction in wind speeds at inland locations is even greater, at over 50% from the eastern coast of Hecate Strait to the inland waters of the CCAA. The highest values measured on the Hecate Strait coast are 39.7 m/s (77 knots) at Bonilla Island and 33.3 m/s (65 knots) at Ethelda Bay (see Figure A-7), compared with maximum measured inland values of 18.4 m/s (36 knots) at Nanakwa Shoal, 17.6 m/s (34 knots) at Kitimat Eurocan and only 11.1 m/s (22 knots) at Kitimat 2. Consistent with the differences in the average and maximum wind speed statistics, the distribution of the wind speeds exhibits major changes between the offshore (Bonilla Island) and inshore areas (Nanakwa Shoal and Kitimat Eurocan), as shown in Figure A-6. Only 4.8% and 6.3% of all winds at Kitimat Eurocan and Nanakwa Shoal, respectively, exceed 10 m/s (18 knots), in sharp contrast to 23.1% of winds exceeding 10 m/s at Bonilla Island.

Table A-2 Wind Statistics for Historical Measurements at Bonilla Island, Nanakwa Shoal and Kitimat Eurocan

Bonilla Island (1994-2005)

	1994/01/01 00:00:00 to 2005/12/11 23:00:00												
	January	February	March	April	May	June	July	August	September	October	November	December	Year
Speed (m/s)	7.8	7.7	7.8	7.3	7.1	6.6	6.0	5.9	6.5	8.0	8.0	8.4	7.3
Most Frequent Direction	SE	SE	SE	SE	SE	N	N	SE	SE	SE	SE	SE	SE
Maximum Hourly Speed (m/s))	28.9	31.9	26.7	27.2	26.4	21.1	21.1	21.7	23.1	33.3	27.2	30.3	33.3
Date (yyyy/dd)	2003/03	1999/11	2003/17	2003/06	1999/05	1996/29	1998/15	2001/20	1999/28	2001/26	1999/23	1996/04	2001/26
Direction of Max. Hourly Speed	S	SE	SSE	SSE	SE	SE	SE	SE	SE	SSE	SE	SE	SSE
Maximum Gust Speed (m/s)	n/a	n/a	n/a	n/a	n/a	n/a	n/a	n/a	n/a	n/a	n/a	n/a	n/a
Date (yyyy/dd)	n/a	n/a	n/a	n/a	n/a	n/a	n/a	n/a	n/a	n/a	n/a	n/a	n/a
Direction of Maximum Gust	n/a	n/a	n/a	n/a	n/a	n/a	n/a	n/a	n/a	n/a	n/a	n/a	n/a
Days with Winds >= 52 km/hr (14.4 m/s)	129	108	121	69	48	34	10	23	53	122	137	147	1001
Days with Winds >= 63 km/hr (17.5 m/s)	74	61	69	38	17	8	1	9	26	71	71	94	539

Kitimat Eurocan (1996-2005)

	1996/10/07 10:00:00 to 2005/01/01 00:00:00												
	January	February	March	April	May	June	July	August	September	October	November	December	Year
Speed (m/s)	5.2	4.4	5.3	4.5	5.2	5.6	5.9	5.3	4.9	4.9	4.7	5.0	5.1
Most Frequent Direction	N	N	N	S	S	S	S	S	S	S	N	N	S
Maximum Hourly Speed (m/s)	17.6	16.7	16.1	14.8	16.7	15.5	16.0	14.3	14.7	16.3	17.3	16.7	17.6
Date (yyyy/dd)	2001/10	2001/28	2004/05	2002/21	1998/27	1997/25	1997/05	2000/30	2004/11	2001/26	2001/15	2004/19	2001/10
Direction of Max. Hourly Speed	SE	W	SSW	W	SSW	SSW	SSW	SSE	E	N	N	E	SE
Maximum Gust Speed (m/s)	n/a	n/a	n/a	n/a	n/a	n/a	n/a	n/a	n/a	n/a	n/a	n/a	n/a
Date (yyyy/dd)	n/a	n/a	n/a	n/a	n/a	n/a	n/a	n/a	n/a	n/a	n/a	n/a	n/a
Direction of Maximum Gust	n/a	n/a	n/a	n/a	n/a	n/a	n/a	n/a	n/a	n/a	n/a	n/a	n/a
Days with Winds >= 52 km/hr (14.4 m/s)	5	3	2	1	2	1	3	0	1	3	2	2	25
Days with Winds >= 63 km/hr (17.5 m/s)	1	0	0	0	0	0	0	0	0	0	0	0	1

Table A-2 Wind Statistics for Historical Measurements at Bonilla Island, Nanakwa Shoal and Kitimat Eurocan (cont'd)

Nanakwa Shoal (1988-2005)

	1988/11/22 22:37:00 to 2005/09/11 21:37:00												
	January	February	March	April	May	June	July	August	September	October	November	December	Year
Speed (m/s)	6.3	4.8	4.5	3.6	3.9	4.3	4.4	4.0	3.7	4.1	4.9	5.5	4.5
Most Frequent Direction	NNE	NNE	NNE	SW	SW	SW	SSW	SSW	SSW	NNE	NNE	NNE	SSW
Maximum Hourly Speed (m/s)	18.4	17.3	16.2	16.1	15.2	13.9	12.0	11.7	12.9	15.4	16.0	18.1	18.4
Date (yyyy/dd)	2000/16	1990/31	2001/24	2000/13	1993/14	2005/18	2003/31	1999/28	2001/29	1996/29	1996/23	1996/26	2000/16
Direction of Maximum Hourly Speed	NE	NNE	NE	NE	SSW	SSW	SW	WSW	S	NNE	NNE	NE	NE
Maximum Gust Speed (m/s)	23.2	20.5	20.2	19.9	17.9	16.7	17.5	15.5	16.6	18.7	20.9	21.5	23.2
Date (yyyy/dd)	2000/16	1990/31	1996/03	2000/13	1993/14	2005/18	1999/14	1999/28	2004/11	1996/29	1996/16	1996/26	2000/16
Direction of Maximum Gust	NE	NNE	SW	NE	SSW	SW	NE	WSW	SSW	NNE	N	NE	NE
Days with Winds >= 52 km/hr (14.4 m/s)	57	11	3	2	2	0	0	0	0	2	10	27	114
Days with Winds >= 63 km/hr (17.5 m/s)	2	0	0	0	0	0	0	0	0	0	0	2	4

Table A-3 Monthly Maximum Wind Speed Statistics for Measurement Sites with 20 Years or More of Historical Data

Bonilla Island (1986-2000)

	1971 to 2000, except maximum values which apply from 1960 to 2000												
	January	February	March	April	May	June	July	August	September	October	November	December	Year
Speed (m/s)						6.6	6.2						
Most Frequent Direction						SE	SE						
Maximum Hourly Speed (m/s)	28.6	39.7	33.1	28.6	23.3	22.8	18.3	21.4	24.2	29.2	35.0	32.2	39.7
Maximum Hourly Speed (km/h))	103	143	119	103	84	82	66	77	87	105	126	116	143
Date (yyyy/dd)	1973/17	1974/20	1977/10	1970/07	1978/01	1968/01	1969/10	1971/18	1968/24	1968/16	1968/28	1968/06	2001/26
Direction of Maximum Hourly Speed	SE	S	SE	S	SE	SE	SE	SE	SE	SE	SE	S	SSE

Ethelda Bay (1971-1991)

	1971 to 1991, except maximum values which apply from 1957 to 1991												
	January	February	March	April	May	June	July	August	September	October	November	December	Year
Speed (m/s)		4.1		3.3	2.9	2.7	2.4						
Most Frequent Direction		NE		SE	SE	SE	NW						
Maximum Hourly Speed (m/s)	25.8	33.3	18.1	19.2	18.1	18.1	13.3	18.1	20.0	23.1	20.6	23.1	33.3
Date (yyyy/dd)	1980/08	1980/14	1979/06	1970/05	1981/01	1981/29	1982/05+	1981/21	1981/30	1980/07+	1979/21+	1981/09+	1980/14
Direction of Maximum Hourly Speed	NE	NE	SE	S	SE	SE	SE	SE	SW	SW	SE	NE	NE
Days with Winds >= 52 km/hr (14.4 m/s)		1		1	0	0	0	0	0				
Days with Winds >= 63 km/hr (17.5 m/s)		0		0	0	0	0	0	0				

Table A-3 Monthly Maximum Wind Speed Statistics for Measurement Sites with 20 Years or More of Historical Data (cont'd)

Nanakwa Shoal (1988-2005)

	1988/11/22 to 2005/09/11												
	January	February	March	April	May	June	July	August	September	October	November	December	Year
Speed (m/s)	6.3	4.8	4.5	3.6	3.9	4.3	4.4	4.0	3.7	4.1	4.9	5.5	4.5
Most Frequent Direction	NNE	NNE	NNE	SW	SW	SW	SSW	SSW	SSW	NNE	NNE	NNE	SSW
Maximum Hourly Speed (m/s)	18.4	17.3	16.1	16.1	15.2	13.9	12.0	11.7	12.9	15.4	16.0	18.1	18.4
Date (yyyy/dd)	2000/16	1990/31	2001/24	2000/13	1993/14	2005/18	2003/31	1999/28	2001/29	1996/29	1996/23	1996/26	2000/16
Direction of Maximum Hourly Speed	NE	NNE	NE	NE	SSW	SSW	SW	WSW	S	NNE	NNE	NE	NE
Maximum Gust Speed (m/s)	23.2	20.5	20.2	19.9	17.9	16.7	17.5	15.5	16.6	18.7	20.9	21.5	23.2
Date (yyyy/dd)	2000/16	1990/31	1996/03	2000/13	1993/14	2005/18	1999/14	1999/28	2004/11	1996/29	1996/16	1996/26	2000/16
Direction of Maximum Gust	NE	NNE	SW	NE	SSW	SW	NE	WSW	SSW	NNE	N	NE	NE
Days with Winds >= 52 km/hr (14.4 m/s)	57	11	3	2	2	0	0	0	0	2	10	27	114
Days with Winds >= 63 km/hr (17.5 m/s)	2	0	0	0	0	0	0	0	0	0	0	2	4

Kitimat 2 (1966-2000)

	1971 to 2000, except maximum values which apply from 1966 to 2000												
	January	February	March	April	May	June	July	August	September	October	November	December	Year
Maximum Hourly Speed (m/s)	11.1	9.4	11.1	8.9	9.7	8.9	8.6	8.1	9.7	10.3	9.7	10.8	11.1
Maximum Hourly Speed (km/h))	40	34	40	32	35	32	31	29	35	37	35	39	40.0
Date (yyyy/dd)	1973/23	1972/15+	1971/07	1966/09	1973/31	1975/20	1966/25+	1967/06+	1970/05	1968/25	1970/27	1968/23	1973/23
Direction of Maximum Hourly Speed	SE	S		SE	SE	SE	SE	SE	SE	S	NW	N	SE

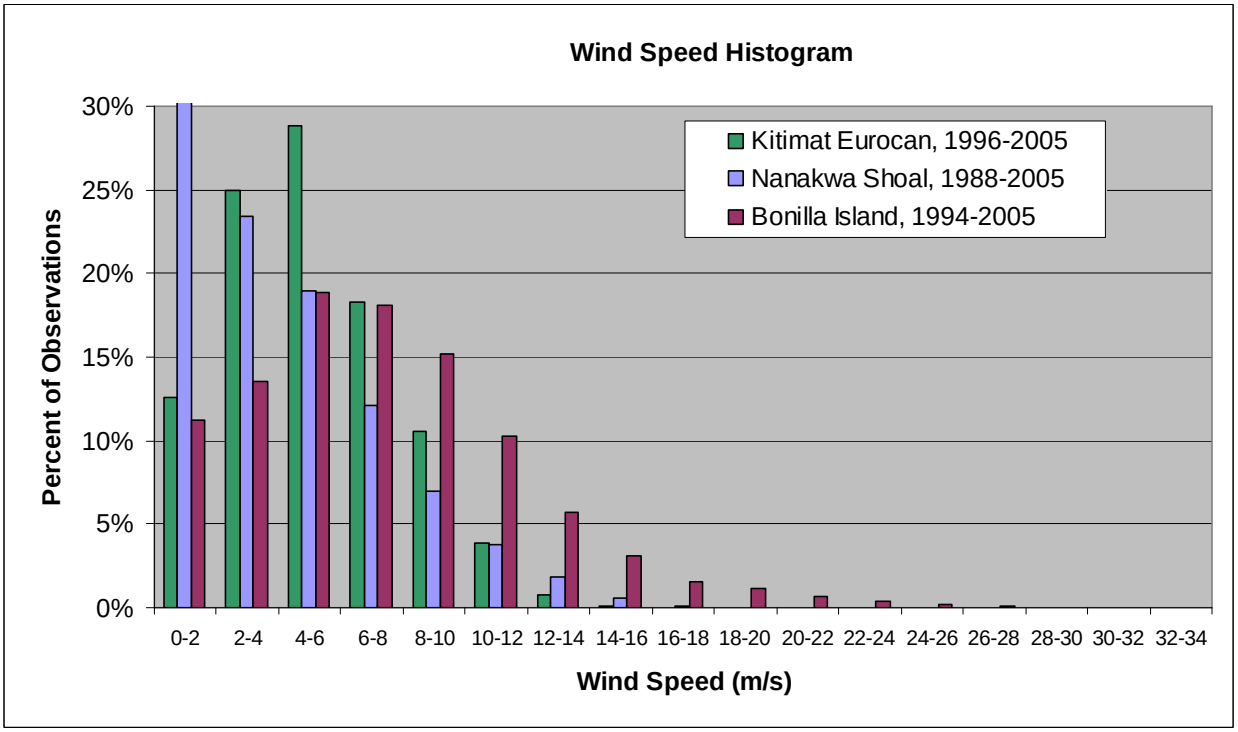

Figure A-6 Observed Distributions of Wind Speeds at Bonilla Island, Nanakwa Shoal and Kitimat Eurocan

Wind speeds exhibit a distinct seasonal pattern, with the highest occurring in fall and winter and the lowest in spring and summer (see Figure A-7). The seasonal cycle in wind speeds is most pronounced in eastern Hecate Strait at Bonilla Island and Ethelda Bay and is less apparent in the inland waters, especially at Kitimat Eurocan where average wind speeds show little change with the seasons. The maximum wind speeds are reduced by 10% to 20% from winter to summer.

In addition to wind speeds being higher in winter, the wind directions (see Table A-2 and Table A-3) change seasonally at inland locations. From October to April, the dominant wind direction at Nanakwa Shoal is from the north, whereas from May to September it is from the south to southwest. At Kitimat Eurocan, northerly winds are dominant from November to March whereas southerly winds are most common from April to October. The predominance of northerly winds in fall and winter is associated with the Arctic outflow conditions, as discussed above, especially for the highest winds in these seasons. These Arctic outflow winds reach maximum hourly values of up to 18.4 m/s (36 knots) at Nanakwa Shoal and approximately 17 m/s (33 knots) at Kitimat Eurocan.

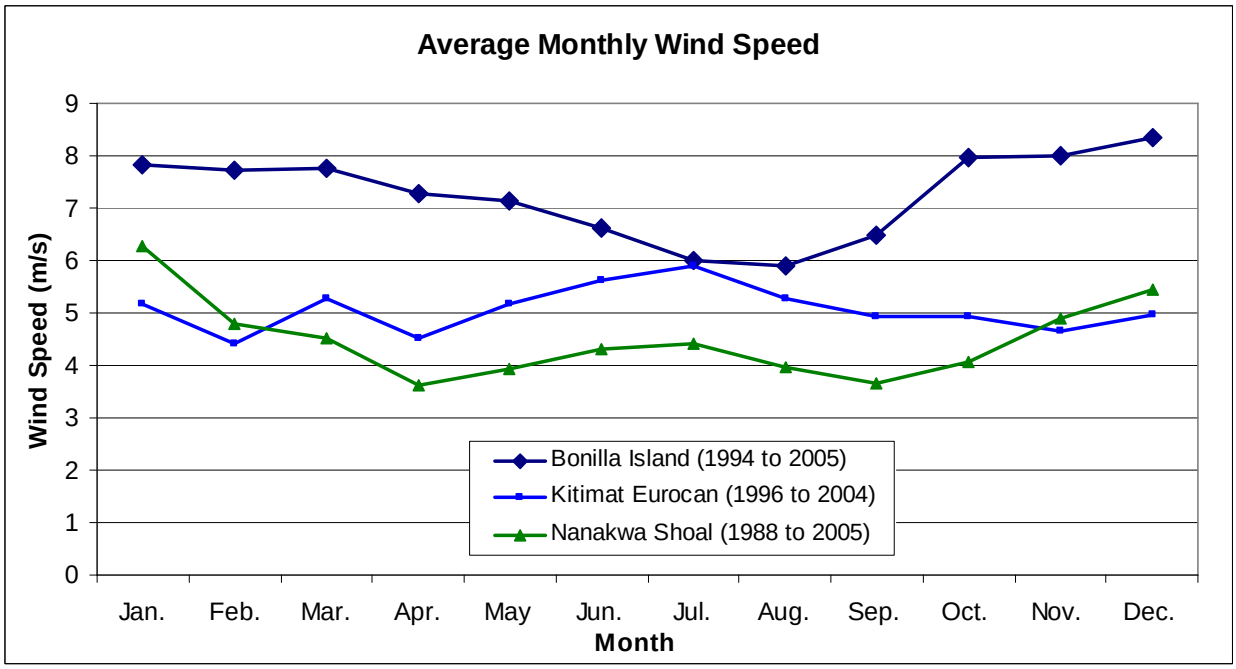

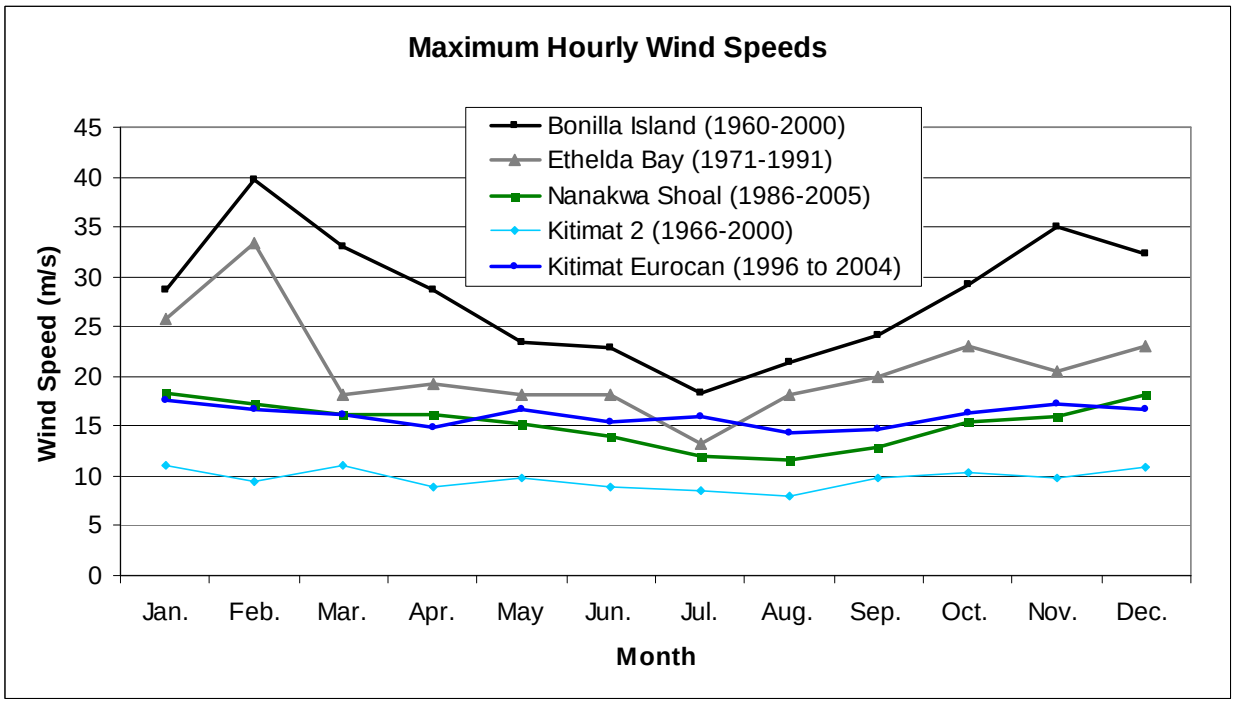

Figure A-7 Average and Maximum Wind Speeds by Month from Historical Wind Data Sets

For plots of wind directions for January, April, July and October, see Figure A-8 through Figure A-10. The length of a pie segment indicates the percentage of time when winds occur from the direction indicated (e.g., the length of the segment at 0 degrees shows the frequency with which the wind blow from the north, whereas the segment length at 270 degrees shows the frequency of winds from the west). The colour coding indicates the relative distribution of wind speeds from each direction. The figures also show the monthly mean and maximum wind speeds (as derived from hourly average wind speed data).

At Bonilla Island (see Figure A-8), the dominant winds are from the southeast to south in all seasons, although northerly and northwesterly winds are more common in spring and especially in summer.

The seasonal distribution of wind directions is very different in the inland waters. At Kitimat Eurocan (see Figure A-9), the winds are more uniformly distributed by direction in April and October, but they show a distinct tendency to be more northerly in January. Note that even though northerly winds predominate in the fall and winter, the less frequent southwesterly winds reach higher speeds (from less than 14 m/s versus up to 17.6 m/s). In July, southerly to southwesterly winds dominate with speeds of up to 14 to 16 m/s. The frequent southerly summer winds at Kitimat reflect the daily convectional winds blowing from Kitimat Arm into the Kitimat Valley because of the higher land-to-water temperature ratio in the summer.

At Nanakwa Shoal (see Figure A-10), the wind direction differences are even more pronounced than those at Kitimat, with northerly winds dominating in January, associated with Arctic outflow winds of up to 18.4 m/s (36 knots). In July, the wind direction is mostly dominated by southwesterly to southerly winds because of the same landward convection effects described in the preceding paragraph.

A.3.3 Air Temperatures and Precipitation

The air temperatures in the CCAA reflect a transition from the Pacific Ocean air masses of the marine climate region of Hecate Strait to the inland waters that cross the Coast Mountain zone. In winter, the warm, moist marine conditions to the west are accompanied by very wet and mild conditions in the inland waters, in conjunction with increased snowfall at higher elevations and with distance to the east. The increased precipitation results from the moist marine air encountering the hills and mountains that border the inland waterways. In summer, the mild marine conditions to the west over Hecate Strait are accompanied by mild scattered showers, again associated with moist marine air encountering mountainous terrain.

The transition in air temperatures from Hecate Strait (Bonilla Island and Ethelda Bay) to the inland locations (Hartley Bay, Kitimat and Kildala) is evident in the statistics derived from long-term measurements of temperature (see Table A-4 and Figure A-11). From October to March, the monthly average air temperatures are reduced by as much (January) as 2.5°C and 6°C at Hartley Bay and Kitimat, respectively, from those at Bonilla Island. In summer, the temperature gradient reverses, with warmer temperatures at inland locations, by 2.2°C and 3.7°C at Hartley Bay and Kitimat, respectively, from those at Bonilla Island.

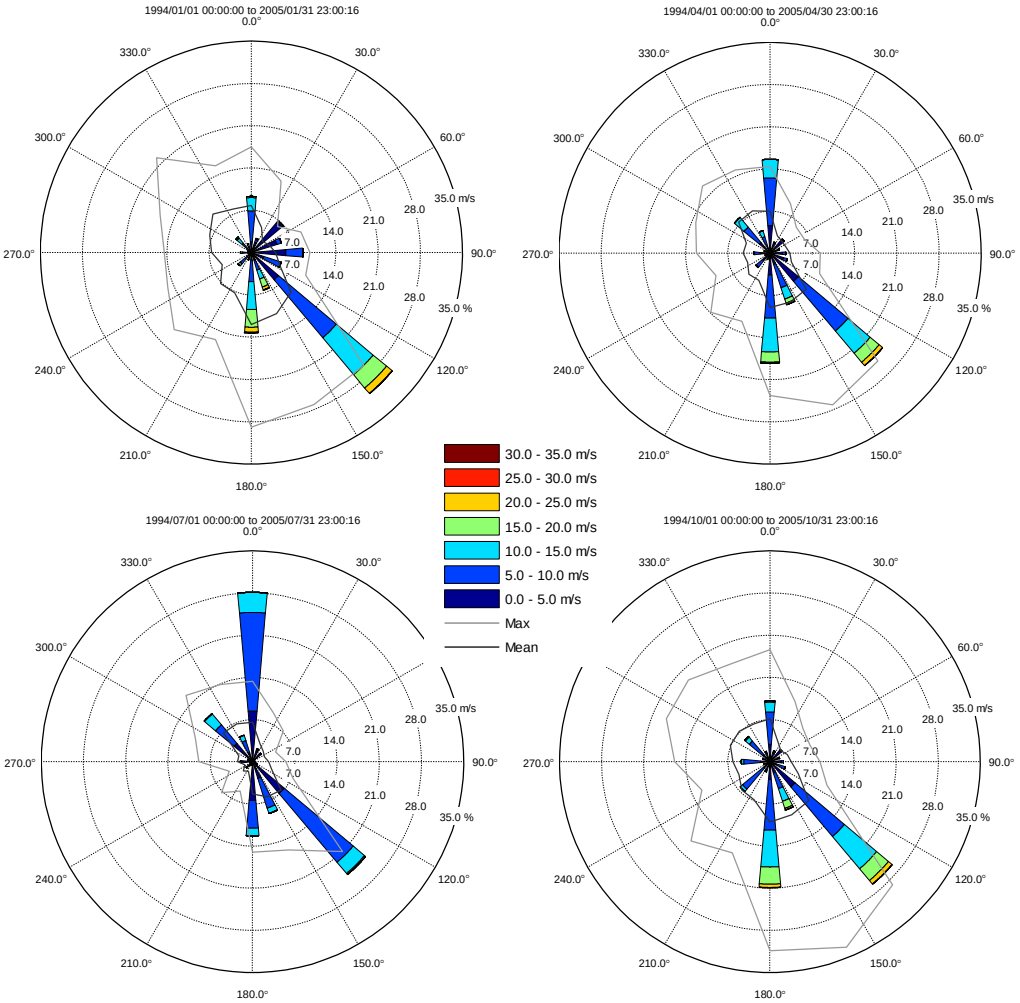

NOTE: January (top left), April (top right), July (bottom left) and October (bottom right)

Figure A-8 Bonilla Island Wind Statistics

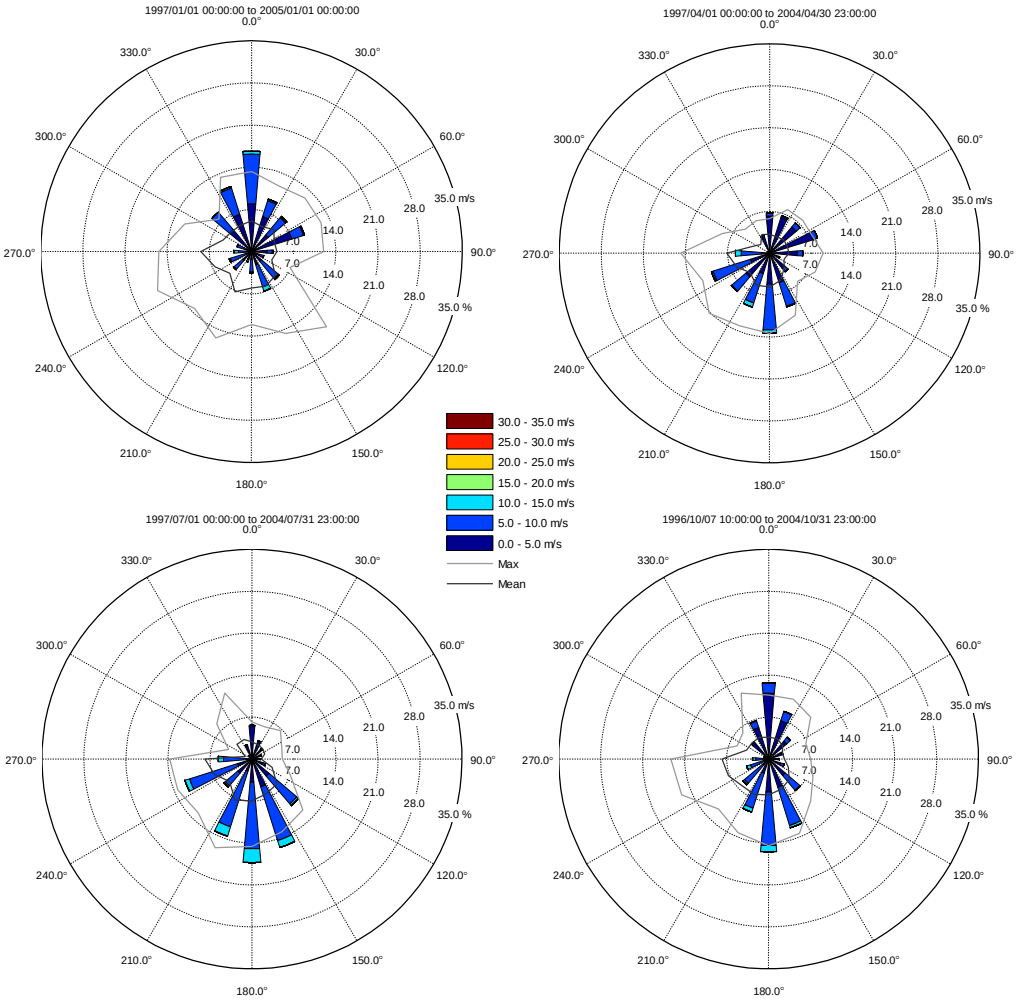

NOTE: January (top left), April (top right), July (bottom left) and October (bottom right)

Figure A-9 Kitimat Eurocan Wind Statistics

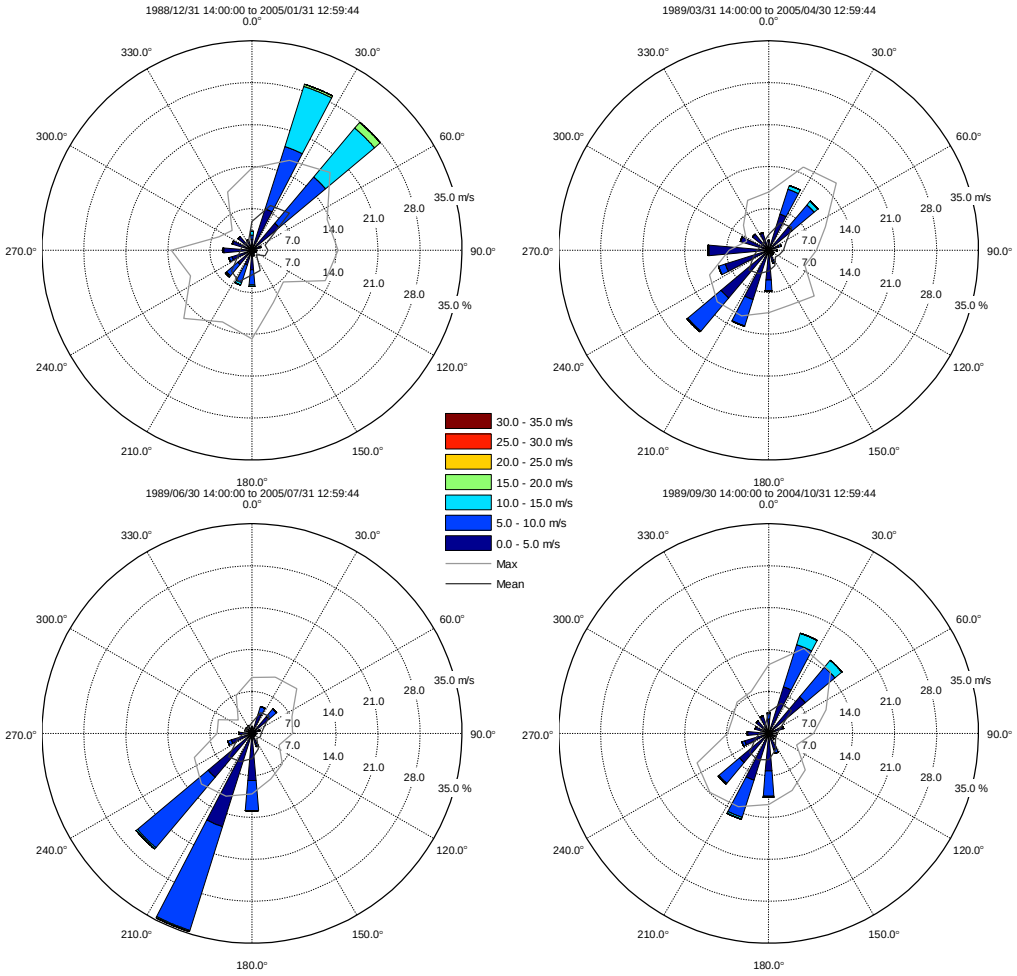

NOTE: January (top left), April (top right), July (bottom left) and October (bottom right)

Figure A-10 Nanakwa Shoal Wind Statistics

Table A-4 Air Temperature Statistics from Weather Stations with Extended Observations

Bonilla Island - All Years (1965 to 2002)

	Jan	Feb	Mar	Apr	May	Jun	Jul	Aug	Sep	Oct	Nov	Dec	Year
Daily Average (°C)	3.8	4.6	5.3	7.0	9.0	11.3	13.0	13.5	12.4	9.7	6.5	4.6	8.4
Daily Maximum (°C)	5.6	6.6	7.4	9.1	11.1	13.3	15.0	15.4	14.2	11.4	8.3	6.4	10.4
Daily Minimum (°C)	1.9	2.7	3.3	4.8	7.0	9.2	11.0	11.6	10.5	7.9	4.7	2.7	6.5
Extreme Maximum (°C)	15.5	15.6	15.5	20.5	22.0	23.5	23.3	22.0	26.5	18.0	18.9	14.5	26.5
Extreme Minimum (°C)	-13.3	-14.5	-8.9	-2.8	2.0	5.5	7.8	7.2	4.4	-5.0	-18.5	-15.0	-18.5

Ethelda Bay- All Years (1957 to 1991)

	Jan	Feb	Mar	Apr	May	Jun	Jul	Aug	Sep	Oct	Nov	Dec	Year
Daily Average (°C)	2.5	3.8	4.5	6.4	8.8	11.3	13.2	13.7	12.0	8.8	5.1	3.1	7.6
Daily Maximum (°C)	4.8	6.4	7.7	10.1	12.8	15.2	17.1	17.5	15.8	11.7	7.4	5.4	10.9
Daily Minimum (°C)	0.2	1.2	1.2	2.6	4.7	7.3	9.3	9.8	8.1	5.8	2.6	0.8	4.4
Extreme Maximum (°C)	16.1	15.0	16.7	23.6	28.3	29.4	26.4	28.4	27.5	20.6	17.8	16.1	29.4
Extreme Minimum (°C)	-16.7	-14.5	-8.9	-7.8	-2.2	-1.1	2.6	1.5	-1.1	-7.6	-18.4	-14.4	-18.4

Hartley Bay - All Years (1973 to 1996)

	Jan	Feb	Mar	Apr	May	Jun	Jul	Aug	Sep	Oct	Nov	Dec	Year
Daily Average (°C)	1.1	2.3	4.1	6.7	10.1	12.9	15.2	15.5	13.0	8.6	4.2	1.8	7.9
Daily Maximum (°C)	3.7	5.2	7.6	11.0	14.7	17.4	19.7	20.3	17.2	11.8	6.7	4.2	11.5
Daily Minimum (°C)	-1.6	-0.6	0.5	2.3	5.5	8.3	10.7	10.7	8.8	5.4	1.6	-0.6	4.2
Extreme Maximum (°C)	13.0	15.0	19.5	24.5	29.0	31.0	32.5	33.3	32.2	20.0	14.4	13.0	33.3
Extreme Minimum (°C)	-14.5	-16.0	-11.7	-3.0	-0.6	2.0	2.5	3.5	1.0	-8.0	-22.0	-16.7	-22.0

Table A-4 Air Temperature Statistics from Weather Stations with Extended Observations (cont'd)

Kildala - All Years (1966 to 2000)

	Jan	Feb	Mar	Apr	May	Jun	Jul	Aug	Sep	Oct	Nov	Dec	Year
Daily Average (°C)	-2.9	-0.2	2.9	6.2	10.0	13.4	15.6	15.7	12.1	7.2	1.9	-1.2	6.7
Daily Maximum (°C)	-0.8	2.4	6.3	10.5	14.6	17.9	20.2	20.2	15.9	9.7	3.7	0.4	10.1
Daily Minimum (°C)	-4.9	-2.8	-0.6	1.8	5.3	8.8	10.9	11.1	8.3	4.6	0.1	-2.8	3.3
Extreme Maximum (°C)	10.0	9.5	17.0	24.4	30.0	31.7	34.5	33.0	29.4	18.0	14.4	12.0	34.5
Extreme Minimum (°C)	-23.9	-18.3	-15.0	-4.4	-2.5	2.5	2.8	2.0	-0.6	-12.0	-23.5	-20.6	-23.9

Kitimat 2 - All Years (1966 to 2002)

	Jan	Feb	Mar	Apr	May	Jun	Jul	Aug	Sep	Oct	Nov	Dec	Year
Daily Average (°C)	-2.4	0.4	3.3	6.7	10.5	14.4	16.7	16.7	13.0	7.8	2.5	-0.9	7.4
Daily Maximum (°C)	0.0	3.1	6.7	11.2	15.6	19.2	21.5	21.4	17.0	10.6	4.7	1.3	11.1
Daily Minimum (°C)	-4.8	-2.4	-0.1	2.2	5.4	9.5	11.8	12.0	8.9	4.9	0.2	-3.1	3.7
Extreme Maximum (°C)	10.5	12.0	19.5	25.6	35.5	33.5	36.0	36.7	33.3	22.0	15.5	12.5	36.7
Extreme Minimum (°C)	-23.3	-18.9	-14.4	-7.8	-2.2	0.5	2.8	2.8	0.0	-12.5	-23.0	-26.0	-26.0

Kitimat Township - All Years (1954 to 2002)

	Jan	Feb	Mar	Apr	May	Jun	Jul	Aug	Sep	Oct	Nov	Dec	Year
Daily Average (°C)	-3.4	-0.3	2.6	6.2	10.3	13.8	16.2	16.1	12.5	7.0	1.6	-1.6	6.9
Daily Maximum (°C)	-0.8	2.6	6.3	10.9	15.6	18.8	21.1	20.9	16.8	9.9	3.9	0.5	10.7
Daily Minimum (°C)	-5.8	-3.2	-1.2	1.5	4.9	8.8	11.3	11.3	8.1	4.1	-0.7	-3.8	3.0
Extreme Maximum (°C)	12.2	11.1	18.0	25.6	32.8	35.6	36.1	36.0	33.3	22.0	13.3	10.0	36.1
Extreme Minimum (°C)	-25.0	-23.9	-19.4	-10.0	-6.7	-0.6	3.9	2.0	-2.0	-13.0	-24.0	-25.0	-25.0

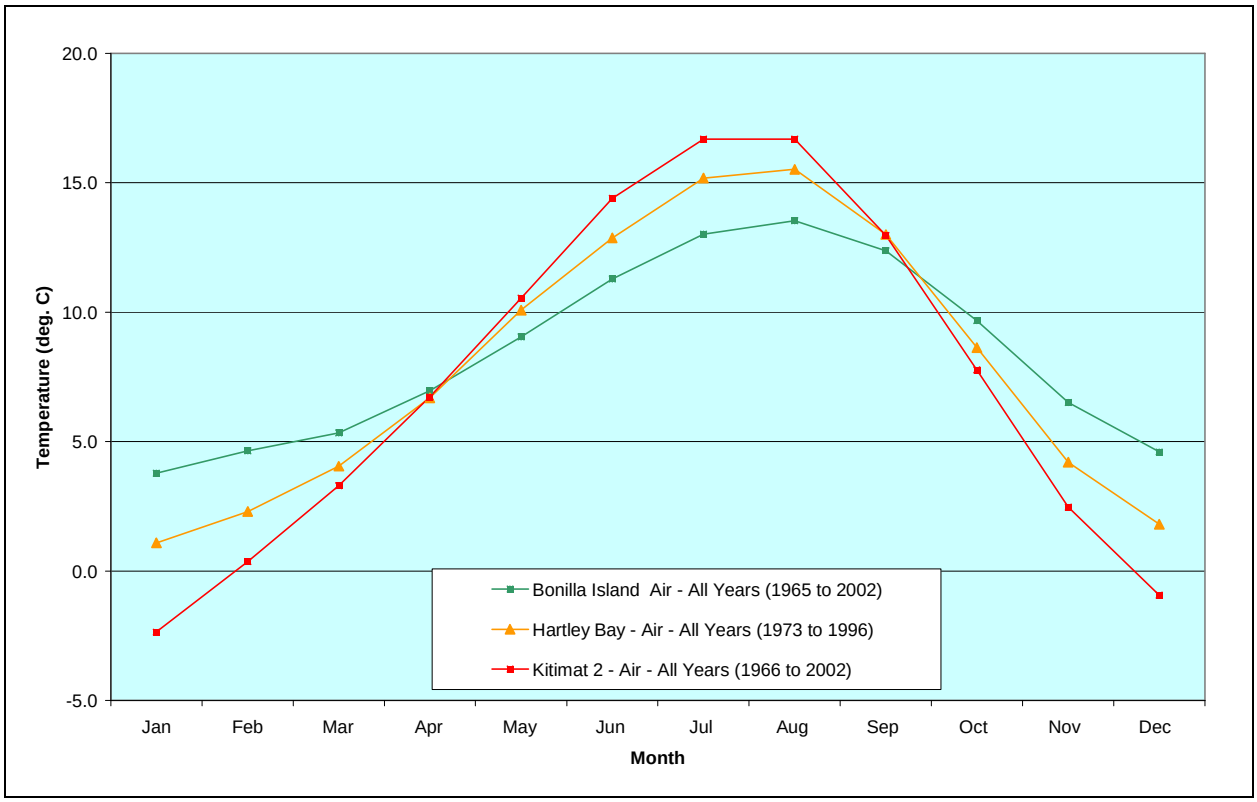

Figure A-11 Monthly Average Air Temperatures at Bonilla Island, Hartley Bay and Kitimat 2 Weather Stations

Large amounts of precipitation occur in the project area because of the mild, moist marine climate. Precipitation occurs primarily as rainfall, with very low snowfall at the seaward end of the CCAA: an average of 52 cm of total annual snowfall at Bonilla Island (see Table A-5). However, at inland locations, where air temperatures are consistently cooler in fall and winter, snowfall amounts increase considerably, with an average of 238 cm of total annual snowfall at Hartley Bay, 338 cm at Kitimat 2 and 460 cm at Kitimat Township. In fact, Kitimat holds the Canadian record for the most snowfall in a five-day period: 246.2 cm from 14 to 18 January 1974 (Heidorn 2004). Nevertheless, even in Kitimat, rainfall precipitation exceeds that of snowfall in all months, on average.

Total precipitation also differs considerably with location, although in a somewhat different pattern from snow-rain ratios. The highest precipitation level of 4,492 mm per year, as measured at Hartley Bay in Douglas Channel, is more than twice the amount at Bonilla Island (2,129 mm) and considerably higher than total precipitation at both Kitimat sites (2,734 and 2,243 mm) and Kildala (2,150 mm). At Hartley Bay (4,492 mm) and at Ethelda Bay (3,275 mm), the higher precipitation values are due to the proximity of these measurement sites to mountainous terrain. Transiting weather systems release large quantities of precipitation, primarily in the form of rain, on approaching these sites. Farther inland at Kitimat and Kildala, the amount of rainfall is somewhat reduced with distance from the open coast of Hecate Strait.

Table A-5 Monthly Precipitation Statistics for Long-Term Weather Stations

Bonilla Island - 1965 to 2002

Monthly Total Precipitation	Jan	Feb	Mar	Apr	May	Jun	Jul	Aug	Sep	Oct	Nov	Dec	Year	Total
Average(mm)	211.8	192.9	180.2	158.6	123.9	98.5	84.1	115.3	171.5	273.0	263.1	255.9	177.4	2,129
Maximum (mm)	380.4	368.0	357.7	318.6	257.5	175.7	192.8	319.5	356.1	458.1	490.5	580.9	232.2	
Minimum (mm)	56.5	19.2	35.9	44.4	30.8	15.9	21.3	10.3	52.4	127.6	107.2	101.8	139.2	
Average Monthly Rainfall (mm)	196.7	181.5	174.7	157.7	123.9	98.5	84.1	115.3	171.5	272.7	258.7	241.4	172.9	2,077
Average Monthly Snowfall (cm)	15.1	11.4	5.4	0.9	0.0	0.0	0.0	0.0	0.0	0.3	4.4	14.5	4.3	52

Ethelda Bay- 1957 to 1991

Monthly Total Precipitation	Jan	Feb	Mar	Apr	May	Jun	Jul	Aug	Sep	Oct	Nov	Dec	Year	Total
Average(mm)	362.2	299.3	284.7	257.6	193.7	138.7	122.9	161.6	255.2	417.9	415.5	365.4	272.9	3,275
Maximum (mm)	578.6	510.4	614.2	532.6	366.4	261.8	289.7	506.8	487.2	599.4	916.6	630.2	442.3	
Minimum (mm)	31.0	34.1	32.8	74.0	67.6	25.3	24.3	4.3	54.2	258.4	159.9	152.8	210.9	
Average Monthly Rainfall (mm)	325.2	276.9	268.4	252.8	193.7	138.7	122.9	161.6	255.2	417.3	405.6	338.1	263.0	3,156
Average Monthly Snowfall (cm)	37.3	22.6	15.9	4.6	0.0	0.0	0.0	0.0	0.0	0.6	9.8	26.0	9.8	117

Hartley Bay - 1973 to 1996

Monthly Total Precipitation	Jan	Feb	Mar	Apr	May	Jun	Jul	Aug	Sep	Oct	Nov	Dec	Year	Total
Average(mm)	449.0	386.6	320.7	316.4	229.9	197.6	175.2	189.6	392.3	679.4	629.5	525.9	374.3	4,492
Maximum (mm)	766.6	721.6	521.2	777.8	532.6	389.5	485.6	446.0	956.4	1020.6	960.9	1241.8	493.4	
Minimum (mm)	61.5	31.1	104.8	108.2	59.0	13.0	18.0	15.3	139.6	441.9	139.8	177.0	227.1	
Average Monthly Rainfall (mm)	378.4	318.5	297.2	311.0	229.7	197.6	175.2	189.6	392.3	678.9	603.0	472.3	353.6	4,244
Average Monthly Snowfall (cm)	70.6	61.7	23.1	5.1	0.1	0.0	0.0	0.0	0.0	0.5	25.2	51.9	19.9	238

Table A-5 Monthly Precipitation Statistics for Long-Term Weather Stations (cont'd)

Kildala - 1966 to 2000

Monthly Total Precipitation	Jan	Feb	Mar	Apr	May	Jun	Jul	Aug	Sep	Oct	Nov	Dec	Year	Total
Average(mm)	262.3	194.1	148.3	132.9	88.4	81.8	81.2	104.3	187.5	316.3	279.5	273.0	179.2	2,150
Maximum (mm)	524.1	297.0	231.1	254.9	202.7	164.3	130.0	196.9	603.0	434.7	479.5	580.3	225.7	
Minimum (mm)	73.9	6.3	51.0	31.8	38.4	18.0	16.1	36.7	65.4	134.1	124.2	92.9	121.7	
Average Monthly Rainfall (mm)	156.4	133.5	123.1	130.4	88.4	81.8	81.2	104.3	187.5	315.1	248.2	200.7	154.3	1,851
Average Monthly Snowfall (cm)	106.0	60.6	25.2	2.5	0.0	0.0	0.0	0.0	0.0	1.5	31.3	72.3	24.9	299

Kitimat 2 - 1966 to 2002

Monthly Total Precipitation	Jan	Feb	Mar	Apr	May	Jun	Jul	Aug	Sep	Oct	Nov	Dec	Year	Total
Average(mm)	337.4	260.6	218.1	172.3	110.6	82.1	70.5	106.9	222.0	405.3	389.5	359.2	227.9	2,734
Maximum (mm)	780.8	616.9	406.2	402.4	206.4	195.8	111.1	224.3	350.9	625.3	673.9	964.8	321.0	
Minimum (mm)	83.3	5.2	60.7	29.6	43.3	16.4	10.8	19.6	53.8	80.3	165.1	85.9	146.9	
Average Monthly Rainfall (mm)	232.3	194.5	189.2	167.9	110.2	82.1	70.5	106.9	222.0	403.7	344.0	274.5	200.4	2,398
Average Monthly Snowfall (cm)	106.2	66.1	28.9	4.3	0.4	0.0	0.0	0.0	0.0	1.6	45.6	85.0	28.1	338

Kitimat Township - 1954 to 2002

Monthly Total Precipitation	Jan	Feb	Mar	Apr	May	Jun	Jul	Aug	Sep	Oct	Nov	Dec	Year	Total
Average(mm)	291.2	218.5	164.7	124.2	82.5	72.8	62.2	98.0	186.6	338.8	303.7	299.9	186.9	2,243
Maximum (mm)	540.9	399.0	416.3	265.5	195.1	310.0	104.2	205.7	572.5	438.5	505.1	614.7	236.0	
Minimum (mm)	101.0	2.5	69.3	49.3	29.2	4.3	13.0	30.4	45.7	77.1	101.2	143.4	123.4	
Average Monthly Rainfall (mm)	145.9	134.0	119.0	115.9	82.1	72.8	62.2	98.0	186.6	330.0	242.5	180.3	147.4	1,769
Average Monthly Snowfall (cm)	144.8	84.6	42.0	8.4	0.4	0.0	0.0	0.0	0.0	4.2	60.0	115.3	38.3	460

Total precipitation exhibits a very marked seasonal cycle (see Table A-5 and Figure A-12). Precipitation is highest in the months of October and November, as frequent and intense Pacific storms approach the area. Gradually through the remainder of the fall and the winter, the average monthly precipitation decreases, reaching the lowest annual levels in June through August. On average, the monthly precipitation in autumn is over twice that experienced in the summer.

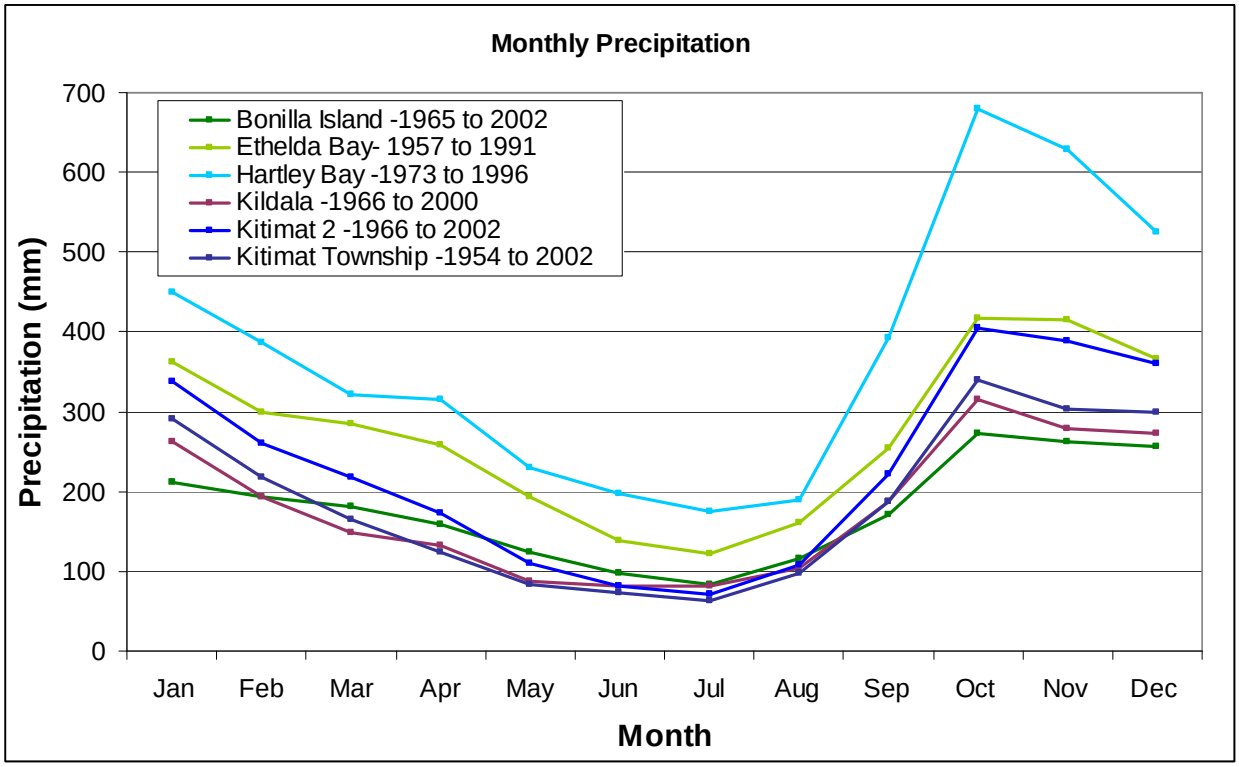

Figure A-12 Monthly Average Total Precipitation at Weather Stations in or near the CCAA

A.3.4 Climate Variability and Climate Change

Scales and Measures of Climate Variability

The climate of the project area, as described above, is based on averages of data collected over long periods (generally 30 years or more). However, significant variability exists within that data on a number of time scales. The shortest scale generally discussed is seasonal variability (see Sections A.3.2 and A.3.3). This variability has the highest range because the seasons differ so greatly (winter weather versus summer weather).

Longer scales include annual variability, which refers to the differences in monthly or seasonal data between different years. These differences are largely a result of variation in the position and strength of the Aleutian Low and North Pacific High pressure systems. These variations can have a significant effect on oceanographic conditions and on biological functions in the coastal ecosystem.

In addition to this normal or local annual variability, climatic changes in other parts of the world, often termed interannual variability, can disrupt local weather patterns on scales of a few months to a few years. El Niño is the most well known of these effects; its pattern of change is called the El Niño Southern Oscillation (ENSO). A change in trade winds off the coasts of Ecuador and Peru causes a reduction in upwelling of cold waters with resulting added heat and moisture brought into these normally arid countries. The added heat in that region also strengthens and alters the path of the jet stream, which can affect weather world-wide. For British Columbia, this generally results in a milder and drier-than-normal winter with the usual winter storms diverted northwards to Alaska and the Yukon (Environment Canada 2006, Internet site). (The complementary phenomenon, which results in colder-than-normal surface water in the tropical Pacific is often called La Niña.) Oceanographers use the ENSO index to monitor and predict changes in ocean conditions in the North Pacific.

Decadal variability refers to changes that take place over tens of years. The Pacific Decadal Oscillation (PDO) is an example of this kind of climate variability that affects Canada's Pacific coast. Information regarding the PDO is actually developed from analysis of sea surface temperature anomalies in the Pacific Ocean north of 20˚N. However, these surface conditions are closely linked to changes in the Aleutian Low and the North Pacific High, so it is still a measure of climate variability. The Aleutian Low Pressure Index is related to the PDO, but is a more direct measure of the sea surface air pressure in the northeast Pacific and, thus, a measure of the intensity of the Aleutian Low (Beamish et al. 1997).

Climate Variability and Trend Analysis

The availability of weather data is limited to between 25 and 45 years at the major meteorological measurement sites (see Table A-1). Trend analyses of average air temperature and precipitation (for the full year and separately for winter and summer) were carried out for measurement sites with at least 30 years of available data.

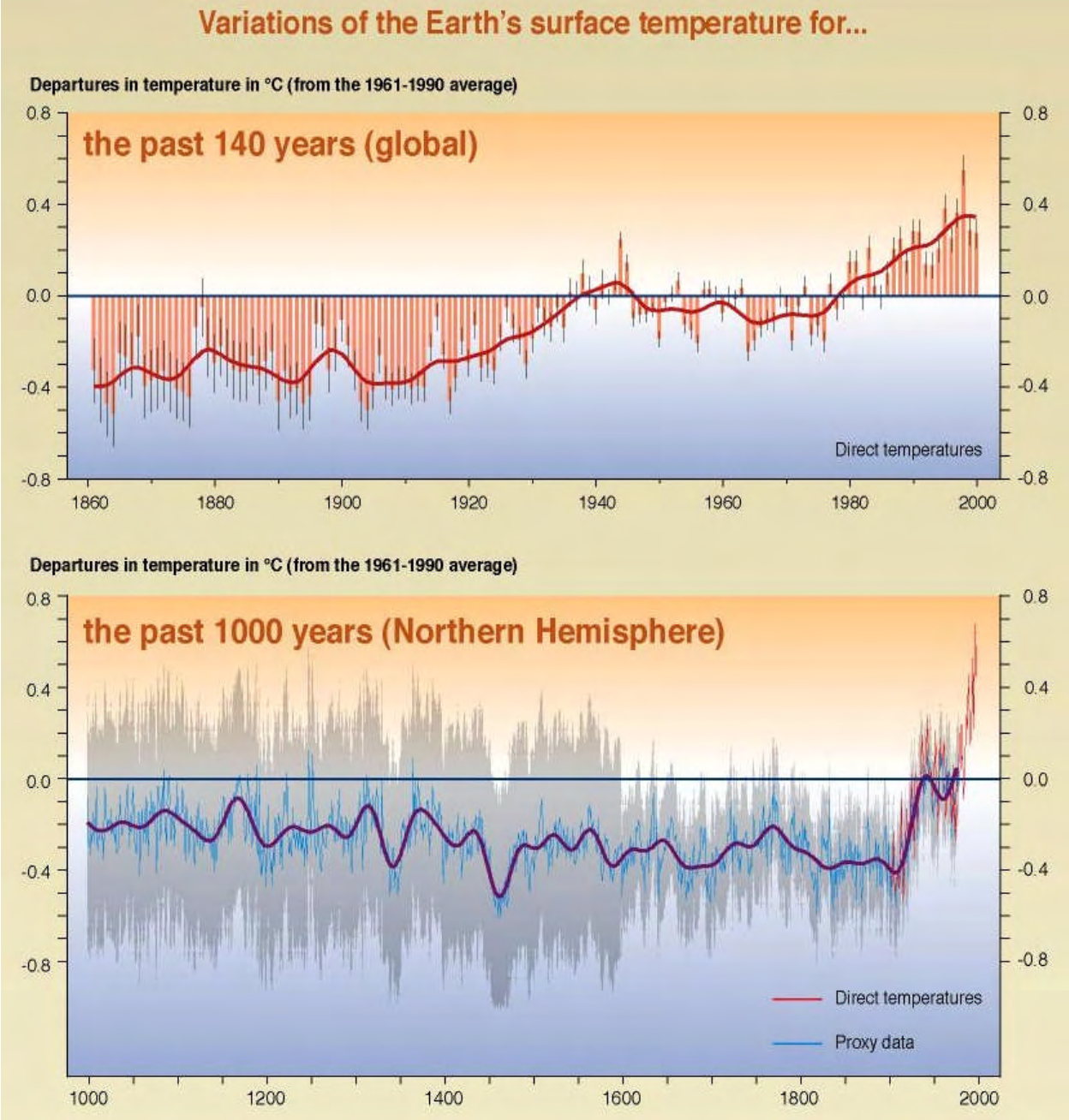

SOURCE: IPCC 2006, Internet site

Figure A-13 Temperature Changes for Global Air from 1861 to 2000 and for the Northern Hemisphere from 1000 to 2000

The results show that most of the interannual variability in temperatures occurs over periods of one to eight years, possibly related to El Niño/La Niña or similar effects. However, a small increase in air temperatures (approximately 1°C) from the 1960s to 2002 was indicated at most locations. This overall change is relatively small compared with the fluctuations over one- to eight-year periods, as can be seen in the case of the Bonilla Island and Kitimat 2 weather observations (see Figure A-14 and Figure A-15). The trend is more consistent in the full-year averages than in either summer or winter seasonal averages. Even in the full-year average values, the correlation statistic (R^2) is only about 0.25, indicating that only 25% of the total variance is actually due to a linear increase in temperature. At the other measurement sites (Ethelda Bay, Kitimat Township and Kildala), the increases in air temperature are smaller and the correlation statistic values even lower, at 0.18, 0.11 and 0.13, respectively.

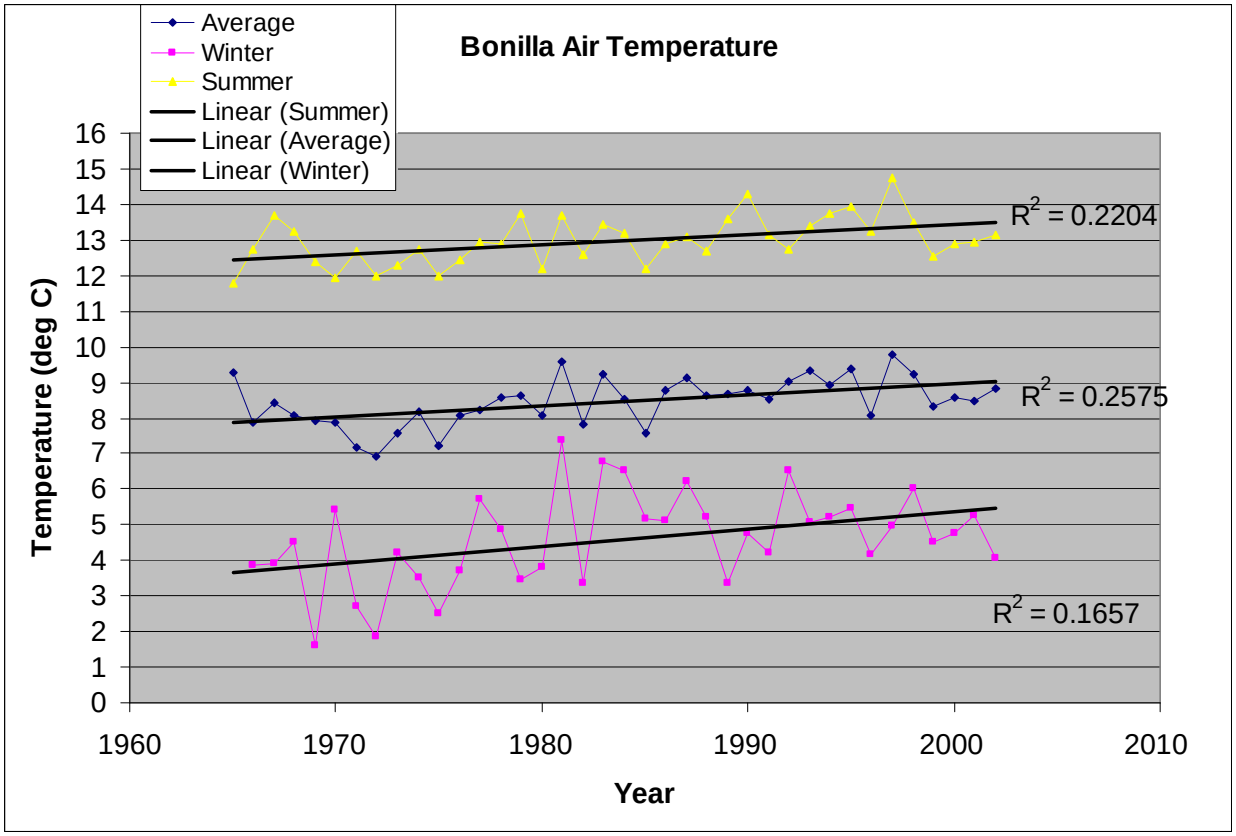

Figure A-14 Long-Term Trends for Annual, Winter and Summer Average Air Temperatures at Bonilla Island

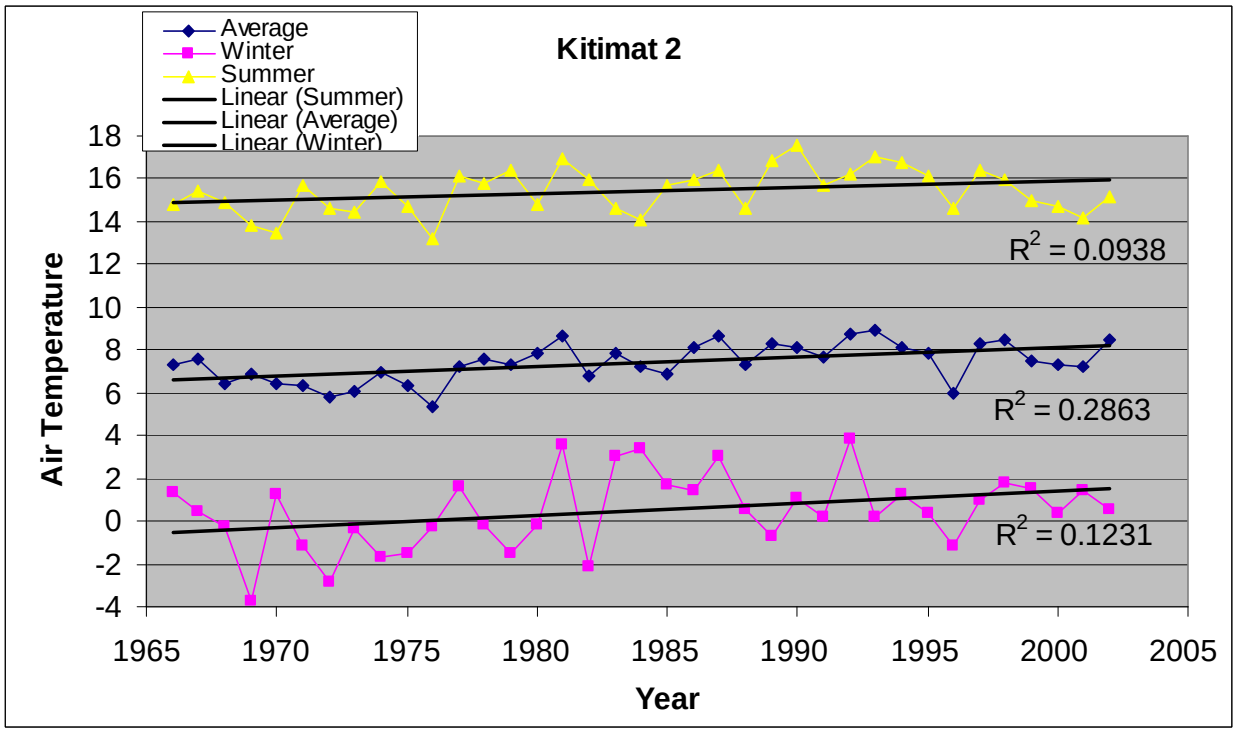

Figure A-15 Long-Term Trends for Annual, Winter and Summer Average Air Temperatures at Kitimat 2 Weather Station

It should be noted that the trend toward a modest increase in air temperatures is not necessarily due, in all or even in part, to global warming as discussed above. Part of this trend may be due to the effect of the Pacific Decadal Oscillation or other natural, long-term variations in climate parameters.

The results of a similar trend analysis carried out on total precipitation at these weather stations indicates only very small changes in precipitation relative to higher levels of variability over periods of one to a few years. The correlation statistic was generally less than 0.05.

A.4 References

A.4.1 Literature Cited

ASL Environmental Sciences Inc. 2010. Weather and Oceanographic Conditions in the CCAA and in Queen Charlotte Sound,Hecate Strait and Dixon Entrance Technical Data Report. Prepared for: Northern Gateway Pipelines Inc. Calgary, AB.

Beamish, R.J., C.E. Neville and A.J. Cass. 1997. Production of Fraser River sockeye salmon (*Oncorhynchus nerka*) in relation to decadal-scale changes in the climate and the ocean. *Canadian Journal of Fisheries and Aquatic Sciences* 54: 543-554.

British Columbia Ministry of Land, Water and Air Protection. 2002. *Indicators of Climate Change for British Columbia 2002*. Victoria, BC.

Chevron Canada Resources Ltd. 1982. *Initial Environmental Evaluation for Renewed Petroleum Exploration in Hecate Strait and Queen Charlotte Sound*. Chevron Canada Resources Ltd. 1. Section 1-3. Calgary, AB.

Environment Canada. 1992. *Marine Weather Hazards Manual: A Guide to Local Forecasts and Conditions*. Gordon Soules Book Publishers. West Vancouver, BC.

Hamilton, K. 1984. *Seasonal Mean North Pacific Sea Level Pressure Charts, 1939-1982*. Manuscript Report. 41. University of British Columbia. Vancouver, BC.

Hall, J., R.F. Addison, J. Dower and I. Jordaan. 2004. *Report of the Expert Panel on Science Issues Related to Oil and Gas Activities, Offshore British Columbia*. Expert Panel Report. RSC.EPR 04-1. The Royal Society of Canada. Ottawa, ON.

Hare, F.K. and J.E. Hay. 1974. The climate of Canada and Alaska. In R.A. Bryson and F.K. Hare (eds.). *Climates of North America*. Amsterdam: Elsevier Scientific. 49-192.

Hayco. 2010. *Wind Observations in Douglas Channel, Squally Channel and Caamaño Sound*. Prepared for Northern Gateway Pipelines Inc. Calgary, AB.

Heidorn, K. 2004. *B.C. Weather Book: From the Sunshine Coast to Storm Mountain*. Fifth House. Calgary, AB.

Hood, D.W and S.T. Zimmerman (eds.). 1986. *The Gulf of Alaska: Physical Environment and Biological Resources*. United States Department of Commerce NOAA, NOS, and United States Department of Interior, MMS, Alaska OCS Region. Anchorage, AK

Houghton, J.T., Y. Ding, D.J. Griggs, M. Noguer, P.J. van der Linden, X. Dai, K. Maskell and C.A. Johnson (eds.). 2001. *Climate Change 2001: The Scientific Basis. Contribution of Working Group 1 to the Third Assessment Report of the Intergovernmental Panel on Climate Change*. Cambridge University Press. Cambridge, UK.

Jacques Whitford Environment Limited. 2001. *British Columbia Offshore Oil and Gas Technology Update*. JWEL Project No. BCV50229. BC Ministry of Energy and Mines. Victoria, BC.

Kendrew, W. and D. Kerr. 1955. *The Climate of British Columbia and the Yukon Territory*. Queen's Printer. Ottawa, ON.

Petro-Canada. 1983. *Offshore Queen Charlotte Islands Initial Environmental Evaluation*. Prepared for: Environment Canada and Ministry of Environment, Lands and Parks Canada, Ottawa, ON.

Ricker, K.E and J.W. McDonald. 1992. *Biophysical Suitability of the North Coast and Queen Charlotte Islands Region of British Columbia for Salmonid Farming in Net Cages: Main Report.* Ministry of Agriculture, Fisheries and Food. Victoria, BC.

Ricker, K.E and J.W. McDonald. 1995. *Biophysical Evaluation of the Central Coast of British Columbia (with Special Reference to Aquaculture): Waldichuk Volume*. Ministry of Agriculture, Fisheries and Food. Victoria, BC.

Scudder, G.G.E and N. Gessler (eds.). 1989. *The Outer Shores: Based on the Proceedings of the Queen Charlotte Islands First International Scientific Symposium, University of British Columbia, August 1984*. Queen Charlotte Islands, BC. Queen Charlotte Islands Museum. University of British Columbia, Vancouver, BC.

Stewart, R.E., D. Bachand, R.R. Dunkley, A.C. Giles, B. Lawson, L. Legal, S.T. Miller, B.P. Murphy, M.N. Parker, B.J. Paruk and M.K. Yau. 1995. Winter storms over Canada. *Atmosphere-Ocean* 33: 223-247.

Thomson, R.E. 1989. The Queen Charlotte Islands: Physical oceanography. In G.G.E. Scudder and N. Gessler (eds.). *The Outer Shores: Based on the Proceedings of the Queen Charlotte Islands First International Scientific Symposium, University of British Columbia, August 1984*. The University of British Columbia. Vancouver, BC. 27-63.

A.4.2 Internet Sites

Canadian Climate Impacts and Adaptation Research Network (CCIARN). 2006. Accessed: January 2006. Available at: http://www.c-ciarn.ca/index-e.asp.

Environment Canada. 2006. *Canadian Climate Normals*. Accessed: January 2006. Available at: http://www.msc-smc.ec.gc.ca/climate/climate_normals/index_e.cfm.

Intergovernmental Panel on Climate Change (IPCC). 2006. Accessed: January 2006. Available at: http://www.ipcc.ch.

Appendix B Ocean Currents

B.1 Introduction

B.1.1 Objectives

The purpose of this appendix is to describe baseline conditions with respect to the ocean currents in the confined channel assessment area (CCAA).

Existing literature was reviewed and field surveys were carried out to gather data for surface currents and subsurface currents in relation to the following:

- water depth
- wind forcing
- tidal forcing
- estuarine circulation (caused by freshwater runoff)

B.2 Methods

B.2.1 Field Surveys

In September 2005, current meters were deployed at four locations in the CCAA (see Figure B-1).These instruments were operated until January 2006 (see Appendix G). One of the current meters was redeployed in in January 2006 for ongoing data collection in Kitimat Arm. The meter, which was near the marine terminal, was located closer to shore than in 2005 (see Appendices H to J). It was operated through to July 2007.

B.2.2 Review of Existing Data Sources

Historical ocean current data sets were identified from a search of published and on-line data inventories (Birch et al. 1985; Fisheries and Oceans Canada 2006, Internet site).

Much of the knowledge of the physical oceanography of the CCAA is contained in the six volume series produced by the IOS in Sidney, British Columbia (as addressed in Webster 1980 and Buckingham 1980) and in proceedings of a workshop on the Kitimat marine environment (Macdonald 1983). These reports present the results of an intensive one-year physical oceanographic study conducted from July 1977 to June 1978, focused on the circulation in the channels that form the seaward approaches to the port of Kitimat. The study included data analyses and description of a tidal circulation model. Currents in the passages are driven by estuarine and tidal forcing and, in the near-surface, by local winds. IOS conducted a follow-up study on chemical and physical oceanography and suspended sediments in Kitimat Arm during 1978 and 1979 (Macdonald et al. 1983).

Summary results for data collected in physical, chemical and geological oceanographic studies from 1977 to 1980 are presented in the Macdonald (1983) workshop proceedings.

For the locations of the project meter data sets as well as those identified from the database and literature search, see Figure B-2. Ten stations with more than one month of data per station in the IOS archive were selected for data analysis (see Figure B-3). For the location coordinates, start and stop times for those records, see Table B-1.

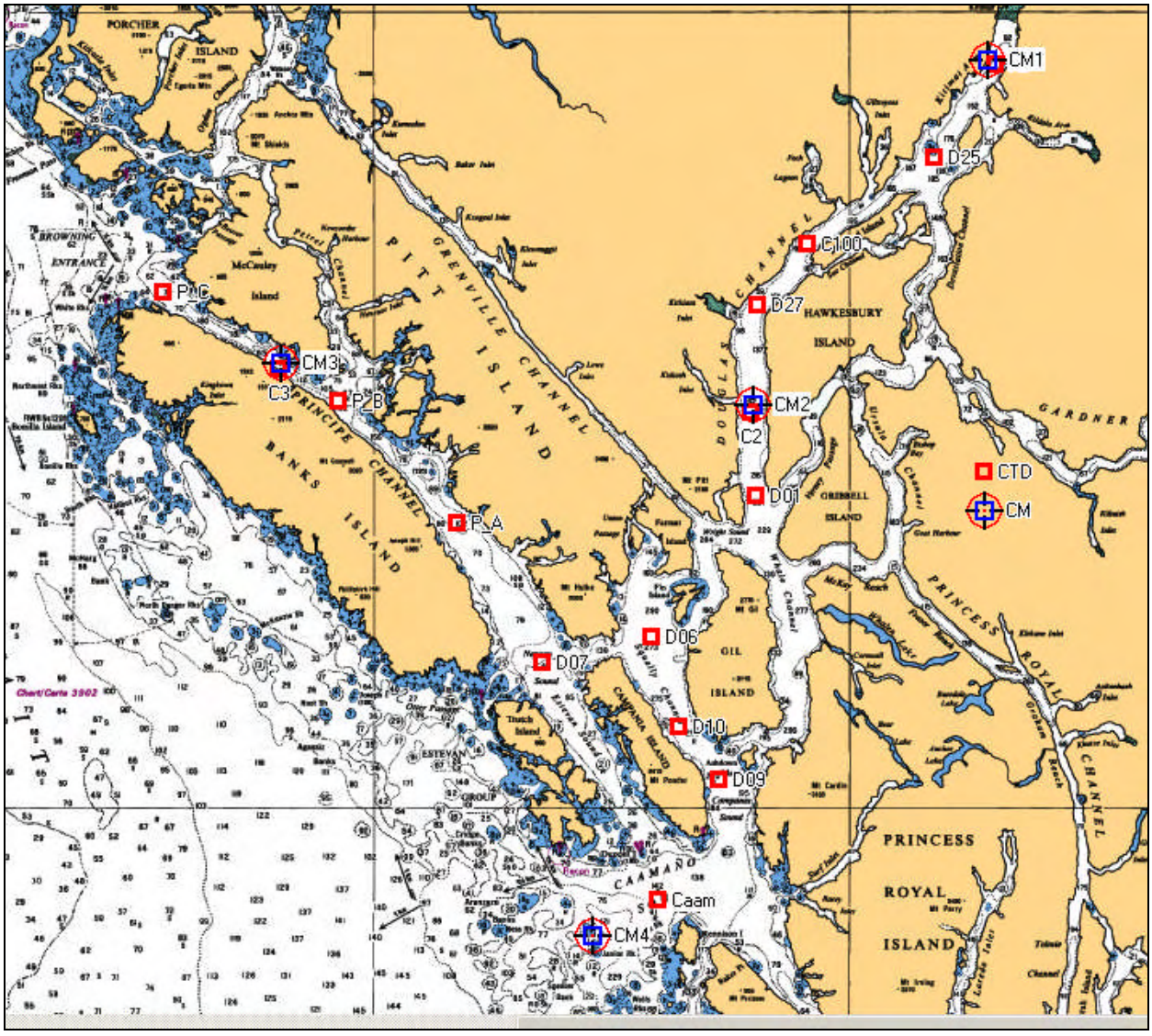

NOTES: Blue squares: Current meter sites September 2005 to January 2006.
Red squares: CTD sites September 2005 and January 2006.

Figure B-1 Project Current Meters and Measurement Sites for Conductivity and Temperature at Various Depths, September 2005 to January 2006

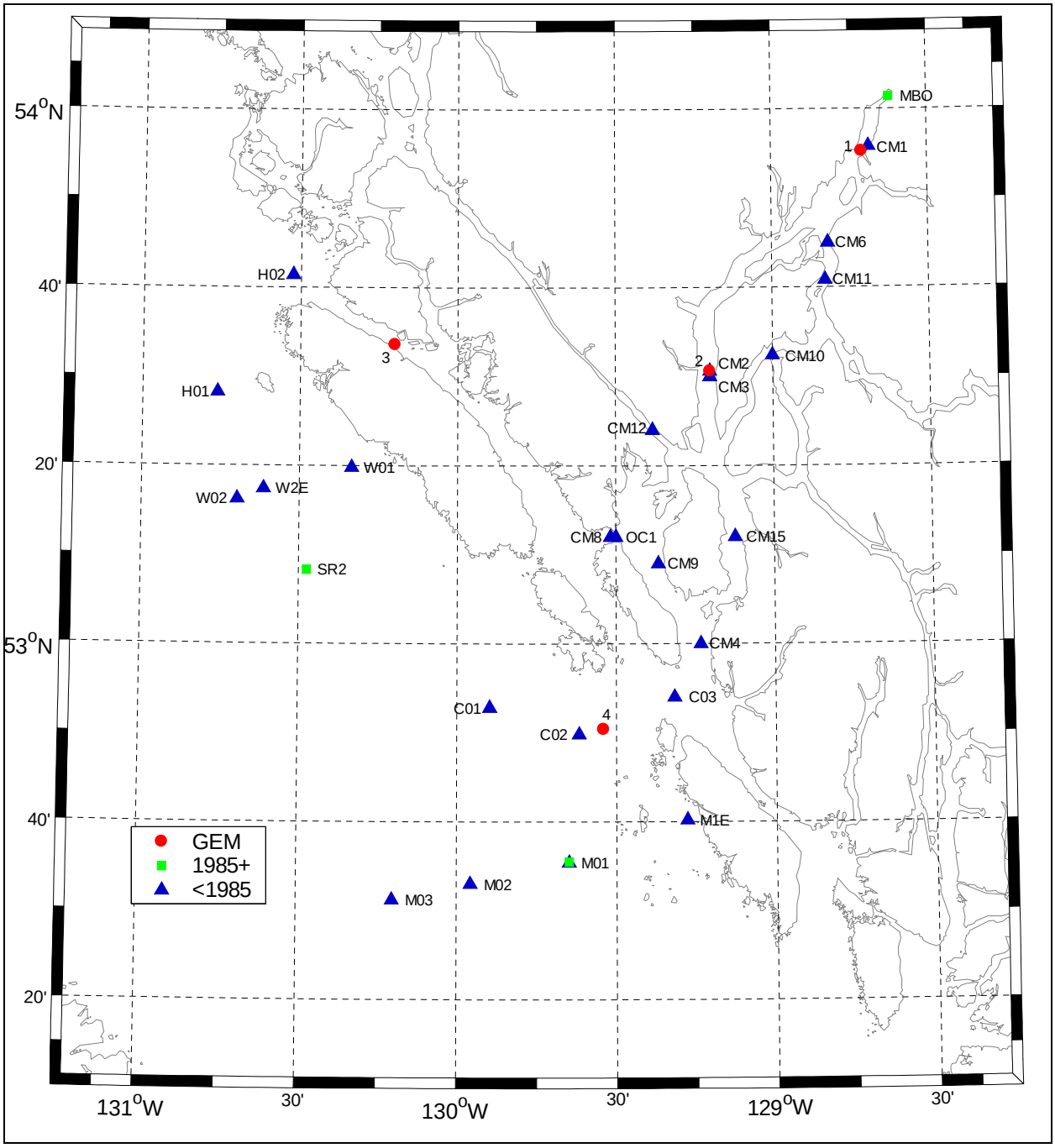

NOTE: Project measurement locations of 2005 to 2006 are indicated by red circles and labelled as GEM.

Figure B-2 Historical and Project Current Meters in the CCAA and Adjoining Portions of Hecate Strait

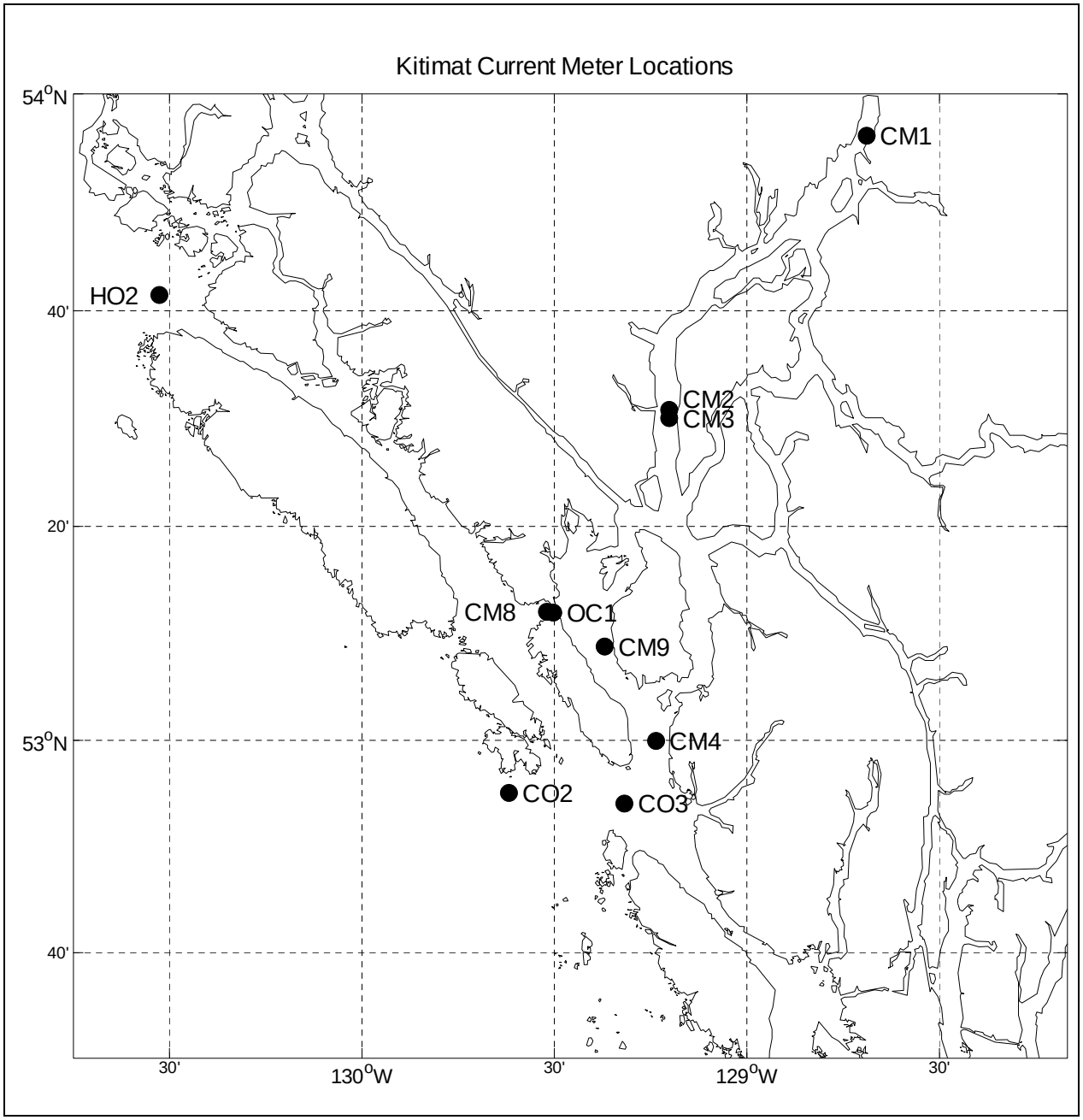

Figure B-3 Historical Current Meters for Data Set Analysis

Table B-1 Historical Current Meter Data Sets, Measurement Depths, Start and End Times

Site	Subarea	Latitude (deg mm. mm)	Longitude (deg mm. mm)	Depth (m)	Start	End
CM1	Kitimat Arm	53 56.07 N	128 41.25 W	40	July 1977	Sept 1997
				104	July 1977	Oct 1977
				168	July 1977	Oct 1977
CM2	Douglas Channel	53 30.78 N	129 12.02 W	40	July 1977	May 1978
				172	July 1977	May 1978
				304	July 1977	May 1978
CM3		53 30.01 N	129 12.01 W	5	July 1977	Dec 1977
				17	July 1977	Feb 1978
CM4	Campania Sound	52 59.88 N	129 14.09 W	40	July 1977	Sept 1977
				153	July 1977	Sept 1977
				266	July 1977	Sept 1977
CM8	Otter Channel	53 12.00 N	129 31.08 W	40	Dec 1977	Feb 1978
				136	Dec 1977	Feb 1978
				228	Dec 1977	Feb 1978
OC1	Otter Channel	53 11.90 N	129 30.10 W	140	May 1977	June 1977
				199	July 1977	Aug 1977
CM9	Squally Channel	53 8.75 N	129 22.05 W	444	Dec 1977	Feb 1978
CO3	Caamaño Sound	52 54.00 N	129 19.00 W	140	June 1977	July 1977
				197	Aug 1997	Oct 1977
CO2	Approaches	52 55.00 N	129 37.00 W	13	Aug 1977	Sept 1977
HO2	Browning Entrance	53 41.30 N	130 31.50 W	20	May 1977	July 1977

NOTE:
deg mm. mm = minutes of longitude or latitude to two decimal places

The results of the analysis of these current meter data sets (21 in total when the different depths are considered) are presented in following sections.

Older historical measurements of surface currents were also reviewed. The only extensive surface current data were measured in the summers of 1953 and 1954 by the Canadian Hydrographic Services (CHS) of Fisheries and Oceans Canada (DFO) (Huggett and Wigen 1983) using a combination of drift pole tracking and current metering. The drift poles, which were 3.6 m long and of a spar buoy design to minimize wind drag, were tracked by surveyors from a small launch using a series of timed sextant fixes to at least three shore-based markers on the nearby coastline. Ship-based mechanical current metering measurements were taken at depths of 1.8, 3.6, 5.5 and 9.1 m. A total of 388 hours of current metering and 1,680 hours of drift pole tracking were taken (see Figure B-4 for the locations). The data were computer scanned and then converted to geographical coordinates. Surface currents were computed from the sequence of drift pole positions and times and various statistical results from these data are presented in this appendix.

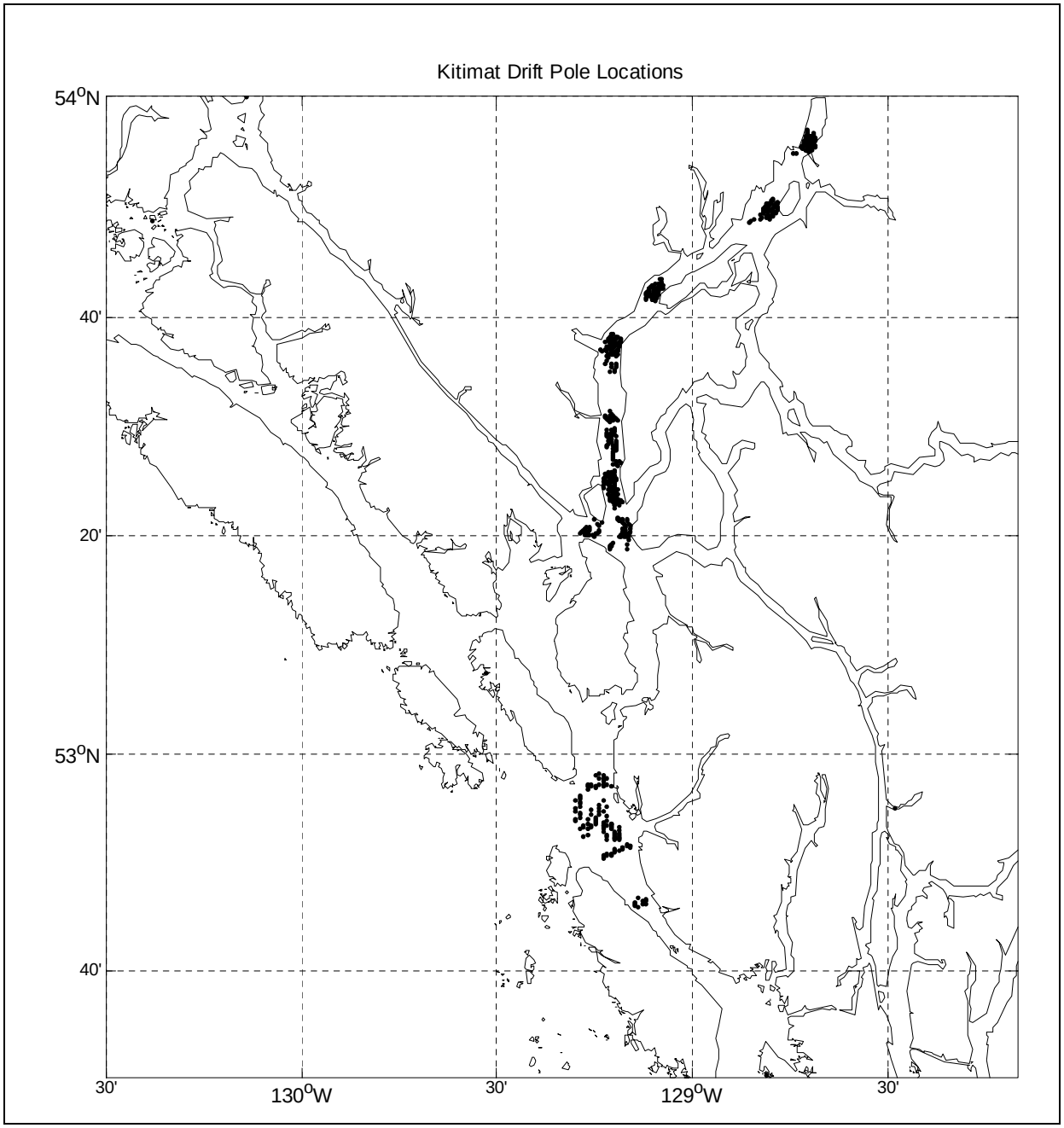

SOURCE: Huggett and Wigen 1983

Figure B-4 Drift Pole Measurement Locations and Tracks in Kitimat Arm, Douglas Channel, Wright Sound and Campania Sound, Summer 1953 and 1954

B.3 Synopsis of Currents and Circulation in the CCAA and PDA

B.3.1 Synopsis of North Pacific Coast Regional Currents and Circulation

The currents of the North Pacific Coast area are dominantly wind driven and are strongly controlled by coastal morphology and continental shelf bathymetry. The shelf waters are also affected by runoff-driven estuarine circulation in the summer, which takes fresh surface waters offshore while counter-currents of deeper ocean water move shoreward over the shelf floor, especially along the deep troughs in Queen Charlotte Sound and Hecate Strait. Winter currents are predominantly northward and tend to flush waters quickly through the area; however, some eddies are thought to retain surface waters. Currents are weaker and more variable in the summer. The coastal inlets are mainly fjords that are often restricted from interactions with open waters by tall underwater sills and long, narrow entrances. Water properties within these inlets are therefore quite distinct from the more open shelf waters. However, estuarine circulation allows regular seasonal renewal of bottom waters in most cases.

All of these conditions are further complicated by variability at a variety of scales. Annual variability in the form of ENSO (El Niño Southern Oscillation) events, known as El Niño conditions (see Appendix A) can significantly change the normal oceanographic conditions of a given season. Changes on a larger scale include decadal oscillations and regime shifts (see Appendix A) that are thought to significantly affect biological productivity in the region. Global warming is also seen to be affecting ocean conditions, most obviously increasing sea surface temperatures over at least the last 50 years (WMO-IPCC 2001).

Tidal Currents

The large tides of the British Columbia coast generate strong tidal currents (see Figure B-5). These currents dominate the surface flows and result in strong tidal mixing, particularly over the banks in Queen Charlotte Sound and shallow portions of Hecate Strait, around the southern and northeastern tips of the Queen Charlotte Islands[1] (Cape St. James and Rose Spit) and the western end of Dixon Entrance (north of the Queen Charlotte Islands).

Wind-Driven Currents

Winds can drive surface currents at speeds up to a few percent of the wind speed. Because of the large-scale atmospheric pressure systems offshore and their resulting regional wind forcing, a strong seasonality occurs in wind-driven current patterns. The winter southeasterly winds result in a general northerly flow of water through the Queen Charlotte Sound and southern Hecate Strait areas (Crawford 2001; Cretney et al. 2002, Internet site). The net transport has been estimated at 300,000 m^3/s (Crawford et al. 1988). Conversely, during the weaker, generally northerly winds of summer, the currents are more variable and little net transport through Hecate Strait occurs (Crawford et al. 1988).

[1] In December 2009, the Queen Charlotte Islands were renamed Haida Gwaii. The previous name is retained for consistency with reviewed literature.

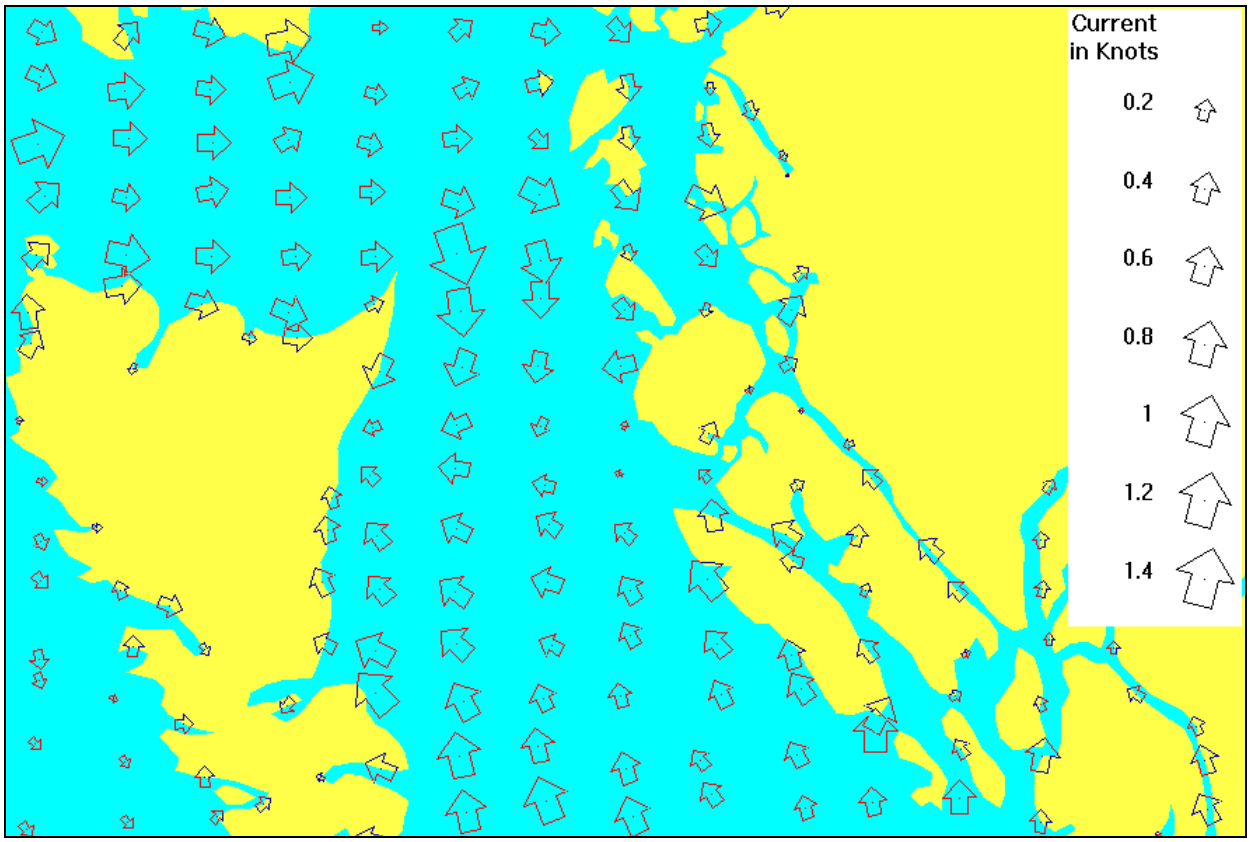

SOURCE: Crawford 2001

Figure B-5 Modelling of Flood Tide Currents in Hecate Strait and Dixon Entrance

Inertial currents are generated primarily by the passage of storms. These currents frequently dominate the surface circulation within Queen Charlotte Sound and Hecate Strait and can be coherent across the width of the sound (Thomson 1981). The associated current speeds are substantial at up to 0.5 m/s near the entrance to Queen Charlotte Sound, reducing to about 0.3 m/s in the eastern portion. They are concentrated in the near-surface layer, but remnants extend down as far as 250 m. The current vectors rotate in a clockwise direction with one rotation approximately every 15.5 hours, which is the inertial period at 51°N latitude. Inertial currents can disrupt the normal tidal flow, making tidal predictions less precise.

Successive storms, with peak winds separated by approximately four inertial periods, were observed to keep the inertial currents in motion for nearly 12 days in June 1977 (Thomson 1981). As the most common gap between successive winter storms is about 2.5 days (i.e., also about four inertial periods), this suggests that storms can result in extended periods of inertial current activity during winter (Thomson 1981).

Internal Waves

The water column often exhibits cyclical oscillations in current and other water properties because of internal waves. Internal waves are like waves at the surface, but instead occur when a stratified fluid interface is perturbed in some way. They are well described in classic texts such as Gill (1981) and Pond and Pickard (1983). These internal waves can have amplitudes of tens of meters while the surface amplitude expression is negligible. One of the most notable and well-studied examples of internal wave generation is that produced by stratified tidal flow over topography. Fluid particles are displaced vertically as they flow over the topography and, because of buoyant restoring forces, internal waves are generated. Numerous studies have been carried out regarding topographically generated internal waves (Baines 1995).

Of relevance to the CCAA are internal waves generated by the flow of a stratified fluid over a topographic feature, such as internal hydraulic jumps and lee waves, as well as internal tides.

Internal Lee Waves and Hydraulic Jumps

A particularly well-known source of internal wave generation is the flow of a stratified fluid over the sill of a fjord. A train of internal lee waves can form on the downstream side of the topography when the flow is sub-critical. However, as internally critical conditions are approached, wave energy accumulates at the topography and a large amplitude lee wave can develop. This wave may break to form an internal jump, which marks the transition from supercritical flow just downstream of the obstacle to subcritical flow (Baines 1984; Kranenburg and Pietrzak 1989). Time-dependent effects can lead to the generation of upstream propagating solitary waves (Maxworthy 1979). Hence, the flow over the topography and the lee wave can influence the flow upstream.

Knight Inlet is perhaps one of the most well-known sites for the generation of such internal waves. Starting with the pioneering work of Freeland and Farmer (1980), Farmer and Smith (1980a, 1980b), Farmer and Freeland (1983) the presence of internal hydraulic jumps, internal lee waves and upstream traveling solitons and bores are now known to have a notable effect on the oceanography of fjord systems. Knight Inlet has become a natural laboratory for the study of internal waves (Farmer and Armi 2001; Cummins et al. 2003, 2006).

Internal Tides

Internal tides and waves may also be generated from the interaction of the tide with bathymetric features such as the shelf break or a prominent sill. In the presence of a sloping bed, cross-shore (barotropic) tidal flow can force the vertical displacement of a stratified fluid and generate internal (baroclinic) tides. These baroclinic tides are actually long-period internal gravity waves with approximately the same period as the tide (Thomson 1981). In contrast to the barotropic tide, internal tides have a small surface amplitude signature; however, they have a large effect on the position of the isopycnals and the vertical structure of the velocity and can lead to enhanced surface currents. This is highlighted in the simple example of barotropic flow versus baroclinic flow (Gill 1981; Figure 6-3). Internal tides have a large-scale effect on a coastal system and can result in much stronger surface currents than those associated with the barotropic tide alone. They also introduce much shorter correlation scales and can cause surface current variations over shorter horizontal distances than one would expect from the barotropic tide alone. Although the

barotropic tidal forcing is constant throughout the year, the internal tides are not. They will vary with the seasonal modulation of the strength of stratification. The strength of the stratification varies, for example, because of seasonal changes in river discharge, surface warming in summer and enhanced mixing in winter.

Internal tides have been studied in northern British Columbia by Cummins and Oey (1997). Internal tides were most evident in Queen Charlotte Sound near the shelf break, but reduced in magnitude toward the shallow waters of northern Hecate Strait (Crawford et al. 1998). Internal waves at Hakai Pass may be related to a cross-channel flow (Province of British Columbia 1998). These waves can also cause horizontal currents of one or more knots, especially in Dixon Entrance (Crawford 2005, pers. comm.). Knight Inlet is also home to many studies on internal tide generation (Farmer and Smith 1980a, 1980b; Freeland 1984; Webb and Pond 1986; Stacey and Pond 1992; Marsden and Greenwood 1994; Stacey, et al. 1995; Yeremy and Stacey 1998; Farmer and Armi 1999a, 1999b; Klymak and Gregg 2003, 2004).

Between July 1977 and June 1978, an extensive study was carried out in the CCAA (see Section B.2.2). Using current meter records obtained at five depths at the CM2 and CM3 locations (see Figure B-3), Webster (1983) investigated the baroclinicity of the semi-diurnal tidal currents in Douglas Channel. He suggested that internal tides were generated by the sill in Douglas Channel, but recognized that his internal Kelvin wave analysis could be further improved. Within Kitimat Arm, the stratification shows a strong seasonal dependence; the resulting effects on the internal tide within the CCAA are explored through an analysis of the year-long CM2 data records (see Section B.3.4).

Runoff and Estuarine Flow

The west coast of North America receives large volumes of freshwater runoff from several major rivers including the Columbia and the Fraser Rivers. These buoyant waters (less dense than seawater) move northward along the Pacific coast from the United States, apparently reaching Queen Charlotte Sound and Hecate Strait (Thomson 1989). These waters are thought to continue into the Gulf of Alaska (and beyond) through the Alaska Coastal Current (Royer 1981). This buoyancy-driven current system serves as a migratory corridor and habitat for salmon and other marine organisms and may advect climate signals (particularly fresh water) over vast distances (Weingartner et al. 2005). Although this flow is persistent and widespread, the associated currents are weak compared with the tidal and wind-driven current components.

In the coastal inlets, or fjords, of northern British Columbia, the estuarine flow is very important in terms of circulation patterns and exchanges of water between the coastal inlets and adjoining water bodies. Within the inlets, the freshwater runoff creates an estuarine circulation with a seaward outflow at surface and a compensating landward flow at depth. The estuarine circulation helps flush the deeper waters, although sills at the entrance often limit this effect. Poor flushing can result in reduced levels of dissolved oxygen, low biological productivity and low species diversity. However, such fjords can also be home to important and often unique species of benthic and planktonic communities (B.C. Ministry of Sustainable Resource Management 2002). See Figure B-6 for some of the processes that occur in British Columbia's coastal inlets and fjords.

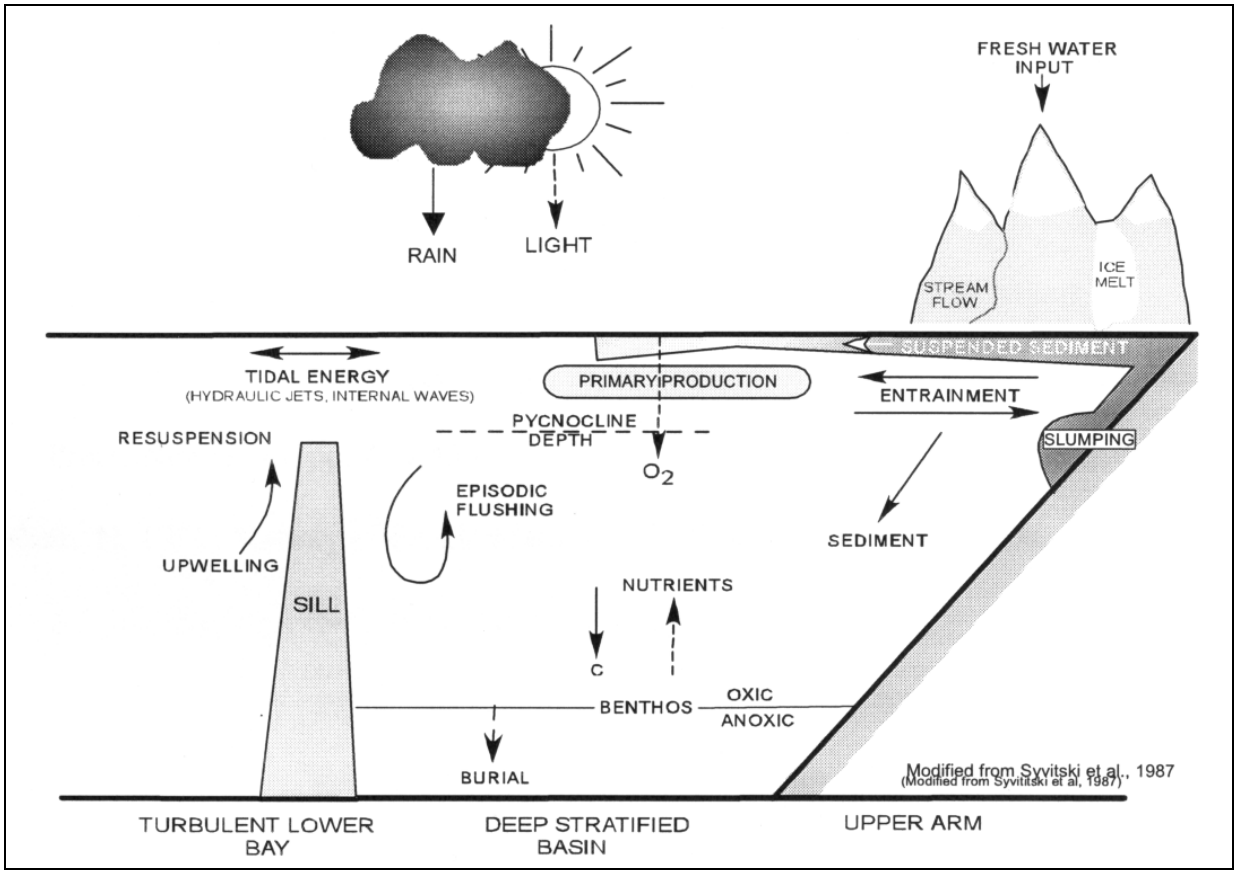

SOURCE: Hooge and Hooge 2002 based on Syvitski et al. 1987.

Figure B-6 Processes Typical of Fjords with a Restrictive Sill at the Entrance

Estuarine flow is generally not uniform. It is strongest during periods of high runoff, but can also be modulated by meteorological forcing and oceanographic conditions offshore.

Within the CCAA, the distribution of temperatures and salinities within the water column is strongly related to freshwater discharges from the myriad of major rivers, smaller rivers and creeks, and from direct precipitation. For the analysis of the resulting water properties and the estimated freshwater discharges, as derived from analysis of historical data, see Appendix C.

River Plumes

River plumes are formed by river outflows discharging into coastal seas or fjords. They occur wherever a buoyant river inflow encounters more dense seawater. River plumes typically form narrow coastal currents; under the influence of the Earth's rotation, in the Northern hemisphere fresher river waters tend to turn to the right on leaving the river mouth. Both the Vancouver Island Coastal Current (Hickey et al. 1991; Foreman and Thomson 1996) and the Columbia River Plume (Garcia Berdeal et al. 2002; Hickey et al. 2005) follow this pattern. Typically, a bulge of fresh water forms in front of the river outlet. Consequently, a sharp density front separating the more buoyant river water from the saltier seawater exists. This also makes them identifiable from satellite images.

Winds have long been recognized as an important factor influencing the dynamics of river plumes (Fong and Geyer 2001). Upwelling favourable winds tend to advect a surface-trapped plume offshore, causing the plume to widen and to thin in the vertical, whereas, downwelling favourable winds tend to advect a plume onshore causing the plume to narrow and to thicken in the vertical. Winds can also reverse the dominant outflow behaviour of a plume (Garcia Berdeal et al. 2002). Effects of tidal straining (Visser et al. 1994; Simpson and Souza 1995) on the vertical structure of the Rhine Plume have been examined by de Boer et al. (2005). Their study showed how tidal pulsing advected the plume onshore and offshore during the tidal cycle.

A number of studies have been conducted on semi-enclosed bodies of water (Kourafalou 1999, 2001). However, there are fewer studies on river plumes in inlets, such as occur in the CCAA. Buckley (1977) studied the circulation of upper Howe Sound, including wind effects in modifying the near-surface estuarine circulation. Aerial photos of Bish Creek, taken in 1947 and 1963 (see Figures F-4 and F-5 in Appendix F) suggest river plumes are present within the CCAA. The characteristic narrow coastal current is visible in both photographs. The plume appears to be associated with the transport of suspended particulate matter.

Numerous rivers discharge into the CCAA. It is likely that they form river plumes; however, as the width of the river inlets is of the order of the Internal Rossby Radius of Deformation, it is likely that inertial effects are also important. Apart from the few photographs, little other evidence suggests their existence in the CCAA. Nonetheless, based on their widespread occurrence as described above, it is likely that they do also form in the CCAA. The numerical model results of the CCAA indicate the presence of tidally pulsed river plumes.

Mean or Residual Currents

Mean or residual currents are net currents averaged over a sufficiently long period so that tidal and other short-term variability are removed.

Time-series records of current data collected by DFO between 1977 and 1995 have been processed to produce vector plots of average currents near-surface and near-bottom for winter (January to March) and summer (July to September) (Crawford 2001; Cretney et al. 2002, Internet site).

The average summer current vectors (see right frame of Figure B-7) show variable currents within Queen Charlotte Sound, because of the weaker, more variable winds during summer. Little net transport occurs through Hecate Strait. However, strong outflow currents near Cape St. James and Cape Scott are likely driven by the summer winds from the northwest. The general southerly wind-driven surface flow is apparently constricted and accelerated by the capes.

Some features, such as the clockwise flow around North Bank and the cross-sound flow of the Aristazabal Island Plume (Thomson et al. 1989; Crawford et al. 1995), are not reflected in the mean currents because there are no current meters in these regions. Limited indications from drifter tracks and satellite photos provide evidence of a counter-clockwise gyre in eastern Dixon Entrance known as the Rose Spit Eddy.

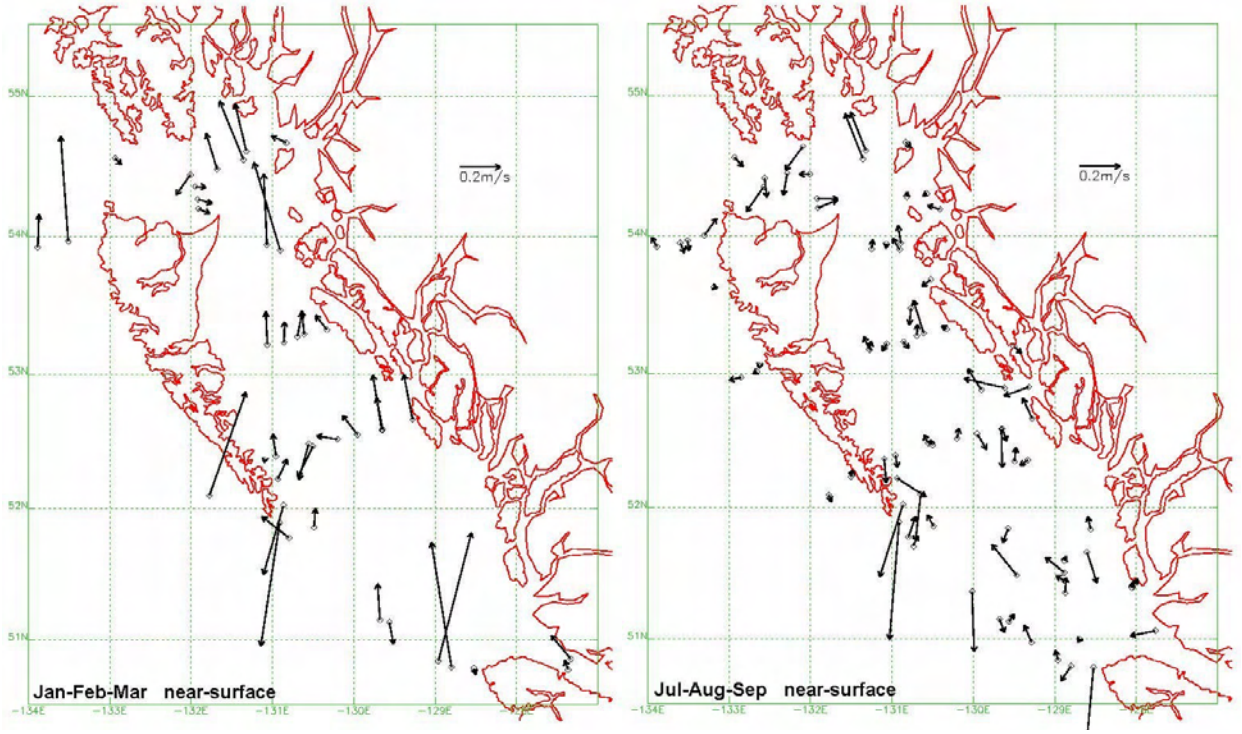

NOTE: Based on 1977-1995 data collected by IOS
SOURCE: Cretney et al. 2002, Internet site

Figure B-7 Average Near-Surface Currents in Winter and Summer

During winter, the winds shift to southerly and intensify. As a result, a general northward drift occurs throughout most of the area, with mean current speeds of 0.2 to 0.6 m/s (see left frame of Figure B-7). However, the high-speed southward outflow persists near Cape St. James, contributing to the formation of the Haida Eddies (Crawford et al. 2002). This outflow is thought to result from the inability of the narrow and shallow northern end of Hecate Strait to accommodate the volume of water flowing into Hecate Strait from the south.

B.3.2 Analysis of Subsurface Current Meter Data Sets

Topography and Bathymetry of the CCAA

The CCAA (see Figure 2-1) consists of the Kitimat fjord system (Macdonald et al. 1983), Caamaño Sound and Principe Channel. The Kitimat system has four entrances: Grenville Channel to the west and Princess Royal Channel to the east, as well as two entrances on the south, Campania Sound and Otter Channel. The CCAA follows the wider western passage through the Kitimat fjord system from Squally Channel through Wright Sound, Douglas Channel and Kitimat Arm. Water exchanged between Kitimat Arm and Campania Sound can also move through the eastern passage of the fjord system through Devastation Channel, Verney Passage (or Ursula Channel and McKay Reach), Wright Sound and Whale Channel. Many inlets and fjords are adjacent to the Kitimat fjord system, including Gardner Canal—by far the largest—and Kildala Arm.

The entrance to the main marine corridor for vessels transiting through Caamaño Sound from the south is through Campania Sound. For vessels transiting through Principe Channel from the west, the entrance to the main marine corridor is through Otter Channel (see Figure B-8). For the water depths along the CCAA, also see Figure B-8.

Statistical Summaries

This section presents the current statistics by depth for the major passes within the CCAA. The measurements have been classified as near-surface at depths of 5 to 20 m, halocline at depths between 20 and 75 m, mid-depth between 75 and 200 m and deep when exceeding 200 m. Except for CM2 data, which spans nearly a year, most of the results were derived from measurements taken over three to four months. The overall speeds and vector average magnitudes are described. Summary statistical results are presented below.

As shown, maximum speeds of 1 m/s occur at the near-surface (see Table B-2), although depending on the site, the near-surface speeds can range between 0.5 and 1.0 m/s. Within Kitimat Arm (CM1), the currents are reduced. Mean speeds in the CCAA are between 20 and 30 cm/s at depths of less than 20 m. Over all, the speeds are reduced with depth, though CM4, located in Campania Sound, must be positioned within a constriction at 266 m depth to register mean speeds of 22 cm/s.

The vector average (net flow considered over the measurement period) can be as high as 20 cm/s at the near-surface in the western approaches to Caamaño Sound (CO2) and Otter Channel (CM8), although speeds within the CCAA are typically under 10 cm/s. The overall trend is for seaward movement of fresher water at the surface and inland movement of denser seawater at depth (estuarine circulation). Measurements in Douglas Channel (CM2 and CM3) show this reversal in net flow direction with depth particularly well. At Douglas Channel sites, the vector average flow direction is south toward the ocean (180°) at the near-surface and halocline depths, but away from the ocean (15 to 20° north-northeast direction) at mid-depth and deep water levels.

Additional current meter measurements were collected for the Project from September 2005 to January 2006 (see Appendix G). Initial Acoustic Doppler Current Profiler (ADCP) measurements in 175 m water depth in the PDA (near the historical CM1 location in Kitimat Arm) are consistent with Kitimat Arm surface drift pole study results that show much stronger currents than were measured at 40 m depth by the CM1 current meter. During that period, 75% of the current speed measurements at 40 m depth exceeded 7 cm/s, and the maximum speed recorded was 24 cm/s (whereas the maximum speed measured in the July to September 1977 period was 8.6 cm/s). One contributing factor for this difference could be the stronger winds present in the fall compared to those in the summer. ADCP provided measurements to within 9 m of the surface. At 9-m depth, the maximum surface current speed measured was 51 cm/s, which is reasonably consistent with the maximum surface current speed of 78 cm/s, observed in 1953 and 1954 drift pole studies, given the strong vertical shear in the current expected in the highly stratified upper layer of Kitimat Arm.

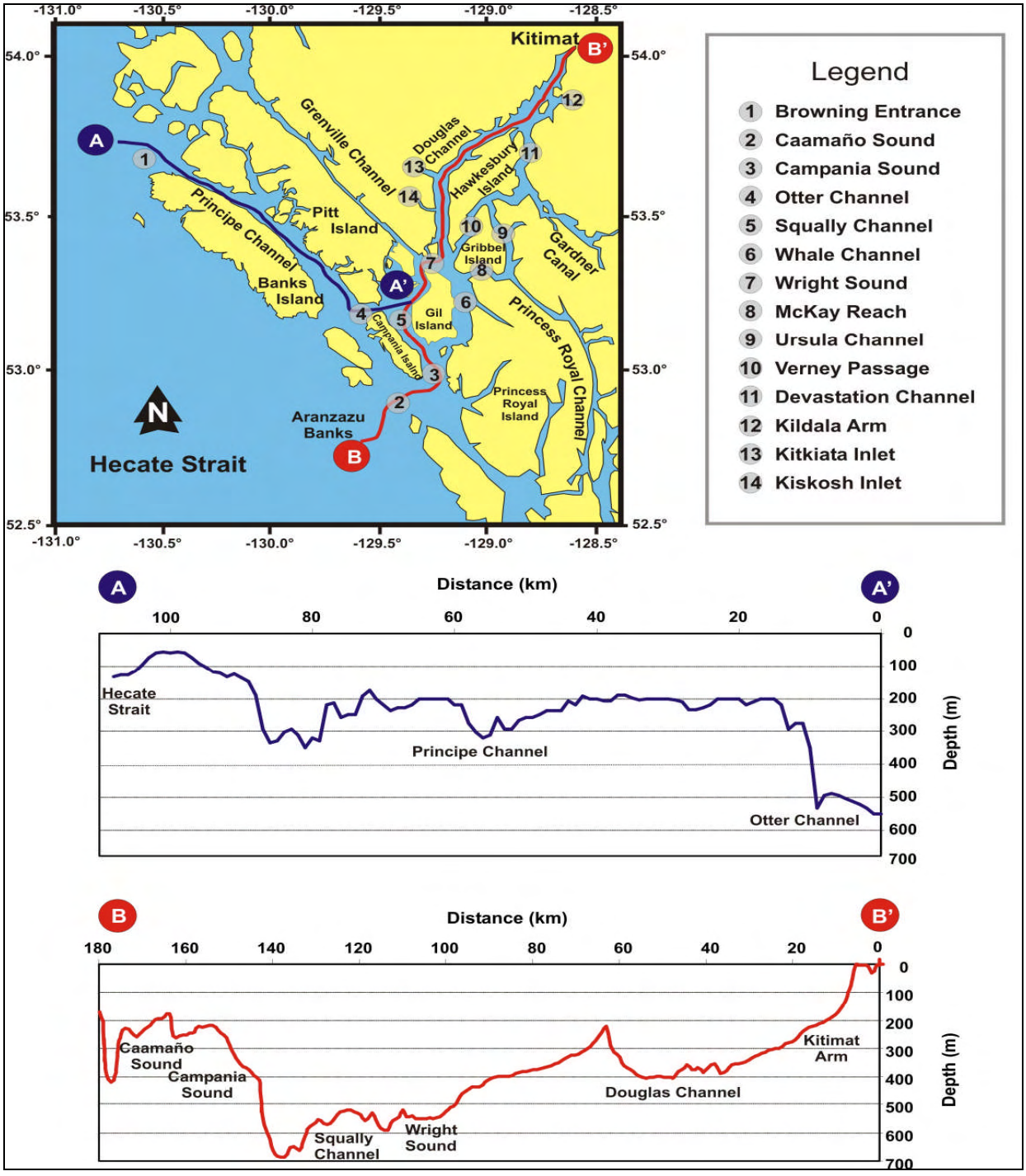

NOTE: Also shown are water depths along two marine corridors: from Browning Entrance in Hecate Strait to Otter Channel (A-A') and from Caamaño Sound to Kitimat Arm (B-B').

Figure B-8 Topography and Bathymetry of the Kitimat Fjord System, Caamaño Sound and Principe Channel

Table B-2 Current Speed Statistics and Vector Average Currents by Site for Near-Surface, Halocline, Mid-Depth and Deep Measurements

		Speed (cm/s)			Vector Average		
Site	**Depth**	**Min.**	**Mean**	**Max.**	**Mag.**	**Dir.**	**SD**
Near-surface (depth <20 m)							
CM3	5	2.1	28.4	91.3	13.6	187.5	28.1
CM3	17	1.5	23.2	70.4	8.3	182.9	24.1
CO2	13	2.6	28.6	100.2	20.1	289.3	26.5
HO2	20	0.0	14.1	54.5	4.4	214.5	15.0
Halocline (depth: 20–75 m)							
CM1	40	1.5	2.4	8.6	0.8	85.5	2.6
CM2	40	0.3	11.3	59.0	1.9	179.5	13.8
CM8	40	1.5	23.0	96.6	20.0	277.4	20.8
CM4	40	1.5	20.7	63.5	8.2	166.6	22.8
Mid Depth (75 m <depth <200 m)							
CM1	104	1.5	2.4	8.6	0.8	183.7	2.6
CM1	168	1.5	2.3	6.5	1.0	75.9	2.4
CM2	172	0.2	6.8	46.3	1.1	20.7	8.1
CM8	136	1.5	13.8	58.4	1.9	310.3	16.4
CM4	153	1.5	15.2	63.1	0.8	182.6	18.0
OC1	140	0.0	9.6	29.8	4.4	114.6	9.9
OC1	199	0.0	9.7	36.2	3.1	135.8	10.8
CO3	140	2.8	19.7	60.1	12.7	257.9	17.8
CO3	197	0.0	15.5	51.7	10.5	257.2	15.0
Deep (depth >200 m)							
CM2	304	1.5	6.7	28.5	1.7	17.8	8.0
CM8	228	1.5	8.8	54.3	2.4	255.1	10.2
CM4	266	1.5	22.3	90.9	16.1	27.1	22.4
CM9	444	1.5	14.8	55.4	0.9	52.3	17.5

NOTES:

Speed statistics represent current speeds (i.e., the length of the current vector regardless of its temporally varying spatial direction). The vector average magnitude represents the “spatially corrected” current speed in the average flow direction (e.g., the extreme example of CM4 at Campania Sound, where the mean current speed, at 75- to 200-m depth, is 15.2 cm/s compared with a 0.8 cm/s velocity average vector magnitude in the southward 186.6° direction).

SD = standard deviation

Distribution of Current Speeds and Directions

Directional distributions of currents during 1977 and 1978 are presented as spoke plots. Each spoke represents the percentage of currents heading in the indicated direction, and each spoke is segmented according to the speed distribution within that directional segment. (Note the 180º difference from a wind rose figure, which shows the direction from which the wind is blowing.)

Excluding the surface currents measured from the drift pole study, the currents at CM1 in Kitimat Arm are small in magnitude and have very little directional dependence (see Figure B-9) compared with other locations.

The near-surface measurements at CM3 in Douglas Channel show strong currents of up to 60 to 80 cm/s aligned along-channel, with a net flow to the south (see Figure B-10). The deeper measurements nearby at Douglas Channel (CM2) (see Figure B-11) are reduced in magnitude and show less tendency to southward flows. At CM2, the current speeds in the fall and winter periods are faster than in the spring and summer seasons.

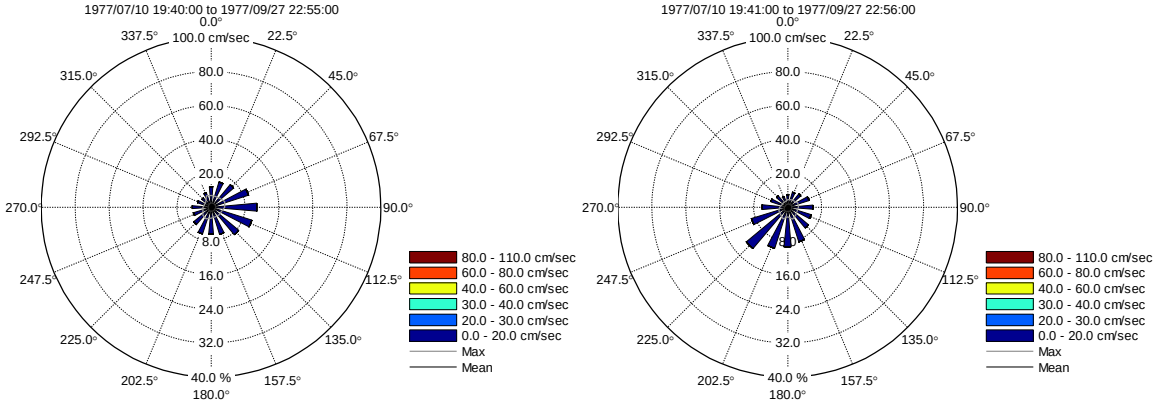

Figure B-9 Joint Speed and Direction Distributions in Kitimat Arm (CM1) for 40-m and 104-m Depths

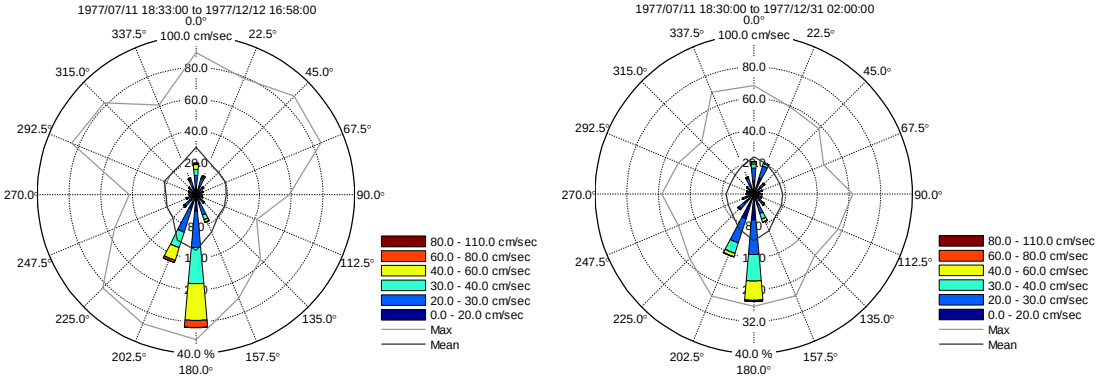

Figure B-10 Joint Speed and Direction Distributions in Douglas Channel (CM3), for 5-m and 17-m Depths

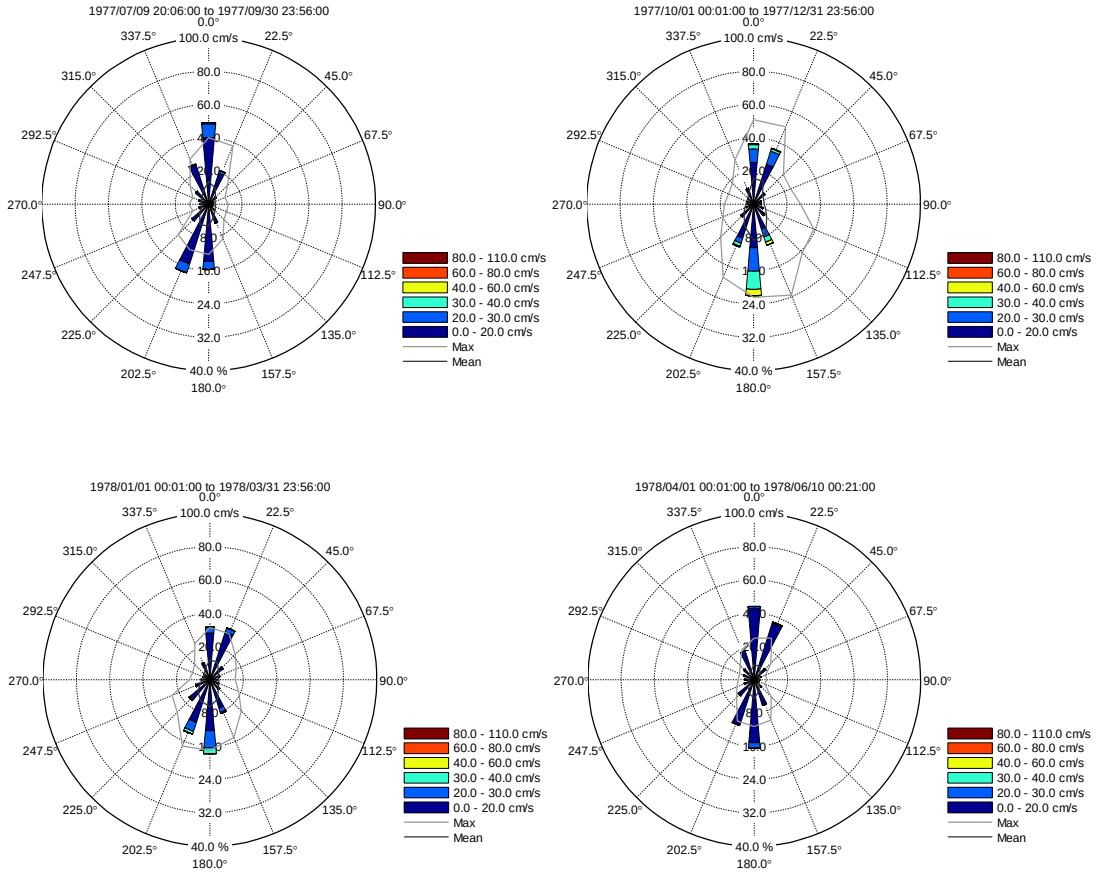

Figure B-11 Joint Speed and Direction Distributions in Douglas Channel (CM2) for 40-m Depth

At CM4 in Campania Sound, strong (40 to 60 cm/s) southward flows are found at near-surface levels, with nearly equal distributions of northerly and southerly directed flows at mid-depth and surprisingly strong (up to 60 to 80 cm/s) northward flows are found at a depth of 266 m (see Figure B-12 and Figure B-13, Plot A).

a b

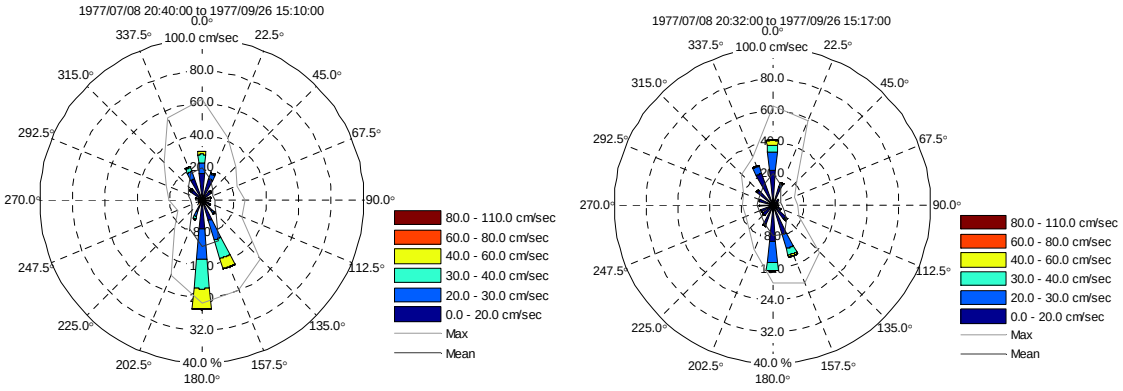

Figure B-12 Plot of Joint Speed and Direction Distributions between July and September at CM4 in Campania Sound (a) 40m Depth (b) 153 m Depth

In Squally Channel, reduced current speeds occur at depth with nearly equal distribution of flow to the north and south (see Figure B-13, Plot B).

In Otter Channel, the December to March currents were westward channelled at the near-surface level, with speeds reaching 60 to 80 cm/s (see Figure B-14, Plot A). The mid-depth level (136 m) continued to show flow along the channel, but with approximately equal distributions of eastward and westward flows as shown in Figure B-14 (Plot B). (Note: The maximum percentage scale for Figure B-14, Plot A is 50% rather than the usual 40%.) However, from May to July at nearly the same depth (140 m), the flows trended more in eastward directions than westward (see Figure B-15, Plot A). Over all, the mid-depth currents had lower speeds in spring and summer than in winter (see Figure B-15, Plot B).

a

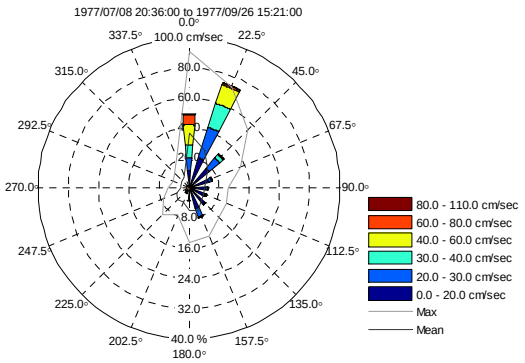

b

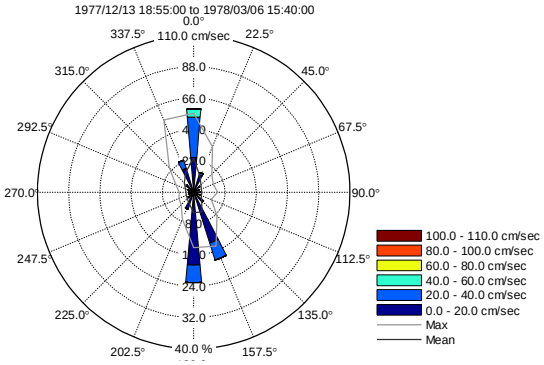

Figure B-13 Joint Speed and Direction Distribution in Campania Sound (CM4) at 266-m Depth in Summer; and in Squally Channel (CM9) at 444-m Depth in Winter

a

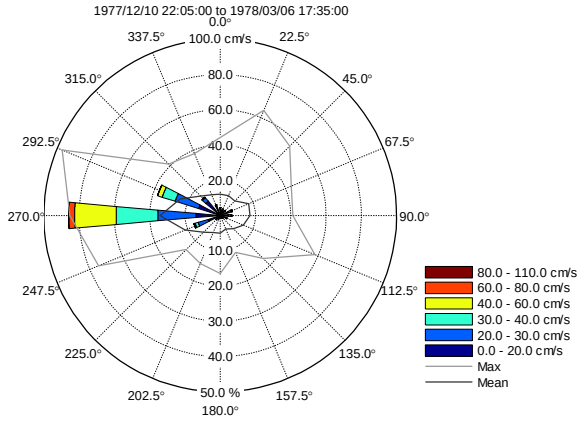

b

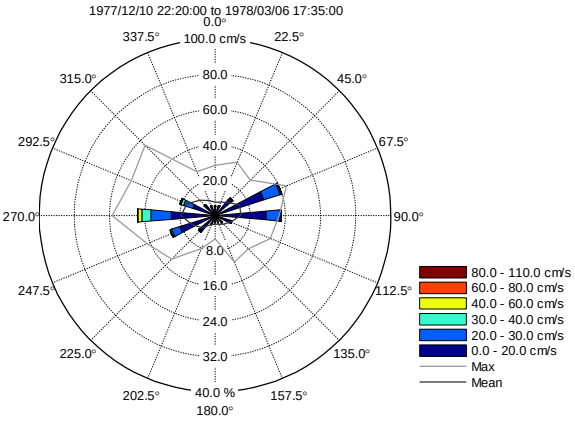

NOTE: In (a), the maximum percentage scale is 50% rather than the usual 40%.

Figure B-14 Joint Speed and Direction Distribution in Otter Channel (CM8) at 40-m Depth and at 136-m Depth in Winter

a b

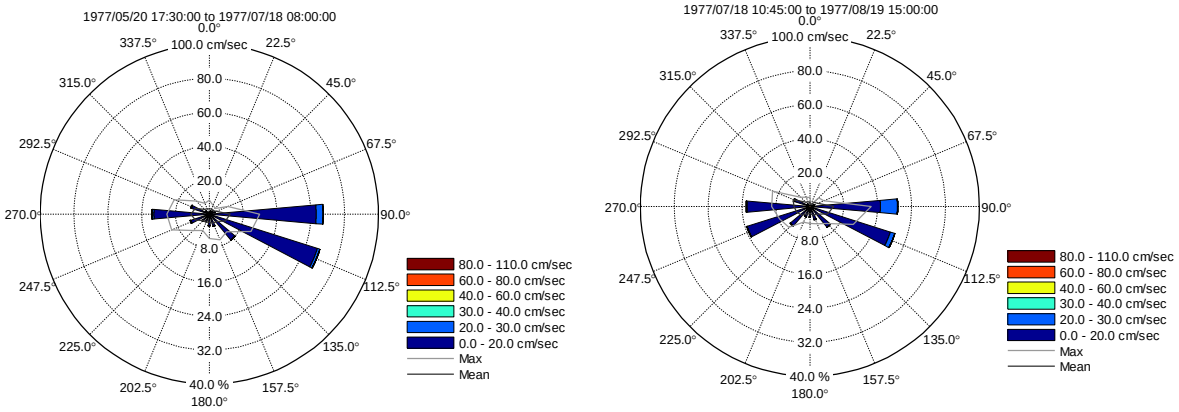

Figure B-15 Joint Speed and Direction Distribution in Otter Channel (OC1) at 140-m Depth, May to July at OC1 in Otter Channel and at 199-m Depth, July to August

Flow rates of 40 to 60 cm/s were measured in the central part of Caamaño Sound at mid-depth during spring and summer, trending to the southwest (see Figure B-16). The near-surface currents further west in the Caamaño Sound approaches (at CO2) trended in a more westerly direction (see Figure B-17, Plot A). The summer near-surface currents in Browning Entrance (H02) were broadly directed toward the west and current speeds were low, usually less than 30 cm/s (see Figure B-17, Plot B).

a b

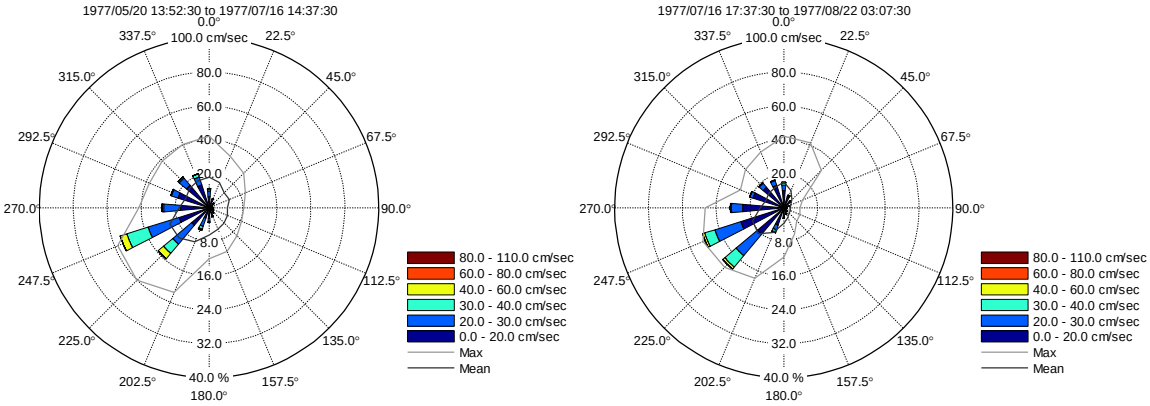

Figure B-16 Joint Speed and Direction Distribution in Caamaño Sound (CO3) (a) at 140-m Depth, May to July and at 195-m Depth, July to August at CO3 in Caamaño Sound

a

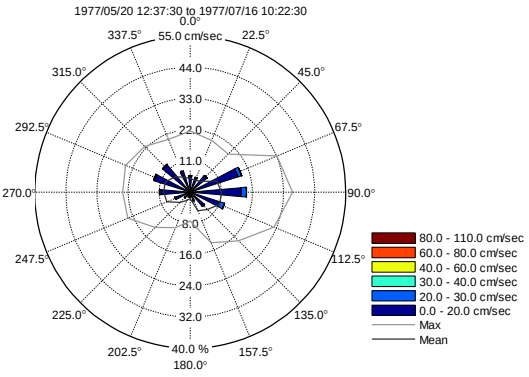

b

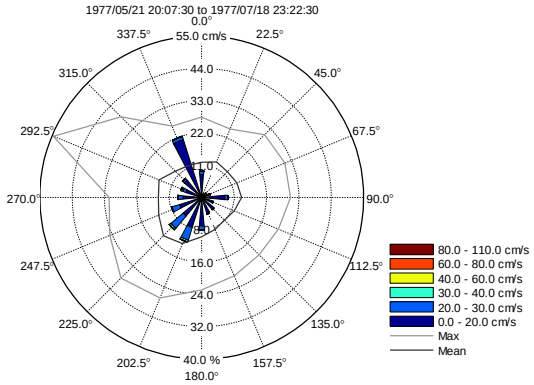

Figure B-17 Joint Speed and Direction Distribution for Western Approach to Caamaño Sound (CO2) at 13-m Depth, August to September, and for Browning Entrance (HO2) at 20-m Depth, July to September

Variability of Currents by Frequency Band and Tidal Analysis

Because of the diurnal astronomical tides, near-surface currents aligned with the axis of a major component current tend to cycle through a high speed in one direction, then to zero speed and then to high speed in the opposite direction. The fluctuating speed pattern for a particular measurement site (see Attachment G1-1 of Appendix G and Attachment H1-1 of Appendix H) is a harmonic time series with a total statistical variance in speed data that can be described mathematically using variance components such as astronomical tide, wind forcing (from prevailing seasonal wind directions) and water density variations by depth and season.

The distribution of statistical variance in the major current component was analyzed mathematically using near-surface measurements at three sites. Current speed data were digitally filtered to compute time series for low frequencies (less than one cycle per day), high frequencies (greater than two cycles per day) and band passed (one to two cycles per day; primarily tidal). The band-passed currents were analyzed using Foreman's (1977) tidal analysis and prediction programs and then subtracting the predicted tidal currents from the original band passed currents. The analysis was carried out on individual current meter data sets of two to three month's duration. For the energy (variance) breakdown for Kitimat Arm, Douglas Channel and Campania Sound, see Figure B-18. Note the very low levels of variance in Kitimat Arm (CM1) in comparison with the other stations. The Kitimat Arm data also show substantial detided variance.

The low frequency band that contributed on time scales exceeding a day were probably caused by wind forcing, though density-driven effects might also be included in this band. At the Douglas Channel sites (CM2 and CM3), in the fall and spring, the winds show considerable low frequency variance, greater than the variance of the astronomical tidal currents. The CM3 measurements show that the influence of low frequency currents increases closer to the surface, particularly in the fall, and the relative importance of the astronomical tides decreases. However, astronomical tides dominate the summer currents in Campania Sound (CM4).

For the variance distribution for the outer parts of the CCAA (Caamaño Sound, Otter Channel and Browning Entrance), see Figure B-19. Except for the Otter Channel measurements, which were made in the winter, the astronomical tide is the dominant contributor. For Otter Channel, the tidal currents and low frequency currents are the significant contributors.

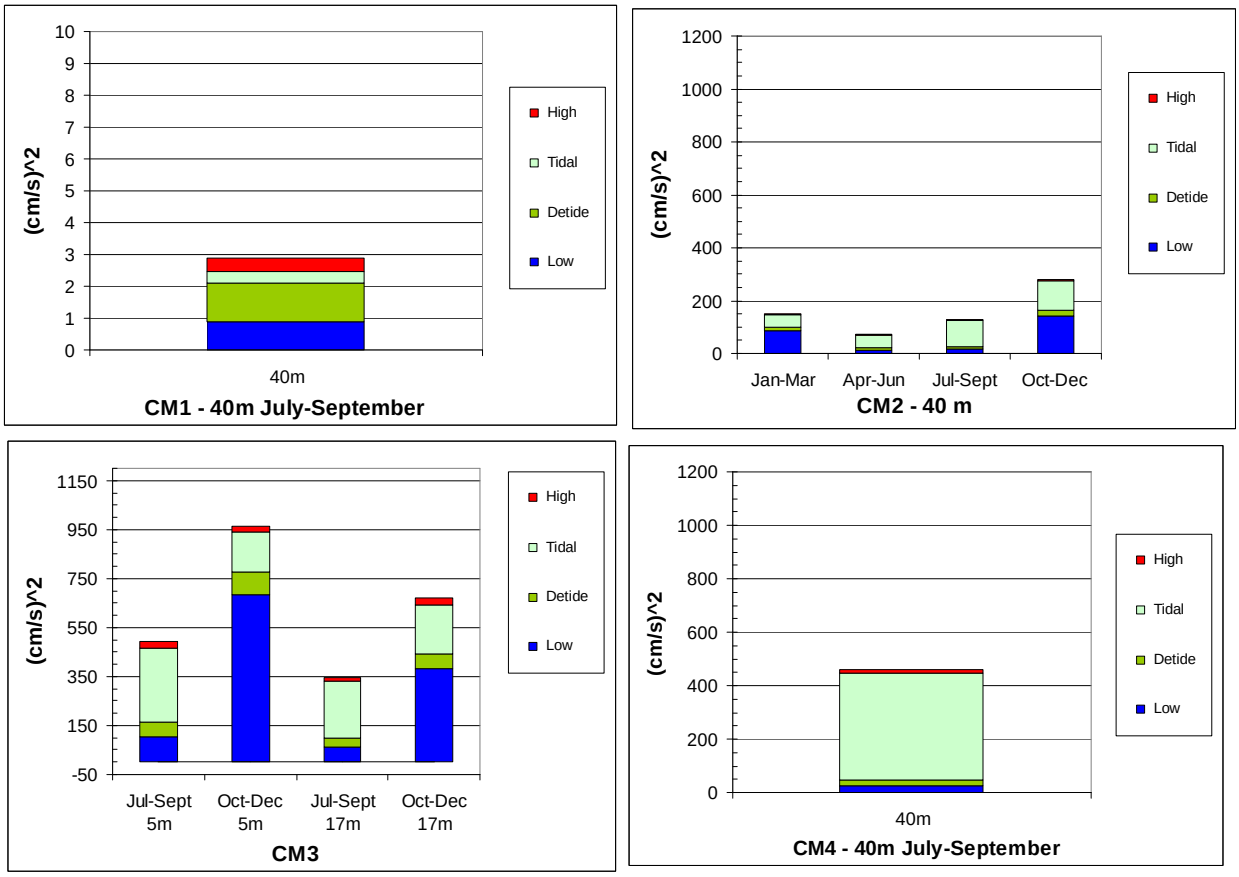

Figure B-18 Speed of Current Variance Distribution between High Frequency, Astronomical Tides, Detided and Low Frequency Bins for Kitimat Arm (CM1), Douglas Channel (CM2, CM3) and Campania Sound (CM4)

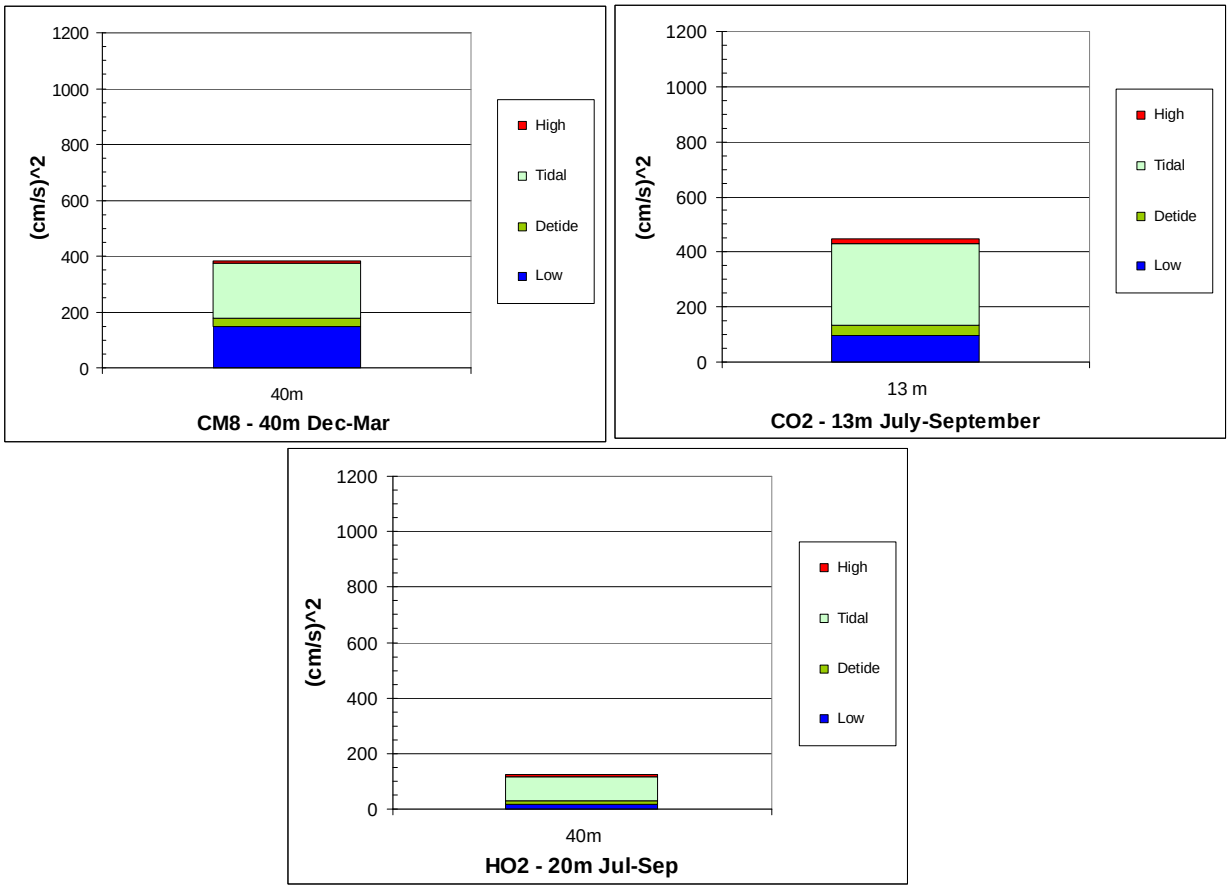

Figure B-19 Speed of Current Variance Distribution between High Frequency, Astronomical Tides, Detided and Low Frequency Bins for Otter Channel (CM8), Western Approach to Caamaño Sound (CO2) and Browning Entrance (HO2)

B.3.3 Analysis of Surface Current Historical Data

Current meters cannot reliably measure currents to within several metres of the surface; however, data from the CHS drift pole study in the summers of 1953 and 1954 (Huggett and Wigen 1983) can be used to better estimate the currents at the surface. In cases where large density gradients exist, it is possible for large differences in current speeds to occur over small vertical distances. The statistics given here, and the tracks illustrated in Figure B-4, are based on drifter locations for which timing information is still readily available. Additional drifter data beyond what is presented here were also collected.

For the speed statistics for the drift pole studies by latitude and region, see Table B-3. The mean current calculations tend to be accurate to within 5 cm/s, though mean speeds of up to 35 cm/s are found in Campania Sound. The strongest currents occur in Campania Sound, Kitimat Arm and Wright Sound (at 81, 78 and 74 cm/s, respectively). Interestingly, even though Kitimat Arm has a mean current speed of

only 17 cm/s in this study, it has a maximum speed of 78 cm/s. Moving from Kitimat Arm toward the approaches, the trend is for mean current speeds to increase.

For the vector averages of the currents measured within each area, as well as the standard deviations, also see Table B-3. A high standard deviation, with respect to the magnitude, partially reflects the measurement of the currents at different phases of the tide.

Table B-3 Surface Current Speeds and Vector Average Speeds by Location

		Speed (cm/s)			Vector Average	
Site	**Latitude**	**Min**	**Mean**	**Max**	**Mag.**	**SD**
	Surface Driftpole					
Kitimat Arm	53.93	4	17	78	11	18
Douglas Channel	53.83	4	18	30	16	11
Douglas Channel	53.77	3	20	43	15	17
Douglas Channel	53.70	2	22	44	4	25
Douglas Channel	53.59	3	19	47	13	17
Douglas Channel	53.44	4	26	64	26	12
Wright Sound	53.36	2	24	74	19	23
Campania Sound	52.96	8	34	81	7	39
Caamaño Sound	52.87	4	28	63	17	18

NOTE:
SD = standard deviation

B.3.4 Response of Currents to Tidal and Wind Forcing

Astronomical and Internal Tidal Currents

Tidal currents driven by astronomical forces are uniform with depth in the absence of frictional or other physical mechanisms. Density gradients within the water column can cause internal tidal currents to develop, which are characterized by marked variations in the tidal current amplitudes and phases with depth as well as marked changes in amplitude and phase at a single measurement level. The effect of internal modes of tidal currents can be seen as changes in the fitted tidal constituents as well as significant residual variance or energy in the semi-diurnal to diurnal band-passed currents. Changes in tidal current variances are shown in Figures B-18 and B-19 indicate that internal tides occur at CM1 (Kitimat Arm), CM2 and CM3 (Douglas Channel), and, to a lesser degree, at CM8 (Otter Channel) and C02 (western approach to Caamaño Sound). Very little detided variance occurs at H02 (Browning Entrance).

To further examine internal tides, a tabulation of the tidal analysis of historical current meter data was prepared of the largest tidal constituent (M2) for values of magnitude, phase, sense of rotation. A parameter denoted as R (see Table B-4), is the ratio of the magnitude of the minor (cross-channel) to major (along-channel) current components for the M2 tidal current. At many sites, the amplitude and

phases of the M2 tidal constituent exhibit large changes with depth. Large amplitude or phase changes are noticeable at CM1 in Kitimat Arm, at CM2 and CM3 in Douglas Channel, especially in the summer and fall, and at CM4 in Campania Sound. The differences are comparatively small in Otter Channel (CM8) and in the outer portions of Caamaño Sound (C02).

In much of the CCAA, the minor component of the tidal current is very small, as indicated by very low absolute values (less than 0.1) of R, consistent with flows primarily along the channel and very small cross-channel flows. Values of R greater than 0.1 are limited to CM8 in Otter Channel (clockwise rotation) and to C02 in the approaches to Caamaño Sound (counter-clockwise). At one level only at CM1 (104 m) in Kitimat Arm, an R value of 0.27 was realized, although at a very small tidal amplitude of only 1.5 cm/s.

Measurements were made at CM2 for nearly a year, allowing the seasonal variability of the M2 tidal current constituent to be examined. Large variations occur in the M2 current amplitude with depth, especially from 40 to 172 m in the summer and fall. These large amplitude variations coincide with the summer period when freshwater content and upper layer stratification reaches its seasonal peak, as well as in the fall when stratification levels are high because of the annual peak in precipitation within the CCAA (see Appendix C). During winter and during spring prior to the river freshet in June, the amplitudes of the M2 tidal constituent are nearly uniform with measurement depth, although even in these seasons, the phase of the M2 tidal constituent at 40 m depth differs by 40 to 45 degrees from the mid-depth measurement level.

Internal tidal currents in the Kitimat system were analysed and modeled by Webster (1980) and Webster (1983). Based on the July to December 1977 measurements at Douglas Channel (CM2 and CM3), Webster computed the non-predictable part of the tidal frequency currents. He found that the amount of non-tidally predictable variance could change on time scales as short as one week, perhaps even less. Webster modeled the internal tides in Douglas Channel using first and second mode Kelvin waves. Thomson and Huggett (1980) show that a similar type of very long period wave mode is possible but unlikely in Johnstone Strait because of rapid dissipation. Webster uses the same logic to consider only Kelvin waves in Douglas Channel. Temperature and salinity information from the CM2 and CM3 current meters and a nearby thermistor chain were used to compute the Eigenfunctions of the first two modes. Using a least squares approach, the theoretical Kelvin waves and the predicted tidal currents were fitted (in both amplitude and phase) to the observed currents subject to assumptions of zero mean flow, as well as a flat bottom, zero friction and linear waves. Webster (1983) suggested that the sill about 10 km to the north of CM2 is a potential trigger of internal waves, although they could be generated elsewhere.

The internal tide for the major M2 tidal constituent is expected to behave as a first-mode Kelvin wave with a horizontal phase speed of 0.8 m/s, which will result in a 555° phase change as it traverses Douglas Channel (about 55 km long), while the second mode will undergo a 885° phase change. A simple astronomical tidal wave (60 m/s phase speed) will only have a 7° phase change over the same distance.

Table B-4 Summary of M2 Tidal Constituent by Site, Time and Depth

Site	Time	Depth (m)	MR Major	R (min/maj)	Rotation Direction	Phase
CM1	Jul – Sep	40	0.35	0.04	ccw	18.2
		104	1.49	0.27	ccw	168.8
		168	1.68	0.01	cw	167.6
CM2	Jan – Mar	40	8.44	0.05	cw	222.7
		172	8.33	0.02	cw	183.8
		304	10.77	0.01	ccw	148.8
	Apr – Jun	40	8.55	0.01	cw	221.3
		172	7.81	0.01	cw	174.9
		304	8.15	0.02	ccw	162.1
	Jul – Sept	40	12.81	0.09	cw	210.0
		172	8.07	0.02	ccw	186.0
		304	8.14	0.05	cw	187.8
	Oct – Dec	40	14.06	0.01	ccw	195.5
		172	6.40	0.02	ccw	185.0
		304	6.80	0.06	cw	168.9
CM3	Jul – Sep	5	21.81	0.02	ccw	184.4
		17	19.46	0.08	cw	198.3
	Oct – Dec	5	15.83	0.01	cw	176.1
		17	18.71	0.04	cw	195.5
CM4	Jul – Sep	40	16.61	0.00	ccw	197.6
		153	19.59	0.14	ccw	191.9
		266	22.88	0.09	cw	196.0
CM8	Dec – Mar	40	16.64	0.23	cw	49.6
		136	13.68	0.13	cw	46.3
CO2	May – Jul	140	8.99	0.04	ccw	332.2
	Jul – Aug	199	11.81	0.01	cw	352.7
CO2	May – Jul	140	16.04	0.00	ccw	306.2
	Jul – Aug	197	13.03	0.27	ccw	318.4

NOTE:
R = the ratio of the magnitude of the minor (cross-channel) to major (along-channel) current components for the M2 tidal current

Wind Forcing of Currents

The winds in the CCAA (see Appendix A) can reach very high values in the Hecate Strait approaches, especially during the fall and winter. Pacific Ocean storms move frequently through the CCAA and generate very strong episodic winds that often reach storm force and occasionally hurricane force wind speeds. In the inland waters, the Pacific storm winds are somewhat moderated by the high-relief terrain of the Coast Mountains. However, in late fall and winter, Arctic outflow winds blowing cold continental air from the north can generate gale force wind episodes, each lasting several days.

Large wind speed events generate surface ocean currents with current speeds of typically 2% to 3% of the wind speed and current directions parallel to the wind in confined waterways. However, the response of the ocean surface layer to wind forcing in the Kitimat system can be more complex, mainly because of the highly stratified and variable estuarine nature of the upper part of the water column, but also because of permutations arising from the complex geometry of adjoining ocean channels.

The general estuarine circulation of surface currents toward the ocean, usually to the south, can be reversed by winds blowing in the opposite direction. At CM2 and CM3, such reversals of the southward flow in Douglas Channel have occurred occasionally in summer, but in fall and winter, the direction of the surface currents are dominated by the wind forcing (Webster 1980), because of the increased wind speeds of these seasons. The response of the surface currents and upper layer water properties in Douglas Channel to wind forcing has been studied by Buckingham (1980) for wind forcing periods of 1 to 11 days. A two-layer frictional model of a stratified inlet (Farmer 1972) agreed reasonably well with observations in explaining the deepening of the surface layer thickness in response to wind forcing and freshwater discharge. However, currents measured at CM3 at a 5 m depth were not explicable as linear coherent responses to wind forcing. The more complicated nature of these current observations may be due to the highly variable stratification, which varied on the same time scales as the wind forcing itself (Buckingham 1980).

B.3.5 Summary of Key Findings

The currents in the CCAA can be characterized by typical flow speeds of about 15 to 30 cm/s at the surface. The highest surface currents have been measured in the outer seaward parts of the CCAA including Campania Sound, Caamaño Sound and Principe Channel, while Kitimat Arm of northern Douglas Channel appears to have slower surface currents. Maximum near-surface currents range from 50 to 60 cm/s in Kitimat Arm, to 90 to 100 cm/s in southern Douglas Channel, to well over 100 cm/s in the seaward portions of the CCAA and in Principe Channel. Analysis of drift pole data in Kitimat Arm, however, suggests that if the currents right at the surface are considered, to the exclusion of those several metres down (near-surface), surface currents are even stronger (up to 78 cm/s) than the aforementioned near-surface current speeds at the respective locations.

The subsurface currents below the main halocline at water depths exceeding 75 to 100 m are typically 3 to 20 cm/s with maximum speeds of 10 to 60 cm/s in the deep inland water basins of Squally Channel, Wright Sound, Douglas Channel and Kitimat Arm. For these inland waterways, the subsurface current speeds generally decrease with increased distance inland from Hecate Strait. In the shallower approaches to the Kitimat system, subsurface current speeds are generally higher, at typical values of 10 to 25 cm/s

and maximum values of 40 to 100 cm/s. Principe Channel has the strongest near-bottom (100-m water depth) currents, with typical speeds of 25 cm/s and maximum speeds of 110 cm/s.

In the confined inland waterways and in some of the narrow passages (e.g., Otter Channel), the current directions are aligned with the axis of the channels themselves and the speeds of cross-channel currents are much slower than those of the along-channel currents. In the more open waters of Caamaño Sound and Browning Entrance, the currents encompass a much greater range of directions.

The average net flows are generally seaward-directed near the surface and landward-directed at depth, consistent with the highly estuarine nature of the Kitimat system. The typical net surface current speeds are 10 to 15 cm/s to the south in Douglas Channel, with a deeper net return flow to the north of 1 to 3 cm/s.

The currents in the CCAA are highly variable because of a combination of wind, tidal and estuarine forcing. The wind forcing is highly episodic and particularly important in the fall and winter under the combined influence of frequent Pacific storms and Arctic outflow winds. Pacific storms result in very strong winds in the outer seaward portions of the CCAA, which while reduced in speed, are still important as strong winds from the south in the inland waterways. The Arctic outflow winds from the north are strongest in the northern portions of the inland waterways. The response of the surface layer to wind forcing, in terms of the magnitude of the resulting current, can be highly variable because of the varying stratification of the water column, which depends on freshwater runoff and precipitation.

The tidal currents exhibit a considerable degree of variability with location and with measurement depth, again because of the underlying effects of the highly variable stratification of the water column. The astronomical tide is highly predictable and uniform with depth and changes little over the length of the system. However, the astronomical tide is often smaller than the internal tide in the upper portions of the water column. The internal tide is much less predictable as it varies in amplitude and phase over periods as short as a few days or less. It also exhibits a high degree of depth dependence, and the horizontal scale of the internal tide is of the order of tens of kilometres as opposed to many hundreds of kilometres for the astronomical tide. Also of relevance to the CCAA are internal waves generated by the flow of a stratified fluid over a topographic feature, such as internal hydraulic jumps and lee waves, as well as internal tides.

B.4 References

B.4.1 Literature Cited

Baines, P.G. 1984. A unified description of two-layer flow over topography. *Journal of Fluid Mechanics* 146: 127-167.

Baines, P.G. 1995. *Topographic Effects in Stratified Flows*. Cambridge University Press. Cambridge.

B.C. Ministry of Sustainable Resource Management. 2002. *British Columbia Marine Ecological Classification: Marine Ecosections and Ecounits*. Resources Inventory Committee. Province of British Columbia. Victoria, BC.

Birch, J.R., E.C. Luscombe, D.B. Fissel and L.F Giovando. 1985. *West Coast Data Inventory and Appraisal. Volume 1. Dixon Entrance, Hecate Strait, Queen Charlotte Sound and Adjoining B.C. Coastal Waters: Physical Oceanography – Temperature, Salinity, Currents, Water Levels and Waves, 1903 through 1984.* Canadian Data Report of Hydrography and Ocean Sciences No. 37. Department of Fisheries and Oceans. Institute of Ocean Sciences. Sidney, BC.

Buckingham, W.R. 1980. *Kitimat Physical Oceanographic Study 1977-1978: Part 5, The Response of Douglas Channel to Meteorological Forces*. Contract Report Series 80-3 (Part 5). Institute of Ocean Sciences. Sidney, BC. Unpublished manuscript.

Buckley, J.R. 1977. *The Currents, Winds and Tides of Upper Howe Sound*. PhD dissertation. University of British Columbia. Vancouver, BC.

Crawford, W.R., J.Y. Cherniawsky, M.G.G. Foreman and J.F.R. Gower. 2002. Formation of the Haida-1998 oceanic eddy, *Journal of Geophysical Research* 107(C7): 10.1029/2001JC000876, 2002. 6-1 to 6-11.

Crawford, W.R. 2001. *Oceans of the Queen Charlotte Islands*. Canadian Technical Report of Fisheries and Aquatic Science 2383. Fisheries and Oceans, Canada. Sidney, BC.

Crawford, W.R., J.Y. Cherniawsky, P.F. Cummins and M.G.G. Foreman. 1998. Variability of tidal currents in a wide strait: A comparison between drifter observations and numerical simulations. *Journal of Geophysical Research* 103: 12743-12759.

Crawford, W.R., W.S. Huggett and M.J. Woodward. 1988. Water transport through Hecate Strait, BC. *Atmosphere-Ocean* 26: 301-320.

Crawford, W.R, M.J. Woodward, M.G.G. Foreman and R.E. Thomson. 1995. Oceanographic features of Hecate Strait and Queen Charlotte Sound in summer. *Atmosphere-Ocean* 33: 639-681.

Cummins, P.F., S. Vagle, L. Armi and D.M. Farmer. 2003 Stratified flow over topography: Upstream influence and generation of nonlinear internal waves. *Proceedings of the Royal Society of London* 459: 1467-1487.

Cummins, P.F., L. Armi and S. Vagle. 2006. Upstream internal hydraulic jumps. *Journal of Physical Oceanography* 36: 753-769.

Cummins, P.F. and L.Y. Oey. 1997. Simulation of barotropic and baroclinic tides off northern British Columbia. *Journal of Physical Oceanography* 27: 762-781.

de Boer, G., J.D. Pietrzak and J.C. Winterwerp. 2005. On the vertical structure of the Rhine Region of freshwater influence. *Ocean Dynamics* 56: 198-216.

Farmer, D.M. 1972. *The influence of wind on the surface waters of Alberni Inlet*. Ph.D. dissertation. University of British Columbia. Vancouver, BC.

Farmer, D.M. and L. Armi. 1999a. Stratified flow over topography: The role of small scale entrainment and mixing in flow establishment. *Proceedings of the Royal Society of London* 455A: 3221-3258.

Farmer, D.M. and L. Armi. 1999b. The generation and trapping of solitary waves over topography. *Science* 283: 188-190.

Farmer, D.M. and L. Armi. 2001. Stratified flow over topography: Models versus observations. *Proceedings of the Royal Society of London* 457A: 2827-2830.

Farmer, D.M. and H.J. Freeland. 1983. The physical oceanography of fjords. *Progress in Oceanography* 12:147-220.

Farmer, D.M. and J.D. Smith. 1980a. Tidal interaction of stratified flow with a sill in Knight Inlet. *Deep Sea Research* 27A: 239-254.

Farmer, D.M. and J.D. Smith. 1980b. Generation of lee waves over the sill in Knight Inlet. In H.J. Freeland, D.M. Farmer and C.D. Levings (eds.). *Fjord Oceanography.* Plenum Publishing. New York.

Fong, D.A. and W.R. Geyer. 2001. The response of a river plume during an upwelling favorable wind event. *Journal of Geophysical Research* 106: 1067-1084.

Foreman, M.G.G. 1977. *Manual for Tidal Heights Analysis and Prediction*. Pacific Marine Science Report, Volume 77-10. Department of Fisheries and Oceans. Institute of Ocean Sciences. Sidney, BC.

Foreman, M.G.G. and R.E. Thomson. 1996. Three-dimensional model simulations of tides and buoyancy along the west coast of Vancouver Island. *Journal of Physical Oceanography* 27: 1300-1325.

Freeland, H.J. 1984. The partition of internal tidal motions in Knight Inlet, British Columbia. *Atmosphere-Ocean* 22: 144-150.

Freeland H.J. and Farmer D.M. 1980. Circulation and energetics of a deep, strongly stratified inlet. *Canadian Journal of Fisheries and Aquatic Science* 37: 1398-1410.

Garcia Berdeal, I.; B.M. Hickey and M. Kawase. 2002. Influence of wind stress and ambient flow on a high discharge river plume. *Journal of Geophysical Research* 107(C9), 3130, doi:10.1029/2001JC000932.

Gill, A. E. 1981. *Atmosphere-Ocean Dynamics*. Academic Press. New York.

Hickey, B.M., R.E. Thomson, H. Yih and P.H. LeBlond. 1991. Velocity and temperature fluctuations in a buoyancy-driven current off Vancouver Island *Journal of Geophysical Research* 96(C6): 10507-10538.

Hickey, B., S.L. Geier, N.B. Kachel and A. MacFadyen. 2005. A bi-directional river plume: The Columbia in summer. *Continental Shelf Research* **25:** 1631-1656.

Hooge, P.N. and E.R. Hooge. 2002. *Fjord Oceanographic Processes in Glacier Bay, Alaska*. USGS - Alaska Science Center, Anchorage, AK.

Huggett, W.S. and S.O. Wigen. 1983. Surface currents in the approaches to Kitimat. In R.W. Macdonald (ed.). *Proceedings of a Workshop on the Kitimat Marine Environment*. Canadian Technical Report of Hydrography and Ocean. Sciences 18. Department of Fisheries and Oceans, Institute of Ocean Sciences. Sidney, BC. 34-65.

Kourafalou, K. 1999. Process studies on the Po River plume, North Adriatic Sea. *Journal of Geophysical Research* 104(C12): 29963-29986.

Kourafalou, K. 2001. River plume development in semi-enclosed Mediterranean regions: North Adriatic Sea and Northwestern Aegean Sea. *Journal of Marine Systems* 30: 181-205.

Klymak, J.M. and M.C. Gregg. 2003. The role of upstream waves and a downstream density pool in the growth of lee waves: Stratified flow over the Knight Inlet sill. *Journal of Physical Oceanography* 33:1446-1461.

Klymak, J.M. and M.C. Gregg. 2004. Tidally generated turbulence over the Knight Inlet sill. *Journal of Physical Oceanography* 34: 1135-1151.

Kranenburg, C. and J.D. Pietrzak. 1989. Internal lee waves in turbulent two-layer flow. *Journal of Hydraulic Engineering American Society of Civil Engineers* 115: 1352-1370.

Macdonald, R.W. (ed.). 1983. *Proceedings of a Workshop on the Kitimat Marine Environmen*t. Canadian Technical Report of Hydrography and Ocean Sciences, 18. Department of Fisheries and Oceans. Institute of Ocean Sciences. Sidney, BC.

Macdonald, R., W. Cretney, C.S. Wong and P. Erickson. 1983. Chemical characteristics of water in the Kitimat fjord system. In R.W. Macdonald (ed.). *Proceedings of a Workshop on the Kitimat Marine Environment*. Canadian Technical Report of Hydrography and Ocean Sciences. 18. Department of Fisheries and Oceans. Institute of Ocean Sciences. Sidney, BC.

Maxworthy, T. 1979. A note on the internal solitary waves produced by tidal flow over a three-dimensional ridge. *Journal of Geophysical Research* 84: 338-346.

Marsden, R.F. and K.C. Greenwood. 1994. Internal tides observed by an acoustic Doppler current profiler. *Journal of Physical Oceanography* 24(6):1097-1109.

Pond, S. and G.L. Pickard. 1983. *Introductory Dynamic Oceanography, 2nd Edition*. Pergamon Press. New York.

Province of British Columbia. 1998. *Coastal Zone Position Paper*. Province of British Columbia Inter-agency Coastal Working Group. Victoria, BC.

Royer, T.C. 1981. Baroclinic transport in the Gulf of Alaska. Part II. A freshwater driven coastal current. *Journal of Marine Research* 39: 251-266.

Simpson, J.H. and A.J. Souza. 1995. Semi-diurnal switching of stratification in the region of freshwater influence of the Rhine. *Journal of Geophysical Research* 100(C4): 7037–7044.

Stacey, M.W. and S. Pond. 1992. A numerical model of the internal tide in Knight Inlet, British Columbia. *Atmosphere-Ocean* 30(3): 383-418.

Stacey, M.W., S. Pond and Z.P. Novak. 1995. A numerical model of the circulation in Knight Inlet, British Columbia, Canada. *Journal of Physical Oceanography* 25: 1037-1062.

Syvitski, J. P. M., D.C. Burrell and J.M. Skei. 1987. *Fjords: Process and Products*. Springer-Verlag. New York.

Thomson, R.E. 1981. *Oceanography of the British Columbia Coast*. Canadian Special Publication of Fisheries and Aquatic Sciences 56. Department of Fisheries and Oceans. Ottawa, ON.

Thomson, R.E. 1989. The Queen Charlotte Islands: Physical Oceanography. In G.G.E. Scudder and N. Gessler (eds.). *The Outer Shores*. Based on the Proceedings of the Queen Charlotte Islands First International Symposium. University of British Columbia. Vancouver, BC. 27-63.

Thomson, R.E, B.M. Hickey and P.H. LeBlond. 1989. The Vancouver Island Coastal Current: Fisheries Barrier and Conduit. In R.J. Beamish and G.A. McFarlane (eds.). *Effects of Ocean Variability on Recruitment and an Evaluation of Parameters Used in Stock Assessment Models.* Canadian Special Publication of Fisheries and Aquatic Sciences 108. Fisheries and Oceans Canada. Ottawa, ON.

Thomson, R.E. and W.S. Huggett. 1980. M_2 baroclinic tides in Johnstone Strait, B.C. *Journal of Physical Oceanography* 10: 1509-1539.

Visser, A.W., A.S. Souza, K. Hessner and J.H. Simpson.1994. The effect of stratification on tidal current profiles in a region of freshwater influence. *Oceanologica Acta* 17(4): 369-381.

Webb A.J. and S. Pond. 1986. A modal decomposition of the internal tide in a deep strongly stratified inlet: Knight Inlet, British Columbia. *Journal of Geophysical Research* 91: 9721-9738.

Webster, I. 1980. *Kitimat Physical Oceanographic Study 1977-1978, Part 3, Estuarine Circulation.* Contract Report Series 80-3 (part 3). Institute of Ocean Sciences, Patricia Bay, BC. Unpublished manuscript.

Webster, I. 1983. The baroclinicity of the semi-diurnal tidal currents in Douglas Channel, BC. In R.W. Macdonald (ed.). *Proceedings of a Workshop on the Kitimat Marine Environment*. Canadian Technical Report of Hydrography and Ocean Sciences 18. Department of Fisheries and Oceans Canada. Institute of Ocean Sciences. Sidney, BC. 14-32.

Yeremy, M.L. and M.W. Stacey. 1998. A two-dimensional numerical model which simulates the temperature, salinity and velocity fields in Knight Inlet, British Columbia. *Atmosphere-Ocean* 36(1): 1-27.

Weingartner, T.J., S. Danielson, and T. C. Royer. 2005. Freshwater Variability and Predictability in the Alaska Coastal Current *Deep-Sea Research*, 52: 169 – 192

World Meteorological Organization. Intergovernmental Panel on Climate Change (WMO-IPCC). 2001 Meteorological Organization Intergovernmental Panel on Climate Change, Third Assessment Report, “Climate Change 2001: Working Group I: The Scientific Basis”, www.grida.no/climate/ipcc_tar/wg1/055.htm

B.4.2 Personal Communications

Crawford, W. 2005. Research Scientist. Institute of Ocean Sciences. Sidney, BC.

B.4.3 Internet Sites

Cretney, W., W.R. Crawford, D. Masson and T. Hamilton. 2002. *Physical Oceanographic and Geological Setting of a Possible Offshore Oil and Gas Industry in the Queen Charlotte Basin*. DFO, Pacific Scientific Advice Review Committee. 2002/004. Canadian Science Advisory Secretariat. Accessed: September 2004. Available at: http://www.pac.dfo-mpo.gc.ca/sci/psarc/

Fisheries and Oceans Canada (DFO). 2006. OSD Data Archive Overview. Accessed: January 2006. Available at: http://www-sci.pac.dfo-mpo.gc.ca/osap/data/SearchTools/aboutarcnew_e.htm

Appendix C Freshwater Discharges and Temperature-Salinity Distributions

C.1 Introduction

This appendix describes the baseline conditions for freshwater discharges and temperature-salinity distribution within the CCAA.

The basic physical oceanographic water property parameters are temperature and salinity. Salinity is related directly to freshwater input, which occurs in large quantities that vary considerably with time and location within the CCAA. For this region, salinity is the dominant contributor to density, so the salinity profiles (variation with depth) are almost identical to the density profiles.

The following data were gathered through a review of existing literature and field surveys:

- estuarine water properties
- temperatures, salinities and densities
- river runoff
- drainage basins
- precipitation

C.2 Methods

C.2.1 Spatial Boundaries

For this report, historical measurements of temperature and salinity profile data within the CCAA (see Figure 1-1), including extended data sets from Environment Canada river and weather stations, were reviewed. In addition, during September 2005 and January 2006, profile measurements of temperature and salinity values were collected at 15 locations within the CCAA (see Figure C-1).

C.2.2 Review of Existing Data Sources

A detailed review of oceanographic information within the CCAA included:

- data inventories
- regional environmental assessment and review documents
- oceanographic and related databases (Institute of Ocean Sciences, Marine Environmental Data Service, Meteorological Services, Inland Waters Directorate)

For the historical measurement locations, see Figure C-2. The available data spanned the years 1951 to 2004 and consisted of CTD profiles, available starting in the 1970s. Prior to that, bottle data were obtained in which thermometers were mounted and water was collected for salinity analysis.

A total of 421 CTD or bottle profile data sets were selected for use in this study.

River runoff measurements are available from the Inland Waters Directorate of Environment Canada. For a summary of the measurements used in this study, see Table C-1.

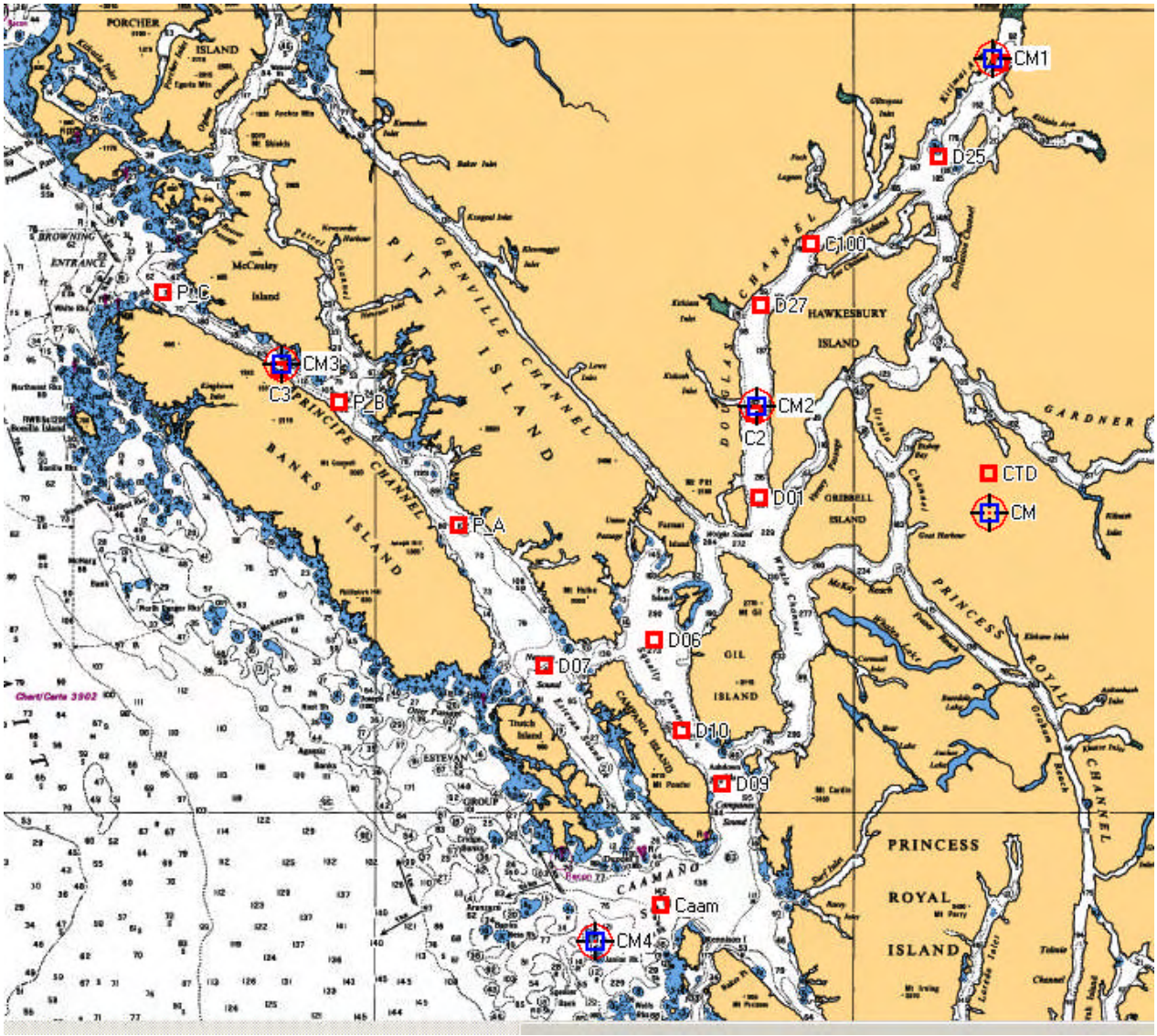

NOTES: Blue squares: Current meter sites September 2005 to January 2006.
Red squares: CTD sites September 2005 and January 2006.

Figure C-1 Conductivity, Temperature and Depth Profiling Sites for the Project, September 2005 and January 2006

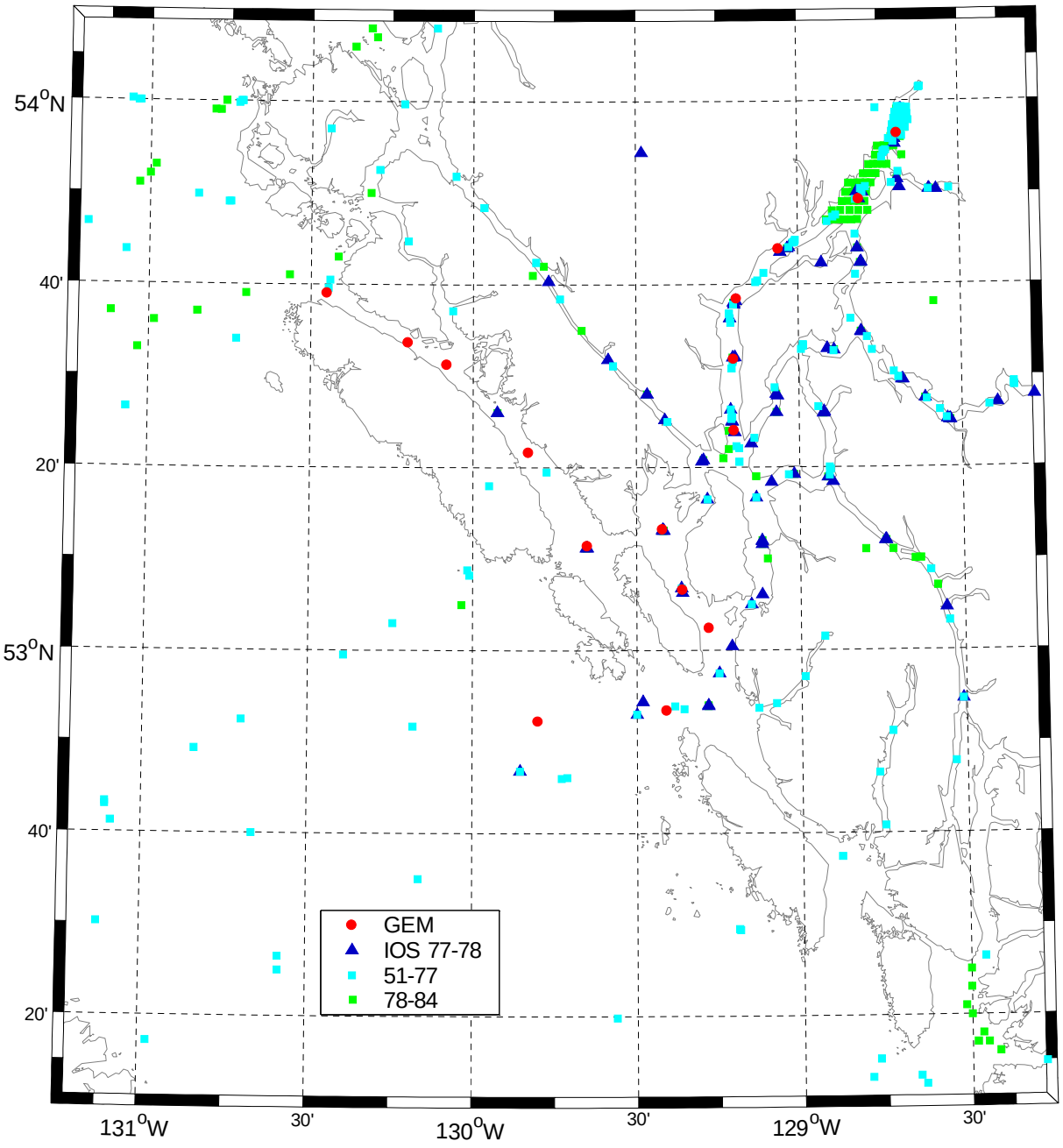

NOTE: Project measurement locations from 2005 to 2006 are indicated by red circles and labelled as GEM.

Figure C-2 Project and Historical Measurement Sites for Conductivity, Temperature and Depth and Bottle Profiles in the CCAA

Table C-1 River Gauging Station Data

EC Station	River (measurement site)	Latitude	Longitude	Drainage Area (km^2)	First Year Observation	Last Year Observation	Average Distance (m^3/s)
08FE002	Kemano Powerhouse	53° 33' 40" N	127° 56' 10" W	(diverted)	1955	2003	96.1
08FE003	Kemano River (above powerhouse Tailrace)	53° 34' 10" N	127° 56' 40" W	583	1972	2003	45.4
08FF001	Kitimat River (below Hirsch Creek)	54° 3' 34" N	128° 40' 29" W	1,990	1964	2003	132.8
08DB001	Nass River (above Shumal Creek)	55° 15' 50" N	129° 5' 10" W	18,500	1929	2003	828.0
08EF001	Skeena River at Usk	54° 37' 50" N	128° 25' 55" W	42,200	1928	2003	914.7
08EF003	Zymoetz River (near Terrace)	54° 32' 10" N	128° 27' 15" W	3,080	1952	1963	138.4
08EF005	Zymoetz River above O.K. Creek	54° 29' 0" N	128° 19' 50" W	2,980	1964	2003	105.3

C.3 Results of Baseline Investigations

C.3.1 Synopsis and Overview

The British Columbia coastal zone is a maze of waterways, inlets and fjords that is exposed to the general offshore climatic patterns, but also has specific characteristics because of the land's topography and the proximity of the Coast Mountains. The steep mountains can cause increased precipitation at the heads of the inlets. Cold winds can flow down from the ice fields at night, while daytime summer heating can generate stiff diurnal breezes. In winter, gaps in the mountains can allow cold polar outbursts of continental air to reach coastal areas (Tyner 1951). The west coast of North America receives large volumes of freshwater runoff from several major rivers including the Columbia and the Fraser. The fresh, buoyant water (less dense than seawater) moves northward along the Washington and British Columbia coast, reaching Queen Charlotte Sound and Hecate Strait (Thomson 1989). The buoyancy-driven current system serves as a migratory corridor and habitat for salmon and other marine organisms and may carry changes in ocean properties (particularly freshwater) over vast distances (Weingartner et al. 2005). Although this flow is persistent and widespread, the associated currents are weak compared with the tidal and wind-driven current component.

British Columbia's glacial-carved fjords tend to be deep (up to 764 m in Finlayson Channel) with steep sides, flat bottoms and sills or shallow ledges where they meet the ocean. Freshwater input is a critical

factor controlling fjord circulation and water properties as the input of freshwater drives the estuarine circulation (Pickard and Stanton 1979). Along the mainland, most fjords attain their maximum freshwater input in the late spring through summer because of snowmelt. Much of the CCAA consists of such fjords.

Mainland fjords are often classified according to the amount of freshwater runoff they receive from snowmelt (Pickard 1961; B.C. Ministry of Sustainable Resource Management 1998, Internet site). The classifications are as follows:

- High runoff: These fjords penetrate far enough inland to tap into glacial watersheds that provide runoff throughout the summer, not just during spring melt. They characteristically have diluted, silt-laden surface layers 3 to 10 m thick that persist through the summer. Estuarine flows are on the order of 10 cm/s. In the CCAA, Douglas Channel is in this category.
- Intermediate runoff: These fjords have less glacial runoff, but sufficient snowpack to produce substantial spring runoff. The surface layer is only about 2 m thick. Examples include Seymour, Belize and Neroutsos Inlets.
- Low runoff: Runoff occurs during spring melt and produces only a partial dilution of the surface layer and weak estuarine flow. The pycnocline (interface between water of differing densities) begins close to the surface. Rupert and Holberg Inlets on Vancouver Island are examples.

The British Columbia coast receives direct discharge from several moderate- to small-sized rivers (see Table C-1 for a partial listing) as well as from innumerable small creeks. It also receives direct runoff outside defined watercourses. Most of the runoff into Queen Charlotte Sound enters at Fitz Hugh Sound, fed by outflow from Rivers Inlet, North and South Bentinck Arms, and Fisher and Dean Channels. Runoff to northern Hecate Strait and Dixon Entrance is dominated by the large Skeena and Nass rivers and from medium-sized rivers such as the Kitimat and Kemano Rivers. For more information on river discharges, see Section C.3.2.

Within the inlets, the freshwater runoff creates an estuarine circulation with a seaward outflow at surface and a compensating landward flow at depth. The estuarine circulation helps flush the deeper waters, although sills at the entrance often limit this effect. Poor flushing can result in reduced levels of dissolved oxygen, low biological productivity and low species diversity. However, fjords with sills can also be home to important and often unique species of benthic and planktonic communities (B.C. Ministry of Sustainable Resource Management 2002).

Appendix B (see Figure B-6) illustrates some of the processes that occur in British Columbia's coastal inlets and fjords. Estuarine flow is generally not uniform. It is strongest during periods of high runoff, but can also be modulated by meteorological forcing and oceanographic conditions offshore. For further information regarding the characteristics of estuarine currents, see Appendix B.

Deepwater renewal occurs because of the estuarine circulation, as deepwaters move up-inlet to replace that lost to entrainment in the seaward-headed surface layer. However, deepwater flushing can be episodic, particularly if a sill or multiple sills at the entrance restrict water movement. Dense water capable of penetrating the deeper portions of the inlet may appear only seasonally, such as during strong coastal upwelling events. Even then, the density of the water penetrating over the sill is often reduced by tidal mixing with surface waters.

Winter intrusions of shelf waters into the Kitimat fjord system at intermediate depths probably occur during periods of katabatic (cold outflow) winds when the surface waters in the inlet system are driven seaward (MacDonald et al. 1983).

C.3.2 Freshwater Inputs

River Discharges

The major rivers in the CCAA are the Kitimat and Kemano Rivers. These rivers are gauged and discharge directly into Kitimat Arm in Douglas Channel and Gardner Canal. Also important are the two major rivers draining into northern British Columbia waters, the Skeena and the Nass. The Skeena and Nass Rivers discharge into coastal waterways north of the CCAA and are important in determining the water properties of northern Hecate Strait and eastern Dixon Entrance.

For the seasonality of the river discharge, see Figure C-3. Larger watershed rivers, such as the Skeena and Nass, have high overall discharge and their broad peak is in the spring and early summer because of snowmelt. At the opposite extreme are the small watershed rivers, often found in islands that have low annual flows and are dominated by rainfall. This results in low summer flows and numerous sudden peaks through the fall and winter because of rainstorms. Between these extremes are the small to medium-sized rivers along the mainland coast, including the Kitimat River. Many of these watersheds include snowfields and glaciers providing high summer flows. However, these rivers are also affected by rainfall and their winter storm-related flow peaks can rival their summer flow level.

The Kemano River has two distinctly different river discharge characteristics. In the mid-1950s, as part of the development of the aluminum smelter at Kitimat, a large power generating facility was built on the Kemano River where water diverted from the Nechako watershed (in the interior region) was transported by tunnel to the Kemano powerhouse for discharge into the Gardner Canal. This discharge is highly regulated through control structures on the Nechako watershed and exhibits little variation throughout the year.

Kemano River basin water is similar in seasonal discharge patterns to the Kitimat River, although the stored discharge of late spring and early summer is somewhat more dominant.

Considerable year-to-year variability is present in the river flow discharges as shown by the Kitimat River annual average discharge rate from 1967 to 2002 (see Figure C-4). In any given year, the actual discharge can differ by up to 20% from the long-term annual average value. The river discharges were unusually low in the mid-1980s and reached a record high value in 1991.

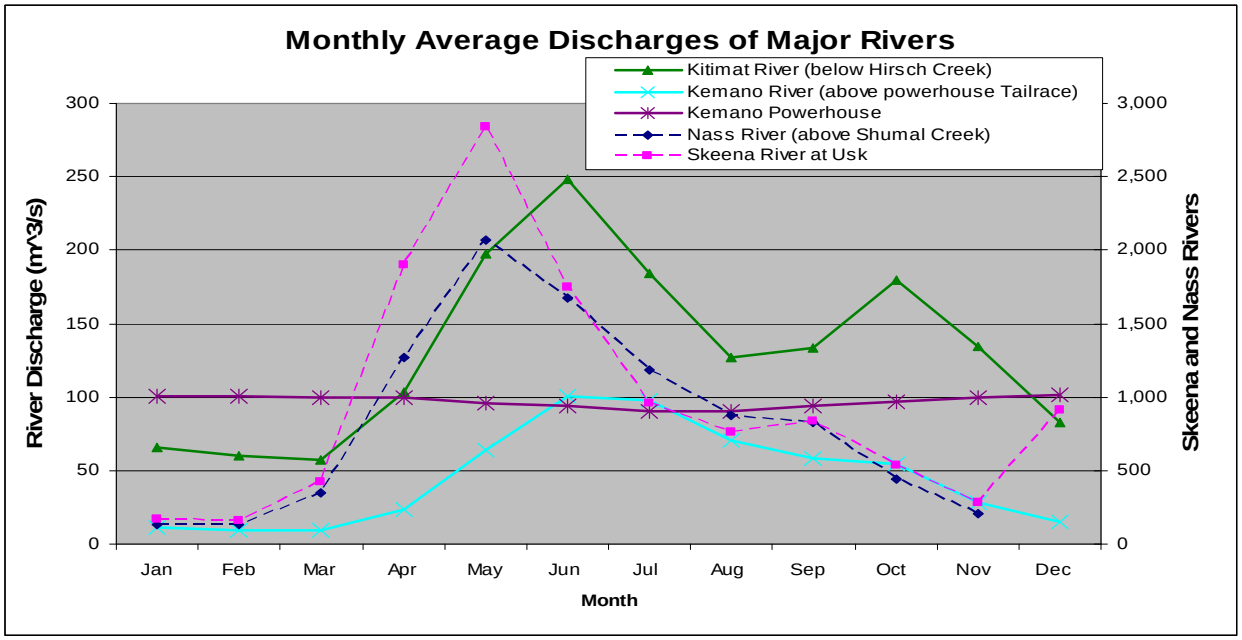

NOTE: The Nass and Skeena River discharge values (dashed lines) are plotted against the right-hand scale, whereas the other rivers are plotted against the left-hand scale.

Figure C-3 Monthly Discharge of the Major Rivers Draining into the Kitimat Fjord System

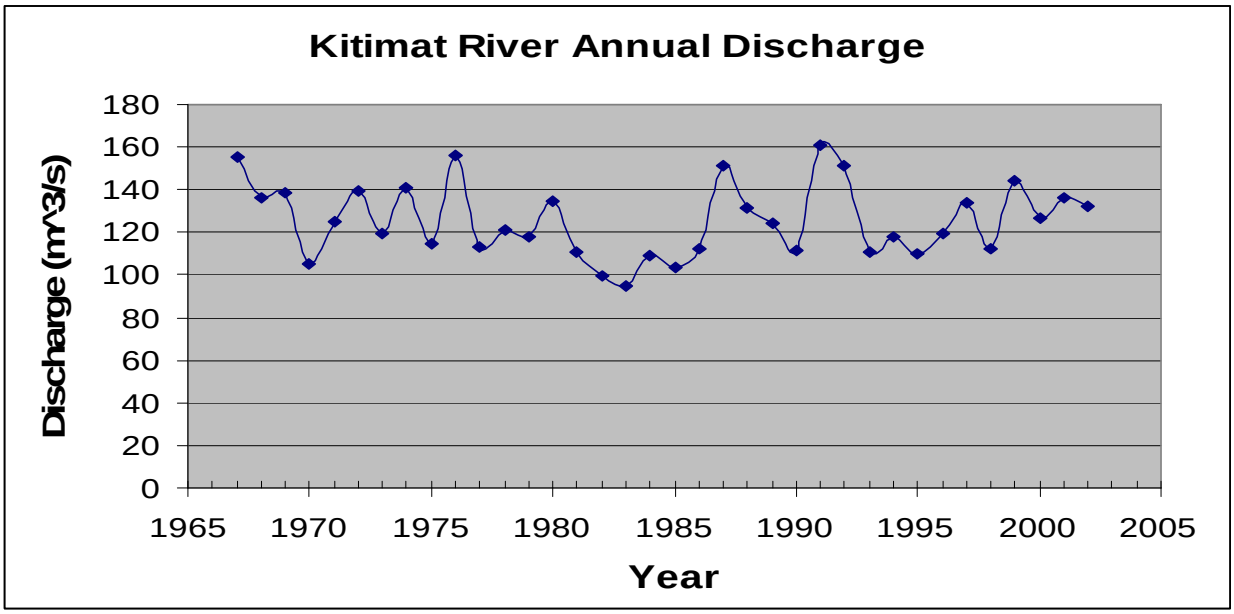

Figure C-4 Yearly Discharge Rate, Kitimat River below Hirsch Creek, 1967 to 2002

CCAA Discharge Basins

Gauged river data are available from only three sites draining into the CCAA, the Kitimat River and the two gauges on the Kemano River. However, the total land area that discharges fresh water into the CCAA covers a much greater total area than the three gauged rivers. An analysis of NTS 1:50,000 topographic maps issued by Natural Resources Canada was carried out to divide the full area of interest into major discharge basins (see Figure C-5). Twenty-nine discharge basins were identified, including the two gauged river basins. For this analysis, the drainage into selected areas adjoining the CCAA was examined, including Gardner Canal, Kildala Arm, Devastation Channel, Verney Passage and Whale Channel. Areas that drain into Grenville Channel and Princess Royal Channel were not included. Not all the fresh water that enters the selected adjoining areas passes through the CCAA, as the actual trajectory of the fresh water will depend on the currents as driven by variable winds and tides (see Appendices B and G).

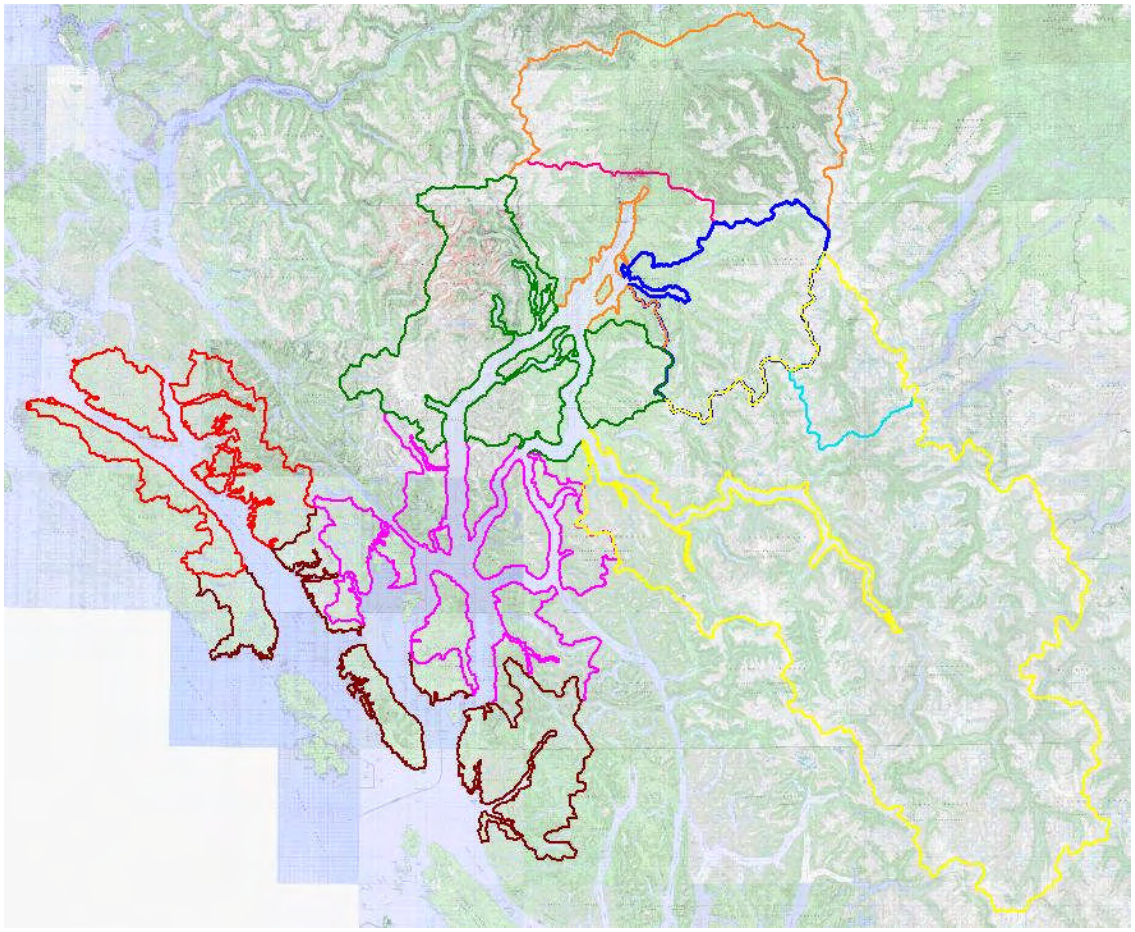

NOTE: The major drainage basins of the extended study area as derived from analysis of 1:50,000 scale National Topographic maps, colour boundaries defined below.

SOURCE: National Topographic Map #103H

Figure C-5 Major Drainage Basins around the CCAA

Each identified basin feature can have either a single major discharge point (a river or similar discharge watercourse, e.g., Jesse Falls) into the marine waterways or can have several smaller discharge points, consisting of a network of small rivers and creeks. Within some of these drainage areas, the single outlet concentrated subareas were identified and mapped. Eight concentrated drainage subareas were identified. Other such drainage subareas also exist in the CCAA. At their outlets, the freshwater discharge into the adjoining ocean waterways will be more concentrated than at other shoreline locations, resulting in small, localized areas where the oceanic surface waters have lower salinities as well as altered temperatures.

The 29 drainage basins were grouped according to distinct portions of the waterways receiving the land-based discharges. The following seven major basins were identified within the CCAA and its environs (indicated on Figure C-5 by the distinct colours of adjoining drainage basins):

- Principe Channel (red)
- Southern waterways: Campania Sound, Caamaño Sound, Squally Channel, Otter Channel, Estevan Sound and southern Principe Channel (brown)
- Southern Douglas Channel, Whale Channel, Verney Channel, Ursula Reach and Mackay Reach (cyan)
- Central Douglas Channel including Devastation Channel (green)
- Kitimat Arm, including northern Douglas Channel (orange)
- Kildala Arm (blue)
- Gardner Canal (yellow)

Table C-2 summarizes the area of each of the seven waterways, along with the adjoining land area, which discharges into the waterway. Note that the water areas exclude major islands that have comparatively high elevations of 300 m or more. The drainage from major islands is assumed to follow the monthly pattern of river discharges. However, for smaller islands with elevations of less than 300 m, the area of these islands is included in the water area. Precipitation falling on these small islands will result in almost immediate direct discharge into the waterway because the land elevations are comparatively low and storage of precipitation in the form of snow will involve only small volumes of water over short periods (see Table C-3).

Freshwater Budget

The amount of fresh water flowing into the CCAA is calculated on a monthly basis for each of the seven waterways identified in Table C-2, after methods of LeBlond et al. (1983). Freshwater input to the ocean consists of two major parts:

- the freshwater input due to land runoff from rivers, creeks and other drainage features
- direct total precipitation (rainfall and snowfall) that enters the ocean directly from the atmosphere or from small, low elevation islands

Table C-2 Total Areas of the Seven Major Waterways and Adjoining Watersheds

Zone #	Name	Water Area (km^2)	Major Islands (km^2)	Land Drainage Area (km^2)
1	Principe Channel	374.8	258.5	725.0
2	Southern Waterways	1,415.7	253.3	953.5
3	S. Douglas, Whale and Verney Channels	705.9	536.4	853.0
4	Central Douglas Channel, Devastation Channel	324.4	309.1	1,351.3
5	Kitimat Arm	142.0	11.3	2,775.0
6	Kildala Arm	22.1		1,064.5
7	Gardner Canal	215.1		6,508.2
Total		**3,200.0**	**1,368.6**	**14,230.5**

Table C-3 Precipitation Sources and Land Discharge Areas

Precipitation Data Sources for Water Area	Land Discharge Areas
Bonilla Island (1/2), Hartley Bay (1/2)	W.Pitt I; NE.Banks I.; Angier I.; S.McCauley I.
Ethelda Bay (1/2), Hartley Bay (1/2)	E.Campania.Sd.; Campania I.; SE.Banks I.; SW.Pitt I.; S.Gil I.
Hartley Bay	E.Whale Chan.; Gribbell I.; SE.Pitt I.; E.Ursula Chan; SE.Grenville Chan; N.Gil I.; S.Hawksbury I.; Farrant I.; Promise I.
Hartley Bay (1/2), Kitimat (1/4), Kitimat Town (1/4)	W.Douglas Chan; E.Devastation Chan; N.Hawksbury I. NE.Verney Passage; Maitland I.; Loretta I.
Kitimat (1/2), Kitimat Twon (1/2)	Kitimat Arm Basin; Eagle Bay Basin; Coste I.
Kildala	Kildala Arm Basin
Kemano	Gardner Canal Basin

The freshwater discharge from river runoff is calculated for each waterway by dividing the total adjoining land drainage area by the drainage area (see Table C-2) of the closest gauged river and then applying this ratio to the monthly values of the gauged river discharge. The freshwater discharge directly from precipitation is calculated from monthly precipitation measurements at the nearest or a combination of the nearest weather stations (see Table C-4) by applying the monthly average rate of precipitation to the total surface area of the waterway (see Table C-2).

Table C-4 Weather Stations with Long-term Measurements in or near the CCAA

Weather Station	Years of Data	Latitude	Longitude	Data Collected
Bonilla Island	1960 - 2002	53° 30' N	130° 38' W	Wind, temperature and precipitation
Ethelda Bay	1957 - 1991	53° 3' N	129° 41' W	Temperature and precipitation
Hartley Bay	1973 - 1996	53° 25' N	129° 15' W	Temperature and precipitation
Kitimat 2	1966 - 2002	54° 1' N	128° 42' W	Temperature and precipitation
Kitimat Town site	1954 - 2002	54° 3' N	128° 38' W	Temperature and precipitation
Kildala	1966 - 2000	53° 50' N	128° 29' W	Temperature and precipitation
Kemano	1951 - 2002	53° 33' N	127° 56' W	Temperature and precipitation

The relative importance of land-derived freshwater runoff to direct precipitation varies considerably among the seven waterways within the CCAA. In the seaward Zones 1 to 3 (see Table C-2), consisting of Principe Channel, the outer southern waterways and southern Douglas Channel, the freshwater contribution from direct precipitation is comparable to or even greater than the river discharge values (see Figure C-6). For the more inland waterways, the river discharge contribution is much greater than direct precipitation because of the larger drainage basins and the smaller size of the receiving waterways. The combined total river runoff for Kitimat Arm (Zone 5) and Kildala Arm (Zone 6) has an average monthly volume of 0.49 km^3, about 24 times more than direct precipitation. Gardner Canal has an average total river discharge of 1.71 km^3 per month, nearly 60 times more than the amount of direct precipitation. About 20% of the total river discharge in Gardner Canal, or 3.1 km^3 per month, is diverted water from the Nechako River basin through the Kemano powerhouse into the Gardner Canal.

For the total freshwater discharge by month for Zones 1, 2 and 3 (southern waterways), Zones 4, 5 and 6 (Central and Northern Douglas Channel including Kitimat Arm and Kildala Arm) and Zone 7 (Gardner Canal), see Figure C-7. The seasonal pattern in all zone combinations is generally similar but somewhat different in the details. In the southern zones, freshwater discharges peak in the fall because of the heavy precipitation associated with the intense autumn Pacific storms. In central Douglas Channel and further north, the river freshet month of June has the largest discharges with a secondary peak in October due to fall storms. In Zone 7 (Gardner Canal), discharges in June and July are dominant with a steady decrease in discharge occurring through the fall. For all zones, the minimum freshwater discharges occur in winter and early spring (January to April).

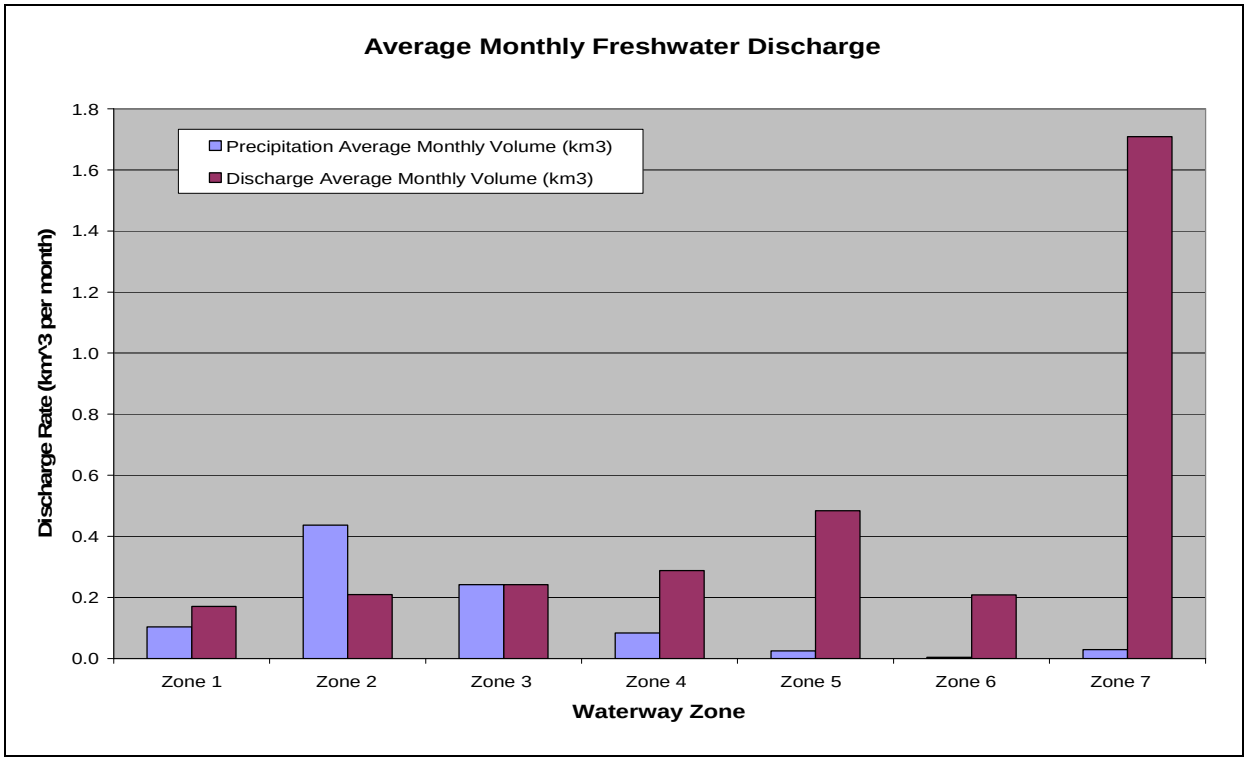

Figure C-6 Monthly Freshwater Input to Waterway Zones, 1967 to 2001

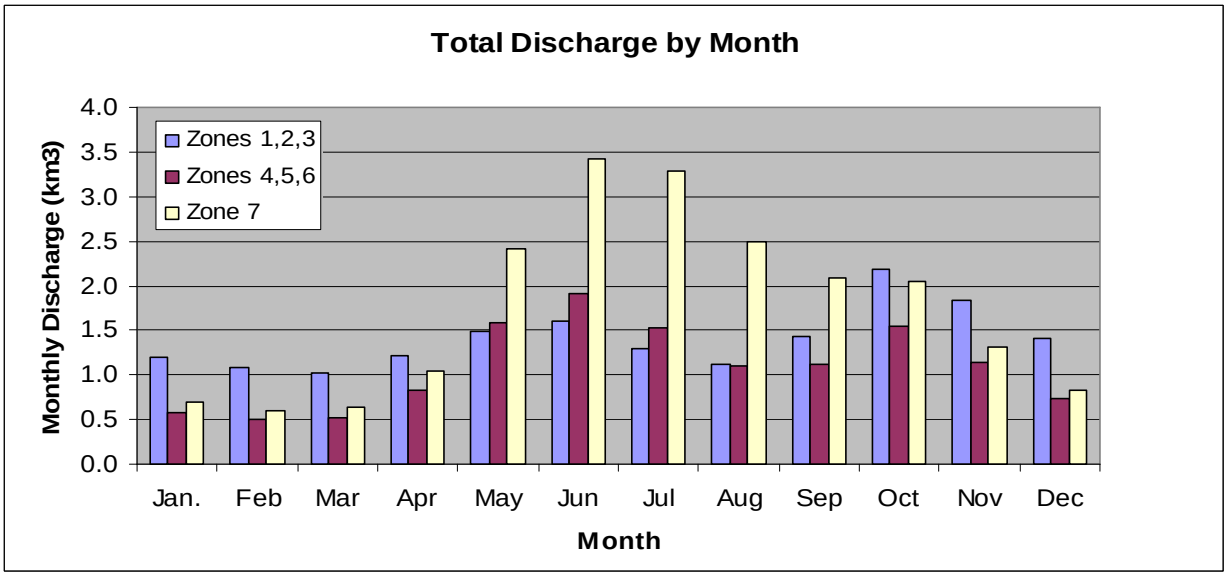

NOTE: Monthly average total discharge volumes (km^3) for the southern zones (Zones 1, 2, 3), Douglas Channel with Kitimat Arm and Kildala Arm (Zones 4, 5, 6) and Gardner Canal (Zone 7)

Figure C-7 Monthly Discharge Volumes for the Southern Zones, Douglas Channel with Kitimat and Kildala Arms, and Gardner Canal

The year-to-year variations in total freshwater discharge (see Figure C-8) are considerable with differences of up to 50%, as seen in the contrast of the low levels of the mid-1980s to the high total discharges of the early 1990s. Notice the high coherence in variations among zones.

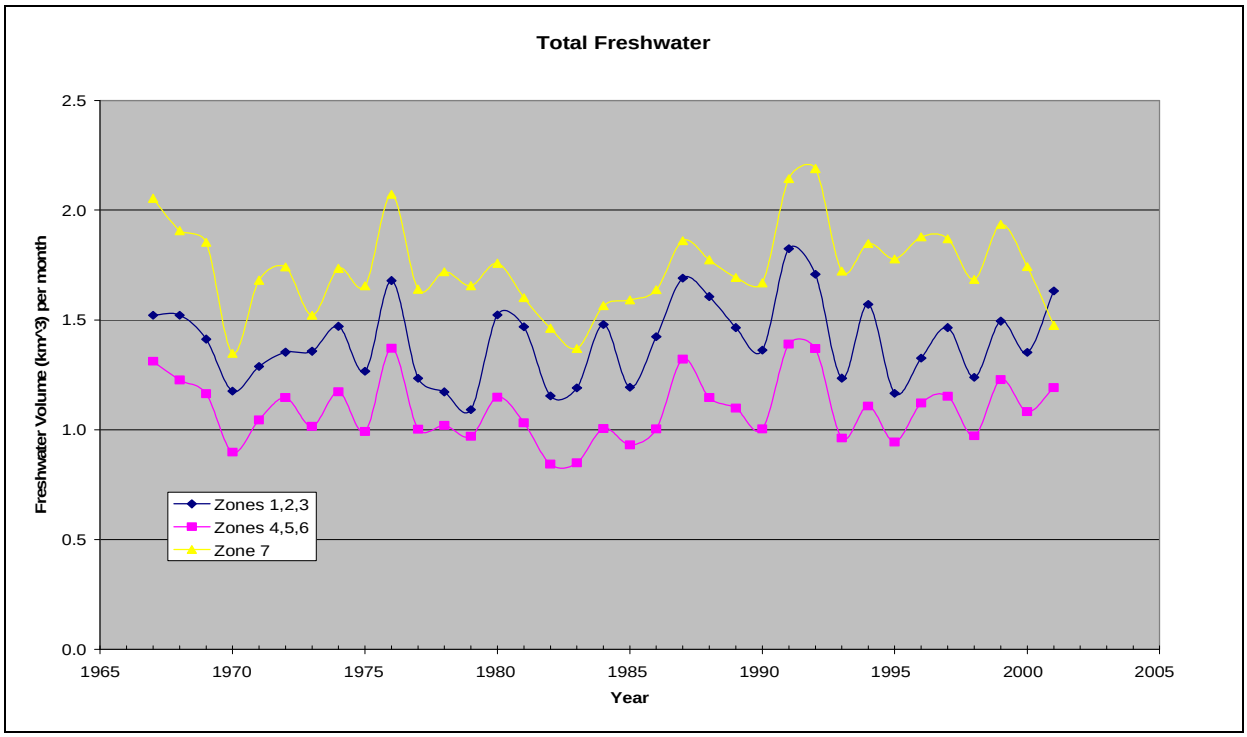

Figure C-8 Total Freshwater Discharge in Groups of Waterway Zones, 1967 to 2001

The total monthly freshwater discharge within each zone can be represented as an equivalent water depth calculated as total discharge divided by surface area of the zone (as shown for each zone and cumulatively for Zones 1 through 7, see Figure C-9). In the outer southern zones, the equivalent monthly depth of fresh water is less than 1 m. In the more inland zones (Zones 4, 5, 6 and 7), the equivalent monthly freshwater depth shows a pronounced increase to 1.2 m in Zone 4 (central Douglas Channel), to 3.6 m in Zone 5 (northern Douglas Channel and Kitimat Arm) and to very large values of 9.6 m and 8.1 m in Kildala Arm and Gardner Canal, respectively.

The deposited fresh water results in an estuarine circulation that carries the fresh water seaward in the surface layer. All fresh water in Kildala Arm (Zone 6) will pass through Zone 5 and then through Zone 4, Zone 3 and Zone 2. The larger freshwater discharges into Gardner Canal will enter Zone 4, but some of this water may travel north through Devastation Channel into Zone 5 before crossing Zones 4, 3 and 2. Consequently, the total freshwater discharge into downstream zones is better represented by the cumulative amount of discharge from more inland zones

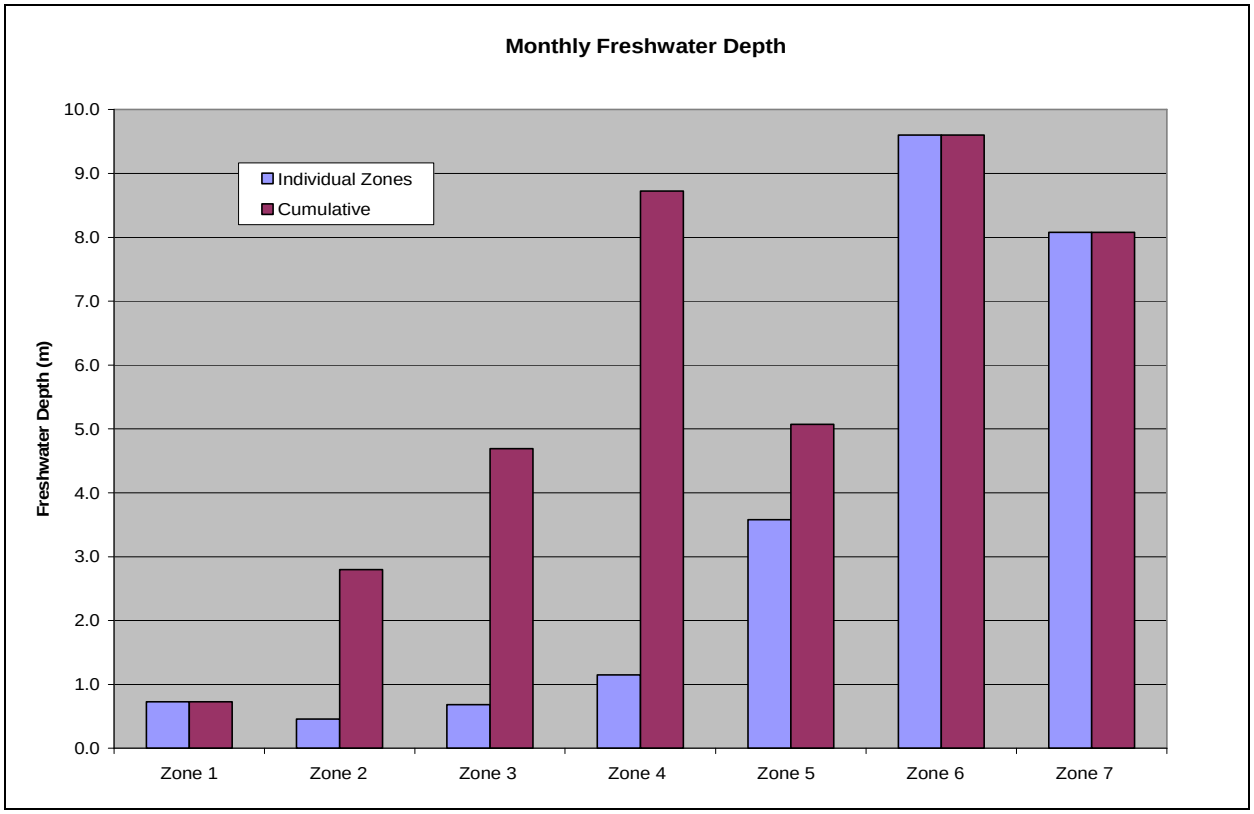

Figure C-9 Equivalent Monthly Freshwater Depth

The equivalent freshwater depth increases to just over 5 m in Zone 5 (northern Douglas Channel and Kitimat Arm) and to nearly 9 m in Zone 4 (central Douglas and Devastation Channels). Further south, in Zones 3 and 2, the channels increase in area because of the greater widths and because there are more channels in total. As a result, the equivalent depth decreases to values of 4.7 and 2.8 m, respectively.

The estimated equivalent freshwater depths are approximate in nature because the advection and dilution rates vary on smaller scales than those of the waterway areas used in these calculations. In addition, wind and tidal currents influence advection rates and the distribution of diluted fresh water in the ocean.

C.3.2.1 Temperature and Salinity

Temperature and Salinity Profile Data Sets

The basic physical oceanographic water property parameters are temperature and salinity. Salinity is directly related to freshwater input, which, as discussed above, occurs in large quantities that vary considerably with time and location within the CCAA. For this region, salinity is the dominant contributor to density, so the salinity profiles (variation with depth) are almost identical to the density profiles. Salinity is measured in practical salinity units (psu), which is functionally equivalent to salt concentration in parts per thousand (ppt).

Temperature-salinity profile data sets (for 421 data sets, for the locations shown in Figure C-2) were selected for analysis and allocated to 15 discrete subareas (shown as boxes A to O, see Figure C-10). Each box typically measures about 15 km in linear dimension. In boxes of this size, spatial changes over smaller distances are not represented. Important horizontal gradients in water properties occur, especially at the mouths of rivers and creeks or because of internal wave features that propagate along the strong density gradient below the upper freshwater layer. The northern section of Kitimat Arm has a considerable small-scale variation in temperature and salinity over distances of hundreds of metres to kilometres (see Figure C-11).

From the mean profiles derived for each box by individual months, the seasonal variability and year-to-year variability of the water properties were calculated and analysed. Different seasonal and interannual patterns are analysed for each box according to data availability.

The temperature and salinity profiles in the CCAA consistently reveal a distinct upper layer up to 10 to 15 m in depth, characterized by much reduced salinities from the underlying deeper waters. From late spring through fall, the salinities are much reduced from those at depth, resulting in a large density gradient between the upper layer and the remainder of the water column. The lower salinities result from the large amounts of freshwater discharge from land runoff and direct precipitation. The upper layer also has higher water temperatures in spring, summer and fall. Based on four summer cruises to the Kitimat system from 1951 to 1960, Pickard (1961) gives the depth of the upper layer at the head of Douglas Channel (Kitimat Arm) as 3 to 7 m, with typical salinities of 3 psu just below the surface and 9 to 21 psu near the bottom of the upper layer. The July 1977 profiles (see Figure C-12) seem to be in reasonable agreement with this characterization.

The high degree of density stratification tends to isolate the upper layer from the remainder of the water column. The less dense, reduced salinity waters have more buoyancy, resulting in a distinct seaward flow of the upper layer. Mixing along the bottom of the low salinity upper layer with the more saline water beneath results in a compensating flow directed up the inlets opposite to the surface layer flow. This flow pattern, called estuarine circulation, is illustrated in Appendix B (see Figure B-6).

In addition to the pronounced seasonal changes in the shallow upper layer salinity and temperature properties, most of the temperature-salinity profiles reveal a mid-water feature (from 5 to 10 m to 50 to 100 m) where a gradual increase in salinity and density, as well as a temperature minimum, occurs from winter through spring (Pickard 1961). The temperature minimum results from fall and winter cooling through heat loss to the surface followed by local warming of the upper layer due to seasonal changes or even from individual weather events. This layer, when present, will be referred to as a cold halocline (cold temperatures accompanied by increasing salinities) or intermediate layer.

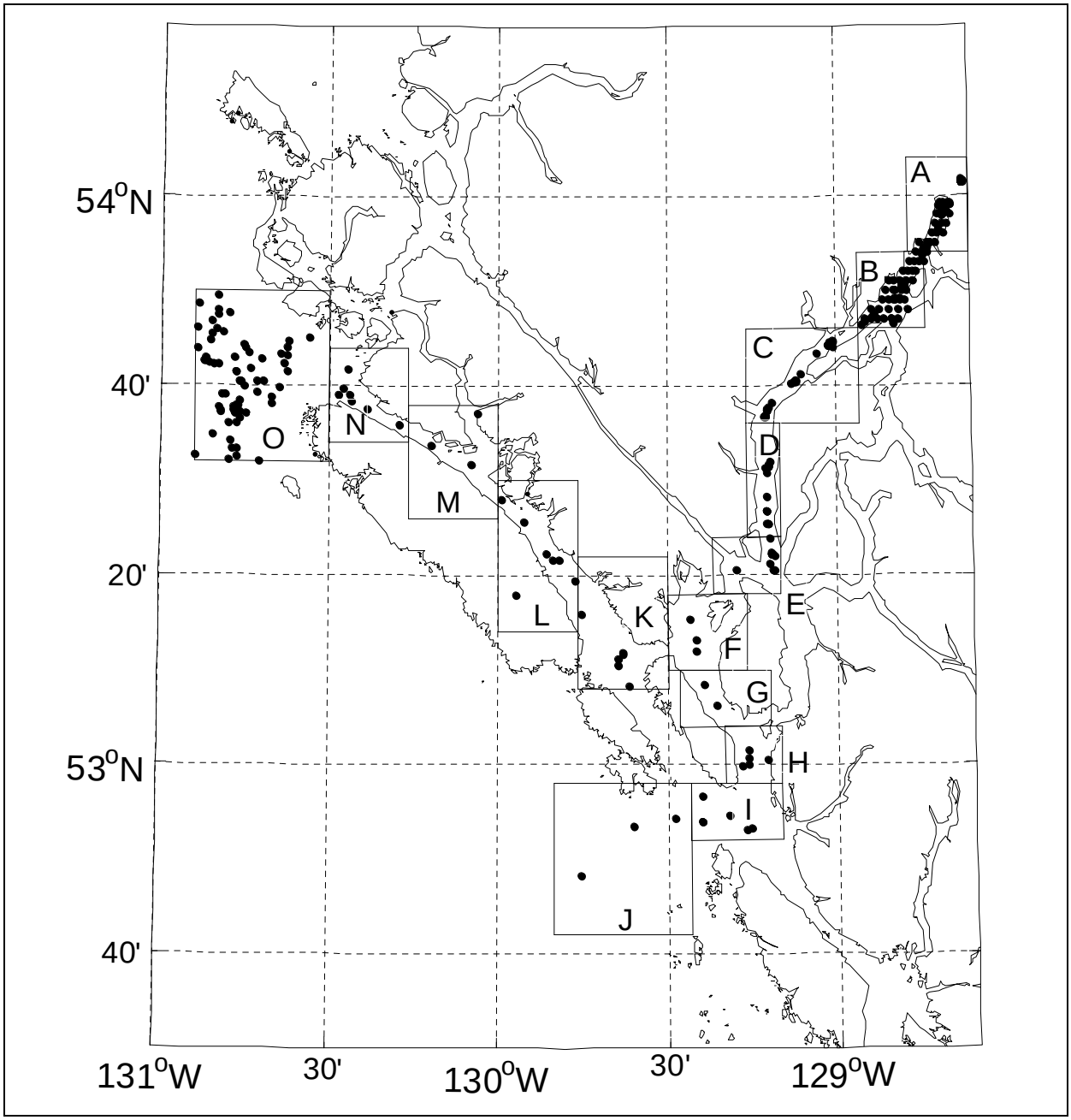

Figure C-10 Boxes for Grouping the Conductivity and Temperature at Various Depths and Bottle Profile Measurement Sites

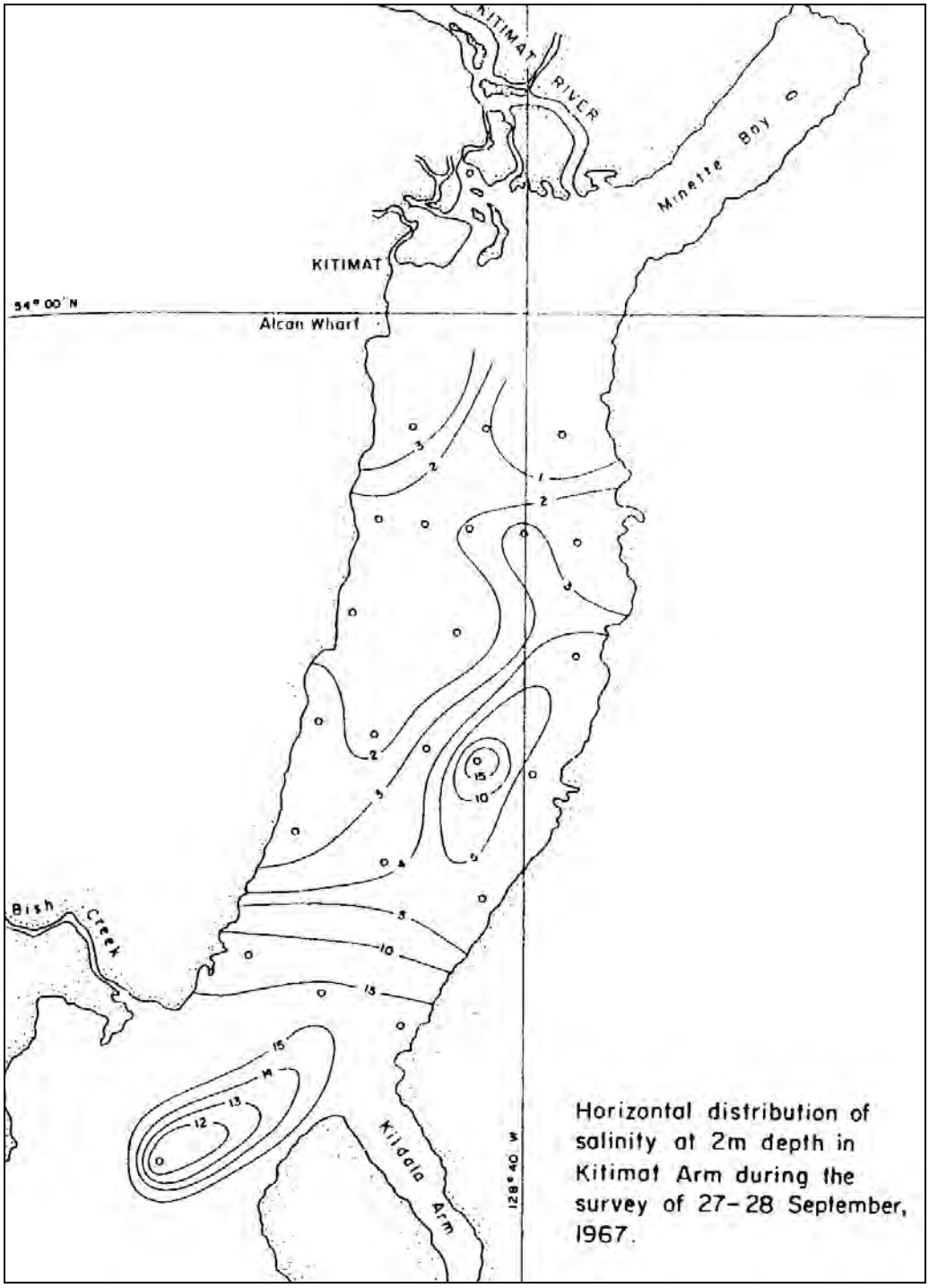

SOURCE: Bell and Kallman 1976 using data collected in 1967 by Waldichuk et al. 1968. Contours are salinity in psu.

Figure C-11 Salinity Distribution at 2-m Depth in Northern Kitimat Arm from Bish Creek to Kitimat River Mouth, 1967

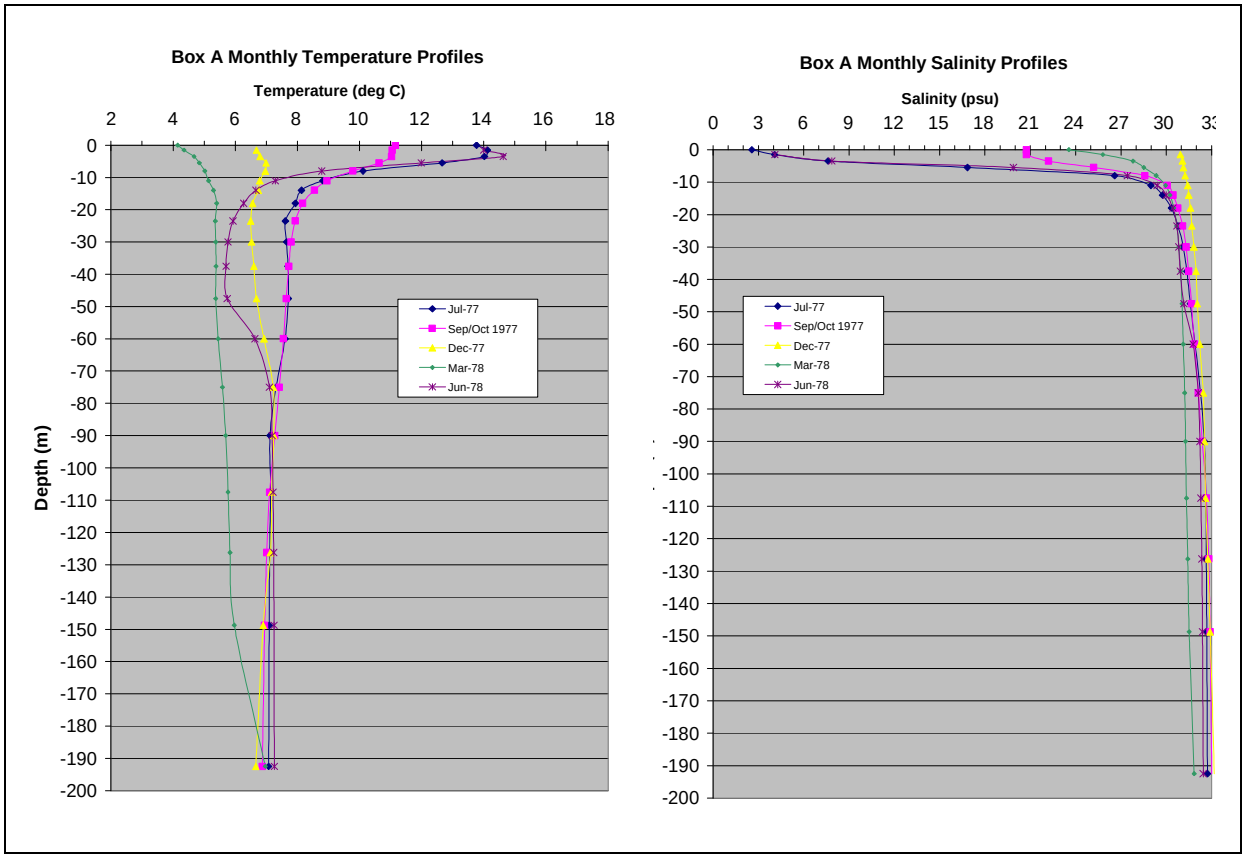

SOURCE: Webster 1980

Figure C-12 Average Temperature and Salinity Profiles in Box A, 1977 and 1978

Surface Temperature and Salinity Distributions

Long-term continuous measurements of surface temperature and salinity are limited to just two data sources in the CCAA: daily temperature and salinity measurements at the Bonilla Island light station at the eastern side of north Hecate Strait (from 1960 to 2005) and surface temperature measurements made at the Nanakwa Shoal weather buoy in northern Douglas Channel (from 1988 to 2005).

The Bonilla Island data (see Figure C-13) show that average monthly surface salinities exhibit a very small or negligible seasonal cycle with the average monthly salinities in a narrow range of values from 31.0 to 31.4 psu. This suggests that the seasonal effects of river runoff at this exposed oceanic location are quite small compared to those in the adjoining inland waters. The seasonal temperature variations appear to follow the seasonal air temperatures with average sea temperatures of 6.5°C in February and 12.5°C in August.

Figure C-13 Monthly Sea Surface Temperature and Salinity at Bonilla Island, 1960 to 2005

Surface temperatures have been measured at the Nanakwa Shoal buoy since 1988. The annual range in monthly average temperatures is much greater than at Bonilla Island (see Figure C-14). The minimum monthly average temperature of 5.2°C occurs in January, while the maximum monthly value of 16.1°C occurs in August. The range from the lowest to the highest measured temperature is much greater at –0.4°C to 22.3°C. The larger range of sea temperatures is similar to the increased range in air temperatures experienced between inland and open-coast weather stations (see Appendix A).

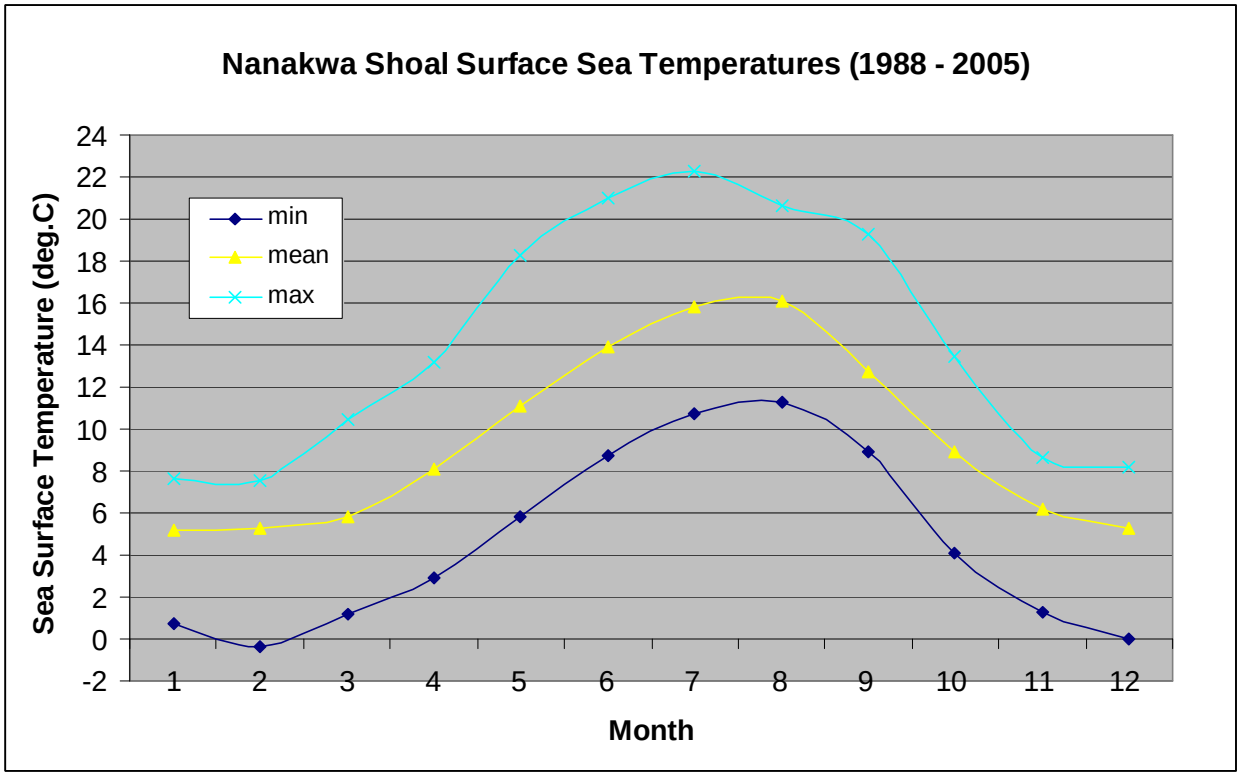

Figure C-14 Monthly Sea Surface Temperature at the Nanakwa Shoal Buoy, 1988 to 2005

There are no continuous measurements of salinity at any inland water location. However, based on the irregularly sampled temperature-salinity profile database (from 1951 to 2004), the surface salinity and temperature statistics for the surface layer can be calculated (see Table C-5). For the selected month, the salinities in Box A, furthest inland in Kitimat Arm, are considerably lower compared to those in Box C (Douglas Channel) and Box E (Wright Sound). Given the limited sample size of only 5 to 35 measurements per month in Box A and fewer measurements in the other boxes, the minimum and maximum values will underestimate the long-term extreme values of near-surface temperatures and salinities.

Table C-5 Surface Temperature and Salinity Values in Kitimat Arm, Douglas Channel and Wright Sound

		Average Temperature					Minimum Temperature						Maximum Temperature					
	Avg. Depth	Mar	May	Jul	Oct	Dec	Avg. Depth	Mar	May	Jul	Oct	Dec	Avg. Depth	Mar	May	Jul	Oct	Dec
Box A	0.0	4.8	10.1	14.3	8.2	2.2	0.0	4.1	7.8	10.9	7.2	2.2	0.0	6.4	11.5	17.3	11.2	2.2
	1.5	4.2	10.1	14.3	9.0	5.2	1.5	3.5	7.8	11.8	7.1	2.3	1.5	5.9	12.0	15.8	11.3	7.6
Box C	0.0		10.1	14.0	10.0	6.6	0.0		9.7	11.4	9.9	6.5	0.0		10.7	17.2	10.1	6.8
	1.5	5.0	9.2	13.2	9.9	6.8	1.5	4.9	8.7	11.2	9.8	6.5	1.5	5.0	9.6	16.9	10.0	7.1
Box E	0.0	5.3	9.3	12.9			0.0	5.2	8.1	11.6			0.0	5.3	10.4	14.4		
	1.5	5.3	8.1	11.9	9.4	6.5	1.5	5.2	8.1	10.7	9.4	6.1	1.5	5.4	8.1	12.7	9.4	6.8
		Average Salinity					Minimum Salinity						Maximum Salinity					
	Avg. Depth	Mar	May	Jul	Oct	Dec	Avg. Depth	Mar	May	Jul	Oct	Dec	Avg. Depth	Mar	May	Jul	Oct	Dec
Box A	0.0	13.0	14.8	3.3	11.0	15.7	0.0	4.4	1.5	0.3	3.7	14.1	0.0	25.6	27.0	7.6	20.8	17.2
	1.5	16.6	15.8	5.2	14.9	25.5	1.5	5.9	1.5	0.3	4.4	14.7	1.5	25.8	27.6	12.7	21.0	31.6
Box C	0.0		21.7	16.7	26.2	24.8	0.0		19.5	12.6	25.4	19.0	0.0		24.8	19.7	26.9	30.6
	1.5	28.7	24.8	17.9	26.3	30.7	1.5	28.2	24.3	15.4	25.7	30.6	1.5	29.4	25.5	19.6	27.0	30.9
Box E	0.0	29.9	26.0	18.7			0.0	29.7	25.8	11.8			0.0	30.2	26.3	24.3		
	1.5	29.9	27.7	21.6	28.7	30.3	1.5	29.8	27.7	17.3	28.7	29.9	1.5	30.2	27.7	25.2	28.7	30.6

Yearly changes in surface temperatures and salinities were also examined for the Bonilla Island light station (see Figure C-15). Changes occur over a few years within a range of 8.2°C to 10.4°C for temperature and 30.6 to 31.6 psu for salinity.

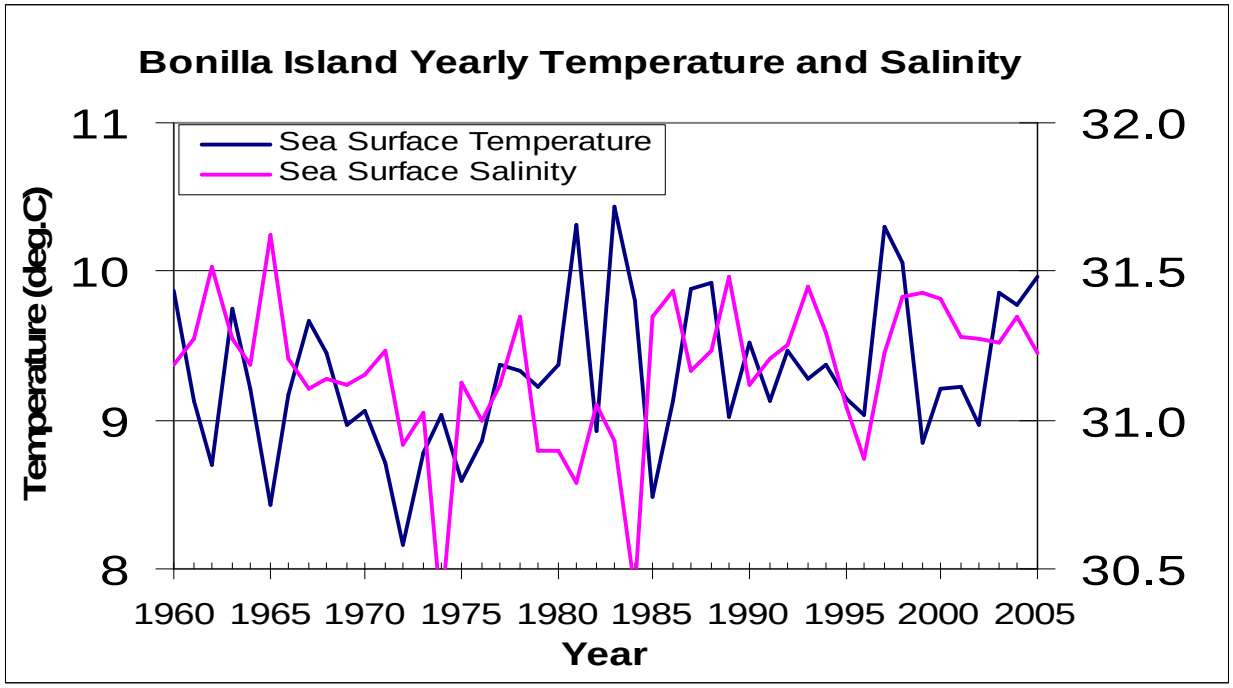

Figure C-15 Annual Sea Surface Temperature and Salinity Values at Bonilla Island, 1960 to 2005

Salinity and Temperature Changes with Distance from Camaaño Sound to Kitimat Arm

The salinity and temperature distributions from Camaaño Sound to Kitimat Arm were calculated for four different months (July 1977, September/October 1977, December 1977 and March 1978) and for July in three different years (1951, 1972 and 1977). These distributions are plotted in Attachment C1.

The distributions for July in three different years show that the intense, but shallow, upper layer extends over the full length of Douglas Channel, with salinities of less than 20 psu and temperatures exceeding 10°C. However, the upper layer in the seaward portions of the CCAA, from Wright Sound through Caamaño Sound, has higher salinities of 20 to 25 psu, although the upper layer temperatures exhibit less change, remaining greater than 10°C.

The salinities in the deeper waters exhibit a modest gradient from beneath the upper layer to values of about 32.5 psu at water depths of 60 to 100 m, depending on the year. At greater depths, the salinities have a narrow range of values from 32.5 to about 33.0 psu. The water temperatures at depth in Douglas Channel are generally in the range of 6°C to 8°C, except when a temperature minimum can occur (observed in 1951 and 1972) with values less than 6°C. Cold temperatures (less than 6°C) also occurred in the deeper waters (greater than 200 to 250 m) of Campania Sound to Wright Sound in July 1977.

The temperature-salinity distributions with depth from July 1977 to March 1978, at approximately three-month intervals, show the expected cooling of the upper layer and a reduction in salinity along with a retreat in the extent of the well-defined, low salinity values. By September and October, upper layer salinities less than 25 psu were confined to boxes A and B, and in December and March, the salinities of the upper layer were close to 30 psu even in Box A (Kitimat Arm).

In the deeper waters, the temperatures had increased in September/October to over 8°C at depths of 40 m and the increase extended to 70 to 160 m in December in the central boxes. This deep temperature maximum may be due to a combination of a remnant of accumulated heat from the previous summer and fall and advection of warmer water into the area from seasonally warmed waters in Hecate Strait. The deepwater temperature remains at less than 7°C.

The deepwater salinities exhibit a tendency to increase from 32.5 to 33 psu from July to September/October and then decrease through December and into March. By March, the deepwater salinities at water depths exceeding 200 m are between 32 and 32.5 psu with some slightly higher salinities near the bottom in central to northern Douglas Channel beyond the sill between Boxes C and D (see Attachment C1).

Seasonal Changes in Salinity and Temperature Distributions

The seasonal changes in the temperature and salinity distributions were examined in more detail for boxes A, D and E (see Figures C-16 to C-18). Box A has the most profile data sets available from three different years for March and October, four years for May and six years for July. The distributions show the development and abatement of the upper layer with the lowest salinities and highest temperatures occurring in July.

The deeper waters show a consistent increase in salinities at depth from May through July to October. The salinity increase amounts to over 0.5 psu in water depths exceeding 200 m. The increase in salinity of the water at depth is accompanied by lower temperatures and lower oxygen concentrations (see Appendix F). The replacement or renewal of the water at depth is driven by upwelling of colder, more saline water in the summer in British Columbia shelf waters, which then flows into the inland waterways at depth and displaces the less dense water. MacDonald et al. (1983) suggest a second mechanism in which the strong winter outflow winds drive the surface waters towards the ocean, which in turn generates an increased flow of more saline water from depth of 30 to 150 m into Douglas Channel. The evidence for this second process occurring on average is not apparent in the temperature-salinity distribution plots calculated from multi-year measurements. However, such a mechanism may be present in particular years. A pronounced increase in salinity and reduction in temperatures was observed in December 1977.

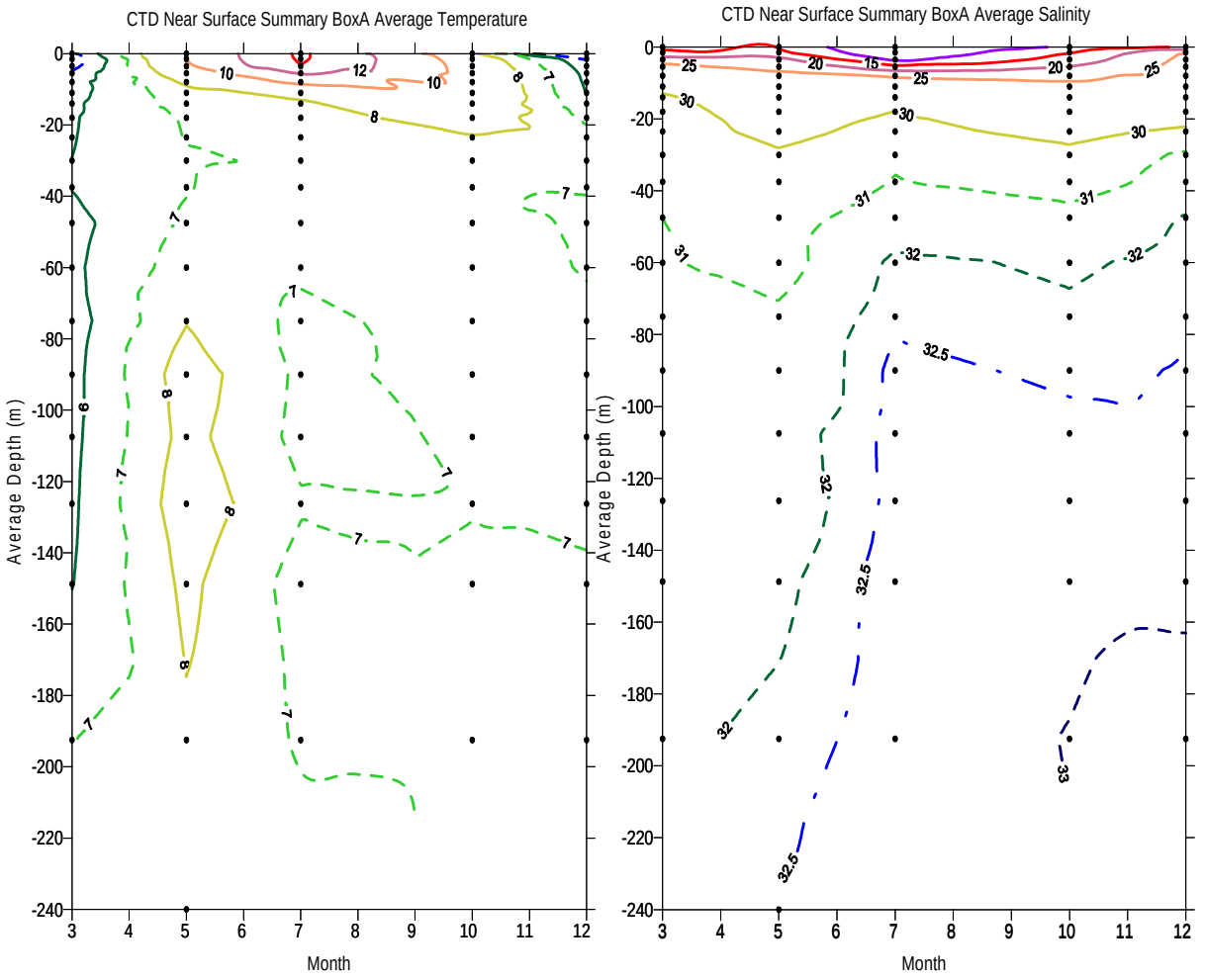

Figure C-16 Temperature and Salinity Depth Distribution for Box A in Kitimat Arm

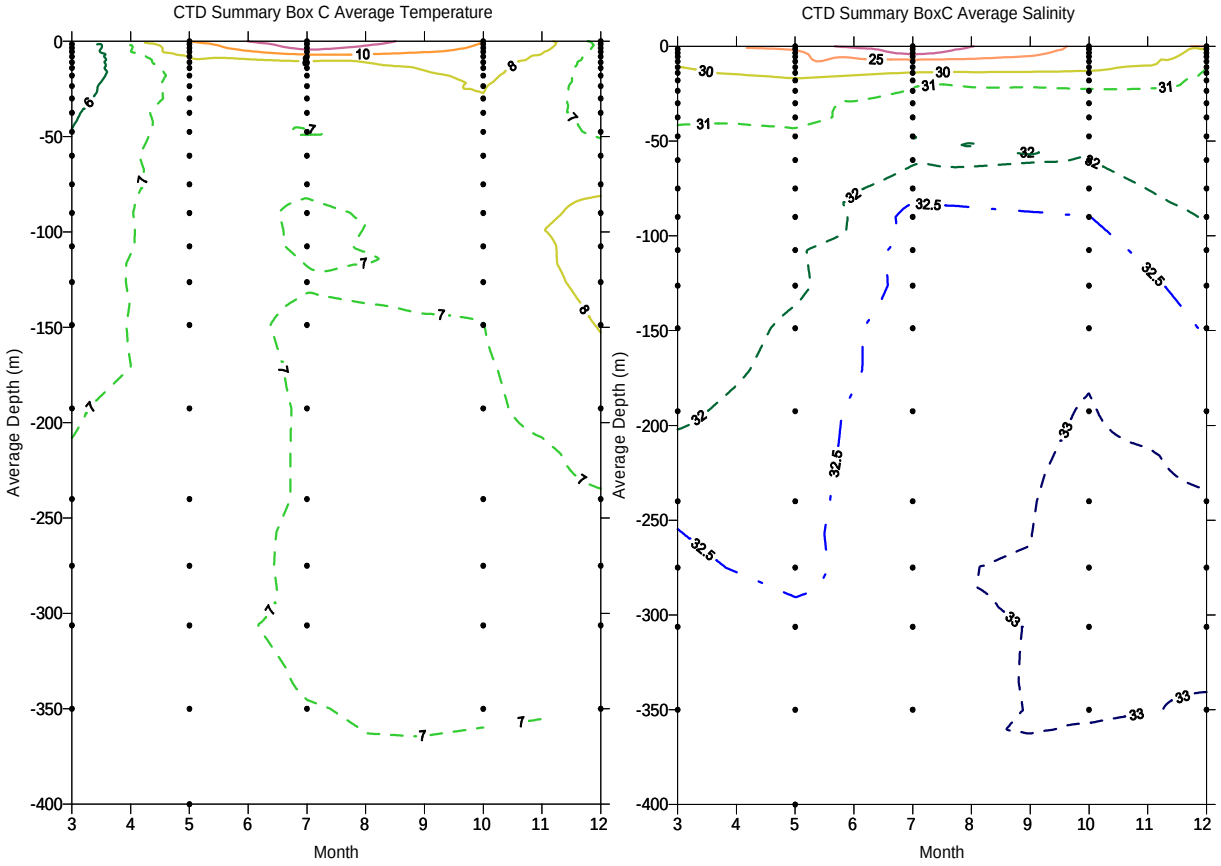

Figure C-17 Temperature and Salinity Depth Distribution for Box C in Central Douglas Channel

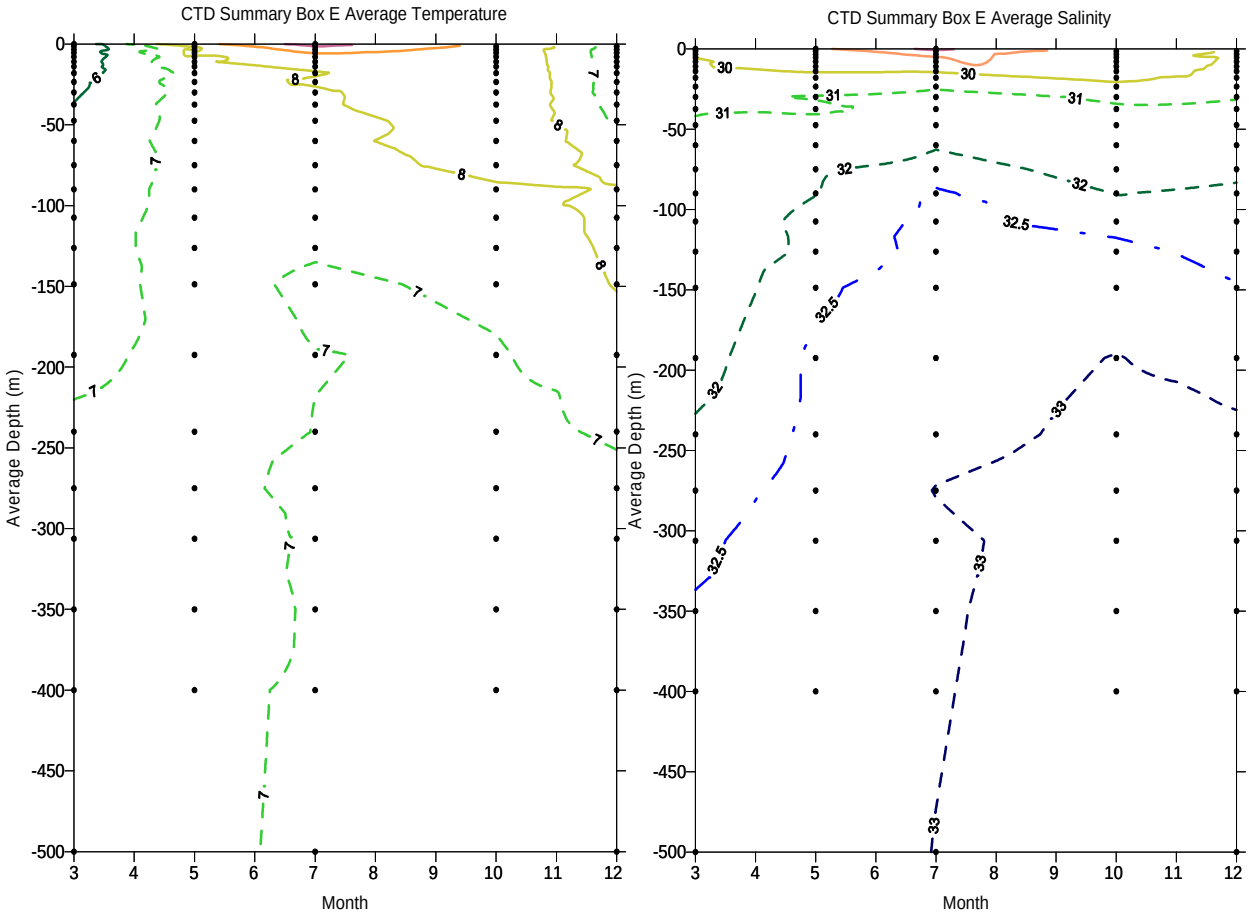

Figure C-18 Temperature and Salinity Depth Distribution for Box E in Wright Sound

Year to Year Variability in Salinity and Temperature Distributions

The variability from year to year was examined by compiling all temperature-salinity profile data sets separately for the months of May and July/August in boxes A, C and E. For Box O in Browning Entrance, data were compiled for the months of May/June and October. The criterion for choosing which month/year data to compile was that at least three profiles must be available for each box considered. For an example of the compilation and analysis, see Table C-6.

An examination of the results indicates that some coherence exists for years with high or low temperature anomalies among Boxes A, C and E, which gives these particular year-month combinations more validity. The level of coherence is small in the upper layer, which likely reflects the small-scale local nature of physical processes in this very dynamic zone. In intermediate and deeper waters, measurements in May indicate that 1966 was unusually cold in the intermediate zone, and the year 1996 was unusually warm. The year 1996 also had unusually low salinity values in the intermediate and deepwater zone.

Table C-6 Temperature and Salinity Measurements in Box A, Kitimat Arm

Avg. Dep	Jul-1951	Jul-1972	Jul-1977	Jul-1981	Jul-1992	Jul/Aug 1993	Aug-1995	Aug-1996	Aug-1999	AVG	SD
Average Temperature											
	16.11	12.88	13.77	14.43		17.50	16.03	15.26		15.14	1.57
1.50		13.73	14.11	14.40	14.39	16.78	15.88	15.34	15.80	15.05	1.06
3.50	15.20	12.01	14.02	14.15	14.14	15.87	15.45	15.16	14.74	14.53	1.14
5.50	12.72	7.28	12.66	13.04	13.72	15.82	15.25	13.57	14.31	13.15	2.46
8.00	8.52		10.11	10.38	13.12	13.79	15.12	12.90	12.04	12.00	2.18
11.00	6.27	6.22	8.81	9.19	8.93	10.77	14.74	11.98	10.27	9.69	2.68
14.00	6.05	5.47	8.13	8.74	8.10	11.65	14.06	8.38	9.12	8.86	2.64
18.00	5.69	5.17	7.94	8.40	7.36	7.82	9.10	6.89	8.04	7.38	1.27
23.50	6.04		7.61	8.22	7.04	6.25	6.46	6.71	7.93	7.03	0.81
30.00	6.39	5.08	7.65	8.09	6.98	6.71	6.69	6.67	8.06	6.39	0.94
37.50	6.60		7.70	8.18	6.99	6.19	7.13	6.69	8.15	7.20	0.74
47.50	6.68	5.59	7.71	8.31		7.41	7.41	7.70	8.13	7.37	0.87
60.00	6.25		7.60				7.50	7.64	7.96	7.39	0.66
75.00		6.40	7.31			7.69			7.34	7.19	0.55
90.00	6.18		7.12						7.18	6.83	0.56
107.50		6.18	7.14			7.68			7.11	7.03	0.62
126.25			7.11						7.07	7.09	0.03
148.75	6.20	6.13	7.09			7.58			7.04	6.81	0.63
192.50	6.21		7.08			7.51			7.04	6.96	0.54
240.00									7.02	7.02	
275.00											
306.25											
350.00											
400.00											
500.00											
Average Salinity											
	3.32	2.07	2.57	5.97		14.74	9.18	4.75		6.09	4.52
1.50		4.35	4.07	6.16	1.94	13.95	9.95	4.91	11.59	7.12	4.21
3.50	7.58	10.87	7.61	9.34	1.99	14.99	20.56	7.58	12.84	10.37	5.31
5.50	16.27	22.68	16.84	15.82	2.33	17.57	26.13	12.48	21.39	16.83	6.82
8.00	28.41		26.58	25.05	10.87	18.31	28.25	13.69	25.99	22.15	6.89
11.00	30.02	27.15	28.99	28.08	26.94	24.90	29.16	16.90	27.96	26.68	3.96
14.00	30.84	30.05	29.76	29.01	27.82	21.30	29.97	26.55	29.27	28.29	2.92
18.00	31.30	30.60	30.34	29.67	29.39	28.66	30.63	29.08	30.40	30.01	0.86

Table C-6 Temperature and Salinity Measurements in Box A, Kitimat Arm (cont'd)

Avg. Dep	Jul-1951	Jul-1972	Jul-1977	Jul-1981	Jul-1992	Jul/Aug 1993	Aug-1995	Aug-1996	Aug-1999	AVG	SD
Average Salinity (cont'd)											
23.50	31.40		30.78	30.19	30.44	29.53	31.07	30.07	31.09	30.57	0.63
30.00	31.75	31.08	31.12	30.59	30.82	30.58	31.35	30.43	31.46	31.02	0.45
37.50	31.90		31.37	30.93	30.88	30.03	31.65	30.57	31.71	31.13	0.64
47.50	32.25	31.75	31.59	31.19		31.70	31.89	32.05	31.92	31.79	0.32
60.00	32.69		31.91				32.18	32.33	32.35	32.29	0.28
75.00		32.46	32.27			32.48			32.75	32.49	0.20
90.00	32.95		32.51						32.84	32.77	0.23
107.50		32.76	32.61			32.62			32.89	32.72	0.13
126.25			32.66						32.92	32.79	0.18
148.75	33.10	32.84	32.69			32.75			32.94	32.86	0.16
192.50	33.07	32.90	32.73			32.83			32.97	32.90	0.13
240.00									33.01	33.01	
275.00											
306.25											
350.00											
400.00											
500.00											

NOTES:
At least three measurements are available within a given month and year.
The highlighted cell values exceed (light yellow) or fall below (light blue) the average by one standard deviation or more.
AVG = average
SD = standard deviation

In July/August observations, 1951 was unusually cold as was 1972 in the intermediate and deep zones. For these same zones, the salinities were unusually low in 1977 and 1999 had unusually high salinities at least in the deep zone.

Overall, the long-term variations in temperature and salinity properties are not large, making it difficult to detect these with the sporadic observations that are available. This long-term trend analysis, when applied to meteorological time series data sets that are available for up to 40 years, indicated that surface air temperatures exhibited a small increasing trend in the annual average values at some measurement sites (see Appendix A).

C.4 References

C.4.1 Literature Cited

Bell, L.M. and Kallman, R.J. 1976. *The Kitimat River Estuary - Status of Environmental Knowledge to 1976.* Special Estuary Series. No. 6. Environment Canada. Vancouver, BC.

British Columbia Ministry of Sustainable Resource Management. 2002. *North Island Straits Coastal Plan*. Coast and Marine Planning Branch. Victoria, BC.

LeBlond, P.H., K. Dyck, K. Penny and D. Cummings. 1983. *Runoff and Precipitation Time Series for the Coasts of British Columbia and Washington State*. Manuscript Report #39, Dept. of Oceanography. University of British Columbia. Vancouver, BC.

MacDonald, R., W. Cretney, C.S. Wong and P. Erickson. 1983. Chemical Characteristics of Water in the Kitimat Fjord System. In *Proceedings of a Workshop on the Kitimat Marine Environment,* Canadian Technical Report of. Hydrography and Ocean Sciences 18. Department of Fisheries and Oceans. Institute of Ocean Sciences. Sidney, BC.

Pickard, G.L 1961. Oceanographic Features of Inlets in the British Columbia Mainland Coast. *Journal of Fisheries Research Board of Canada* 18: 907-982.

Pickard, G.L. and B.R. Stanton. 1979. *Pacific Fjords - A Review of their Water Characteristics*. Manuscript Report. 34. University of British Columbia, Department of Oceanography.

Thomson, R.E. 1989. The Queen Charlotte Islands: Physical Oceanography. In G.G.E. Scudder and N. Gessler (ed.). *The Outer Shores*. Proceedings of Queen Charlotte Islands First International Symposium, August 1984. University of British Columbia. Vancouver, BC. 27-63.

Tyner, R. 1951. *Paths Taken by the Cold Air in Polar Outbreaks in British Columbia*. Meteorological Technical Circular. 18. Meteorological Division. Government of Canada. Ottawa, ON.

Waldichuk, M., J.R. Markert and J.H. Meikle. 1968. Physical and Chemical Oceanographic Data from the West Coast of Vancouver Island and the Northern BC Coast, 1957-1967. *Vol. II Fisher Channel, Cousins Inlet, Douglas Channel, Kitimat Arm and Prince Rupert Harbour and its Contiguous Waters*. Fisheries Research Board Canada Manuscript Report Series 990. Fisheries Research Board. Ottawa ON.

Webster, I. 1980. *Kitimat Physical Oceanographic Study, 1977-78, Part 3, Estuarine Circulation*. Contractor Report Series 80-3 (Part 3). Department of Fisheries and Oceans. Institute of Ocean Sciences. Sidney, BC.

Weingartner, T.J., S. Danielson, and T. C. Royer. 2005. Freshwater Variability and Predictability in the Alaska Coastal Current *Deep-Sea Research* 52: 169 – 192

C.4.2 Internet Sites

British Columbia Ministry of Sustainable Resource Management. 1998. *Central Coast LCRMP Marine Planning Workbook.* B.C. Ministry of Sustainable Resource Management, Coast and Marine Planning Branch. Accessed September 2004. Available at: http://www.ilmb.gov.bc.ca/slrp/lrmp/nanaimo/cencoast/docs/AIP_coastal_zone_plan.pdf

Attachment C1 Salinity and Temperatures Changes with Distance from Camaaño Sound to Kitimat Arm

The salinity and temperature distributions from Camaaño Sound to Kitimat Arm were for four different months (July 1977, September /October 1977, December, 1977 and March 1978) and for three different years (1951, 1972 and 1977) in the month of July (see Figures C1-1 to C1-6).

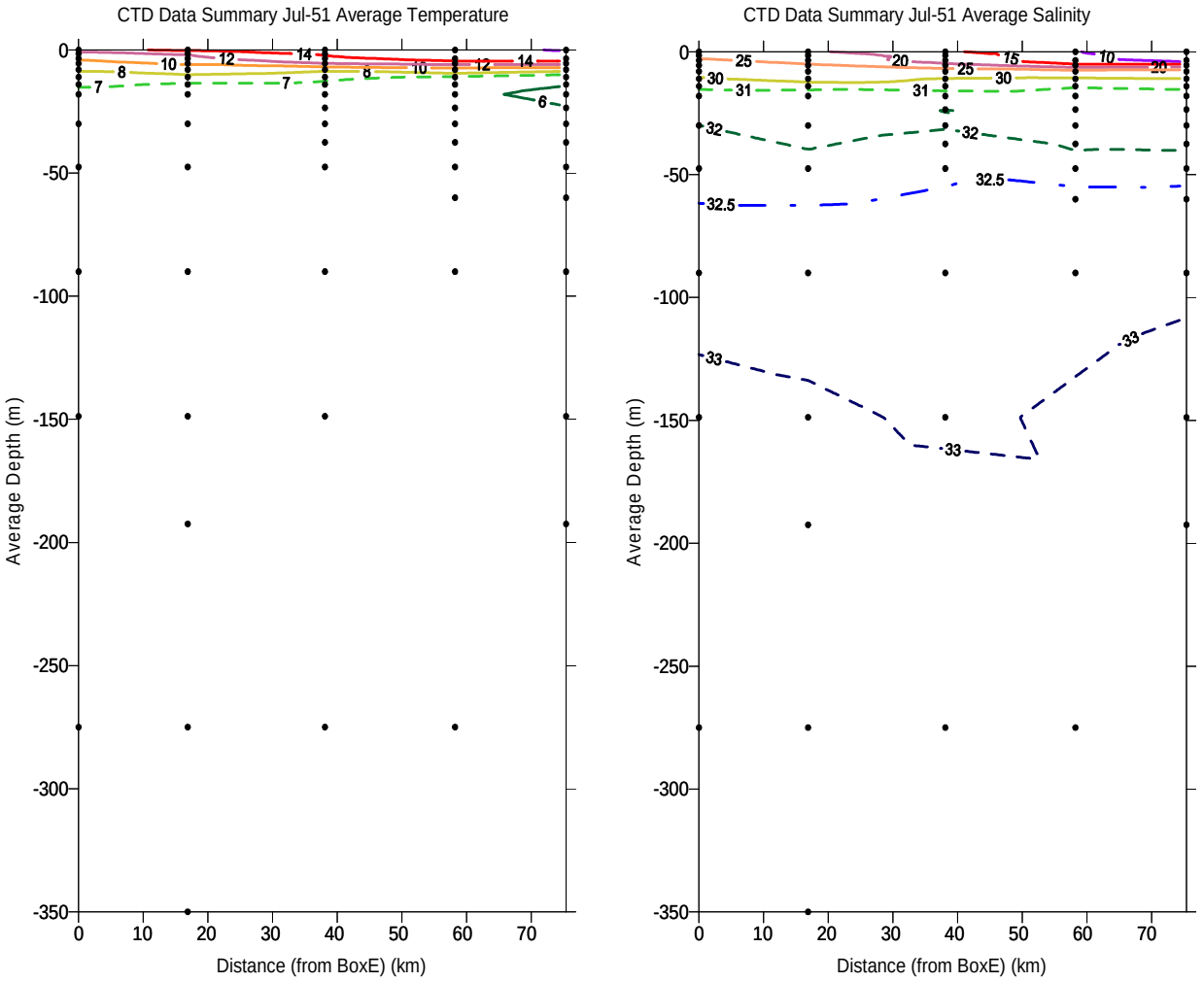

NOTE: Temperature and salinity distribution measured in July 1951 in Douglas Channel (Boxes E, D, C, B and A)

Figure C1-1 Temperature and Salinity Distribution in Douglas Channel, July 1951

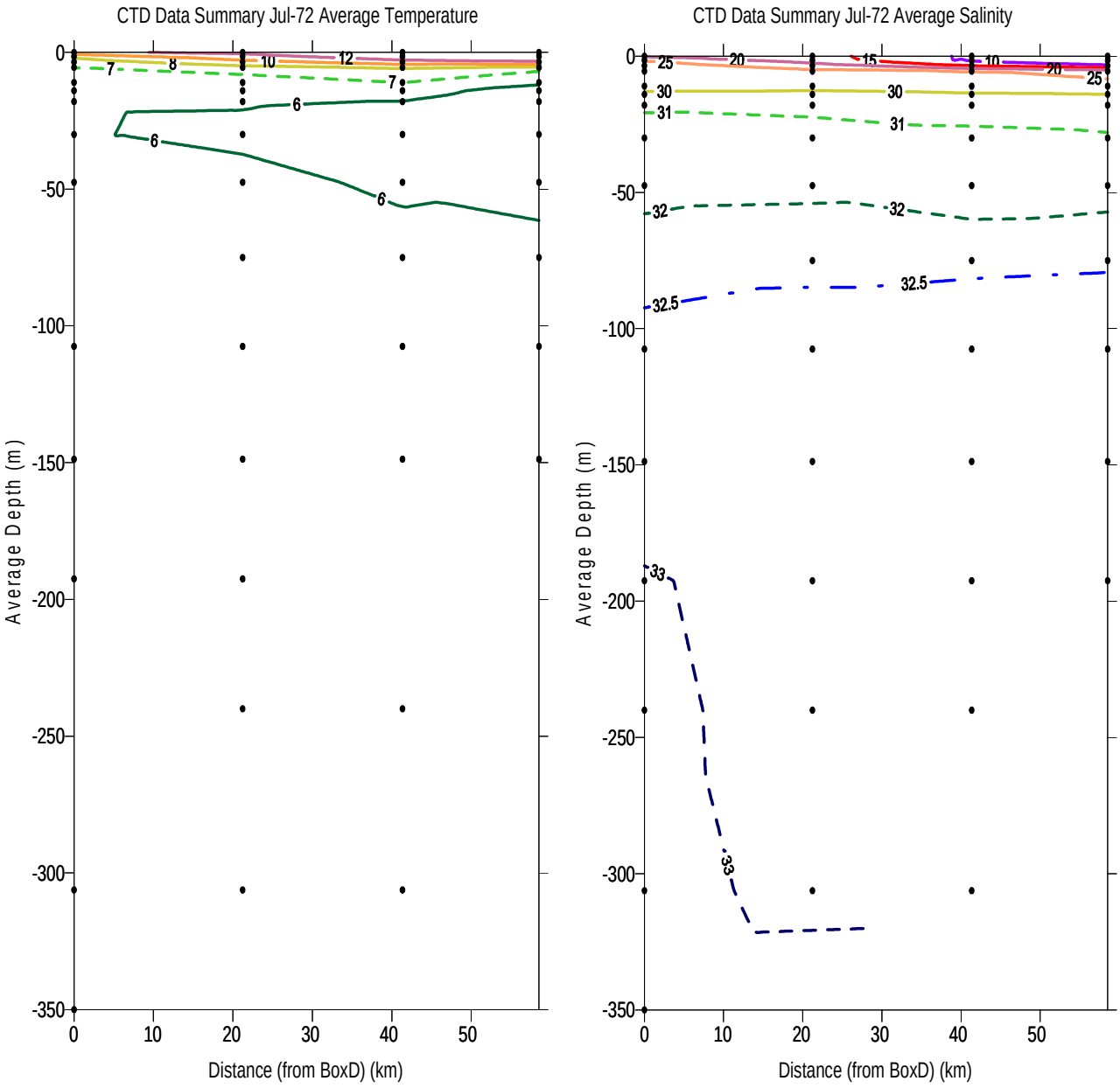

NOTE: Temperature and salinity distribution of July 1972 measured in Douglas Channel (Boxes D, C, B and A)

Figure C1-2 Temperature and Salinity Distribution in Douglas Channel, July 1972

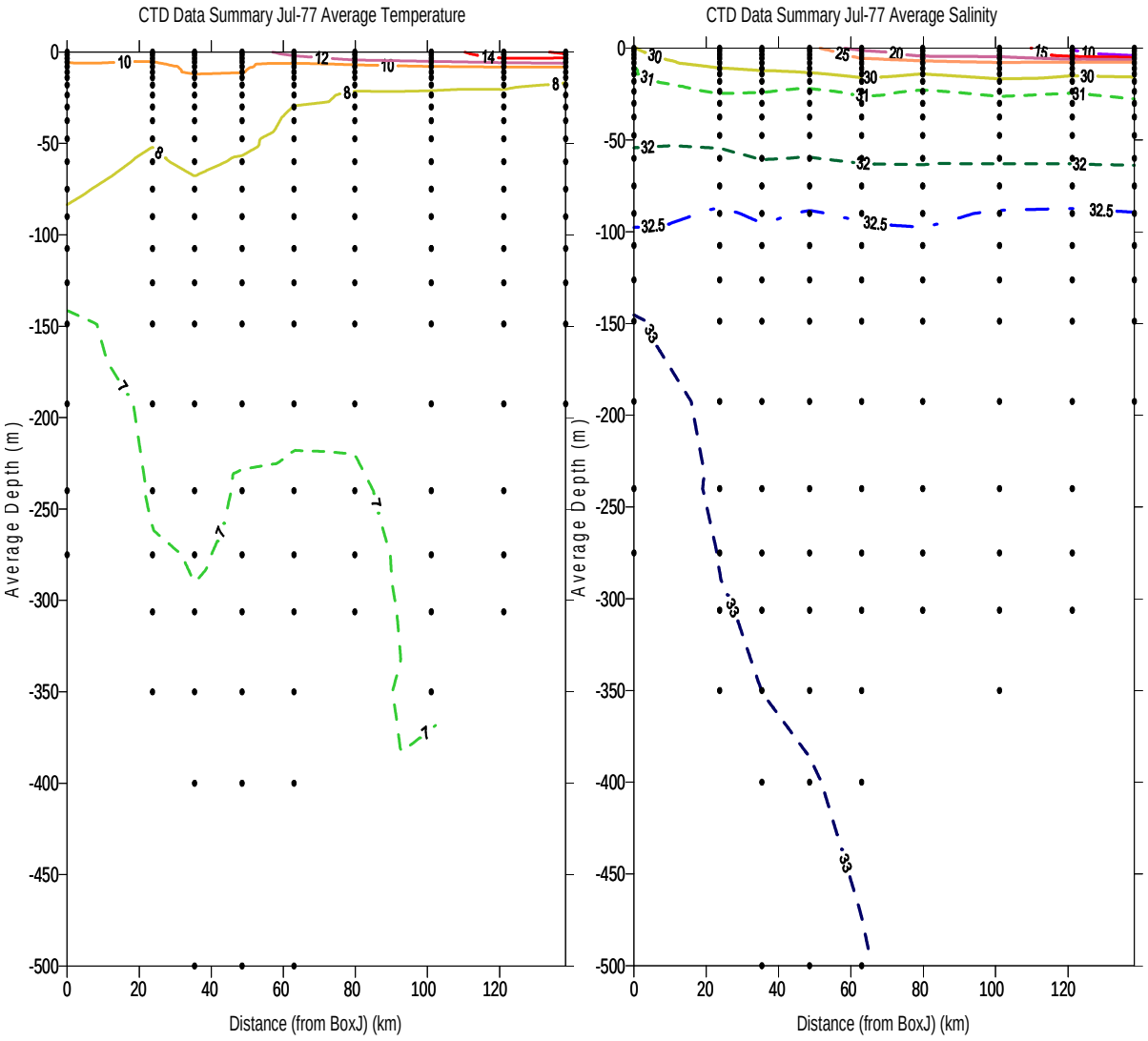

NOTE: Temperature and salinity distribution measured in July 1977 from Caamaño Sound to Kitimat Arm (Boxes J, H, G, F, E, D, C, B and A)

Figure C1-3 Temperature and Salinity Distribution from Caamaño Sound to Kitimat Arm, July 1977

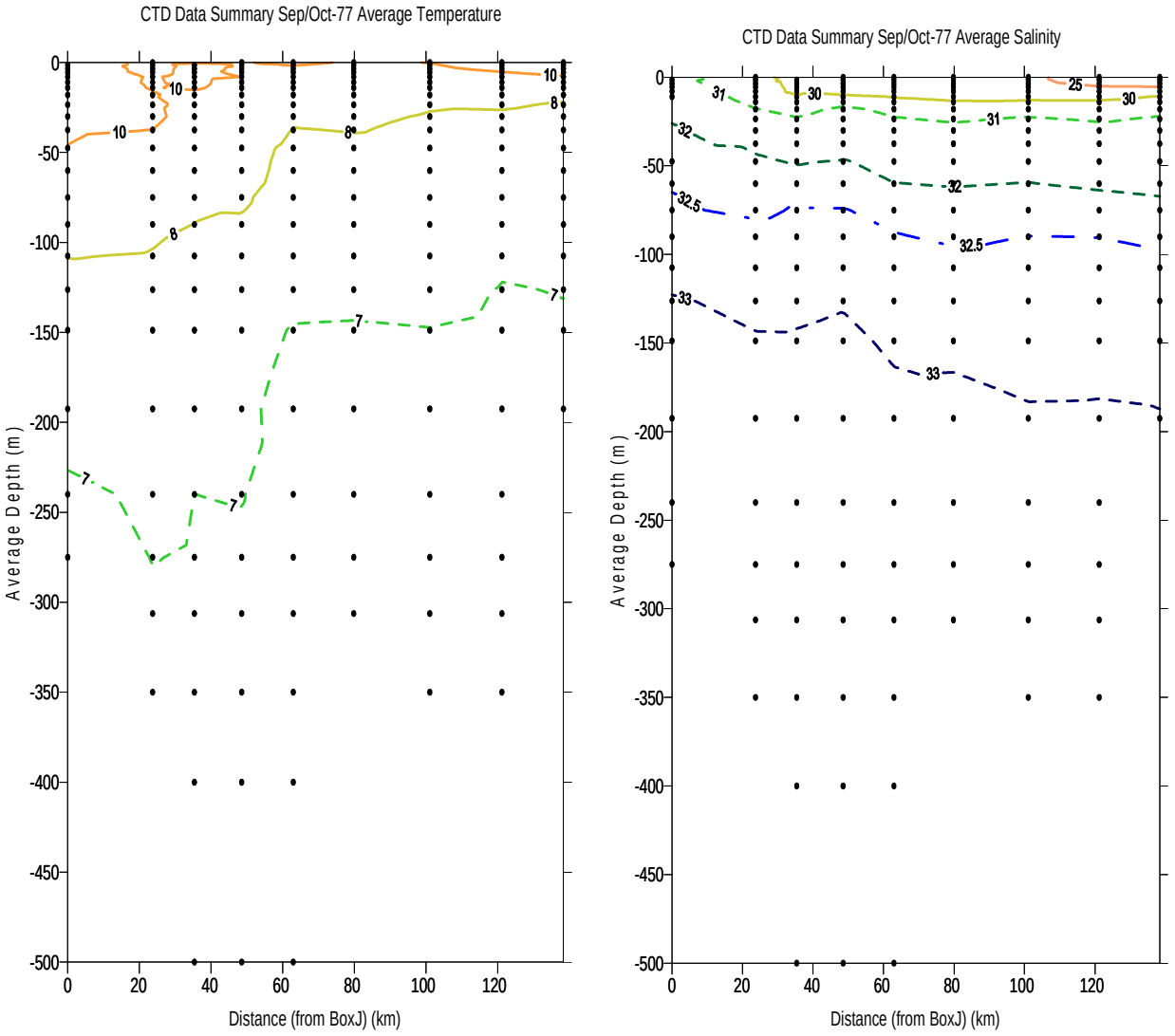

NOTE: Temperature and salinity distribution measured in September to October 1977 from Caamaño Sound to Kitimat Arm (Boxes J, H, G, F, E, D, C, B and A)

Figure C1-4 Temperature and Salinity Distribution from Caamaño Sound to Kitimat Arm, Fall 1977

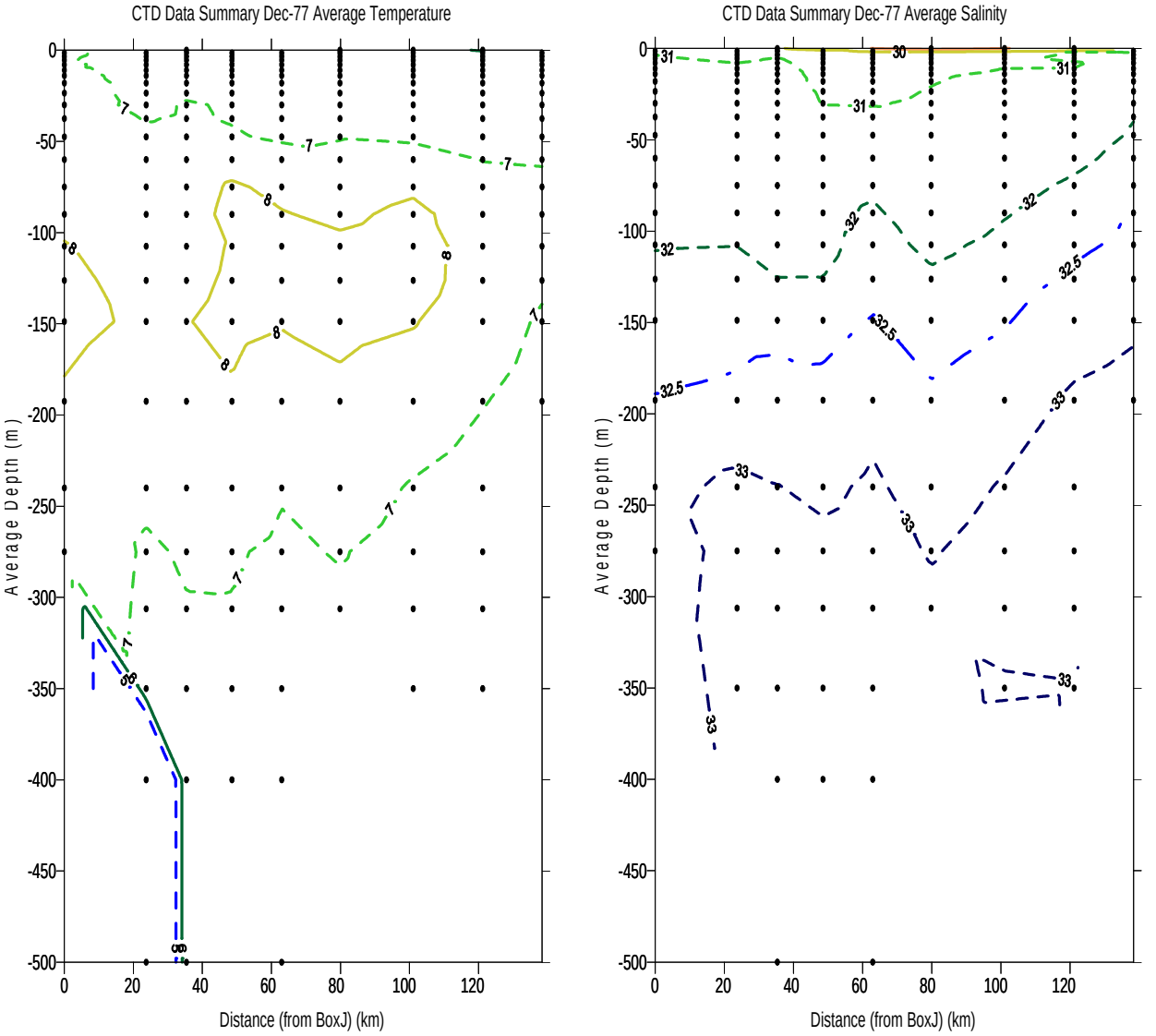

NOTE: Temperature and salinity distribution measured in December 1977 from Caamaño Sound to Kitimat Arm (Boxes J, H, G, F, E, D, C, B and A)

Figure C1-5 Temperature and Salinity Distribution from Caamaño Sound to Kitimat Arm, December 1977

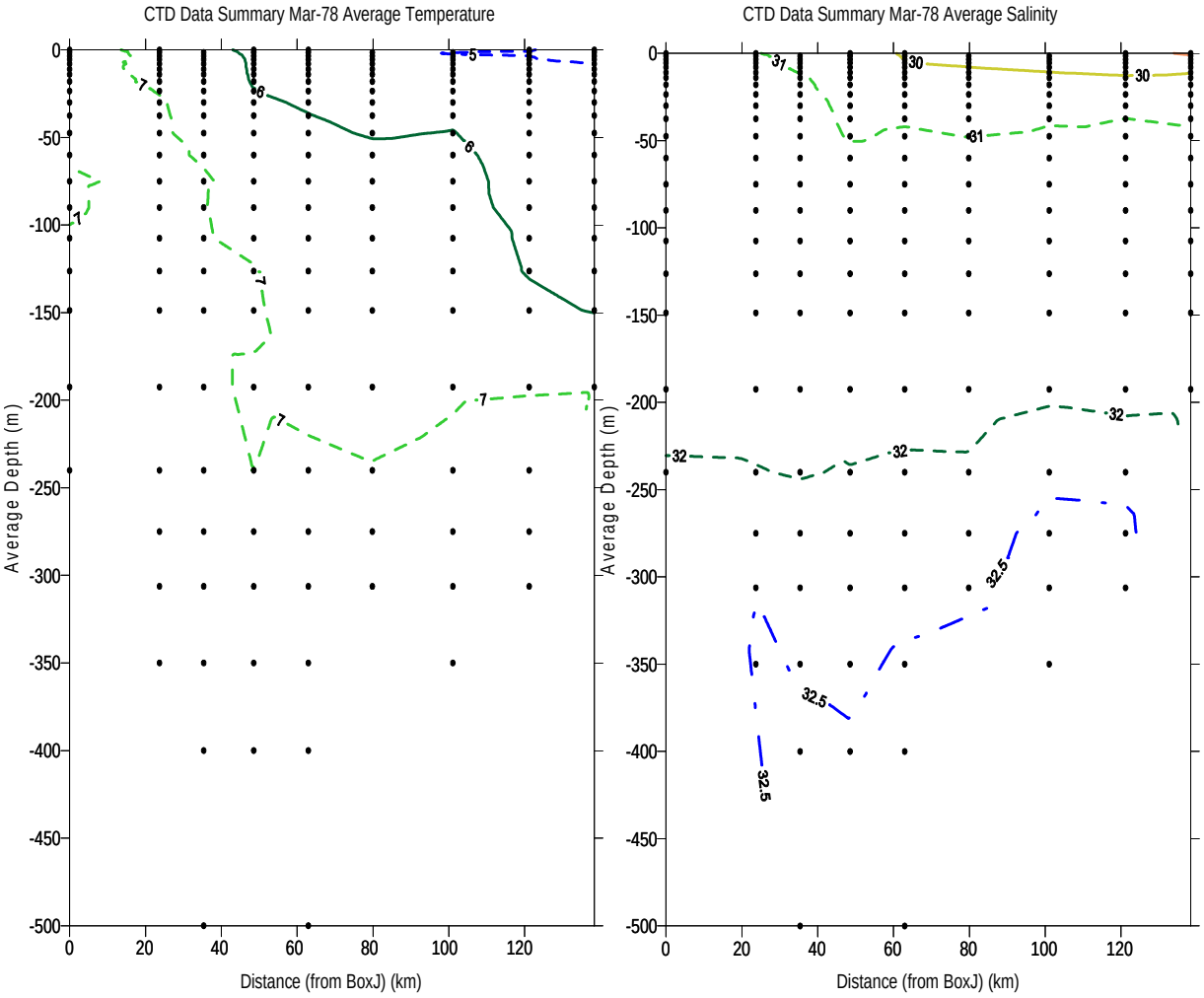

NOTE: Temperature and salinity distribution measured in March 1978 from Caamaño Sound to Kitimat Arm (Boxes J, H, G, F, E, D, C, B and A)

Figure C1-6 Temperature and Salinity Distribution from Caamaño Sound to Kitimat Arm, March 1978

Appendix D Water Levels and Waves

D.1 Introduction

D.1.1 Objectives

The purpose of this document is to describe baseline conditions with respect to water levels and waves within the CCAA to support the environmental assessment for the Project. Information has been sourced and summarized from existing literature and field surveys for the following key data categories:

- tides
- waves
- storm surges and inverted barometer effect (air pressure drop leading to sea level rise)
- tsunamis
- seasonal and long-term sea level changes

D.2 Methods

D.2.1 Confined Channel Assessment Area Boundaries

CCAA for Existing Data Review

The CCAA consists of Douglas Channel and its approaches, Principe Channel and Caamaño Sound, which emerge into the open waters of Hecate Strait (see Figure 1-1).

CCAA for Field Surveys

Data were collected at four mooring sites within the CCAA. Water levels were measured at all four sites, i.e., Kitimat Arm, Douglas Channel, Principe Channel and Aranzazu Bank. Directional wave data were collected at the Aranzazu Bank site.

D.2.2 Review of Existing Data Sources

Data sources reviewed for this section consist of published literature, databases and publications of the CHS and Environment Canada. Specific sources are listed as references in the text.

D.2.3 Field Surveys

Field survey work, extending from the seaward end of the CCAA to landward to the proposed marine terminal, was carried out from September 2005 to January 2006. As part of that program, water levels were measured at four mooring sites (Sites 1, 2, 3 and 4, see Figure D-1).

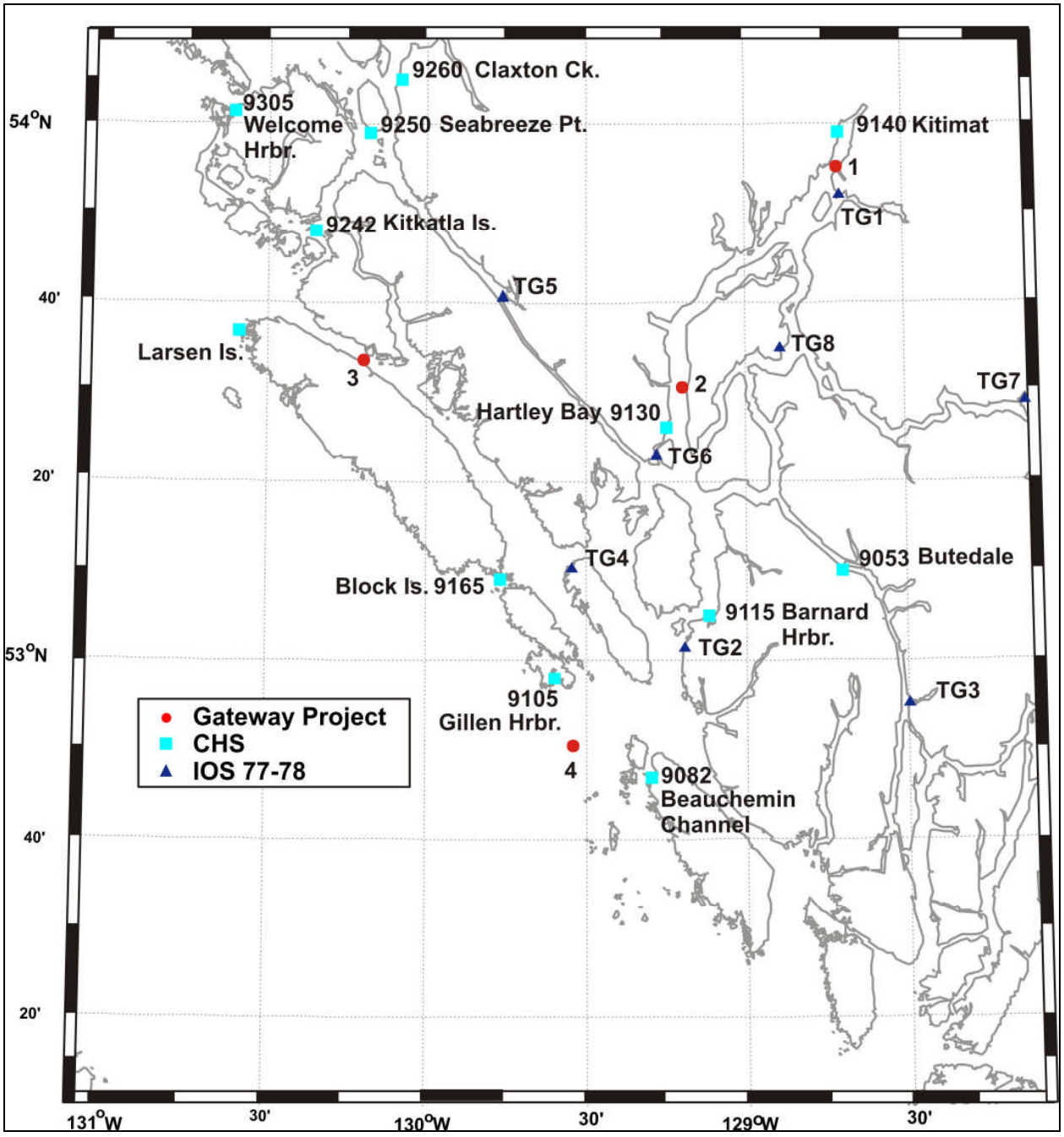

Figure D-1 Water Level Measurement Sites

D.3 Results of Baseline Investigations

Changes in sea level, related to the mean sea level, along the British Columbia coast are primarily due to the tides; however, other episodic and seasonal factors can affect water levels. Ocean waves are the result of wind generation in regional and local waters, as well as of the occasional occurrences of very long period swell waves in Hecate Strait that can originate from other parts of the Pacific Ocean.

D.3.1 Tides

The gravitational pull of the sun and moon on the ocean waters causes the periodic rise and fall in water level known as the tide. This astronomical tide accounts for most of the variations in sea level along the central British Columbia coast. The mean tidal range (low to high water level difference) for the central coast region is about 3.6 m, with large ranges up to 6 m (CHS 2005).

The tides along the British Columbia central coast are classified as mixed, mainly semi-diurnal (two highs and two lows per 24.75 hour period, but successive highs or lows are of unequal differential height). Figure D-2 shows the typical tidal curve for Kitimat. A spring-neap cycle of about 14 days occurs as the gravitational forces of the sun and moon reinforce each other at full and new moons. Tidal ranges during these spring tides are about twice those that occur during the weaker neap tides. The spring tide range at Kitimat is 6.5 m, reducing to about 3 m during neap tides.

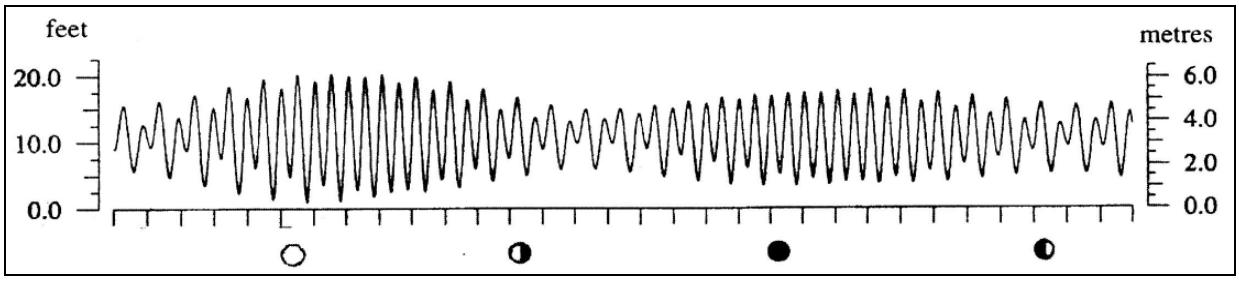

SOURCE: Modified from CHS 2005

Figure D-2 Monthly Tidal Cycle in Kitimat Arm

After entering Queen Charlotte Sound, the tide travels northward up Hecate Strait, meeting (in northern Hecate Strait) the tide that entered through Dixon Entrance (see Figure D-3). The tidal range increases both because of a decrease in depth and because of positive reinforcement with the tidal wave from Dixon Entrance. Thus, the tidal ranges are largest in the area where the two components meet. As the tide moves up Hecate Strait, the mean tide range increases from about 3 m at the entrance to Queen Charlotte Sound to about 5 m midway up Hecate Strait. Part of the tide reflects back from northern Hecate Strait, resulting in what may be a standing wave (Thomson 1989; Foreman et al. 1993).

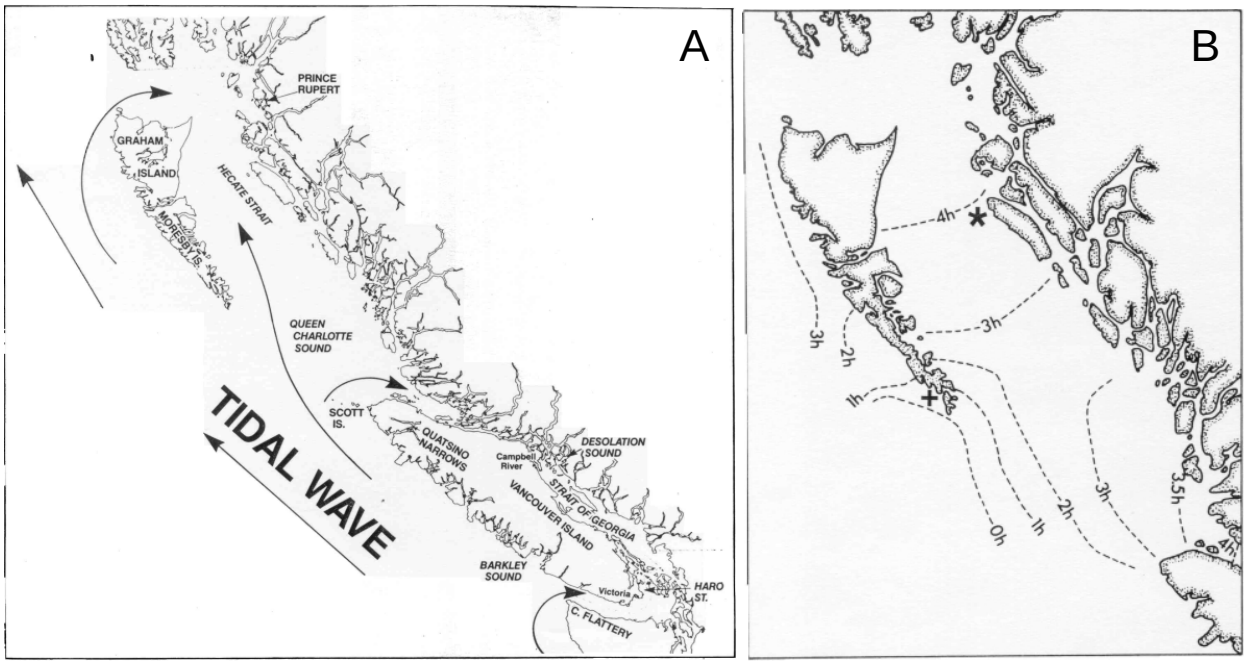

SOURCE: Thomson 1989

Figure D-3 Path (A) and Relative Timing (B) of Tidal Progression, Northern British Columbia Coast

The tide in the CCAA is driven by the tide in Hecate Strait, but is modified by the network of channels and inlets. Tidal information in the area is available from stations where data have been collected by the CHS, as well as from tide gauges deployed as part of the Kitimat Physical Oceanographic Study (KPOS) carried out in 1977 to 1978 by the Institute of Ocean Sciences (Narayanan 1980).

For the tidal ranges at each of the CHS sites and Principe Channel Site 3 for mean and large tides (CHS 2005), see Figures D-4 and D-5, respectively. The tidal range increases with northward distance along the coast of the region, by about 25% from Station 9082 (Beauchemin Channel) in the southeast to Station 9305 (Welcome Harbour) in the northwest. Tidal range also increases from the mouth to the head of the inlet system, but by a much smaller amount (approximately 6% between Caamaño Sound and Kitimat). The greatest range occurs at Site 3 in Principe Channel.

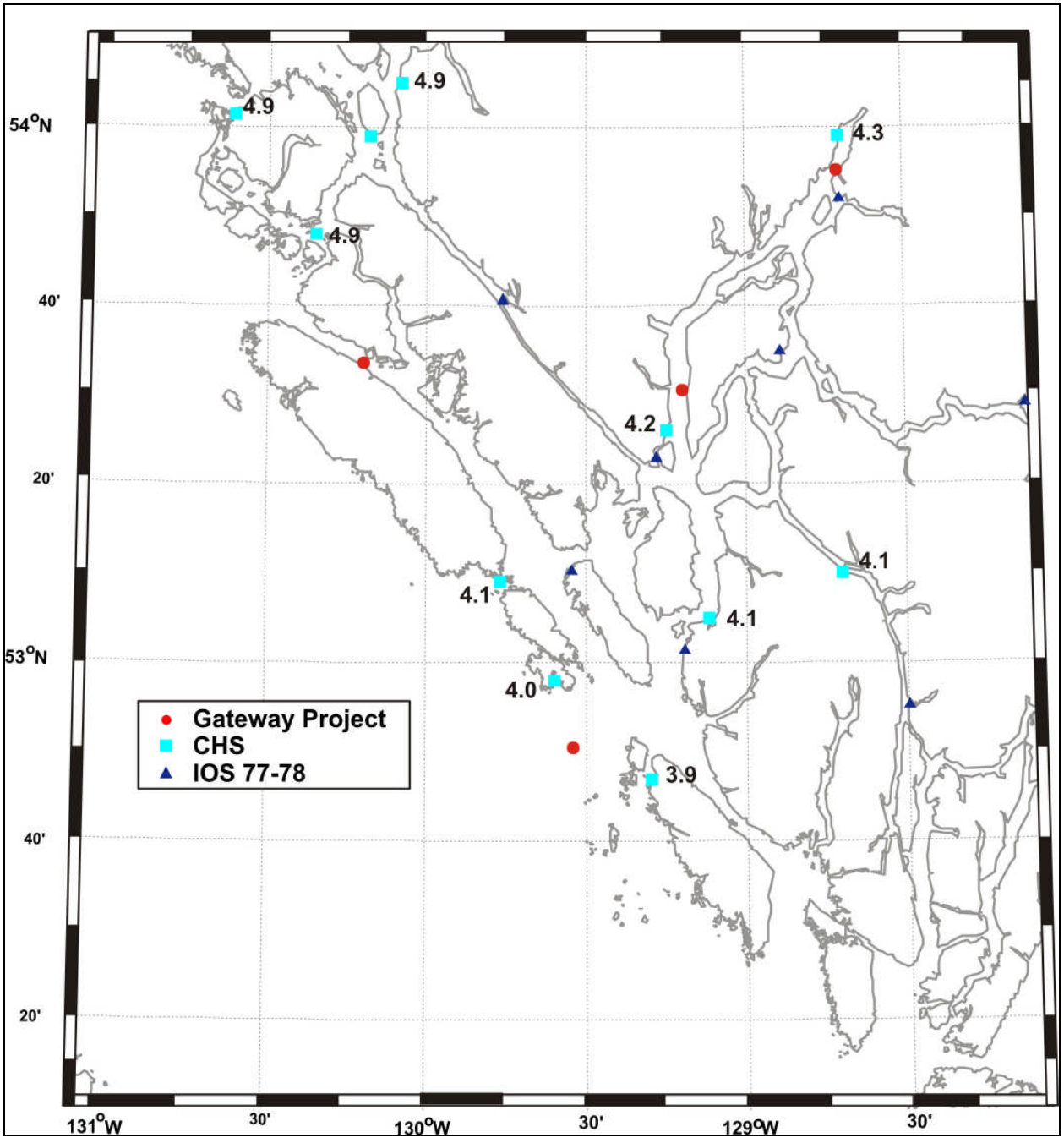

Figure D-4 Tidal Range for Mean Tides

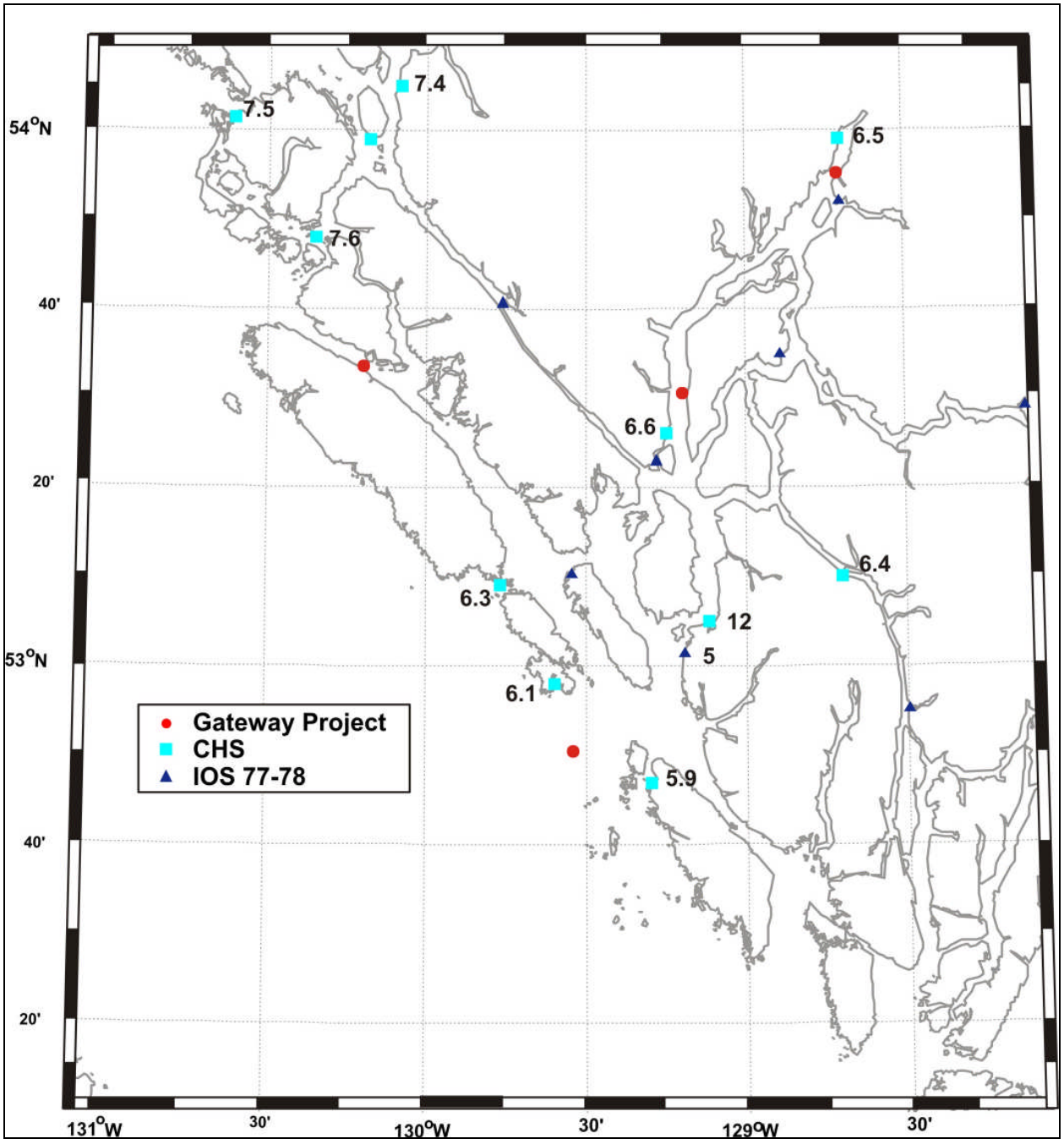

Figure D-5 Tidal Range for Large Tides

The tide is a very long wave of complex form; for the purposes of prediction, it may be resolved into a number of simple sinusoidal components related to the astronomical forcing. The two largest components of the tidal range in the region are the M2 (principal lunar semi-diurnal) and K1 (soli-lunar declinational diurnal) constituents. For the amplitudes of these constituents at each site, see Figures D-6 and D-7. (The range of a constituent is equal to twice its amplitude; e.g., at Kitimat, the M2 constituent is responsible for 3.3 m of the 6.5 m range at large tides.) The amplitude of the M2 constituent increases with northward distance along the coast and with landward distance towards the head of the inlet system to a greater degree than does the tidal range, whereas the amplitude of the K1 constituent varies only slightly. The largest values for these constituents are found at Site 3 in Principe Channel, consistent with its having the greatest range at large tides. The tidal range is determined by the combination of constituents (many other smaller constituents also contribute, but the M2 and K1 are the largest); the relative constancy of the K1 accounts for its smaller variance compared to that of the M2 constituent.

For the time of the peak amplitude of the M2 and K1 at each site, relative to its occurrence at Station 9082 (Beauchemin Channel), see Figures D-8 and D-9. The times for the M2 constituent increase with northward distance along the coast, but show only a few minutes increase between the mouth and head of the inlet system. The times for the K1 constituent also increase with northward distance along the coast, but show a great deal more variation with location in the inlet. Narayanan (1980) states that the harmonic analysis of the tidal data collected in the Douglas Channel system during the KPOS showed a significant amount of seasonal dependence in the phase (equivalent to the relative arrival times discussed above) of the K1 constituent, whereas the phase of the M2 constituent was stable. Those seasonal variations are likely caused by changes in the water column stratification and so may be expected to vary from year to year as well. The K1 arrival times at the KPOS sites in Figure D-9 are derived from yearly averages of the phase. The instability in the K1 phase will cause some deviations from the predicted tide, in addition to non-tidal effects, but they may be expected to be less than 25 cm (half the K1 amplitude).

The K1 arrival time at Site 3 (Principe Channel) differs significantly from all the others. The water level record at this site was collected between September 2005 and January 2006, and the K1 phase computed from the tidal analysis is in fact consistent with the K1 phases computed for the KPOS sites for the same season. It may therefore be expected that the K1 phase at Site 3 would exhibit similar seasonal variability and that its yearly average would be more consistent with that of other sites.

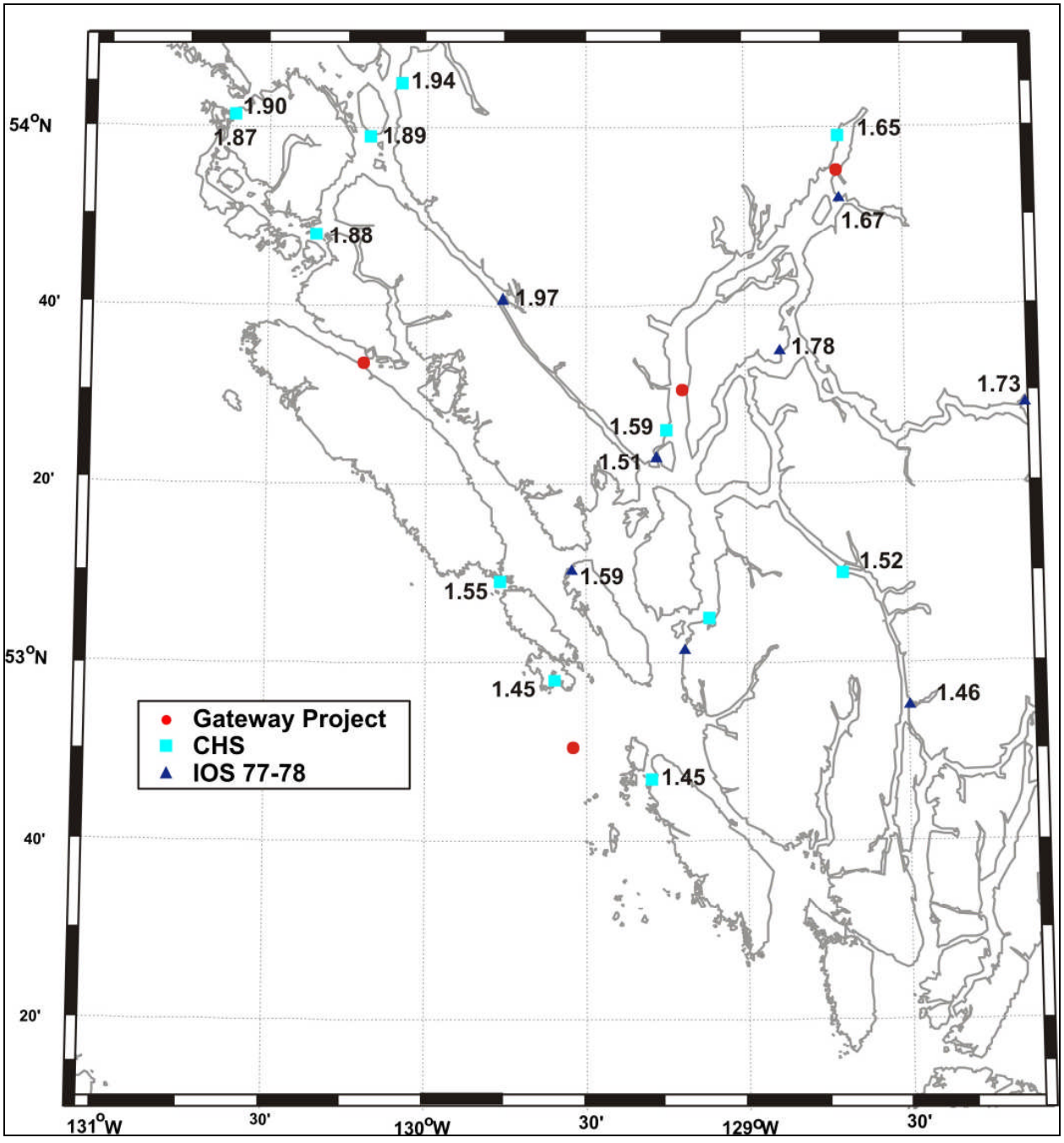

Figure D-6 Amplitude of the M2 Tidal Constituent

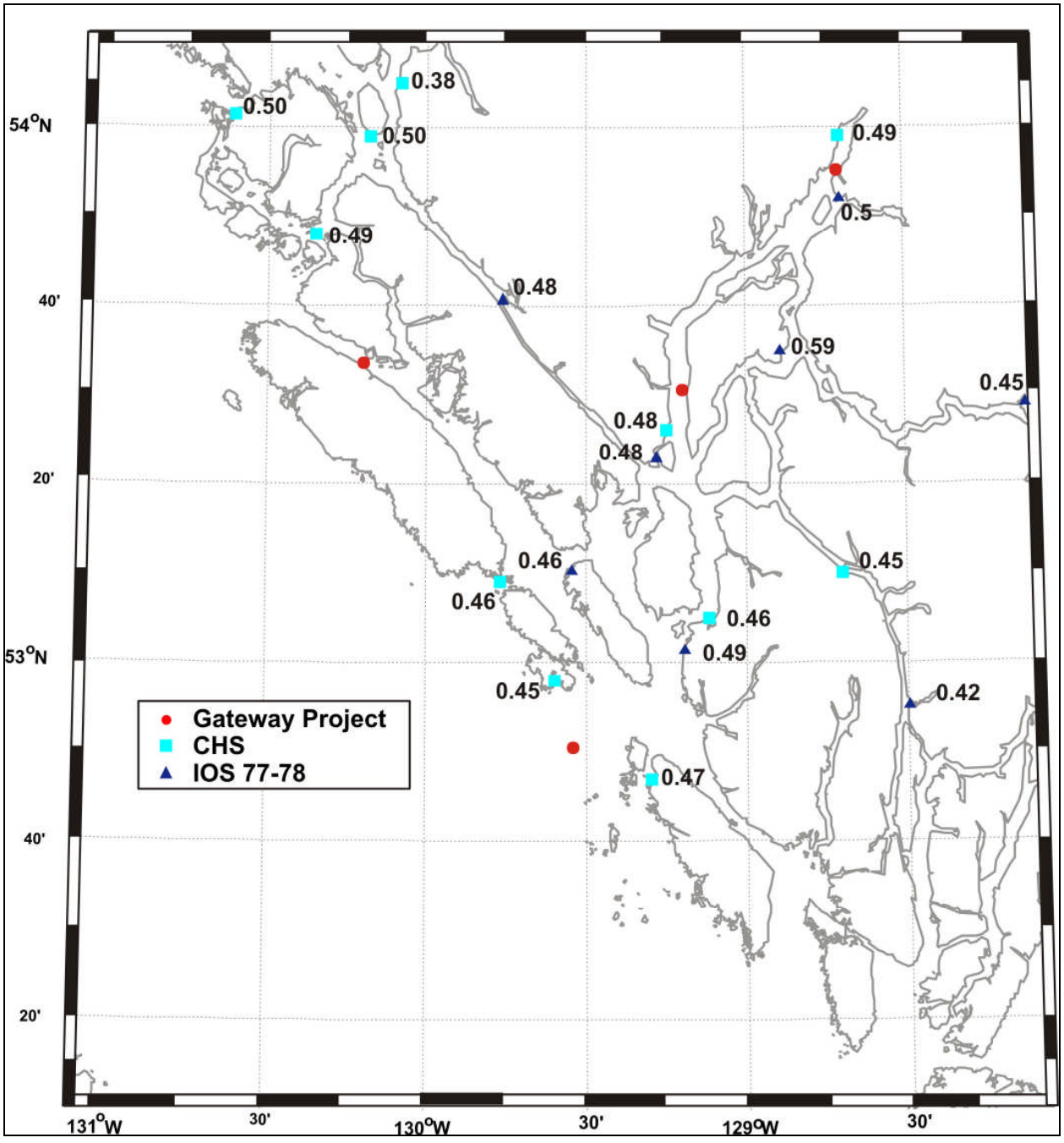

Figure D-7 Amplitude of the K1 Tidal Constituent

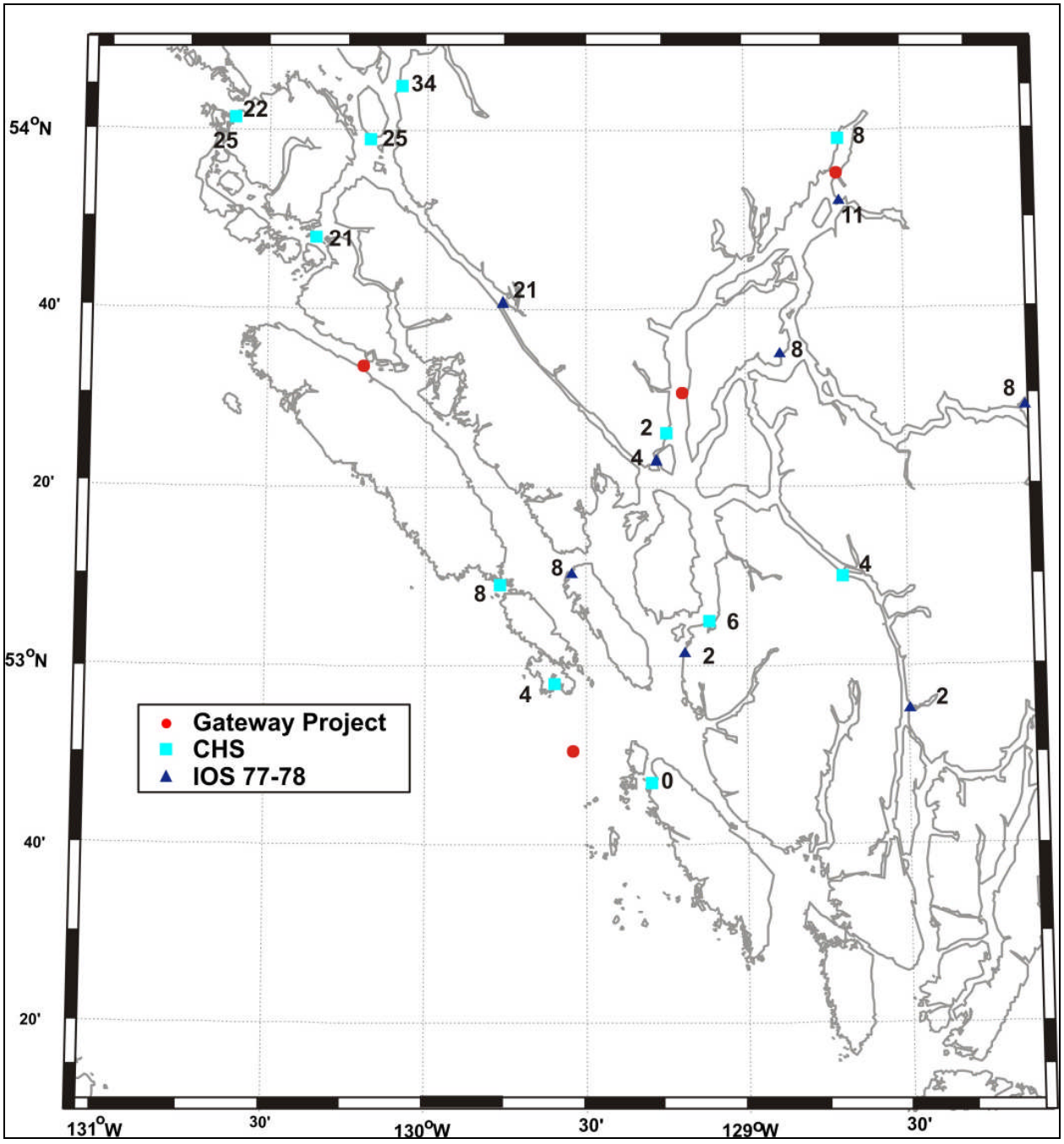

Figure D-8 Relative Times for the M2 Constituent (minutes)

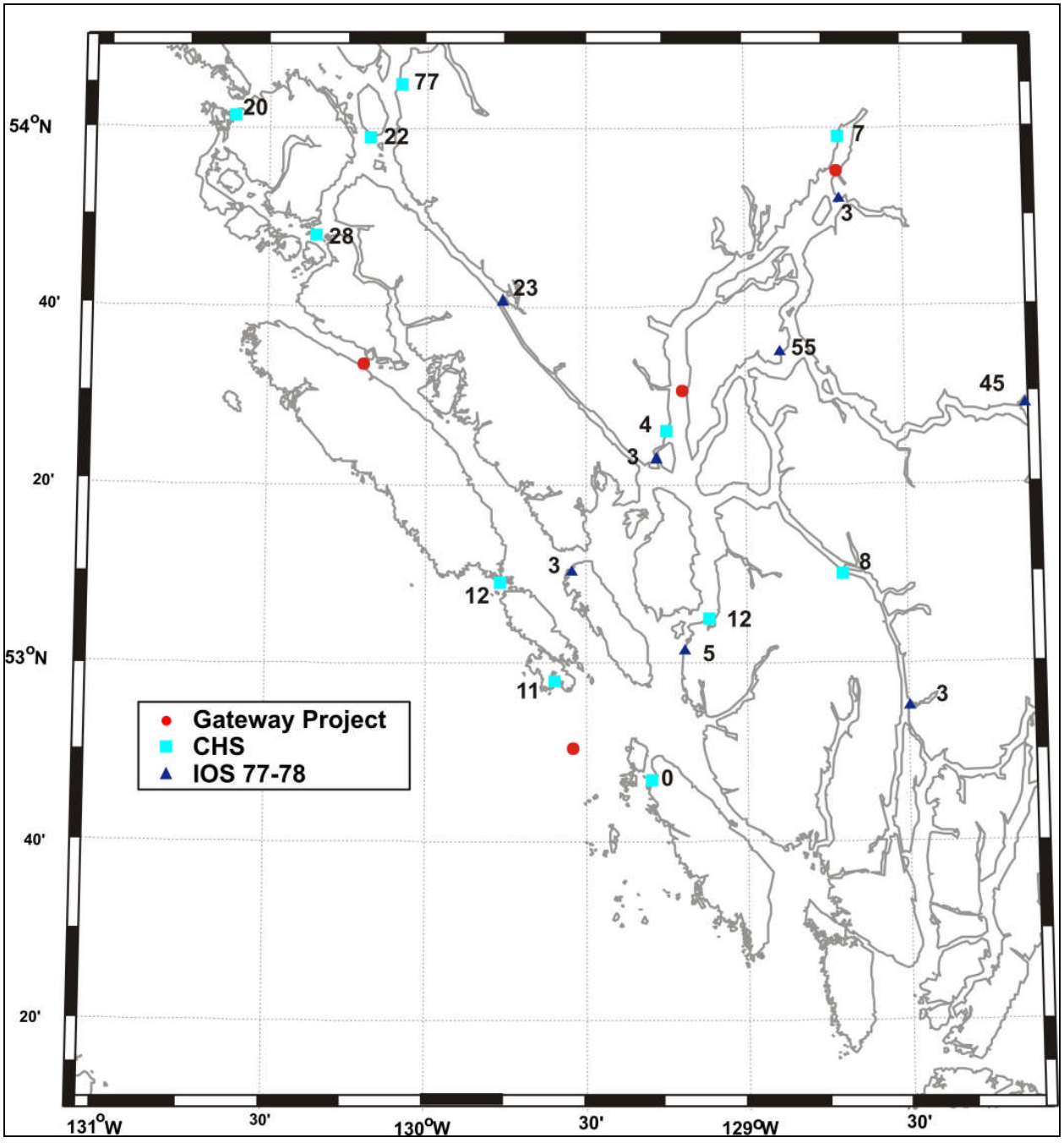

Figure D-9 Relative Times for the K1 Constituent (minutes)

D.3.2 Waves

Regional Wave Conditions

The waters of Hecate Strait and Queen Charlotte Sound are open to large fetches, particularly from the southwest, and can receive long-period swells (16- to 22-second period) although average wave periods are generally about 5 to 10 seconds for most months (Thomson 1989). During winter, seas with significant wave height[1] in excess of 3.5 m occur 20% to 30% of the time offshore, reducing to 10% along the coast (Thomson 1989). Episodes of large waves during winter have a two-to-three-day periodicity, consistent with the interval between the passages of frontal systems. Storm-force winds (gusting to 90 to 100 knots), accompanied by significant wave heights of 6 to 8 m, occur several times each winter (Environment Canada 1992). The increase in winter winds generally occurs quickly in early fall.

An extensive study of waves resulting from severe storms between 1957 and 1989 (Canadian Climate Centre 1992) indicated that significant wave heights of 5.5 m or more are almost always associated with strong winds from the southwest to southeast (see Table D-1). Statistical extrapolation methods were used to estimate the largest significant and maximum wave height expected over a 100-year period. From the extrapolated results of the wave distributions, the 100-year return period wave is estimated to have a significant wave height of nearly 14 m and a maximum wave height of nearly 25 m in Hecate Strait.

The coastal waterways, including inlets and fjords, are generally more sheltered with weaker winds and reduced fetch. However, strong winds, particularly when combined with an opposing tide, can generate steep, choppy wave conditions of 1 to 2 m height. For example, on the outer edge of the Broughton Group, summer afternoon winds can rise to gale-force westerlies and during ebb tide, seas can become large. Arctic outflow winds during fall and winter can produce rough seas even in the inlets. For example, waves of up to three metres have been reported in Knight and Rivers Inlets (Province of British Columbia 2001); similar effects are expected in the Douglas Channel system.

Major variations in the winter storm climate occurred from 1949 to 1998 along the British Columbia coast, with an increase in the number of intense storms and a shift of the storm tracks to the south (Graham et al. 2002). These changes are estimated to have resulted in an increase, over those 50 years, of the yearly 95th percentile wave value by as much 2 m off California, but only 0.3 m off the British Columbia central coast (Graham and Diaz 2002).

[1] Significant Wave Height (Hs) represents the average of the largest one-third of all waves present. Based on normal wave statistics, the maximum wave height is usually about 1.8 times larger than the significant wave height value.

Table D-1 Estimated Significant Wave Height Statistics in Hecate Strait from 1957 to 1989

SIGNIFICANT WAVE HEIGHT STATISTICS
WEST COAST AREA 3 – HECATE STRAIT

PERCENTAGE FREQUENCY OF OCCURANCE BY DIRECTION
Annual
ODGP

	Direction – Coming From									
	N	NE	E	SE	S	SW	W	NW	Total	Num Obs
0.0m									2.7	239
> 0.0 - < 0.5 m	0.4	0.1	0.5	1.0	0.9	3.2	4.8	1.4	12.4	1009
0.5 - < 1.0 m	0.2	0.1	0.5	0.9	1.0	6.6	5.9	3.8	19.7	1730
1.0 - > 1.5 m	0.3	0.1	0.2	0.9	2.3	5.8	2.8	2.6	14.9	1310
1.5 - > 2.0m	0.2	0.0	0.2	0.8	2.5	5.1	1.0	0.8	16.7	934
2.0 - > 2.5 m	0.1	0.0	0.1	0.6	3.0	4.4	0.5	0.3	9.1	800
2.5 - > 3.0 m	0.0	0.0	0.1	0.5	2.0	4.0	0.3	0.1	7.0	612
3.0 - > 3.5 m	–	0.0	0.1	0.5	2.7	2.2	0.1	0.1	5.8	506
3.5 - > 4.0 m	–	0.0	–	0.4	2.5	1.9	0.1	–	5.0	438
4.0 - > 4.5 m	–	0.0	0.0	0.3	1.8	1.1	–	–	3.3	287
4.5 - > 5.0 m	–	0.0	0.0	0.2	1.2	0.9	0.0	–	2.4	212
5.0 - > 5.5 m	–	–	0.1	0.2	1.1	0.3	–	–	1.9	166
5.5 - > 6.0 m	–	–	–	0.2	0.8	0.4	–	–	1.4	124
6.0 - > 6.5 m	–	–	–	0.1	0.8	0.4	–	–	1.3	118
6.5 - > 7.0 m	–	–	–	0.1	0.5	0.1	–	–	0.7	65
7.0 - + m	–	–	–	0.1	1.1	0.2	–	–	1.5	134
Total	1.2	0.3	1.8	6.9	25.2	36.9	15.6	9.1		

MONTHLY DATA STATISTICS
Waverider/ODGP

	Mean	Std Dev	Med	Max	Min	Upper 95% Lim	Lower 95% Lim	Most Freq Dir	Num Obs
January	2.6	1.7	2.1	13.1	0.3	0.0	0.0	S	1115
February	1.9	1.4	1.6	9.5	0.0	4.6	0.0	S	1295
March	1.9	1.2	1.6	8.7	0.1	4.3	0.7	S	1451
April	1.7	1.2	1.3	8.0	0.2	4.2	0.6	SW	1204
May	1.4	0.9	1.2	6.1	0.2	3.1	0.5	SW	1149
June	1.2	0.7	1.0	5.1	0.2	2.6	0.5	SW	943
July	1.0	0.6	0.8	4.3	0.2	2.3	0.3	W	1352
August	1.0	0.7	0.8	6.6	0.2	2.3	0.3	W	1004
September	1.3	1.1	1.0	9.2	0.2	3.2	0.4	SW	996
October	1.9	1.2	1.6	8.7	0.2	4.1	0.6	SW	1196
November	2.8	1.7	2.3	12.7	0.5	0.2	0.9	SW	1156
December	2.2	1.6	1.9	14.3	0.2	5.2	0.6	S	1345
Annual	1.8	1.4	1.4	14.3	0.0	4.4	0.5	SW	14199

SOURCE: Canadian Climate Centre 1992

Waves in the CCAA

Environment Canada buoy sites were used for the wave data in this review (see Table D-2). Directional wave measurements were also made as part of the project field studies from September 2005 to January 2006 at the Aranzazu Bank mooring (Site 4), using an Acoustic Doppler Current Profiler equipped with wave measurement firmware.

Table D-2 Wave Buoy Data Sources

MEDS ID	Name	Start Date	End Date	Type	Lat. (deg)	Long. (deg)	Sea Depth (m)	Number of Records	Good Days	Total Days
C468181	Nanakwa Shoal	11/22/88	6/21/2005	AE	53.82	128.84	21	104,349	4,894	6,055
MEDS118	Kitimat	10/8/1977	3/22/1978	WR	53.98	128.65	37	1,188	152	165
MEDS213	Bonilla Island	11/27/1984	04/01/1990	WR	53.32	130.72	159	36,623	1,325	1,951
C46183	Hecate Strait North	5/15/91	6/21/2005	AE	53.57	131.14	62	113,881	4,451	5,151

The available wave measurements collected at the Hecate Strait North buoy since the completion of the Canadian Climate Centre (1992) study have been analyzed, as have the available wave data sets for Nanakwa Shoal in northern Douglas Channel and Kitimat.

The waves in the CCAA are much lower in amplitude than those of the exposed waters of Hecate Strait as can be seen from the measured distributions of significant wave heights (see Figure D-10). At Nanakwa, less than 5% of all observations exceed 0.5 m in significant wave height, whereas at Hecate Strait North, 80% of all observations are greater than 0.5 m in significant wave height. The maximum measured significant wave height value at the Hecate Strait North site is 9.54 m, as compared to 2.02 m at Nanakwa Shoal and only 0.63 m from the 1977 to 1978 wave measurements in Kitimat Arm.

As well as much lower wave heights, the periods and wavelengths of the waves in the inland waters are considerably reduced, as shown by the scatter plots of significant wave height (H_s) versus peak period (T_p, peak of the wave energy spectrum, i.e., the period of the most energetic component of the wave spectrum) (see Figures D-11 and D-12). At Nanakwa, most wave periods are 2.5 to 5 s, with a few at 7 s, whereas at Hecate Strait North, nearly all peak periods are greater than 4 s and the largest waves have peak periods of 9 to 14 s.

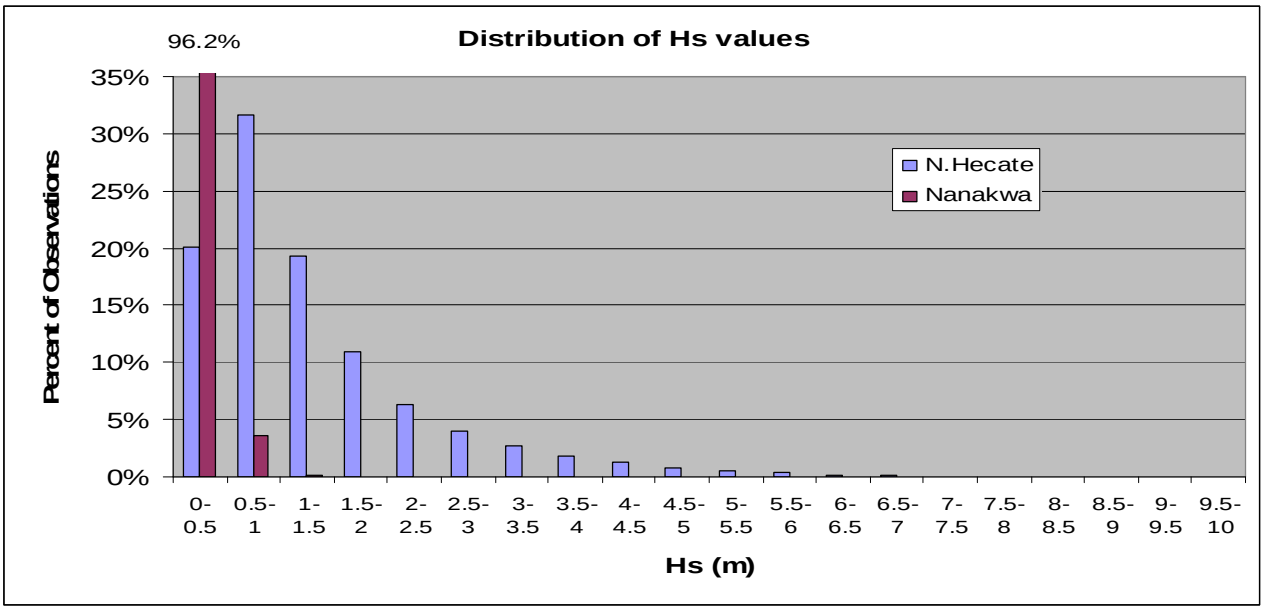

Figure D-10 Distribution of Measured Significant Wave Heights at Nanakwa Shoal and N. Hecate Strait Wave Buoys

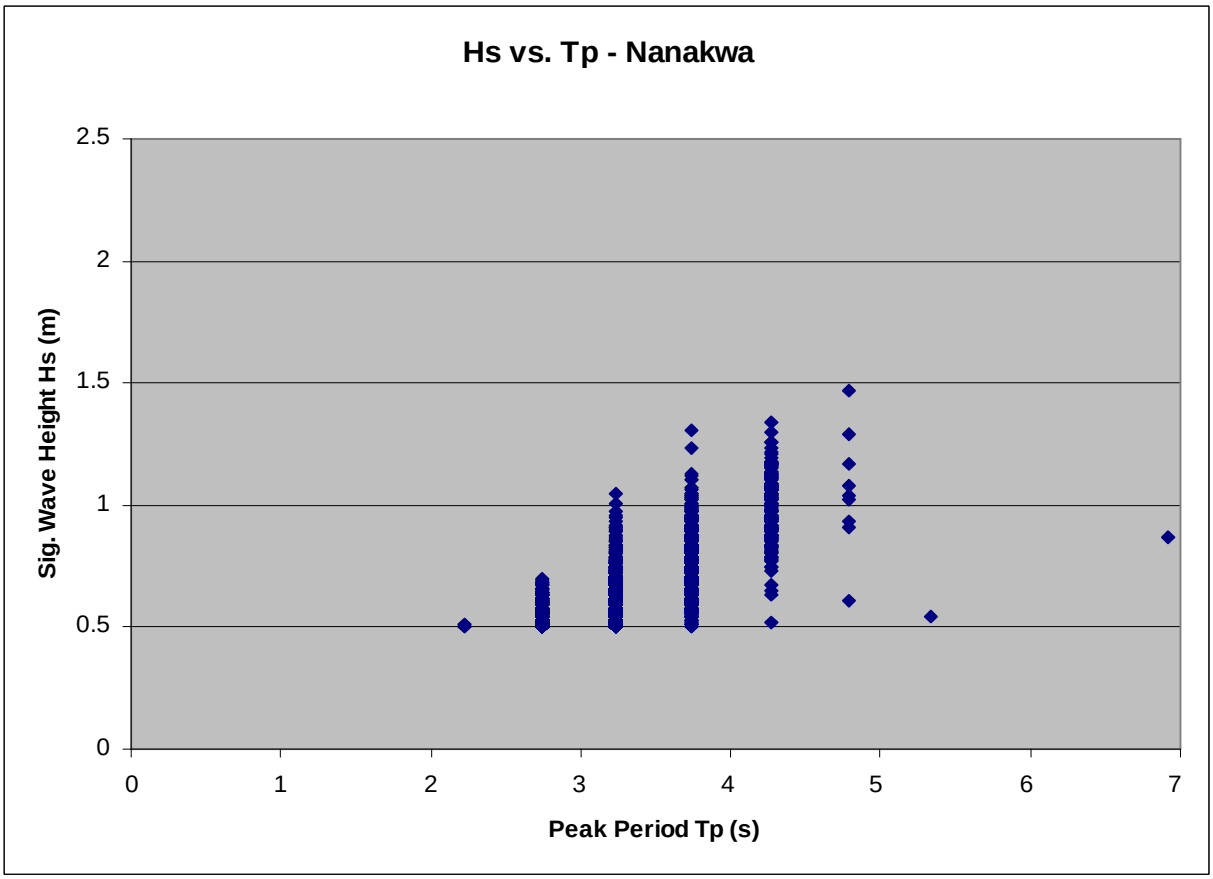

Figure D-11 Scatter Plot of Significant Wave Height vs. Peak Period for Nanakwa Shoal Buoy Data (H_s >0.5 m)

Wave heights are strongly related to wind direction, reflecting the importance of the wind fetch (distance that the wind blows over the water). Scatter plots of H_S and wind speed versus wind direction illustrate the importance of the wind direction in determining the ultimate height of waves (see Figures D-13 and D-14). This influence is particularly apparent at Nanakwa, where the largest waves are clearly due to the strong (winter) outflow winds from the north-northeast, whereas a secondary peak in wave height is evident for winds from the south-southwest blowing up Douglas Channel towards Kitimat. The polarity of the wave heights in response to wind direction is not as severe in the open waters of northern Hecate Strait, with the major broad peak in wave heights associated with winds from the southeast to south, which are the highest.

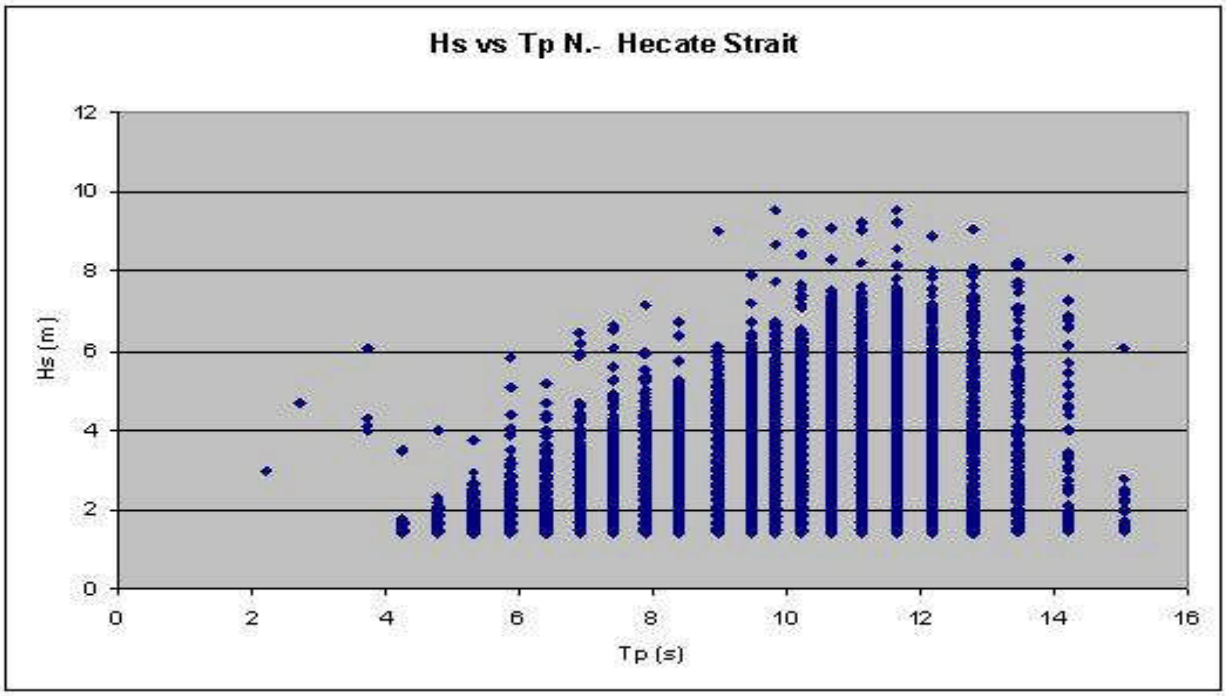

Figure D-12 Scatter Plot of Significant Wave Height vs. Peak Period for N. Hecate Strait Data (H_s >1.4 m)

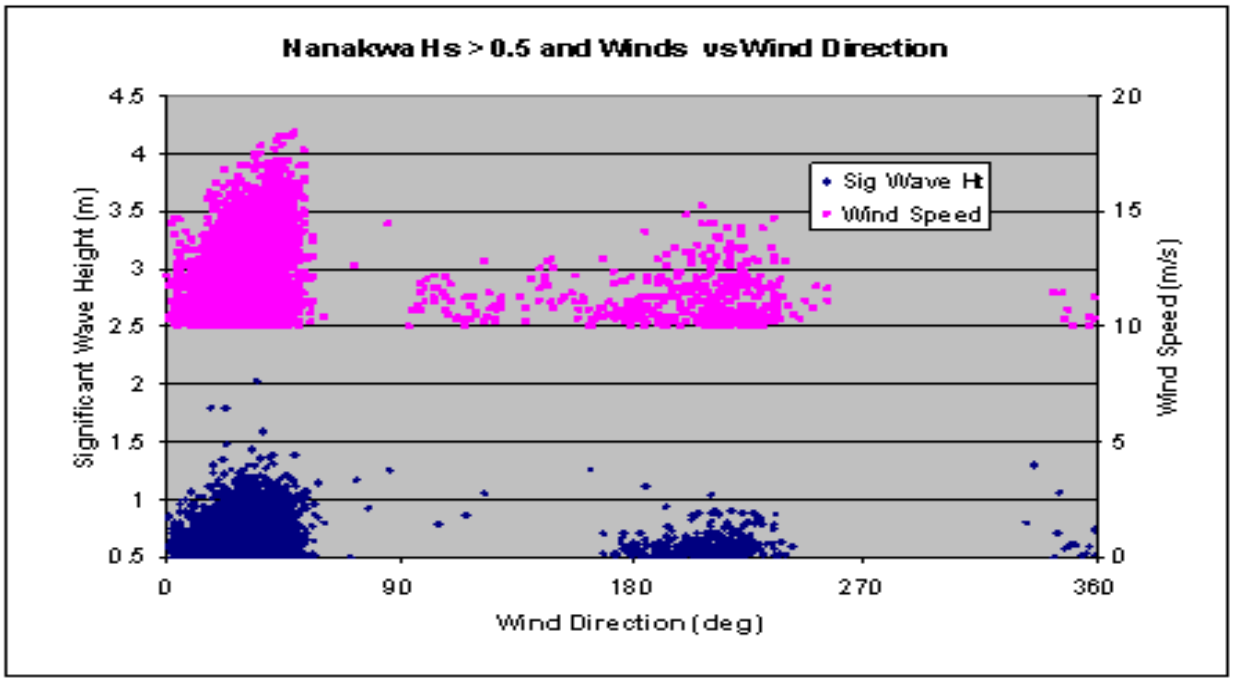

Figure D-13 Plot of Significant Wave Heights (H_S) and Winds vs. Wind Direction at Nanakwa Shoal for H_s >0.5 m

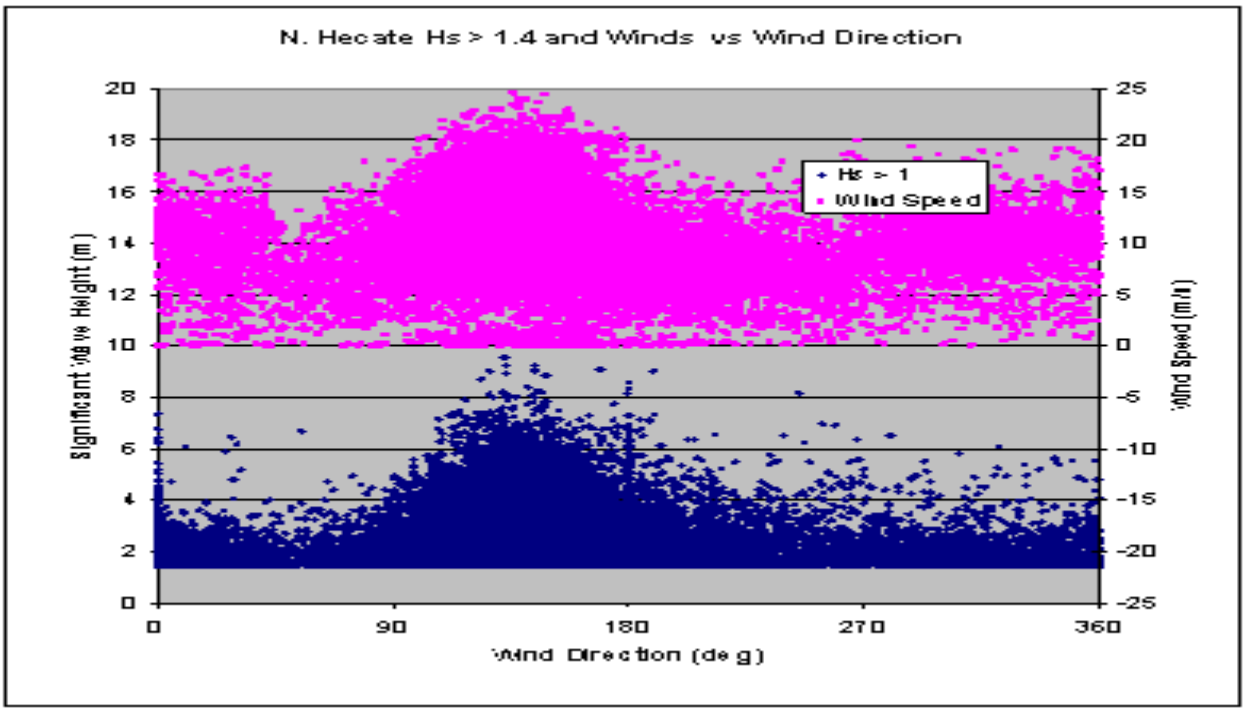

Figure D-14 Plot of Significant Wave Heights (H_s) and Winds vs. Wind Direction at N. Hecate Strait for H_s >1.4 m

D.3.3 Storm Surges and Inverted Barometer Effect

Storm surges are caused by wind stress acting on the water surface causing a direct set-up of the sea level. Storm surges have the greatest effect in shallow water and low-lying coastal areas such as the Mackenzie Delta of the Arctic Ocean. This is generally not the case along the British Columbia coast. Surge levels are usually greater along the eastern side of Hecate Strait than the western side. The inverted barometer effect (higher atmospheric pressure depresses the sea surface; low atmospheric pressure raises the sea surface) can change the water level about 1 cm for every 100 Pa change in air pressure. This is particularly noticeable during winter with sea level changes on the order of 30 cm common (Crawford 1980).

D.3.4 Tsunamis

Tsunamis are giant ocean waves that can be extremely destructive and endanger human lives where they strike populated coastlines. Tsunamis are very long period waves (15 to 90 minutes) that travel rapidly from the source. Generally, they are the result of an earthquake, less commonly a result of an underwater landslide or surface landslide that enters the water. This leaves the British Columbia coast susceptible to three types of tsunamis: far field (originating at great distances) as monitored by the Pacific warning system (Titov et al. 2005a); landslides; and a possibly devastating submarine mega-thrust earthquake associated with the Cascadia subduction zone (Nedimovic et al 2003).

The British Columbia coast is susceptible to submarine earthquakes, and submarine landslides and related tsunamis have been recorded along this coast (Rabinovich et al. 2003). Funnelling in the inlets can result in increasing wave height as a tsunami penetrates up the inlet. The extent of flooding and damage to the affected coastal areas depends on factors such as the bathymetry and distance from the source. The March 1964 earthquake that caused major damage to Port Alberni (Wigen and White 1964; Thomson 1981) penetrated the central British Columbia coast and resulted in high water levels at Bella Bella and damage at Ocean Falls (Spaeth and Berkman 1967). Based on historical and sediment records, a large subduction earthquake is believed to have caused a giant tsunami about 300 years ago that devastated the southern British Columbia coast (Hyndman et al. 2002, Internet site). Recurrence intervals for mega-thrust earthquakes are unknown, but are estimated to be about 300 to 500 years (Hyndman et al. 2002, Internet site). Given the time since the last subduction earthquake, the possibility of another in the lifetime of the Project should be considered. The Sumatra-Andaman earthquake (Vigny et al. 2005) has further raised the awareness of the threat of a mega-thrust earthquake (Titov et al. 2005b).

On a smaller geographic scale, localized slumping and avalanches due to steep terrain and high rainfall can cause tsunami-type waves in the coastal areas as a result of their displacing a large volume of water. A submarine slide in Kitimat inlet in April 1975 resulted in a wave estimated at 8.2 m height (Murty and Brown 1979). A November 1994 underwater landslide in Skagway Harbor (southeastern Alaska) generated a tsunami that was estimated to be 5 to 6 m high in the harbour, increasing to 9 to 11 m as it hit the far shore (Kulikov et al. 1996). Known submarine landslides and related tsunamis for the coasts of Alaska, British Columbia and Washington were recently summarized in Rabinovich et al. (2003); some specific examples are discussed in Bornhold et al. (2007) and Rabinovich et al. (2008).

D.3.5 Seasonal Effects on Sea Level

During winter, the northerly movement of water due to the prevailing southerly winds, combined with the rightward deflection due to the Coriolis Force, results in an average 10 to 20 cm rise in the coastal sea level along the central British Columbia coast. The opposite happens in summer with a corresponding, but smaller, drop in the coastal sea level (Thomson and Crawford 1997). The El Niño-Southern Oscillation cycle can cause further fluctuations in water levels on a scale of several years. During an intense El Niño, the northerly surge of warm water reaches Queen Charlotte Sound, causing water levels to increase by almost 40 cm (see Figure D-15).

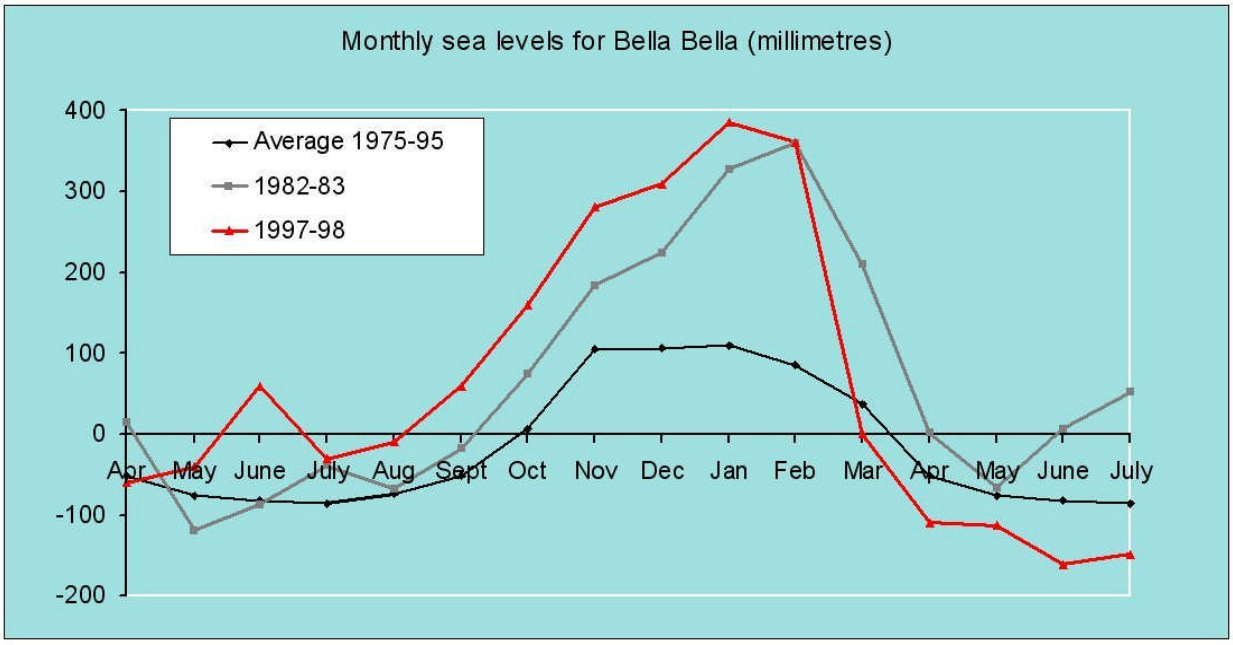

SOURCE: Crawford 2004, pers. comm.

Figure D-15 Monthly Sea Levels at Bella Bella, 20-Year Average and El Niños of 1982-83 and 1997-98

D.4 References

D.4.1 Literature Cited

Bornhold, B.D., J.R. Harper, D. McLaren and R.E. Thomson. 2007. Destruction of the First Nations village of Kwalate by a rockfall-generated tsunami. *Atmosphere-Ocean.* 45(2):123-128.

Canadian Climate Centre. 1992. *Wind/Wave Hindcast Extremes for the West Coast of Canada, Volume 1*. Environment Canada. Ottawa, ON.

Canadian Hydrographic Service (CHS). 2005. *Canadian Tide and Current Tables 2005, Vol. 7, Queen Charlotte Sound to Dixon Entrance*. Fisheries and Oceans Canada. Ottawa, ON.

Crawford, W.R. 1980. *Sea Level Changes in British Columbia at Periods of Two Days to a Year.* Pacific Marine Science Report 80-8. Institute of Ocean Sciences, Department of Fisheries and Oceans. Sidney, BC.

Environment Canada. 1992. *Marine Weather Hazards Manual: A Guide to Local Forecasts and Conditions.* Gordon Soules Book Publishers. West Vancouver, BC.

Foreman, M.G.G., R.F. Henry, R.A. Walters and V.A. Ballantyne. 1993. A finite element model for tides and resonance along the north coast of British Columbia. *Journal of Geophysical Research* 98(C2): 2509-2532.

Graham, N.E. and H.F. Diaz. 2002. Evidence for intensification of North Pacific winter cyclones since 1948. *Bulletin of the American Meteorological Society* 82: 1869-1893.

Graham, N.E., R.R. Strange and H.F. Diaz. 2002. Intensification of North Pacific Winter Cyclones, 1948-98: Impacts on California Wave Climate. In *Proceedings of the 7th International Workshop on Wave Hindcasting and Forecasting*, October 2002, Banff, AB. Environment Canada. Ottawa, ON. 60-69.

Kulikov E.A., A.B. Rabinovich, R.E. Thomson and B.B. Bornhold. 1996. The landslide tsunami of November 3, 1994, Skagway Harbor, Alaska. *Journal of Geophysical Research* 101: 6609-6615.

Murty, T.S. and R.E. Brown. 1979. *The Submarine Slide of 27 April, 1975 in Kitimat Inlet and the Water Waves that Accompanied the Slide.* Pacific Marine Science Report No. 79-11. 1979. Institute of Ocean Sciences. Department of Fisheries and Oceans. Sidney, BC.

Narayanan, S. 1980. *Kitimat Physical Oceanographic Study 1977-1978, Part 4, Tidal Circulation Model.* Contract Report Series 80-3 [Part 4], Institute of Ocean Sciences, Department of Fisheries and Oceans. Sidney, BC.

Nedimovic, M.R., R.D. Hyndman, K. Ramachandran and G.D. Spence. 2003. Reflection signature of seismic and aseismic slip on the northern Cascadia subduction interface. *Nature* 424: 416-420.

Province of British Columbia. 2001. *CCLCRMP-Coastal Zone Strategic Plan*. Ministry of Sustainable Resource Management. Victoria, BC.

Rabinovich, A.B., R.E. Thomson, B.B. Bornhold, I.V. Fine and E.A. Kulikov. 2003. Numerical modeling of tsunamis generated by hypothetical landslides in the Strait of Georgia, British Columbia. *Pure and Applied Geophysics* 160: 1273-1313.

Rabinovich, A.B., R.E. Thomson, V.V. Titov, F.E. Stephenson and G.C. Rogers. 2008. Locally Generated Tsunamis Recorded on the Coast of British Columbia. *Atmosphere-Ocean.* 46(3): 343-360.

Spaeth, M.G. and S.C. Berkman. 1967. *The Tsunami of March 28, 1964 as Recorded at Tide Stations*. U.S. Coast and Geodetic Survey Technical Bulletin 33. US Department of Commerce. National Oceanic and Atmospheric Administration. Washington, DC.

Thomson, R.E. 1981. *Oceanography of the British Columbia Coast.* Canadian Special Publication of Fisheries and Aquatic Sciences 56. Department of Fisheries and Oceans, Ottawa, ON.

Thomson, R.E. 1989. The Queen Charlotte Islands: Physical Oceanography. In G.G.E. Scudder and N. Gessler (eds.). *The Outer Shores, Proceedings of Queen Charlotte Islands First International Symposium, August 1984.* University of British Columbia. Vancouver, BC. 27-63.

Thomson, R. E. and Crawford, W. R. 1997. Processes Affecting Sea Level Change along the Coasts of British Columbia and the Yukon. In *Responding to Global Climate Change in British Columbia and the Yukon, Volume I of the Canada Country Study: Climate Impacts and Adaption.* Proceedings of workshop held on February 27-28, 1997 at Simon Fraser University. 4-1 to 4-19. Environment Canada and British Columbia Ministry of Environment, Lands and Parks. Victoria, BC.

Titov, V.V., F.l. Gonzalez, E.N. Bernard, M.C. Eble, H.O. Mofjeld, J.C. Newman and A.J. Venturato. 2005a. Real-time tsunami forecasting: Challenges and solutions. *Natural Hazards* 35(1): 41-58.

Titov, V.V., A.B. Rabinovich, H.O. Mofjeld, R.E. Thomson and F.I. Gonzalez. 2005b. The global reach of the 26 December 2004 Sumatra tsunami. *Science* **309**: 2045-2048.

Vigny, C., W.J.F. Simons, S. Abu, R. Bamphenyu, C. Satirapod, N. Choosakul, C. Subarya, A. Socquet, K. Omar, H.Z. Abidin and B.A.C. Ambroius. 2005. Insight into the 2004 Sumatra-Andaman earthquake from GPS measurements in southeast Asia. *Nature* 436: 201-206.

Wigen, S.O. and W.R. White. 1964. *Tsunami of March 27-29, 1964, west coast of Canada*. Department of Mines and Technical Surveys. Ottawa, ON.

D.4.2 Personal Communications

Crawford, W.R. 2004. Oceanographer. Institute of Ocean Sciences. Fisheries and Oceans Canada. Sidney, BC. Meeting, 2004.

D.4.3 Internet Sites

Hyndman, R.D., G.C. Rogers, H. Dragert, K. Wang, D. Oleskevich, J. Henton, J.J. Clague, J. Adams and P.T. Bobrowsky. 2002. *Giant earthquakes beneath Canada's west coast.* Available at: http://www.pgc.nrcan.gc.ca/seismo/hist/megapap.htm. Accessed: February 2006.

Appendix E Underwater Acoustics

E.1 Introduction

E.1.1 Objectives

The purpose of this document is to describe baseline conditions with respect to underwater acoustics within the CCAA to support the environmental assessment for the Project. This information will be used to identify construction and operational measures required to minimize or avoid adverse environmental effects and to support the assessment of project effects on marine acoustics.

Information has been sourced and summarized from existing literature and field surveys for the following key data categories:

- fundamental concepts, including frequency and intensity level, and their respective measurement units and references
- underwater ambient noise
- underwater sound propagation characteristics and acoustic modelling

E.2 Methods

E.2.1 Confined Channel Assessment Area Boundaries

CCAA for Existing Data Review

The assessment area for the existing data review was the CCAA, which consists of Kitimat Arm and Douglas Channel and its approaches, Principe Channel and Caamaño Sound, (see Figure 1-1).

CCAA for Field Surveys

Field surveys were carried out at four locations in the CCAA – Principe Channel, Caamaño Sound, Wright Sound and Emsley Creek Estuary (see Figure E-1 and Marine Acoustics [2006] Technical Data Report [TDR] [JASCO 2006]).

E.2.2 Review of Existing Data Sources

The review of existing data sources has been confined to general sources describing underwater acoustics, as no acoustic data sets are available specifically for the CCAA. Some limited measurements of ambient noise were made in Queen Charlotte Sound in the summer of 1982 (Lemon et al. 1984). The seafloor properties of Douglas Channel (required to model acoustic propagation in the area) have been described in Bornhold (1983).

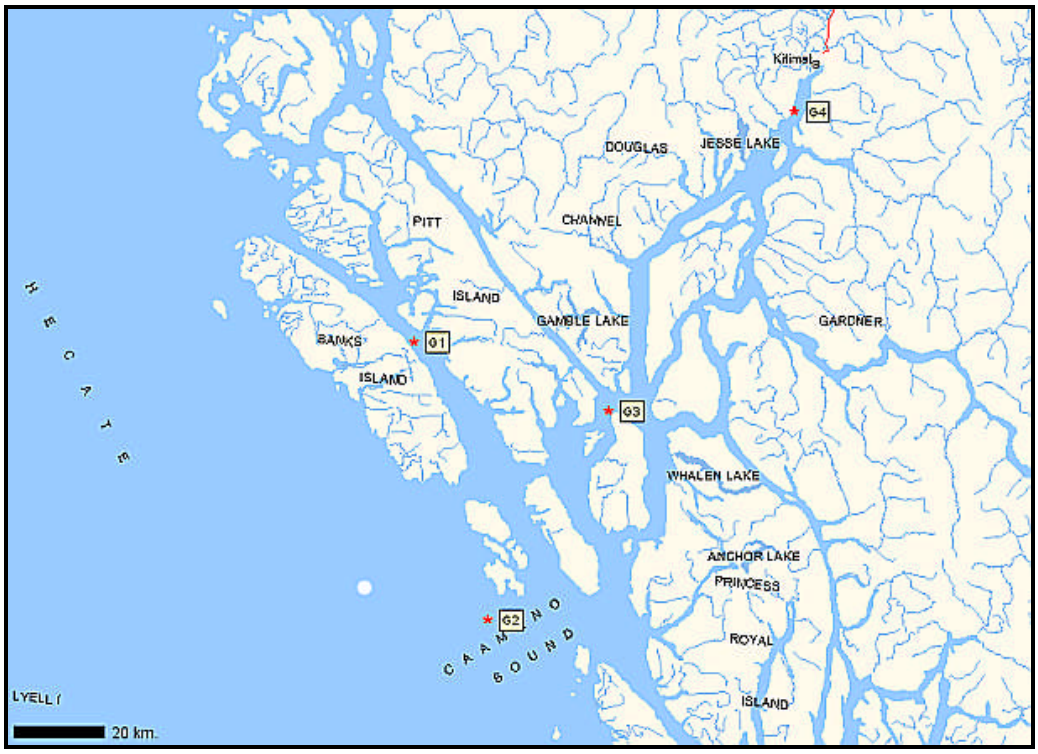

SOURCE: JASCO 2006

Figure E-1 Acoustic Measurement Locations

E.2.3 Field Surveys

Field surveys for ambient noise and transmission loss were carried out between September 28 and October 1, 2005 (JASCO 2006); the locations and measurement methods as reported are given below.

Measurements were made at four survey sites (see Figure E-1). At each of these locations, an autonomous on-bottom-hydrophone (OBH) system was deployed to record sound levels over a 13-hour period. For the OBH deployment locations and water depths for the respective measurement sites, see Table E-1.

Table E-1 Acoustic Measurement Locations

Station	Site Name	Date	Latitude	Longitude	Depth (m)
G1	Principe Channel	28 Sept 2005	53° 26.375’ N	129° 56.328’ W	142
G2	Caamaño Sound	29 Sept 2005	52° 54.617’ N	129° 39.317’ W	214
G3	Wright Sound	30 Sept 2005	53° 19.592’ N	129° 17.401’ W	90
G4	Douglas Channel (Emsley Creek Estuary)	01 Oct 2005	53° 53.989’ N	128° 46.799’ W	5
SOURCE: JASCO 2006					

E.3 Results of Baseline Investigations

E.3.1 Fundamental Concepts

Sound is a pressure wave that propagates through any compressible medium; the most common examples are air, water and solid materials, such as the Earth's crust. Sound waves are longitudinal; the variations in pressure and density they produce occur along the direction of propagation. Electromagnetic radiation, in contrast, is a transverse wave and can therefore be polarized, unlike sound. Sound waves require a material medium to exist and can be characterized by their frequency, amplitude and speed of propagation through the medium. The frequency can be thought of as the rate at which the pressure fluctuates at a point in the medium, whereas the amplitude describes the magnitude of the pressure variations. The energy carried by the wave is determined by the mean square of its amplitude, called the intensity.

A purely sinusoidal wave contains only one frequency and is sometimes referred to as a pure tone. Actual sound waves are never purely sinusoidal, but may be thought of as composed of many pure sinusoidal waves over a range of frequencies, each with its own amplitude. The distribution of the intensity of those composite waves with frequency is described by the power spectrum of the sound. If that energy is concentrated near a single frequency, it is referred to as a narrow-band sound field. If it is spread over a large range, then it is referred to as broad-band. The speed at which sound travels depends strongly on the medium; in general, the denser the medium, the greater the speed of sound. Thus, sound travels at about 350 m/s in air, 1,500 m/s in seawater and 4,300 m/s in iron.

In terms of human hearing, the frequency of a sound wave describes its pitch, and its amplitude or intensity describes its loudness. Human beings can detect sounds within only a certain range of frequencies and intensities: from 20 to 20,000 Hz in frequency and between 1 and 140 decibels in intensity. The decibel (abbreviated as dB) is a logarithmic measure of sound intensity or energy relative to a reference value; as different references are used in different areas of acoustical research and engineering, confusion can easily arise.

Sound magnitude can be measured either as the pressure of the acoustic wave, or as the energy carried by the wave, usually referred to as the intensity. The energy carried by the wave depends on the pressure and on the medium in which the wave is traveling; it depends on its specific acoustic resistance, which is the product of the density of the medium and the speed of sound in it. Both the reference level and the measure used for sound magnitude must be clearly defined in any statement about sound levels. For example, the reference level for sound pressure in air is 20 micropascals (μPa), whereas the standard reference for underwater sound is 1 μPa (Chapman and Ellis 1998). Therefore, a sound pressure of 140 dB in air, which is the threshold of pain for human hearing (Kinsler et al. 1982), would be 166 dB in water because of the difference in the reference pressures used for water and air. The sound intensity is proportional to the square of the pressure, divided by the specific acoustic impedance (the product of the medium density and the sound speed in it). The specific acoustic impedance of water is approximately 3,600 times greater than that of air; an underwater acoustic wave carrying the same energy as that at 140 dB in air would have an intensity of 202 dB. It is also important to understand whether a sound level is a source or received level. Source levels are normally given as the sound intensity at a reference distance of one metre from the source. At greater distances, the received sound level will be less, depending on the sound transmission characteristics of the medium. Spherical spreading from the source

causes an intensity decrease of 6 dB for every doubling of the distance; thus, the received level from a 202 dB underwater source would be 196 dB at 2 m, 184 dB at 8 m and 162 dB at 100 m.

E.3.2 Underwater Sound Environment

The ocean has an ambient noise background that is produced by natural processes (physical and biological) and human activities (see Figure E-2). Physical causes include wind and surface waves, rainfall and seismic activity, whereas biological causes include the sounds produced by marine mammals, fish and crustaceans. Shipping, shoreline industrial activity and seismic exploration are some of the main human sources of ocean ambient noise.

Little specific information is available concerning the ambient noise environment in Kitimat Arm. Lemon et al. (1984) recorded ambient noise at three frequencies (4.3, 8 and 14.5 kHz) at two locations in outer Queen Charlotte Sound for three weeks in the late summer of 1982. The noise spectrum levels ranged from a low of 38 dB (re 1μPa^2/Hz) in the 14.5 kHz band to a high of 63 dB (re 1μPa^2/Hz) in the 4.3 kHz band and were mainly dependent on the wind speed at the ocean surface.

At present, vessel traffic is the main anthropogenic contributor to the ambient noise environment and is highest in summer.

Ambient noise measurements collected in the fall of 2005 at the four sites listed above are given in the Marine Acoustics (2006) TDR. Their measurements were made in the 10 Hz to 20 kHz band for 13 hours at each location (part of the period was also used for transmission loss measurements). The minimum ambient noise levels in the channels were between 82 and 84 dB (equivalent to an average noise spectrum level of 39 to 41 dB [re 1μPa^2/Hz]), with the exception of Caamaño Sound, where the level was about 10 dB higher. The higher level was attributed to its exposure to the open waters of Hecate Strait and their greater wind and wave noise. Transient higher noise levels were observed when vessels or marine mammals were present.

E.3.3 Sound Propagation

The propagation speed of sound in the ocean is a function of the temperature, salinity and pressure of the water, as well as the properties of the seafloor. The ocean is almost always stratified and, as a result, the speed of sound varies with depth. Sound leaving a source does not travel in a straight line, but is refracted by the variations in the sound speed with depth. The sound waves are bent towards regions of lower sound velocity; a velocity minimum may therefore trap sound and allow it to propagate to great distances with relatively little loss. The sound speed profile may also produce shadow zones, into which very little sound penetrates even though the source may be quite close. The reflective properties of the seafloor determine how sound encountering it is reflected, scattered or transmitted into sediments, and that also will influence how sound from a source travels through the sea.

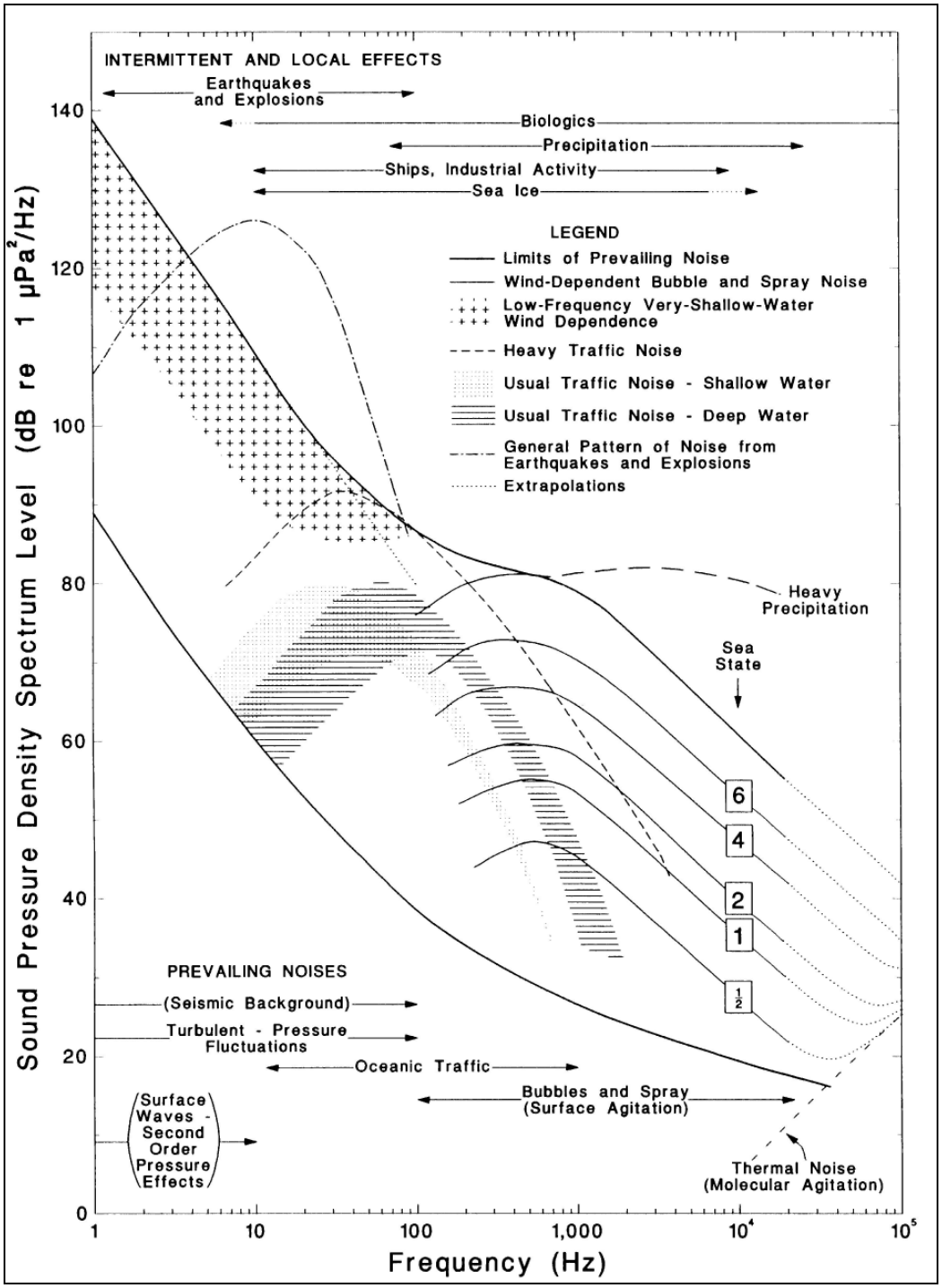

NOTE: Sea state numbers refer to the roughness of the sea surface, ½ being rippled and 6 very rough.
SOURCE: Richardson et al. 1995

Figure E-2 Oceanic Ambient Noise Spectra

During the marine acoustics study (see Marine Acoustics [2006] TDR) transmission loss measurements were taken at each of the four survey locations (see Figure E-1). The measurements were made by towing a calibrated acoustic projector away from each of the receivers and recording the position of the projector as a function of time. The recorded sound levels were then used to compute the decrease in sound level with distance for a series of frequency bands. The loss as a function of distance can be used to predict the expected sound intensity from a source, such as a vessel, at various distances.

Because of the complexity of sound propagation in the ocean, numerical propagation modelling is required to predict the effects of an acoustic source. A number of propagation models can be used, but they all depend critically on the quality of the environmental information available. For a summary of the temperature and salinity data available to characterize the sound speed environment, see Appendix C. Detailed characterization of the acoustic properties of the ocean floor is lacking for nearly all of the northern British Columbia coast; however, data are available for the Douglas Channel system from a series of studies performed by the Geological Survey of Canada and Fisheries and Oceans Canada. These data have been reviewed in the Marine Acoustics (2006) TDR, where it is concluded that "The sediment descriptions given are suitable for ascribing the geoacoustic parameters for the present sediment types that are required by the acoustic model."

The transmission loss data and geoacoustic parameters are used as inputs for follow-on modelling studies (see the Marine Acoustics [2006] TDR).

E.4 References

E.4.1 Literature Cited

Bornhold, B.D. 1983. Sedimentation in Douglas Channel and Kitimat Arm. In R.W. Macdonald (ed.). *Proceedings of a Workshop on the Kitimat Marine Environment*. Canadian Technical Report of Hydrography and Ocean Sciences No. 18. Institute of Ocean Sciences. Department of Fisheries and Oceans. Sidney, BC.

Chapman, D.M.F. and D.D. Ellis. 1998. The elusive decibel: Thoughts on sonars and marine mammals. *Canadian Acoustics* 26(2): 29-31.

JASCO Research Ltd. 2006. *Marine Acoustics (2006) Technical Data Report*. Prepared for Enbridge Northern Gateway Pipelines Inc. Calgary, AB.

Kinsler. L.E., A.R. Frey, A.B. Coppens and J.V. Sanders. 1982. *Fundamentals of Acoustics.* Wiley. New York.

Lemon, D.D., D.M. Farmer and D.R. Watts. 1984. Acoustic measurements of wind speed and precipitation over a continental shelf. *Journal of Geophysical Research* 89(C3): 3462-3472.

Richardson, W.J., C.R. Greene Jr., C.I. Malme and D.H. Thomson. *Marine Mammals and Noise*. Academic Press, San Diego, CA.

Appendix F Other Water Properties

F.1 Introduction

F.1.1 Objectives

The purpose of this document is to describe baseline conditions with respect to other marine water characteristics (i.e., dissolved oxygen, nutrients, pH and turbidity) within the CCAA to support the environmental assessment for the Project. Information has been sourced and summarized from existing literature and field surveys for the following key data categories:

- dissolved oxygen
- nutrients (dissolved phosphate, silicate and nitrate)
- pH and turbidity

F.2 Methods

F.2.1 Confined Channel Assessment Area Boundaries

CCAA for Existing Data Review

The CCAA consists of Douglas Channel and its approaches, Principe Channel and Caamaño Sound and the immediately adjacent waters of Hecate Strait (see Figure 1-1).

CCAA for Field Surveys

No field surveys were undertaken for these data categories.

F.2.2 Review of Existing Data Sources

Data sources for this review consisted of published literature and data reports. Specific sources are listed as references in the text.

F.2.3 Field Surveys

No field surveys were undertaken for these data categories.

F.3 Results of Baseline Investigations

The properties of the central British Columbia coast waters are variable both spatially and temporally, influenced by oceanic as well as coastal processes. The offshore oceanic waters are generally more saline than those near shore. The coastal waters are subject to runoff, bathymetric influences and wind-induced upwelling or downwelling. Strong tidal currents and shallow depths can cause intense mixing, often increasing the salinity and nutrients in the surface waters but decreasing the temperature and dissolved oxygen.

The properties of the coastal inlet waters are influenced by the amount of runoff and exchange with the offshore waters. Shallow sills, if present, restrict the exchange and flushing of the deeper inlet waters and

can result in oxygen depletion. The water properties of the area vary seasonally, with winter and summer extremes. The associated large-scale wind shifts between winter and summer (see Appendix A), and the resulting changes in overall current patterns, control the makeup of the water masses.

The inlet system comprising Kitimat Arm and Douglas Channel is listed by Pickard (1961) as a member of the A.1 class of coastal fjords, those that have a relatively high runoff, resulting in low (less than 3 psu) surface salinity at the head and surface salinities at the mouth between 5 and 20 psu. Such inlets are characterized by an estuarine circulation, with fresher water flowing seaward at the surface and a deeper return flow of oceanic water. Sills separating the deep inner basins of these inlets from the outside usually limit the replacement of the bottom water to periodic episodes. The portion of the system lying within the CCAA is divided bathymetrically into two main basins, Maitland Basin and Gil Basin (see Figure F-1; Macdonald et al. 1983a). For the general characteristics of the circulation of the Kitimat fjord system, as they are relevant to the CCAA, see Appendix B.

Dissolved oxygen measurements were taken in Kitimat arm and Douglas Channel by the University of British Columbia Institute of Oceanography in 1951, 1962, 1963 and 1966 (Institute of Oceanography 1953, 1963, 1964, 1967). The Pacific Oceanographic Group collected water property data in the system in 1964 and 1967 (Waldichuk et al. 1968), but the most comprehensive data set is that collected in a series of cruises conducted from 1977 to 1979 by the Institute of Ocean Sciences (Macdonald et al. 1983b). During these cruises, concentrations of dissolved oxygen, nitrate, silicate and phosphate were measured along with temperature and salinity.

F.3.1 Dissolved Oxygen

The amount of dissolved oxygen (DO) in the water is critical to the ability of the ocean to support life. Oxygen is added to the water by surface mixing and photosynthesis; it is consumed by animals, fish, bacteria and decomposition. The less dense surface waters are generally higher in DO than the denser deeper waters, and runoff tends to increase DO levels near shore. Without replenishment, waters become oxygen-depleted and eventually anoxic. This can occur in the bottom waters of coastal inlets where a shallow sill often limits flushing of the deep water. During summer, deep water upwells from offshore, bringing denser, more saline, but low-oxygen, water onto the shelf. The near-surface waters remain relatively well oxygenated (greater than 6 ml/l); however, the deeper water DO levels fall below 4 ml/l. During winter, the more oxygenated surface waters pile up along the coast, downwelling occurs and DO levels in the deeper water increase by about 1 to 2 ml/l.

Dissolved oxygen concentrations in coastal inlets such as the Kitimat system depend in a complex manner on the circulation in the inlet and on biological processes taking place in it. Generally, near-surface oxygen concentrations are at or above saturation and are below saturation in the deeper water (Pickard 1961). Anoxic conditions are rare, but have been observed in the deeper water of Minette Bay, at the head of Kitimat Arm, as it has only a very shallow connection to the Arm (Pickard 1961); therefore, the deeper water is exchanged only infrequently. Oxygen concentration maxima, with supersaturated values, have been observed beneath the halocline in Douglas Channel and are attributed to production by phytoplankton (Pickard 1961; Macdonald et al. 1983a). The deep water in the basins is renewed regularly (Macdonald et al. 1983a). Two different processes appear to be involved. The first is the usual deepwater renewal process, in which cold, dense, low-oxygen water produced by upwelling on the shelf flows over

the sill and replaces the bottom water in the basins in the spring and summer. In the second, strong winter outflow winds drive the inlet surface waters seaward to produce a rapid influx of water from 30- to 150-m depth in Hecate Strait into Douglas Channel (Macdonald et al. 1983a).

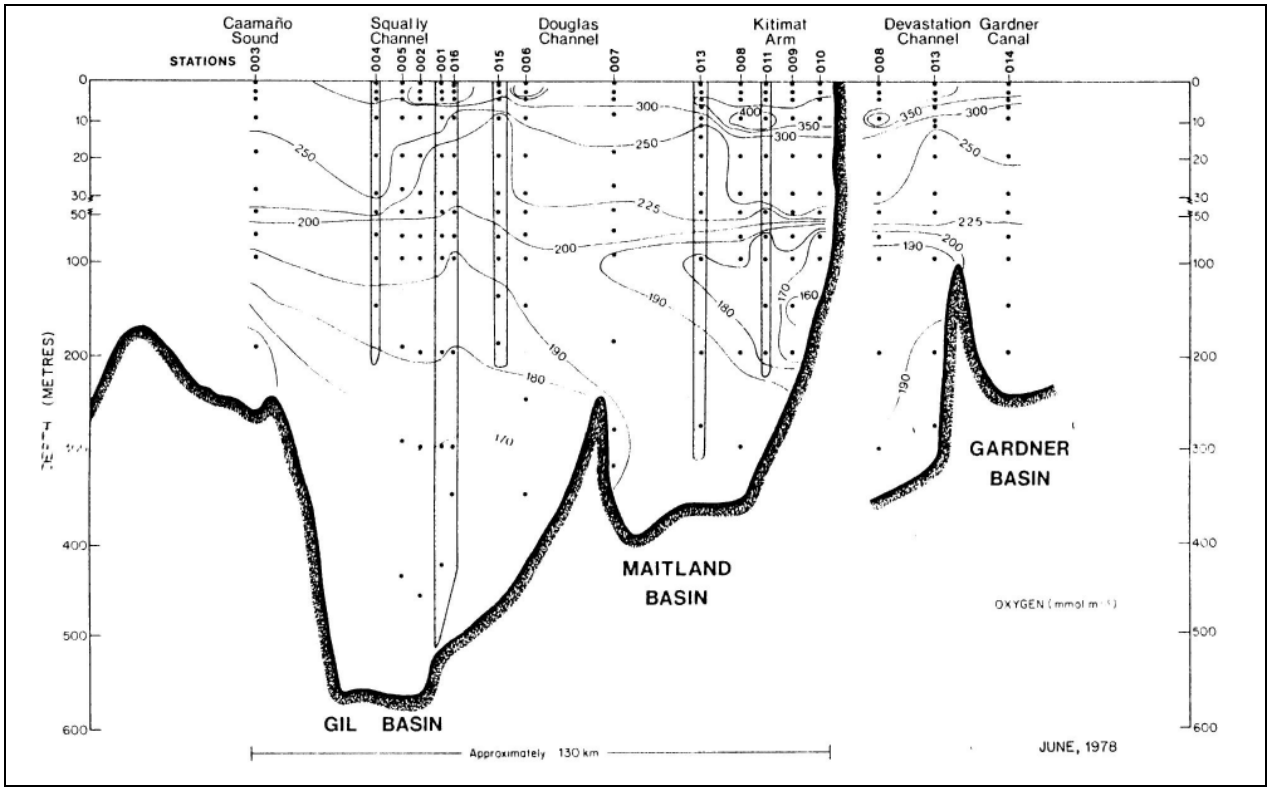

NOTE: Concentrations in mmol/m^3, where ~44.66 ml/l = 1 mmol/m^3 of O_2

SOURCE: Macdonald et al. 1983

Figure F-1 Oxygen Concentration Observed in June 1978

The summer renewals proceed inwards from one basin to the next, progressively uplifting old basin water and replacing it. Figure F-1 shows a longitudinal section of dissolved oxygen in the Kitimat system observed in June 1978 (Macdonald et al. 1983b), near the completion of a deepwater renewal. The deep water in Gil Basin has been completely replaced, while the flushing of Maitland Basin is still in process, as may be seen by the low oxygen concentrations between 100 and 200-m depth at the head of the inlet, representative of the old bottom water uplifted from the basin.

High oxygen concentrations are apparent near 10-m depth in Kitimat Arm; for example, the vertical profile from Station 011 (see Figure F-2) shows that those concentrations are supersaturated and correspond to a minimum in silicate concentration, illustrative of the oxygen production and nutrient depletion produced by phytoplankton growth in Douglas Channel as noted by Pickard (1961) and discussed above.

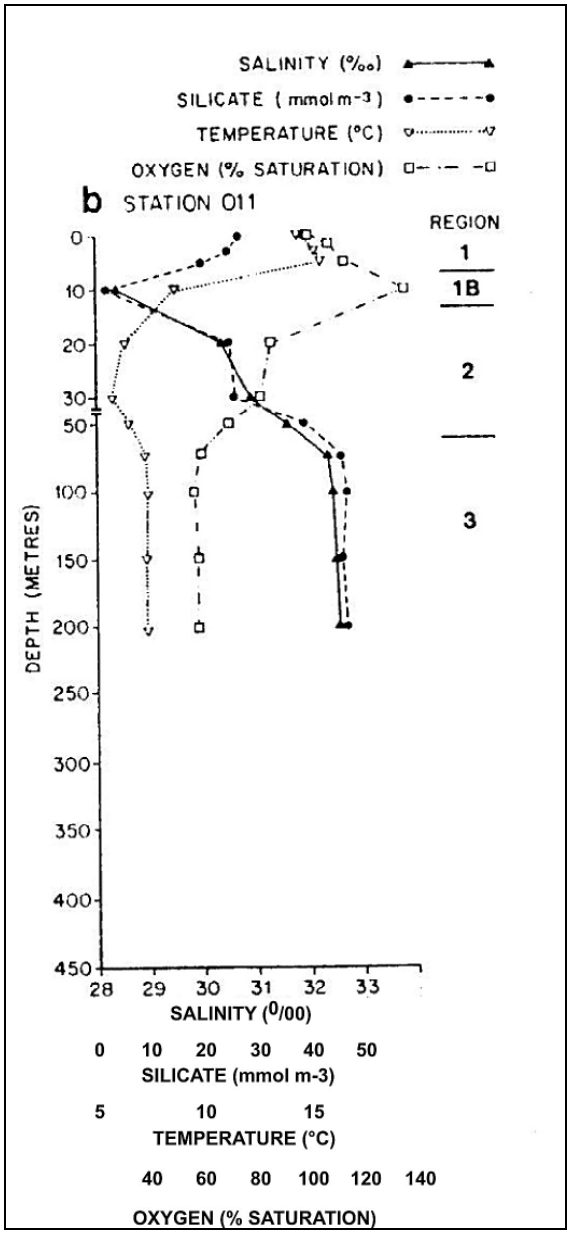

SOURCE: Macdonald et al. 1983

Figure F-2 Vertical Profile of Water Properties at Station 011, June 1978 Nutrients

Phytoplankton are the small plants that form the base of the oceanic food chain and they require nutrients for growth and reproduction. The phytoplankton also require adequate light for photosynthesis and this occurs only in the upper layer, the euphotic zone. Although in much of the upper layer of the world's oceans the nutrient levels are too low for plankton to grow, on relatively shallow continental shelves, such as those of the British Columbia coast, nutrient levels are high, making these areas among the most productive in the world.

Nutrients are supplied to coastal waters in various ways, including:

- land runoff from nutrient-rich rivers
- upwelling of deep nutrient-rich water
- estuarine circulation that draws deep water shoreward to replace waters entrained into the surface, seaward-flowing layer
- remineralization of organic materials in shallow sediments

Often nutrients exist in the deeper waters beneath the euphotic zone, but they are unavailable to plankton unless they can be brought into the surface layer. This is accomplished by mixing processes, both tidal and wind mixing, as well as by upwelling and estuarine circulation. Tidal mixing is most effective over shallow areas such as the banks, in restricted passageways and around points of land. Winter storms mix the shelf waters, bringing nutrients up from depth; however, low levels of sunlight prevent plankton from taking advantage of this abundance. Plankton productivity is greatest during the spring and summer, with the increased sunlight and the stratification of the water column. The stratification results from runoff (both rain and river runoff) and solar heating.

The main nutrients include nitrogen (nitrate NO_3), phosphorus (phosphate PO_4), silica (silicate SiO_2) and ammonia (NH_4), as well as carbon from carbon dioxide (CO_2). Plankton also require small amounts of trace elements such as iron (Fe) and zinc (Zn). Nitrogen is used by plankton to synthesize protein and phosphorus is required to convert sunlight and for cellular growth. Reduced amounts of nitrogen and phosphorus in marine waters often limit marine plant growth. Nitrate supply is believed to limit plankton production in British Columbia coastal waters. Plankton such as diatoms require silica as part of their structure. Concentrations of dissolved silica are generally high on continental shelves with significant runoff. The reaction pathways of the main nutrients in the ocean are often complex and have been, and continue to be, the subject of extensive research (Parsons 1965; Parsons et al.1984; Fisheries and Oceans Canada 2003, Internet site; University of British Columbia 2006, Internet site).

The shelf waters of the British Columbia central coast have been termed coastal waters based on the nutrient supply and utilization (Whitney et al. 1998). These waters are characterized by relatively high levels of silica, apparently from the solution of terrestrial-derived silicate material. Nutrient levels in the coastal waters of the central shelf region decline to an annual low during summer because of nutrient uptake by the plankton. The near-surface layer is particularly depleted, resulting in a nutrient maximum at about 50-m depth. Surface nutrient enhancement, with resulting increases in plankton levels, occurs in areas of summer upwelling (Freeland and Denman 1982), strong tidal mixing and river runoff.

Nutrients enter the Kitimat inlet system through river runoff and through intrusions of oceanic water from Hecate Strait. Macdonald et al. (1983b) measured the dissolved nutrients, phosphate, nitrate and silicate, in a series of four cruises in Douglas Channel and Kitimat Inlet between February 1977 and February 1979. Kitimat River water, observed in the surface layer in the summer (see Figure F-2) is characterized by high silicate concentrations (30 to 40 mmol/m^3), and low phosphates and nitrates. These characteristics were well defined in the surface layer in Kitimat and Kildala Arms during the summer. Below the pycnocline a silicate minimum is accompanied by oxygen super-saturation, as a result of phytoplankton growth. The surface layer takes on more oceanic characteristics by the entrance to Douglas Channel at Wright Sound, where the near-surface silicate enrichment was no longer evident (see Figure F-3).

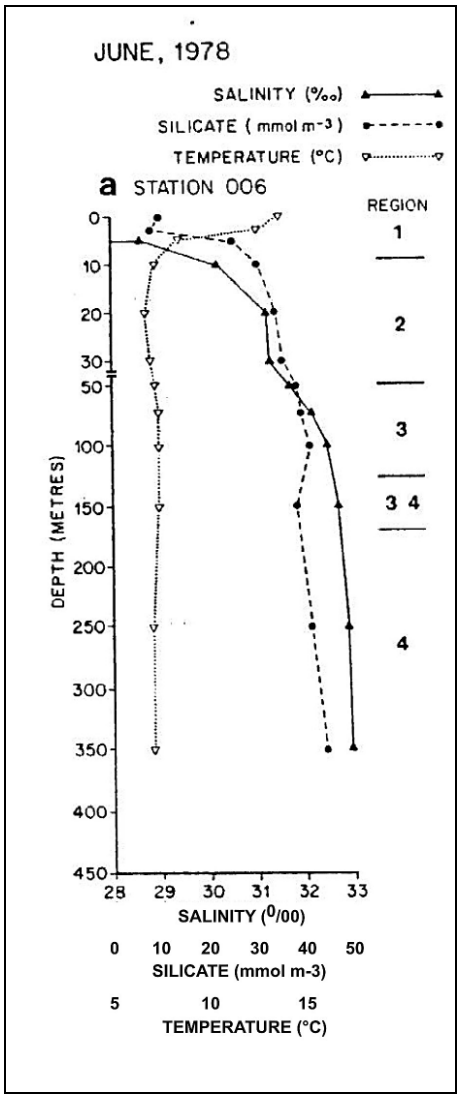

SOURCE: Macdonald et al. 1983

Figure F-3 Vertical Profile of Water Properties at Station 6 (Douglas Channel entrance), June 1978

The highest nutrient concentrations (phosphate 2.4, silicate 54, nitrate 29.7 mmol/m^3) were found in June 1978 at depth inside the Gil Basin sill, as a result of the deepwater renewal process underway at the time.

During the fall and winter cruises, less upper-layer nitrate depletion was found because of reduced phytoplankton growth; in the winter, reduced surface-layer silicate in the upper reaches of the inlet occurred because of the lower river flow. Evidence also suggested the intrusion of low-silicate mid-depth Hecate Strait water (50 to 150 m) in response to outflow winds driving surface waters out of the inlet.

F.3.2 pH and Turbidity

The pH value is a measure of the acidity of the water. Pure water at pH 7 is neutral, whereas lower numbers are acidic and higher are basic. Seawater is slightly basic, with a pH of 7.8 to 8.3. The pH value varies with DO and with CO_2. CO_2 acts as a buffer: adding acid to the water produces CO_2; adding CO_2 to the water increases acidity (Sverdrup et al. 1942). When the upper euphotic zone is low in CO_2 because of plant use, pH values are high.

Within the inlets and fjords, surface pH is usually high, except in the presence of low pH (acidic) runoff. Freshwater discharge, particularly in areas affected by acid rain, can reduce pH values. Many of the streams sampled on the British Columbia central coast during 1982 to 1983 were acidic (Sullivan et al. 1985), having low pH values (e.g., 6 to 6.5 near Rivers Inlet). Values for pH would tend to be low in deep waters, particularly if the water is low in DO because of poor flushing or the buildup of organic debris. For example, in a stagnant deep-water Norwegian fjord, where H_2S was present, pH levels were as low as 7.0 (Strom 1936). No direct measurements are available of pH levels in the Kitimat system.

Turbidity is a measure of the cloudiness or opacity of water caused by suspended particles and dissolved material. Turbidity levels within the fjords are generally higher in summer because of suspended particles in the freshwater input, sometimes called rock flour. Most of the particulates are resistant to dissolving and do little to alter the water chemistry. For high-runoff fjords, a secchi-disk, used to quantify water clarity, may be visible only within the first 10 to 30 cm (Pickard 1961). Plankton and brownish humic acid runoff also decrease water clarity. For aerial photographs of the Bish Creek region of Kitimat Inlet in 1947 and 1963, see Figures F-4 and F-5. The two images illustrate the considerable variability that occurs in the surface opacity.

For photosynthetic plankton, turbidity reduces the depth of the euphotic zone and requires mixing of nutrients above the halocline. Whether natural (rock flour), or anthropogenic (e.g., logging debris), turbid waters result in reduced primary productivity. Turbidity levels tend to decrease toward the mouths of inlets. Often turbidity levels increase in the last 50 to 100 m of the water column above the inlet bottom. High near-bottom turbidity is thought to be due to turbidity currents and landslides or avalanches. Turbidity plumes have been observed in Moses and Rivers Inlets. Avalanches and landslides, as in Dean Channel, often scar the steep sides of the inlets. Highly turbid waters can be detrimental to filter feeders (e.g., shellfish) causing them to silt up, and turbidity currents from underwater mudslides would be harmful to any benthic creatures in their path.

The highest nutrient concentrations (phosphate 2.4, silicate 54, nitrate 29.7 mmol/m^3) were found in June 1978 at depth inside the Gil Basin sill, as a result of the deepwater renewal process underway at the time.

During the fall and winter cruises, less upper-layer nitrate depletion was found because of reduced phytoplankton growth; in the winter, reduced surface-layer silicate in the upper reaches of the inlet occurred because of the lower river flow. Evidence also suggested the intrusion of low-silicate mid-depth Hecate Strait water (50 to 150 m) in response to outflow winds driving surface waters out of the inlet.

F.3.2 pH and Turbidity

The pH value is a measure of the acidity of the water. Pure water at pH 7 is neutral, whereas lower numbers are acidic and higher are basic. Seawater is slightly basic, with a pH of 7.8 to 8.3. The pH value varies with DO and with CO_2. CO_2 acts as a buffer: adding acid to the water produces CO_2; adding CO_2 to the water increases acidity (Sverdrup et al. 1942). When the upper euphotic zone is low in CO_2 because of plant use, pH values are high.

Within the inlets and fjords, surface pH is usually high, except in the presence of low pH (acidic) runoff. Freshwater discharge, particularly in areas affected by acid rain, can reduce pH values. Many of the streams sampled on the British Columbia central coast during 1982 to 1983 were acidic (Sullivan et al. 1985), having low pH values (e.g., 6 to 6.5 near Rivers Inlet). Values for pH would tend to be low in deep waters, particularly if the water is low in DO because of poor flushing or the buildup of organic debris. For example, in a stagnant deep-water Norwegian fjord, where H_2S was present, pH levels were as low as 7.0 (Strom 1936). No direct measurements are available of pH levels in the Kitimat system.

Turbidity is a measure of the cloudiness or opacity of water caused by suspended particles and dissolved material. Turbidity levels within the fjords are generally higher in summer because of suspended particles in the freshwater input, sometimes called rock flour. Most of the particulates are resistant to dissolving and do little to alter the water chemistry. For high-runoff fjords, a secchi-disk, used to quantify water clarity, may be visible only within the first 10 to 30 cm (Pickard 1961). Plankton and brownish humic acid runoff also decrease water clarity. For aerial photographs of the Bish Creek region of Kitimat Inlet in 1947 and 1963, see Figures F-4 and F-5. The two images illustrate the considerable variability that occurs in the surface opacity.

For photosynthetic plankton, turbidity reduces the depth of the euphotic zone and requires mixing of nutrients above the halocline. Whether natural (rock flour), or anthropogenic (e.g., logging debris), turbid waters result in reduced primary productivity. Turbidity levels tend to decrease toward the mouths of inlets. Often turbidity levels increase in the last 50 to 100 m of the water column above the inlet bottom. High near-bottom turbidity is thought to be due to turbidity currents and landslides or avalanches. Turbidity plumes have been observed in Moses and Rivers Inlets. Avalanches and landslides, as in Dean Channel, often scar the steep sides of the inlets. Highly turbid waters can be detrimental to filter feeders (e.g., shellfish) causing them to silt up, and turbidity currents from underwater mudslides would be harmful to any benthic creatures in their path.

Figure F-4 Aerial Photograph of the Bish Creek Area, 1947

Figure F-5 Aerial Photograph of the Bish Creek Area, 1963

F.4 References

F.4.1 Literature Cited

Freeland, H.J. and K.L. Denman. 1982. A topographically controlled upwelling centre off southern Vancouver Island. *Journal of Marine Research* 40: 1069-1093.

Institute of Oceanography. 1953. *British Columbia Inlet Study, 1951. Data Report 1*. University of British Columbia. Vancouver, British Columbia.

Institute of Oceanography. 1963. *British Columbia Inlet Cruises, 1962. Data Report 25*. University of British Columbia. Vancouver, British Columbia.

Institute of Oceanography. 1964. *British Columbia Inlet Cruises, 1963. Data Report 23*. University of British Columbia. Vancouver, British Columbia.

Institute of Oceanography. 1967. *British Columbia and Alaska Inlets and Pacific Cruises, 1966. Data Report 26*. University of British Columbia. Vancouver, British Columbia.

Macdonald, R.W., B.D. Bornhold and I. Webster. 1983a. The Kitimat Fjord system: An introduction. In R.W. Macdonald (ed.). *Proceedings of a Workshop on the Kitimat Marine Environment.* Canadian Technical Report of Hydrography and Ocean Sciences No. 18. Institute of Ocean Sciences. Sidney, British Columbia. 2-13.

Macdonald, R.W., W.J. Cretney, C.S. Wong and P. Erickson. 1983b. Chemical characteristics of water in the Kitimat Fjord system. In R.W. Macdonald (ed.). *Proceedings of a Workshop on the Kitimat Marine Environment.* Canadian Technical Report of Hydrography and Ocean Sciences No. 18. Institute of Ocean Sciences. Sidney, British Columbia. 66-87.

Parsons, T. 1965. A general description of some factors governing primary production in the Strait of Georgia, Hecate Strait and Queen Charlotte Sound, and N.E. Pacific Ocean. MS Report Series (Oceanography and Limnology) 193. Fisheries Research Board Canada. Ottawa, Ontario.

Parsons, T., M. Takahashi and Hargrave, B. 1984. *Biological Oceanographic Processes*. Pergamon Press. New York.

Pickard, G.L. 1961. Oceanographic features of inlets in the British Columbia mainland coast. *Journal of the Fisheries Research Board of Canada* 18: 907-999.

Strom, K.M. 1936. Landlocked Waters: Hydrography and bottom deposits in badly-ventilated Norwegian fjords with remarks upon sedimentation under aerobic conditions. Skrifter Institut Matematisk-naturvidenskapelig-Klasse 7. Norske Videnskaps Akademi. Oslo, Norway.

Sullivan, M.A., S.C. Samis, J.A. Servizi and R.W. Gordon. 1985. *Survey of Selected British Columbia and Yukon Salmon Streams for Sensitivity to Acidification from Precipitation*. Canadian Technical Reports on Fisheries and Aquatic Sciences 1388. Fisheries and Oceans Canada. Ottawa, ON.

Sverdrup, H.U., M.W. Johnson and R.H. Fleming. 1942. *The Oceans: Their Physics, Chemistry and General Biology*. Prentice Hall. New York.

Waldichuk, M., J.R. Markert and J.H. Meikle. 1968. *Physical and Chemical Oceanographic Data from the West Coast of Vancouver Island and the Northern British Columbia Coast, 1957–67, Volume II, Fisher Channel – Cousins Inlet, Douglas Channel – Kitimat Arm and Prince Rupert Harbour and its Contiguous Waters.* Fisheries Research Board of Canada, Manuscript Report Series #990. Ottawa, ON.

Whitney, F.A., C.S. Wong, and P.W. Boyd. 1998. Interannual variability in nitrate supply to surface waters of the northeast Pacific Ocean. *Marine Ecology Progress Series* 170: 15-23.

F.4.2 Internet Sites

Fisheries and Oceans Canada. 2003. *Hecate Strait Ecosystem Project*. Available at: http://www-sci.pac.dfo-mpo.gc.ca/sa-hecate/default.htm/. Accessed May 2006.

University of British Columbia. 2006. *Stratogem Project*. Available at: http://www.stratogem.ubc.ca/. Accessed May 2006.

Appendix G GEM Oceanography Program, September 2005 to January 2006

G.1 Introduction

G.1.1 Objectives

The purpose of this document is to describe physical oceanographic measurements made to support the environmental assessment for the Project. Oceanographic measurements were undertaken for the Project spanning a four-month period from September 2005 to January 2006. This appendix presents the results of the measurement program, including:

- subsurface currents
- waves
- water levels
- CTD profiles (conductivity, temperature and depth)

New data are compared with historical knowledge in Appendices B through D.

G.2 Methods

G.2.1 Confined Channel Assessment Area for Field Surveys

In September 2005, a series of nine current meters was deployed at four locations in the CCAA. These instruments continuously collected measurement data until January 2006, when eight of the nine instruments were recovered. The ninth instrument was recovered later and contained data to November 6, 2005. In January 2006, one of the current meters was redeployed in the immediate vicinity of the proposed marine terminal. During the September 2005 and January 2006 oceanographic cruises in the area, profiles of temperature and salinity values (CTD measurements) were made at 15 locations within the CCAA.

G.2.2 Data Gathering Methods and Instruments

Acoustic Doppler Current Meters

Nine acoustic Doppler current meters were deployed at the four locations in the CCAA (see Table G-1 and Attachment G1).

Table G-1 Locations, Deployment Times and Water Depths for Each Current Measurement Site

Site	Area	Deployment Time Date (PDT)	Lat, Long (WGS84)	Water Depth to Sea Floor (m)	Recovery Time Date (PDT)	Instrument Depth or Depth Range
1	Kitimat Arm, Offshore of Bish Creek Terminal	14 Sept 2005 10:02	53 56.468 128 42.461	179	17 Jan 2006 10:40	1. ADCP 300 kHz: 9-97m @ 2m bins. Battery dead at recovery. Last good data 01 Jan 2006. 2. Single Level CM: 165m + WL
2	Douglas Channel	13 Sept 2005 16:00	53 30.574 129 12.150	380	15 Jan 2006 16:02	3. ADCP 300 kHz: 7-57m @ 2m bins (upward looking) 4. ADCP 300 kHz: 67-151m @ 2m bins (downward looking) 5. Single Level CM: 212m + WL 6. Single Level CM: 312m + WL
3	Principe Channel	12 Sept 2005 10:15	53 33.772 130 11.834	135	06 Nov 2005 20:00 _____ 13 Jan 2006 15:15	7. 300 kHz ADCP: 10-80m @ 2m bins (upward looking); broke free of mooring on 06 Nov 2005. 8. Single Level CM: 123m + WL, direction data on this instrument was adjusted to align with channel.
4	West Approach to Caamaño Sound, Yates Shoal (Aranzazu Banks)	12 Sept 2005 17:30	53 50.235 129 32.555	34	12 Jan 2006 12:40	9. ADCP 600 kHz: 10-33m @ 1m bins With directional wave measurements. Acoustic release on pop-up canister was not recovered.

NOTES:
CM = current meter
PDT = Pacific Daylight Time
WL = Water Level Measurement
WGS84 = World Geodetic System 1984

Of the nine instruments, five were ADCPs. Four of these ADCPs were 300-kHz instruments operated on taut line mooring systems in the water column. At Site 4, in the west approach to Caamaño Sound, a 600-kHz instrument ADCP was operated from a bottom frame to allow the measurement of directional waves as well as ocean current profiles. At Site 3 (in Principe Channel), the 300-kHz ADCP contained valid data to November 6, 2005, at which time it broke free of its mooring. The Site 3 ADCP was recovered later washed up on a beach. The ADCPs also measure water temperature and acoustic backscatter return values as well as internal instrument functional parameters. The 600-kHz ADCP operated at Site 4 also measured pressure which was used to compute water levels.

The four other Doppler current meters were current meters that use the Doppler measurement principle to measure ocean currents at a single level. These current meters also measured pressure (for water-level computations) as well as temperature and internal parameters. The Site 3 Aquadopp meter exhibited some problems with the current direction measurements and post-processing corrections were applied to the data set.

For the detailed location maps for each ocean current measurement site, see Figures G-1 through G-4. Nearby sites where current measurements were made in the past are also shown to facilitate comparisons with the historical data previously discussed in Appendices B through D.

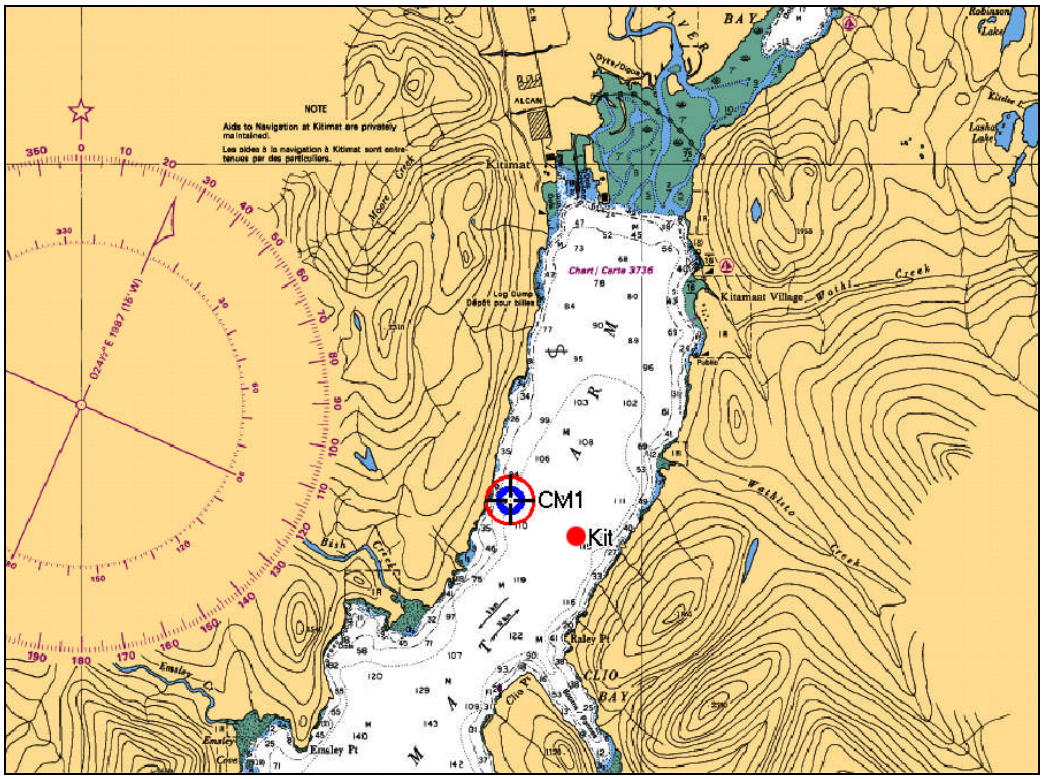

NOTE: Also shown is the location of a current meter mooring "Kit" operated in this area in the summer and fall of 1977.

Figure G-1 Location of the GEM Marine Current Meter Mooring CM1 at Site 1 in Kitimat Arm

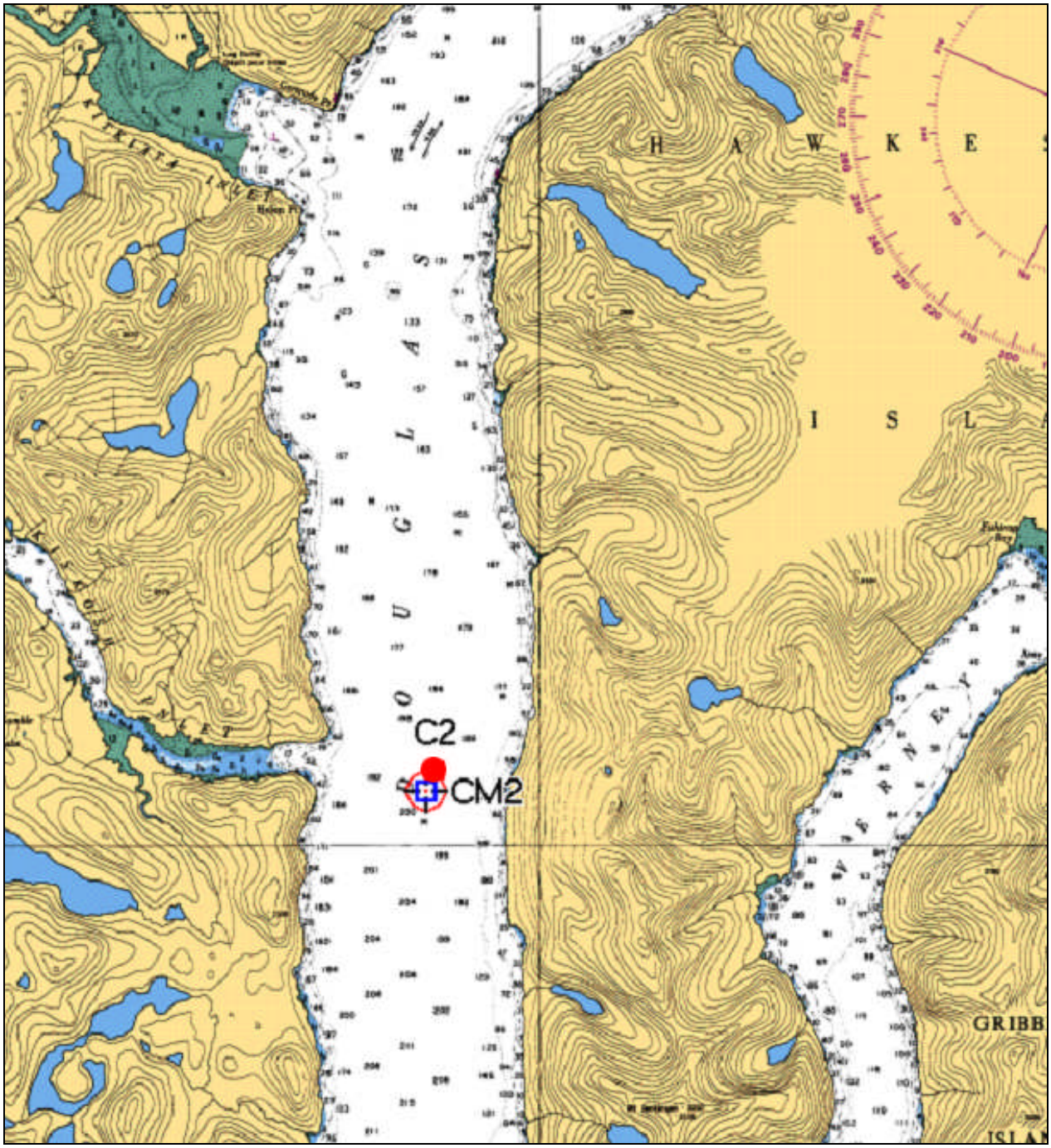

NOTE: Also shown is the location of a current meter mooring “C2” operated in this area in 1977-1978.

Figure G-2 Location of the GEM Marine Current Meter Mooring CM2 at Site 2 in Douglas Channel

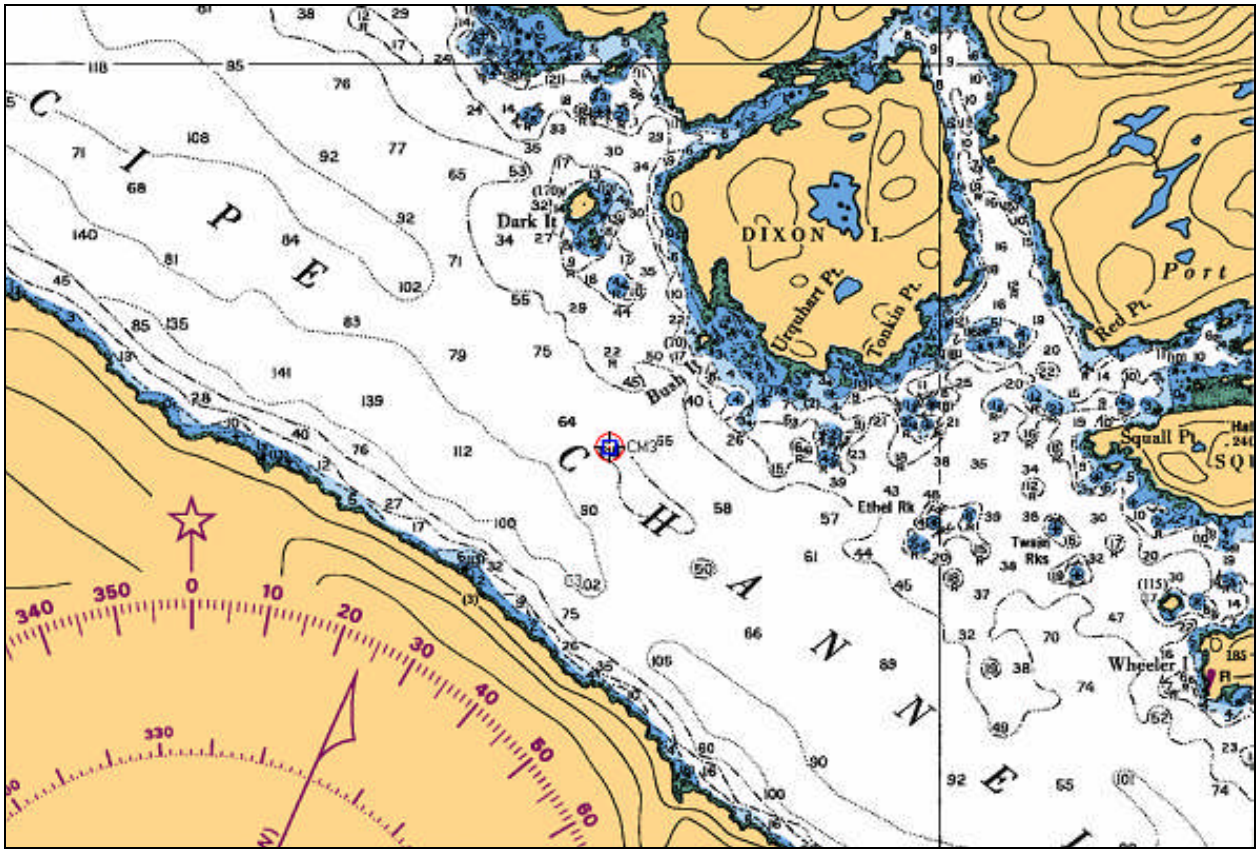

Figure G-3 Location of the GEM Marine Current Meter Mooring CM3 at Site 3 in Principe Channel

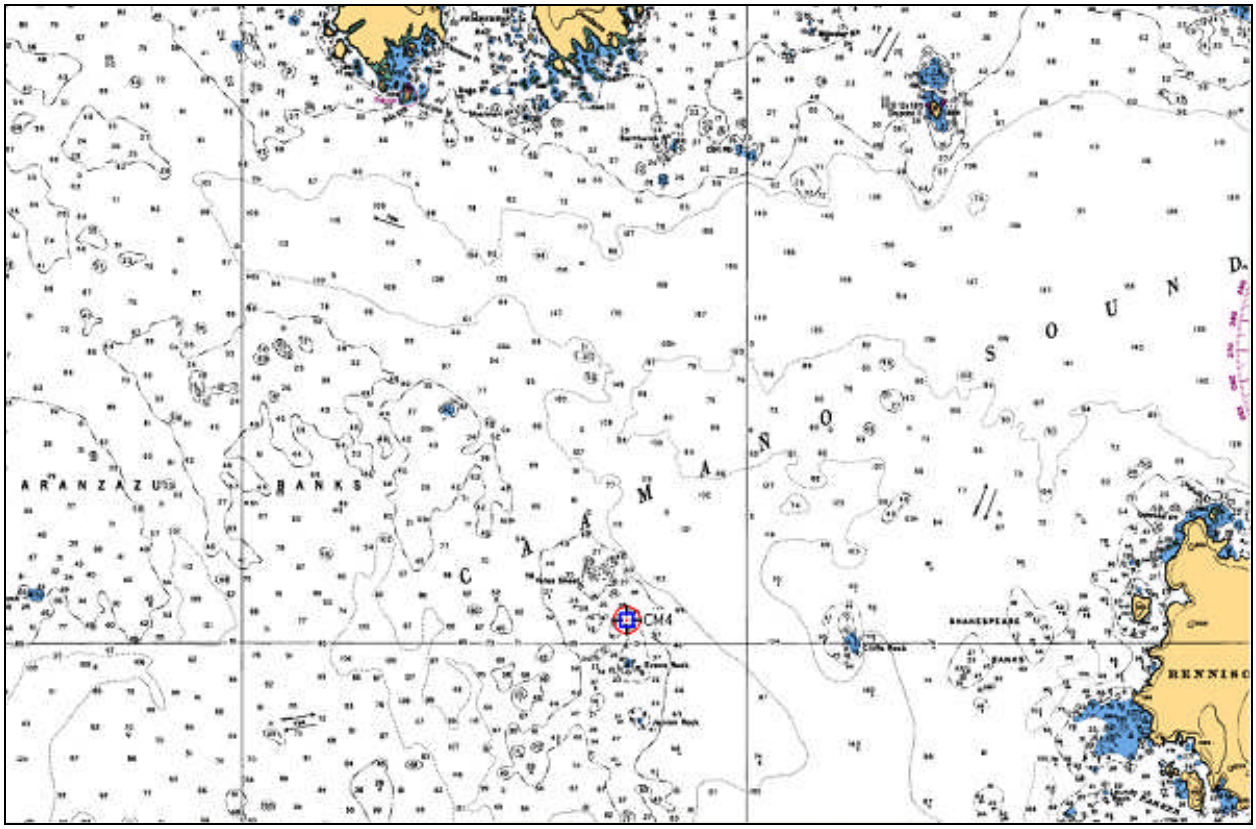

Figure G-4 Location of the GEM Marine Current Mooring CM4 at Site 4 in Caamaño Sound

CTD Profile Measurements in September 2005 and January 2006

During the deployment cruise in September 2005 and again in January 2006, as part of the recovery cruise, CTD profile data were obtained at 15 locations within the study area. For the location coordinates, times and dates of the CTD data collected in September 2005, see Table G-2 and, for the data collected in January 2006, see Table G-3.

All CTD data were collected with an Applied Microsystems STD12+ CTD instrument (sn 736).

Table G-2 CTD Stations Occupied in September 2005

Area	Comments	Time Date (PDT)	Lat, Long (WGS84)	Water Depth/ Deepest CTD Measurement (m)	CTD File Name	Map ID
Principe Chan	Near CM Site 3	12 Sept 05 10:30	53 33.781 130 12.05	188/160	Site3.xls	C3
Caamaño Sound	Near Dobrocky #08	12 Sept 05 18:45	52 53.144 129 24.373	271/250	Caamaño.xls	Caam
Douglas Chan	Near CM Site 2; near Dobrocky #28	13 Sept 05 13:25	53 30.108 129 12.586	370/360	Site2.xls	C2
Douglas Chan	Between CM Sites 1&2; off Maitland Is, near Dobrocky #26; wire angle ~25°	13 Sept 05 17:45	53 42.73 129 5.27	394/375	Ctd100.xls	C100
Douglas Chan	same as Dobrocky #25, off Nanakwa Shoal	13 Sept 05 18:15	53 49.25 128 49.359	335/320	Ctd101.xls	D25
Douglas Chan	Near Kitimat	14 Sept 05 08:30	53 56.25 128 41.71	210/200	Dobkit.xls	Kit
Douglas Chan	Dobrocky #27	15 Sept 05 08:30	53 38.18 129 11.69	360/340	Dob27.xls	D27
Wright Sound	Dobrocky #01	15 Sept 05 11:00	53 23.85 129 11.90	415/400	Dob01.xls	D01
Squally Chan	Dobrocky #06	15 Sept 05 14:30	53 13.2 129 25.2	510/450	Dob06.xls	D06
Nepean Sound	Dobrocky #07	16 Sept 05 10:00	53 11.2 129 39.0	180/170	Dob07.xls	D07
Principe Chan A	Southern End of Principe Channel	16 Sept 05 11:30	53 21.8 129 49.6	188/180	Princ_A.xls	P_A
Principe Chan B	Middle of Principe Channel	16 Sept 05 13:00	53 31.0 130 4.6	204/185	Princ_B.xls	P_B
Principe Chan C	Northern End of Principe Channel	16 Sept 05 15:30	53 39.2 130 26.8	140/130	Princ_C.xls	P_C
Squally Chan	Dobrocky #10	15 Sept'05 16:00	53 06.3 129 21.6	650/450	Dob10.xls	D10
Campania Sound	Dobrocky #09	15 Sept 05 17:00	53 01.8 129 16.4	390/370	Dob09.xls	D09

Table G-3 CTD Stations Occupied in January 2006

Area	Comments	Time Date (PST)	Lat, Long (WGS84)	Water Depth/ Deepest CTD Measurement (m)	CTD File Name	Map ID
Principe Chan	Near CM Site 3	13 Jan 06 14:40	53 33.781 130 12.05	150/140	Site3.xls	C3
Caamaño Sound	Near Dobrocky #08	12 Jan 06 15:35	52 53.144 129 24.373	255/255	CamanoSD.xls	Caam
Douglas Chan	Near CM Site 2; near Dobrocky #28, Did 2 casts at this site	15 Jan 06 11:05	53 30.108 129 12.586	390/360	Site2.xls & Site2B.xls	C2
Douglas Chan	Between CM Sites 1&2; off Maitland Is, near Dobrocky #26	15 Jan 06 14:10	53 42.73 129 5.27	390/375	C100.xls	C100
Douglas Chan	same as Dobrocky #25, off Nanakwa Shoal	17 Jan 06 14:00	53 49.25 128 49.359	340/320	D25.xls	D25
Douglas Chan	Near Kitimat	17 Jan 06 12:42	53 56.25 128 41.71	210/200	Site1.xls	Kit
Douglas Chan	Dobrocky #27	15 Jan 06 13:16	53 38.18 129 11.69	370/350	D27.xls	D27
Wright Sound	Dobrocky #01	15 Jan 06 09:55	53 23.85 129 11.90	440/410	D01.xls	D01
Squally Chan	Dobrocky #06	14 Jan 06 18:35	53 13.2 129 25.2	550/443	D06.xls	D06
Nepean Sound	Dobrocky #07	14 Jan 06 17:25	53 11.2 129 39.0	200/190	D07.xls	D07
Principe Chan A	Southern End of Principe Channel	14 Jan 06 11:30	53 21.8 129 49.6	190/180	Princ_A.xls	P_A
Principe Chan B	Middle of Principe Channel	14 Jan 06 14:20	53 31.0 130 4.6	204/190	Princ_B.xls	P_B
Principe Chan C	Northern End of Principe Channel	13 Jan 06 16:40	53 39.2 130 26.8	140/140	Princ_C.xls	P_C
Squally Chan	Dobrocky #10	13 Jan 06 08:45	53 06.3 129 21.6	650/450	D10.xls	D10
Campania Sound	Dobrocky #09	12 Jan 06 17:30	53 01.8 129 16.4	360/360	D09.xls	D09

NOTES:
CM = current meter
PDT = Pacific Daylight Time
WL = Water Level Measurement
WGS84 = World Geodetic System 1984

G.3 Results of GEM Marine Data Collection, September 2005 to January 2006

G.3.1 Subsurface Current Meter Data Sets

Statistical Summaries

In this section, the current statistics are given by depth for four instrumented sites in the CCAA. For the current meter measurements, see Attachment G2. The measurements have been classified as near-surface (depths of 5 to 20 m), halocline depths (between 20 and 75 m), mid- to near-bottom (Kitimat Arm and Principe Channel, depths between 75 and 200 m), and deep water (Douglas Channel where water depths exceed 200 m). The overall speeds and vector average magnitudes are described. Summary statistical results are presented below.

Maximum speeds at the near-surface levels in Caamaño Sound, Douglas Channel and Principe Channel were 92, 106 and 111 cm/s, respectively (see Table G-4). The maximum current speeds in Kitimat Arm are notably lower at 51 cm/s. Near-surface mean speeds in the study area are only 8 cm/s in Kitimat Arm, but considerably larger (between 16 and 39 cm/s) in Caamaño Sound, Douglas Channel and Principe Channel. The current speeds in Kitimat Arm, Douglas Channel and Caamaño Sound exhibit a marked reduction with depth, with the mean current speeds in the halocline layer reduced by a factor of two from near-surface levels (see Table G-4 and Figure G-5). Current speeds are generally reduced further at water depths below 75 m. However, in Principe Channel the mean currents are more uniform with depth. Also the maximum current speed measured at all sites and depths was 113 cm/s in Principe Channel at 80-m depth.

In the near-surface layer the vector average magnitude (net flow speed considered over the measurement period) was typically about 4 to 9 cm/s, reading 12 cm/s at both the shallowest measurement level (7 m) in Douglas Channel and 10 m in Principe Channel. However, in the Kitimat Arm, the net near-surface flow was much smaller at 0.5 to 1.6 cm/s. The overall pattern in net current direction is one of seaward movement at the surface and inland movement at depth as indicated by the Douglas Channel vector-averaged speeds. This is consistent with an estuarine circulation where lower salinity waters move seaward at surface, with a compensatory landward movement of more saline oceanic water at depth.

Table G-4 Current Speed Statistics and Vector Average Currents by Site for Near-surface (<20 m), Halocline (20-75 m), Mid-depth (75-200 m) and Deep (>200 m) Measurement Locations

Site	Depth	Speed (cm/s)			Vector Average		
		Min.	Mean	Max.	Mag. (cm/s)	Dir.	SD (cm/s)
Near-surface (depth <20 m)							
Site 1 Kitimat	9	0.0	7.5	50.8	1.6	194.8	9.7
	15	0.0	5.3	39.9	0.5	206.0	6.9
Site 2 Douglas	7	0.1	24.5	106.3	12.0	173.4	27.8
	15	0.0	16.2	69.8	3.6	165.8	19.2
Site 3 Principe	10	0.1	38.7	110.7	11.8	301.5	43.3
Site 4 Caamaño	6	0.3	26.0	91.5	5.8	334.9	28.7
	10	0.2	25.9	84.1	8.7	335.9	27.8
	19	0.1	21.8	69.9	5.8	337.1	23.9
Halocline (depth: 20-75 m)							
Site 1 Kitimat	41	0.0	3.4	24.3	0.4	190.5	4.2
Site 2 Douglas	41	0.1	12.6	57.3	8.0	4.7	12.9
	67	0.1	10.2	42.7	6.8	339.6	10.0
Site 3 Principe	20	0.3	36.4	98.0	0.2	41.5	42.1
	40	0.3	36.1	96.6	16.5	118.0	38.6
Site 4 Caamaño	33	0.1	13.1	43.6	4.0	321.8	14.5
Mid-depth (75 m <depth <200 m)							
Site 1 Kitimat	81	0.0	2.9	13.1	0.2	210.4	3.4
	165	0.0	3.4	14.4	0.9	175.8	3.9
Site 2 Douglas	91	0.1	9.0	32.6	3.7	326.1	9.9
	121	0.0	8.1	33.2	1.5	313.2	9.5
	151	0.0	8.4	31.8	1.0	301.2	9.9
Site 3 Principe	80	0.3	31.9	113.3	8.8	111.6	37.8
	125	0.1	25.3	109.4	2.0	86.3	31.3
Deep (depth >200 m)							
Site 2 Douglas	250	0.0	8.9	24.8	1.2	166.5	9.8
	350	0.0	6.4	18.0	1.0	353.5	7.2

NOTE:
SD = standard deviation

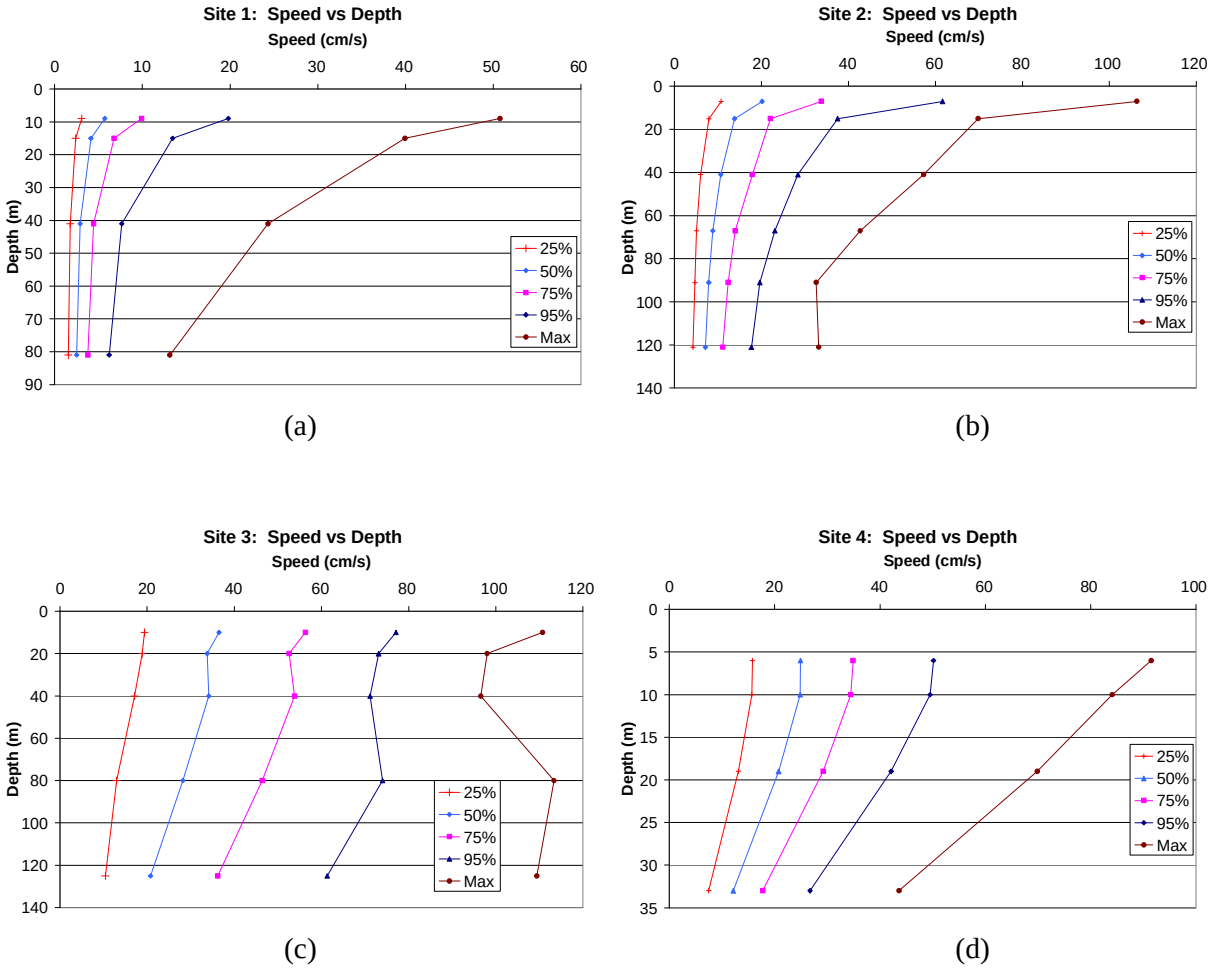

Figure G-5 Current Speed vs. Depth for Kitimat Arm (a), Douglas Channel (b), Principe Channel (c) and Caamaño Sound (d)

Distribution of Current Speeds and Directions

Directional distributions of currents are presented as spoke plots. Each spoke represents the percentage of currents heading toward the indicated direction, and each spoke is segmented according to the speed distribution within that directional segment. Also shown are the maximum and mean currents for each directional segment.

The currents in Kitimat Arm are small in magnitude, but they exhibit a pronounced bimodal directional distribution consistent with the tendency for the tidal flows to be along the axis of the channel (see Figure G-6).

Douglas Channel shows strong currents of 60 to 80 cm/s aligned along-channel, at near-surface levels and 20 to 40 cm/s at larger depths, but with a net flow to the south (see Figure G-7). The bias of the net southerly currents at the near-surface level is very prominent, as is the northerly bias of the currents in the halocline layer at 41-m depth. The deeper measurements are considerably reduced in magnitude and show a bias toward northerly flows.

The directional distribution of currents in the banks at the approaches to Caamaño Sound is less bimodal in character, although few flows are directed toward the southeasterly quadrant (see Figure G-8). The most common current direction is northeasterly or directed toward the Sound and entrance to the inland waterway. However, the vector average or net flow direction is toward the northwest.

The currents measured in Principe Channel align northwest-southeast along the axis of the channel (see Figure G-9). The preferential flow to the northwest at 10-m depth, switching to southeast at 40 and 80-m depths, is consistent with an estuarine circulation with fresher surface waters flowing out to the northwest and more saline water returning near bottom. The single-point current meter at 125-m depth shows a more evenly split northwest-southeast flow that appears to be somewhat inconsistent with the deeper ADCP direction distributions, even considering only the shorter section of the 125-m record up to November 6 when the ADCP broke free of its mooring.

Variability of Currents by Frequency Band and Tidal Analysis

The distribution of variance in the major current component is presented in the following results. The currents were digitally filtered to compute time series for low frequencies (less than 1 cycle per day), high frequencies (greater than 2 cycles per day) and band passed (1 to 2 cycles per day; mainly tidal). The band-passed currents were then analyzed by using Foreman's (1978) tidal analysis and prediction programs and subtracting the predicted tidal currents from the original band-passed currents to separate the tidal and non-tidal contributions. The low-frequency band that had contributions on time scales exceeding a day were likely due primarily to wind forcing, though density-driven effects might be included in this band. Energy in the high-frequency band is likely related to internal waves and seiches. For the energy (variance) breakdown for Kitimat Arm, Douglas Channel, Principe Channel, see Figure G-10 and Aranzazu Banks at the entrance to Caamaño Sound.

a

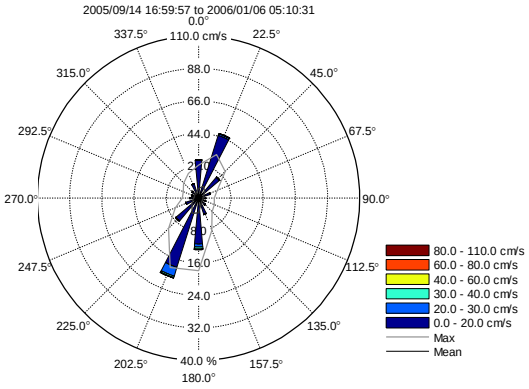

b

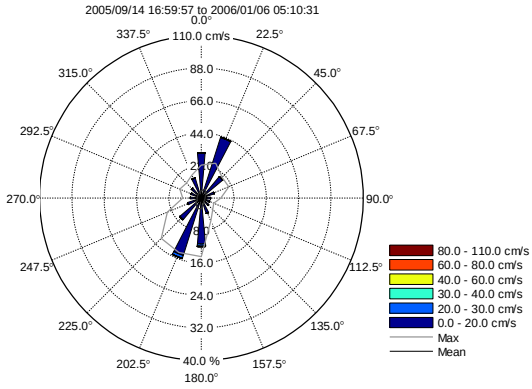

c

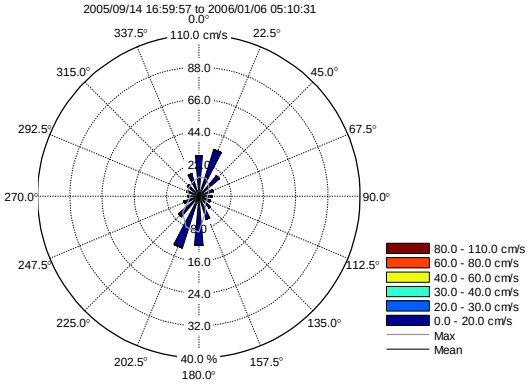

d

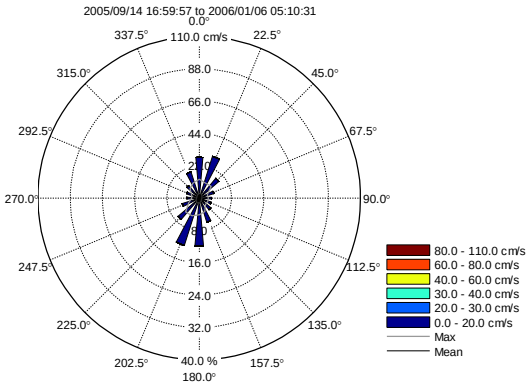

e

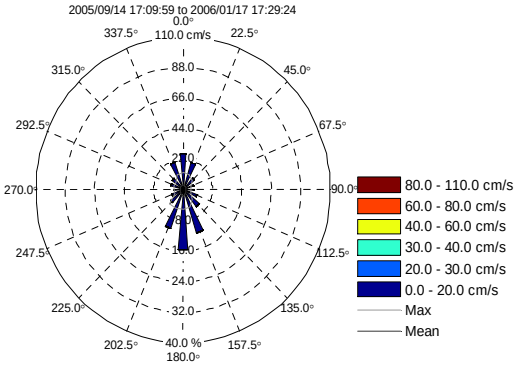

Figure G-6 Speed-Direction Joint Frequency Plot in Kitimat Arm for (a) 9-m Depth, (b) 15-m Depth, (c) 41-m Depth, (d) 81-m Depth and (e) 165-m Depth

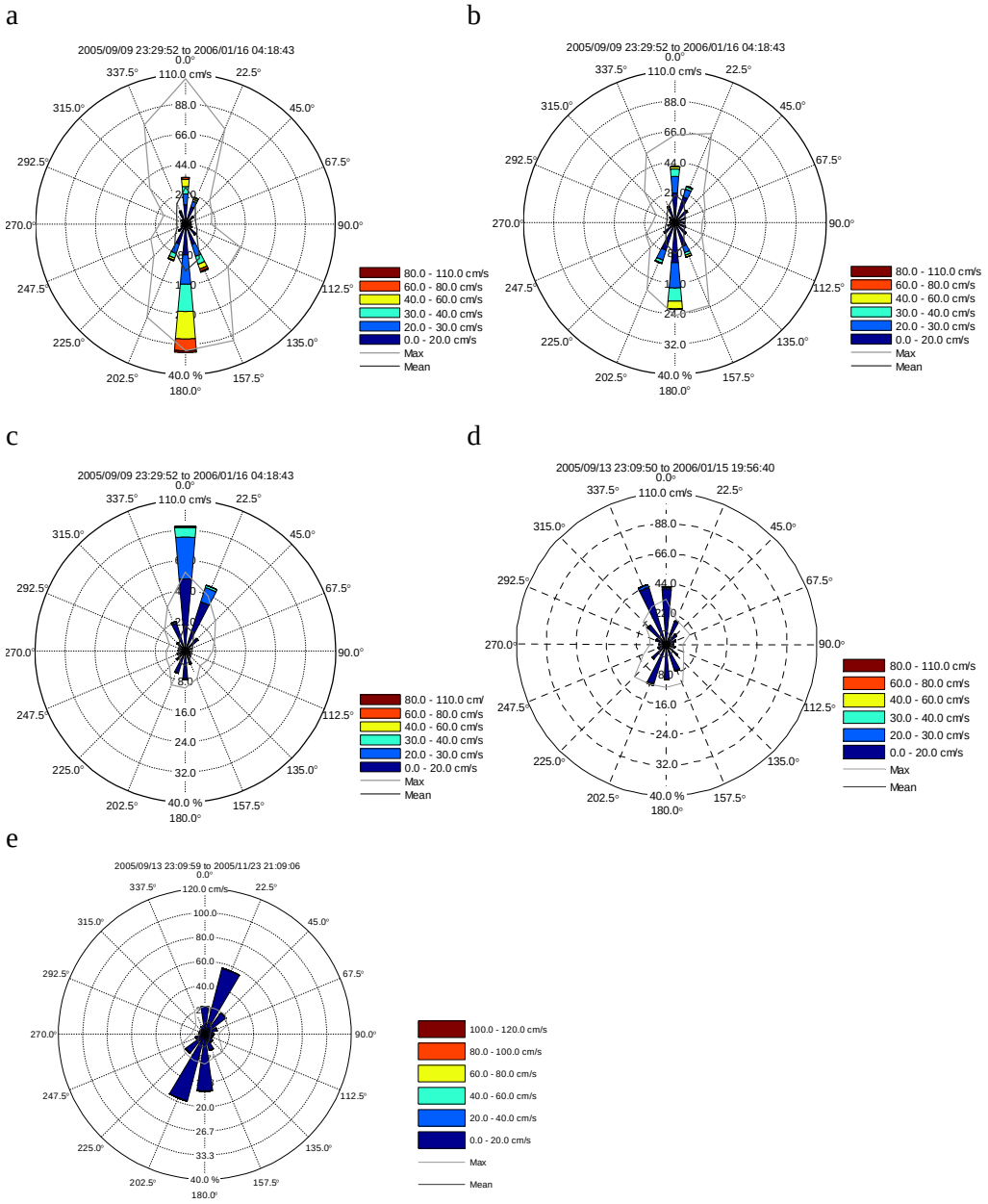

Figure G-7 Speed-Direction Joint Frequency Plot for (a) 7-m Depth, (b) 15-m Depth, (c) 41-m Depth, (d) 121-m Depth and (e) 250-m Depth in Douglas Channel

a

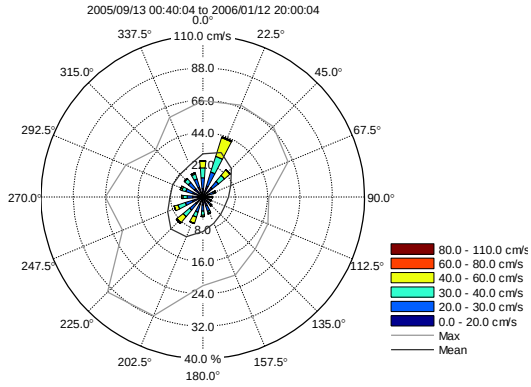

b

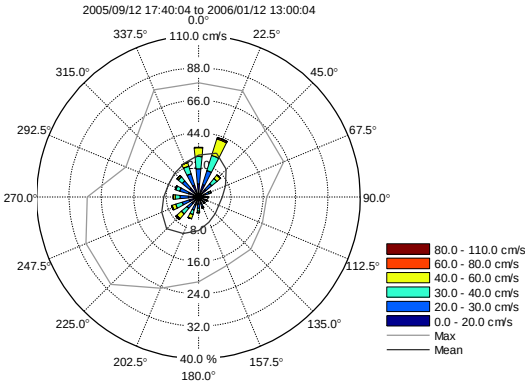

c

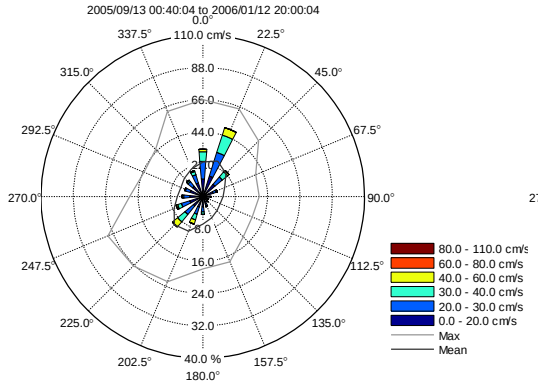

d

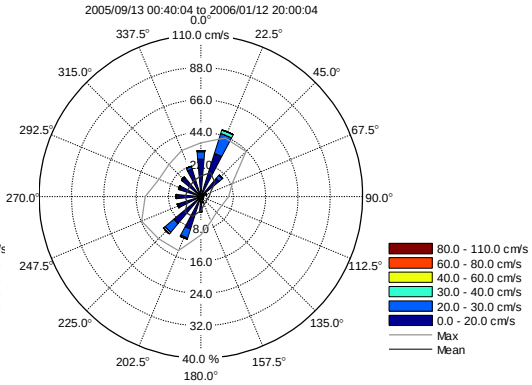

Figure G-8 Speed-Direction Joint Frequency Plot for (a) 6-m Depth, (b) 10-m Depth, (c) 19-m Depth and (d) 33-m Depth in Caamaño Sound

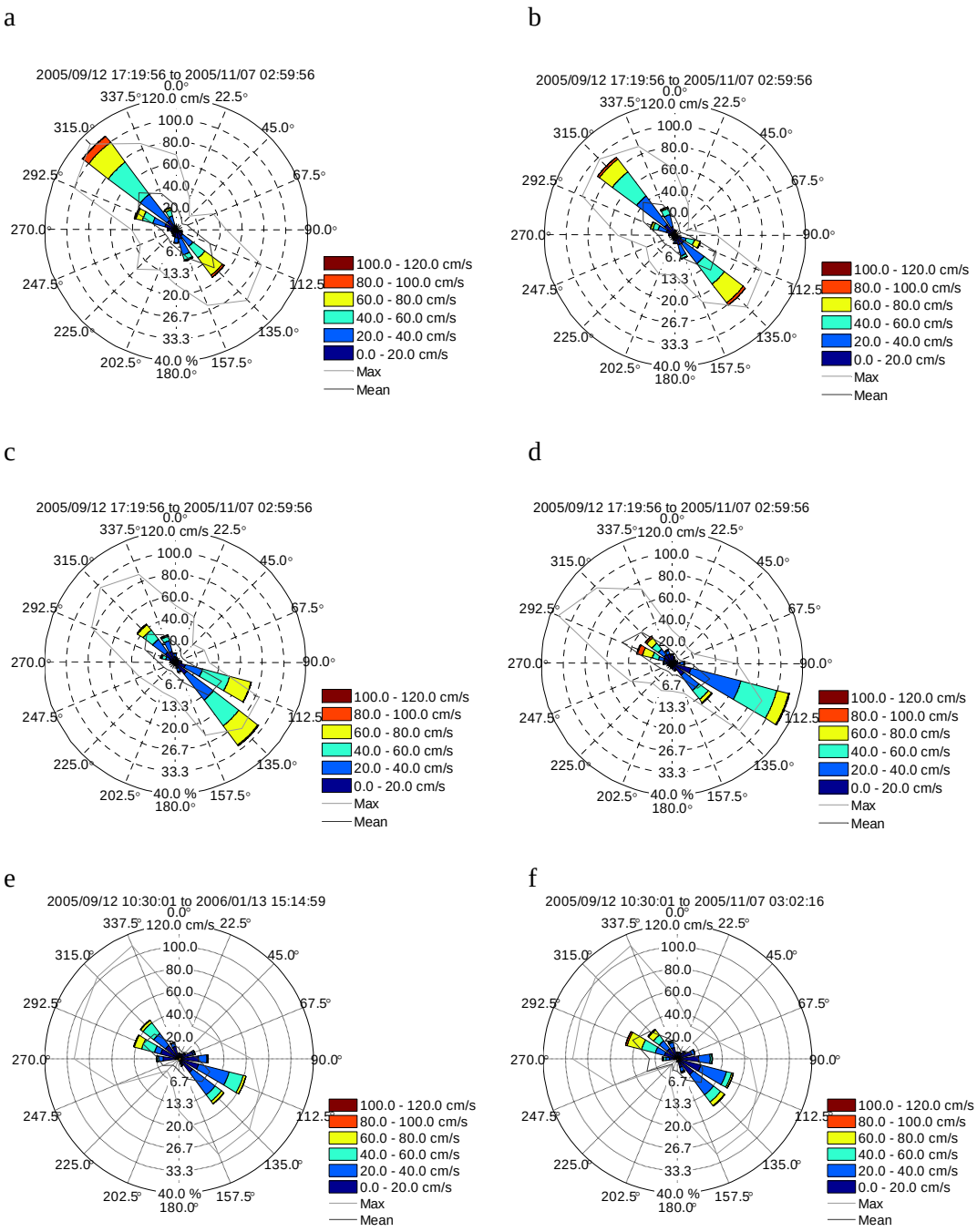

Figure G-9 **Speed-Direction Joint Frequency Plot for (a) 10-m, (b) 20-m, (c) 40-m, (d) 80-m, (e) full 125-m Data Record and (f) Partial 125-m Data Record Coinciding with Shallower Depths in Principe Channel**

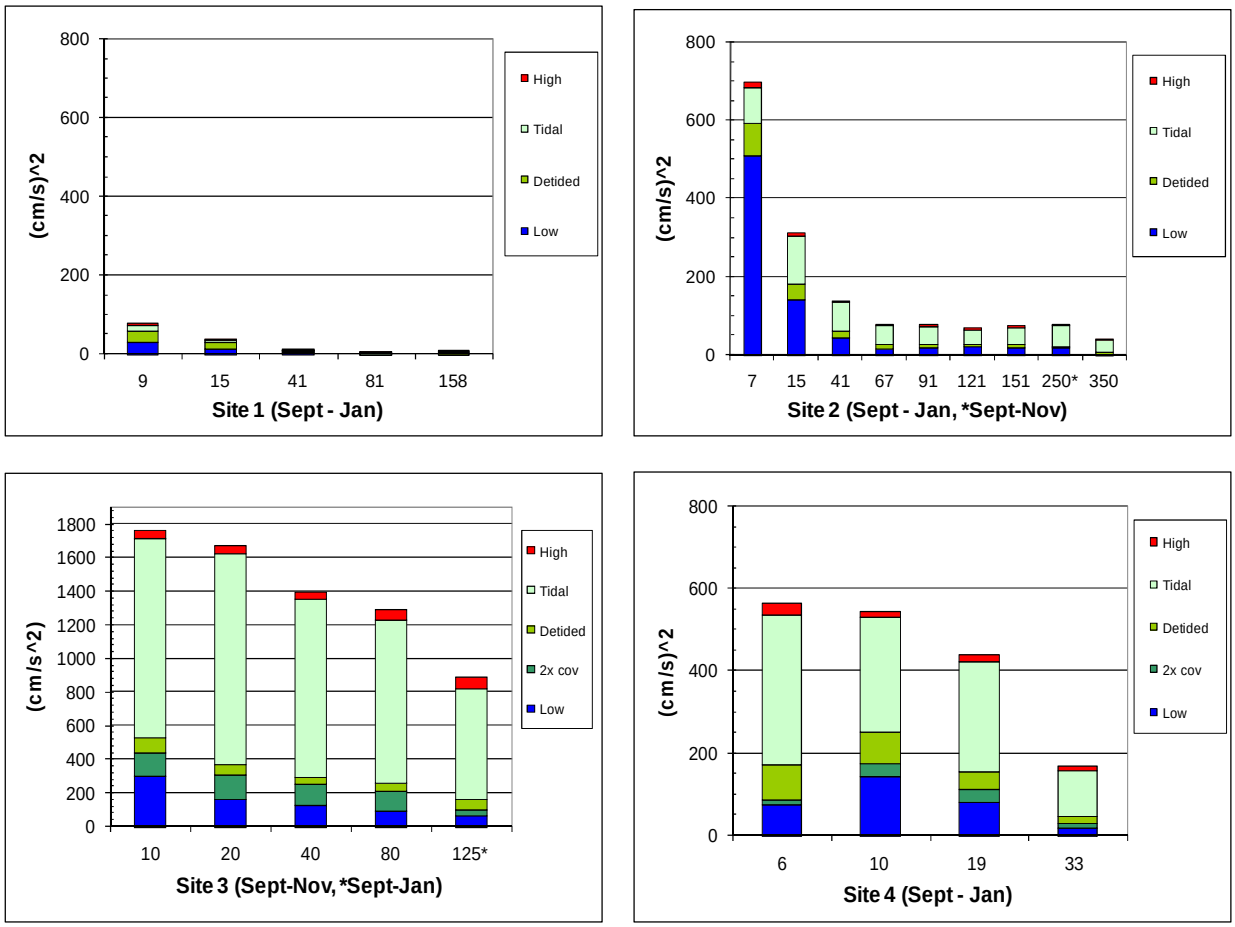

Figure G-10 Speed of Current Variance Distribution among High-Frequency, Astronomical Tides, Detided, and Low-Frequency Bins for Site 1 (Kitimat Arm), Site 2 (Douglas Channel), Site 3 (Principe Channel) and Site 4 (Caamaño Sound)

Note the very low levels of variance in Kitimat Arm (Site 1) compared with the other stations. The Kitimat Arm data also show a relatively large amount of detided variance.

In Douglas Channel, the winds result in large amounts of low-frequency variance, which is larger than the variance of the astronomical tidal currents at near-surface levels. The large current speeds in Principe Channel required plotting on a scale twice as large as at the other sites. The currents at all levels in Principe Channel are dominated by the tides. The Caamaño Sound measurements show that the currents on the shallow banks are also dominated by the astronomical tides.

G.3.2 Response of Currents to Tidal Forcing

Astronomical and Internal Tidal Currents

Tidal currents driven by astronomical forces are uniform with depth in the absence of frictional or other physical mechanisms. In the presence of density gradients within the water column, internal tidal currents can develop. Internal tidal currents are characterized by large depth-dependent variations in the tidal current amplitudes and phases as well as marked changes in amplitude and phase at a single measurement level. The effect of internal modes of tidal currents can be seen as changes in the fitted tidal constituents as well as significant residual variance or energy in the semi-diurnal to diurnal band-passed currents. From the variance distribution plots of Figure G-10, the detided current variances and changes in tidal current variances indicate that internal tides occur in Kitimat Arm and Douglas Channel, especially in the upper layer, and to a lesser degree in Caamaño Sound and Principe Channel.

For the tidal stream constituents for 125-m depth in Principe Channel, see Table G-5. As at the other sites in the study area, the M2 is the dominant constituent. To further examine internal tides, a tabulation of the tidal analysis of the measured current meter data was prepared for the largest tidal constituent (M2) for values of magnitude, phase, sense of rotation and a parameter that will be denoted as R (see Table G-6). The parameter R is the ratio of the magnitude of the minor (cross-channel) to major (along-channel) current components for the M2 tidal current. At many sites, the amplitude and phases of the M2 tidal constituent exhibit largely changes with depth. Large amplitude and phase changes are noticeable in Kitimat Arm and Douglas Channel, especially in the upper 50 m of the water column.

The minor component of the tidal currents in Kitimat Arm, Douglas Channel and Principe Channel is very small, as indicated by very low values (less than 0.1) of R, consistent with flows primarily along the channel axis and very small cross-channel flows. Much larger values of R of 0.1 to 0.24 are evident in Caamaño Sound where local bathymetry provides much less in the way of constraints to current flow directions.

G.3.3 Water Levels and Tidal Heights Results

For the statistics of tidal heights, with respect to mean sea level, for Sites 1 through 4, see Table G-7. These tidal height statistics do not include corrections for variations in atmospheric pressure over the deployment. The tidal ranges at Site 1 in Kitimat Arm are about 6.0 m from maximum to minimum and only 4.4 m from the 5% exceedance level to the 95% exceedance level. At Site 2 in Douglas channel, the tidal range is similar at 4.3 m at the 95% exceedance level (6.2 m max-min). At Site 3 in Principe Channel, the tidal range is 5.8 m at the 95% exceedance level (8.4 m max-min). At Site 4 in the approaches, the tidal range is 3.8 m at the 95% exceedance level (5.5 m max-min).

Table G-5 Tidal Stream Constituents for 125-m Depth in Principe – September 12, 2005 – January 13, 2006

	NAME	SPEED	MAJOR	MINOR
2	MM	0.001512	0.066	0
3	MSF	0.002822	0.059	-0.002
4	ALP1	0.034397	0.355	0.003
5	2Q1	0.035706	0.216	-0.022
6	Q1	0.037219	0.157	0.047
7	O1	0.038731	2.263	-0.21
8	NO1	0.040269	0.511	-0.072
9	P1	0.041553	1.103	0.142
10	K1	0.041781	4.428	-0.435
11	J1	0.043293	0.873	0.112
12	OO1	0.044831	0.429	0.257
13	UPS1	0.046343	0.171	0.019
14	EPS2	0.076177	1.001	-0.063
15	MU2	0.077689	4.493	-0.108
16	N2	0.078999	7.395	0.587
17	M2	0.080511	32.975	-0.695
18	L2	0.082024	2.17	-0.383
19	S2	0.083333	14.811	-0.317
20	K2	0.083561	3.001	-0.218
21	ETA2	0.085074	0.95	0.115
22	MO3	0.119242	0.381	0.253
23	M3	0.120767	0.753	-0.141
24	MK3	0.122292	1.19	0.101
25	SK3	0.125114	0.829	-0.041
26	MN4	0.159511	1.005	-0.26
27	M4	0.161023	1.499	-0.322
28	SN4	0.162333	0.238	-0.008
29	MS4	0.163845	1.559	-0.417
30	S4	0.166667	0.345	0.143
31	2MK5	0.202804	0.29	-0.017
32	2SK5	0.208447	0.111	0.054
33	2MN6	0.240022	0.178	-0.02
34	M6	0.241534	0.137	-0.08
35	2MS6	0.244356	0.191	-0.023
36	2SM6	0.247178	0.072	-0.016
37	3MK7	0.283315	0.021	-0.003
38	M8	0.322046	0.013	0.001
39	M10	0.402557	0.01	-0.002

Table G-6 Summary of the M2 Tidal Stream Constituent by Site, Time and Depth

Site	Time	Depth (m)	M2 Major	M2 Minor	R (min/maj)	Rotation Dir	Phase
Site 1	Sept-Jan	9	5.0	-0.11	-0.02	cw	214.9
		15	2.4	-0.04	-0.02	cw	257.3
		41	0.6	0.03	0.05	ccw	218.0
		81	1.6	0.06	0.04	ccw	129.8
		158	2.0	-0.09	-0.05	cw	133.9
Site 2	Sept-Jan	7	13.1	0.72	0.06	ccw	183.3
	Sept-Jan	15	15.6	-0.66	-0.04	cw	185.9
	Sept-Jan	41	12.3	-0.61	-0.05	cw	197.9
	Sept-Jan	67	9.9	-0.09	-0.01	cw	193.0
	Sept-Jan	91	9.6	-0.29	-0.03	cw	190.5
	Sept-Jan	121	8.6	0.15	0.02	ccw	181.0
	Sept-Jan	151	9.3	-0.27	-0.03	cw	174.8
	Sept-Nov	250	9.8	-0.61	-0.06	cw	175.6
	Sept-Jan	350	8.0	-0.31	-0.04	cw	170.2
Site 3	Sept-Nov	10	47.6	-2.25	-0.05	cw	158.8
	Sept-Nov	20	49.2	-0.86	-0.02	cw	342.2
	Sept-Nov	40	44.5	-1.67	-0.04	cw	349.3
	Sept-Nov	80	41.0	0.26	0.01	ccw	354.3
	Sept-Jan	125	33.0	-0.69	-0.02	ccw	359.3
Site 4	Sept-Jan	6	23.2	-5.58	-0.24	cw	172.7
		10	22.7	-4.18	-0.18	cw	328.8
		19	22.5	-3.56	-0.16	cw	165.3
		33	15.0	-1.72	-0.11	cw	148.1

Table G-7 Summary of the Water Levels by Site and Depth

(m)	Min	1%	5%	25%	50%	Mean	75%	95%	99%	Std	Max	Valid	Total Number
Site 1 AQD	-3.10	-2.79	-2.27	-1.02	0.03	0.00	1.07	2.08	2.53	1.33	2.85	18003	18003
Site 2 ADCP	-3.05	-2.74	-2.23	-1.03	0.04	0.00	1.06	2.07	2.51	1.32	3.15	17838	18223
Site 3 AQD	-4.48	-3.82	-3.05	-1.37	0.07	0.00	1.42	2.74	3.38	1.78	3.94	17741	17741
Site 4 ADCP	-2.93	-2.55	-2.03	-0.88	0.07	0.00	0.93	1.80	2.22	1.18	2.53	17541	17541

G.3.4 Wave Results from Site 4 in Caamaño Sound

For the directional and non-directional wave parameters computed from the wave spectra measured at Site 4 in Caamaño Sound, see Figure G-11. The wave heights are highly episodic in nature, reflecting the passage of storms at intervals of a few to several days. Several wave episodes had significant wave heights exceeding 4 m (corresponding to maximum wave heights of 7.6 m), while the largest wave event on January 5, 2006 had a peak significant wave height of 6.3 m (peak period T_p= 18 s and peak direction D_p = 153°) corresponding to a maximum wave height of 11.7 m. The most common wave directions were from the south to southwest. Waves generated from the south and southeast sectors have the maximum fetch over which to develop and may then undergo refraction to arrive from the south to southwest.

For the minimum, mean, median and maximum significant wave height (H_s), peak period (T_p) and peak direction (D_p), see Table G-8. The significant wave height versus peak period shows how the largest waves (H_s greater than 4 m) had typical peak periods between 10 and 20 s (see Figure G-12). In the middle panel, Figure G-12 illustrates the significant wave height versus peak direction. It shows that the most common wave direction is from 200^o to 250^o, with a smaller but important number of events originating from 135^o to 200^o, including the two largest wave heights measured. The latter group of waves arrive from the south to southeast, apparently travelling along the coastline. The scatter plot of peak period versus peak direction (bottom panel) indicates that waves arriving from the southeast represent a full range of wave periods and are not limited to higher-frequency, shorter-wavelength waves that are less likely to be refracted by the local bathymetry.

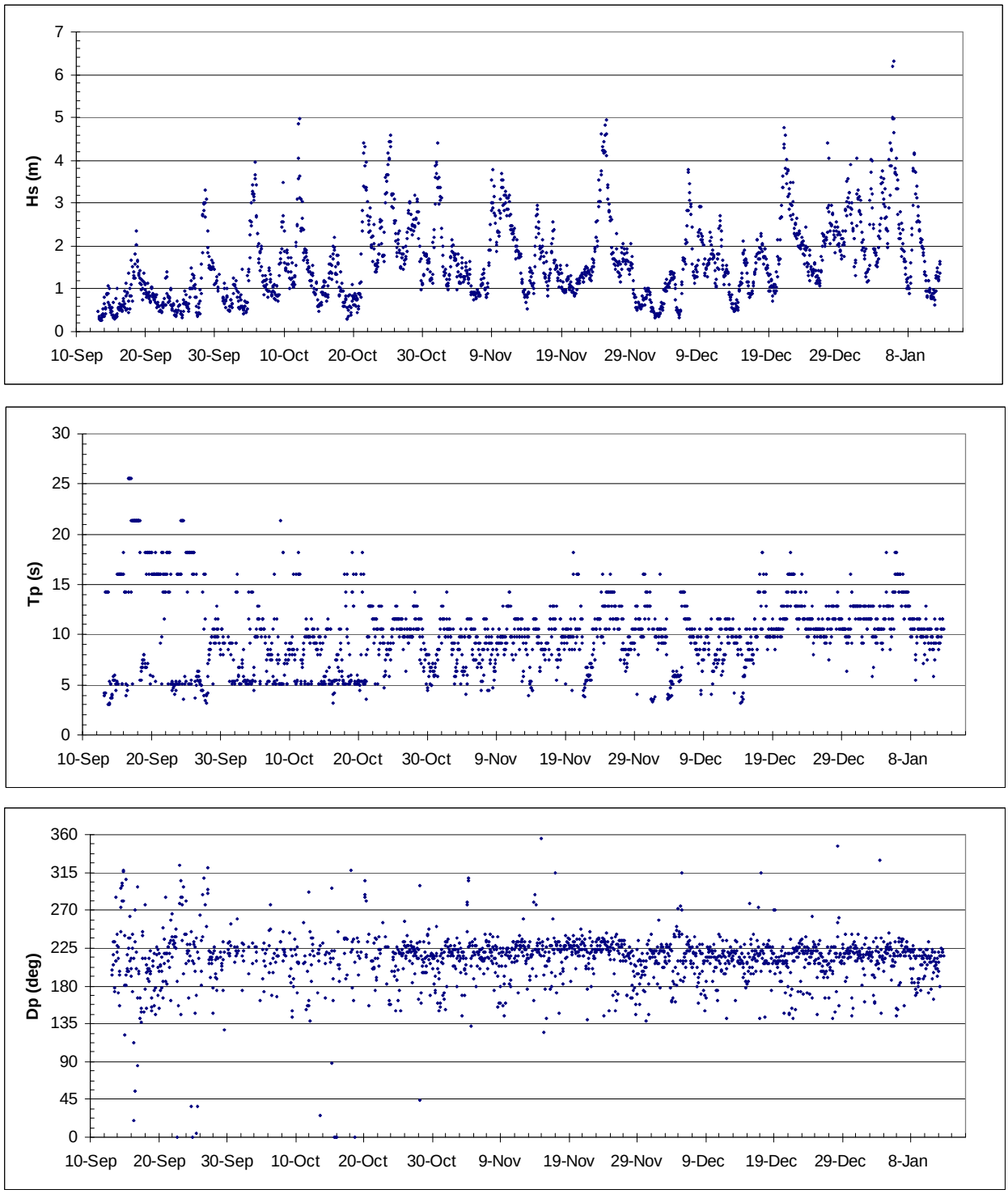

Figure G-11 Significant Wave Height (H_s), Peak Period (T_p) and Peak Direction (D_p) in Caamaño Sound (180^o = Waves from the South)

Table G-8 Significant Wave Height, Peak Period and Peak Direction Statistics at Site 4

	H_s (m)	T_p (s)	D_p (deg true)
Min	0.3	3.0	5.0
Mean	1.7	10.0	212.3
Median	1.5	9.8	216.0
Max	6.3	25.6	356.0

For the non-directional and directional spectra from three wave events, see Figure G-13. The non-directional spectra indicate the energy distribution with frequency as measured by the pressure sensor (red curve), the velocity sensor (green curve) and the surface tracking (blue curve). Generally, the three sensors have good agreement, although occasionally the velocity-derived significant wave heights will give marginally smaller results. Because of the optimization of the instrument for use with this sensor, the velocity-derived results have been used as the primary sensor source for wave parameters.

As in most of the large wave events, the low-frequency contribution was important. Taking the largest event from January 5, 2006 as an example, the Bonilla Island winds (see Figure G-15) exceeded 10 m/s around 01:00. The peak period was already about 11 seconds, even though this is the period that might be expected for a fully developed sea (the winds had been under 10 m/s for over 18 hours leading up to this event). These long periods indicate that part of the contribution at the long frequencies was due to the arrival of these large waves from greater distances than Hecate Strait. The winds peaked at 20 m/s around 06:00, but remained above 13 m/s until about 22:00. Within about 24 hours, the winds were back under 10 m/s. The maximum significant wave height of 6.3 m and 18.2-second peak period at 16:00 PDT (15:00 PST) are similar to that which might be expected for a fully developed sea. The point of this example, however, is to show that even on days where the local seas are calm, swell activity — known as forerunner waves — may occur because of the propagation of waves from a distant storm in the northeast Pacific Ocean.

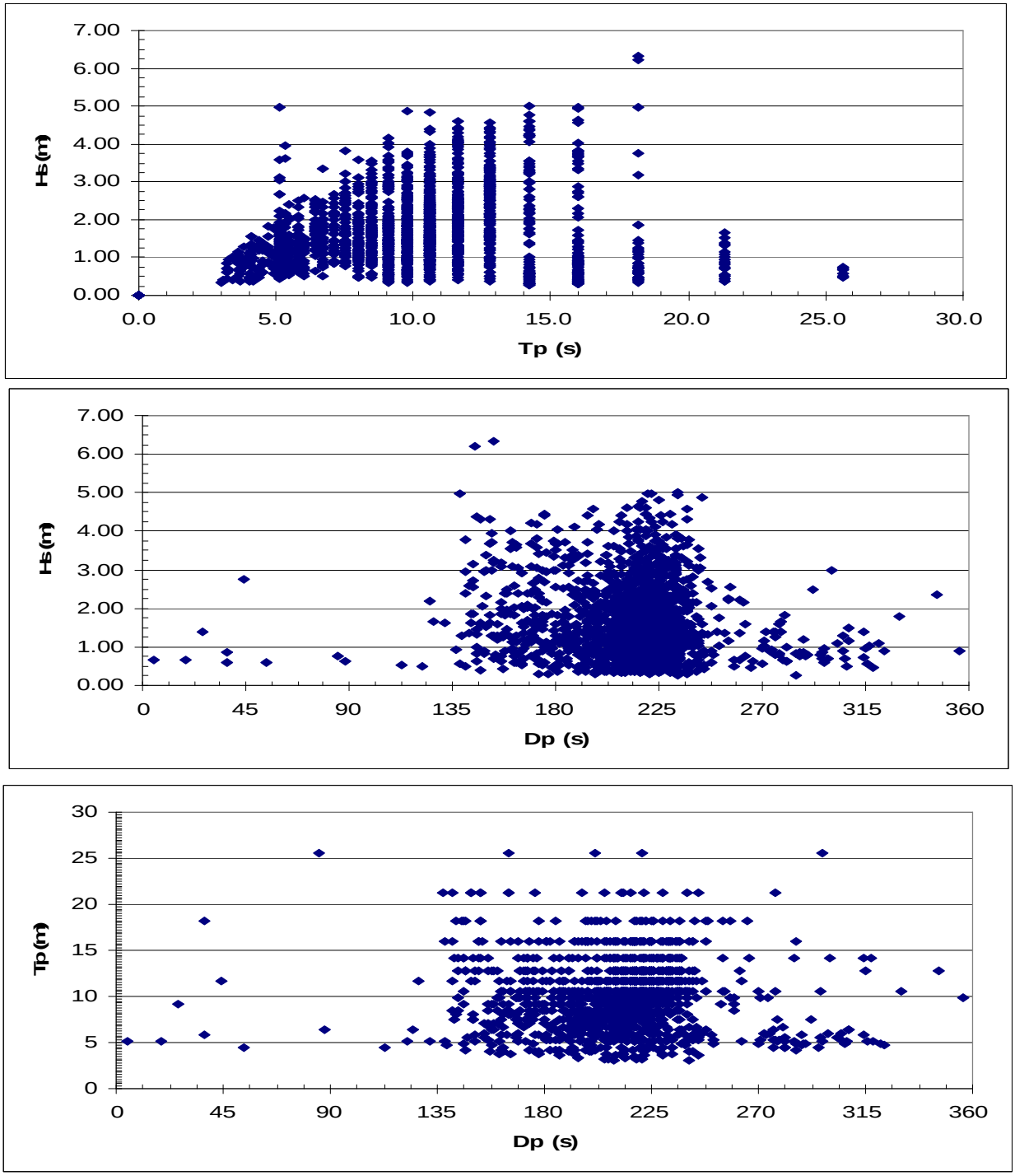

Figure G-12 **Caamaño Sound (a) Significant Wave Height (H_s) versus Peak Period (T_p) (b) H_s versus Peak Direction (D_p) (c) T_p versus D_p (180^o = Waves from the South)**

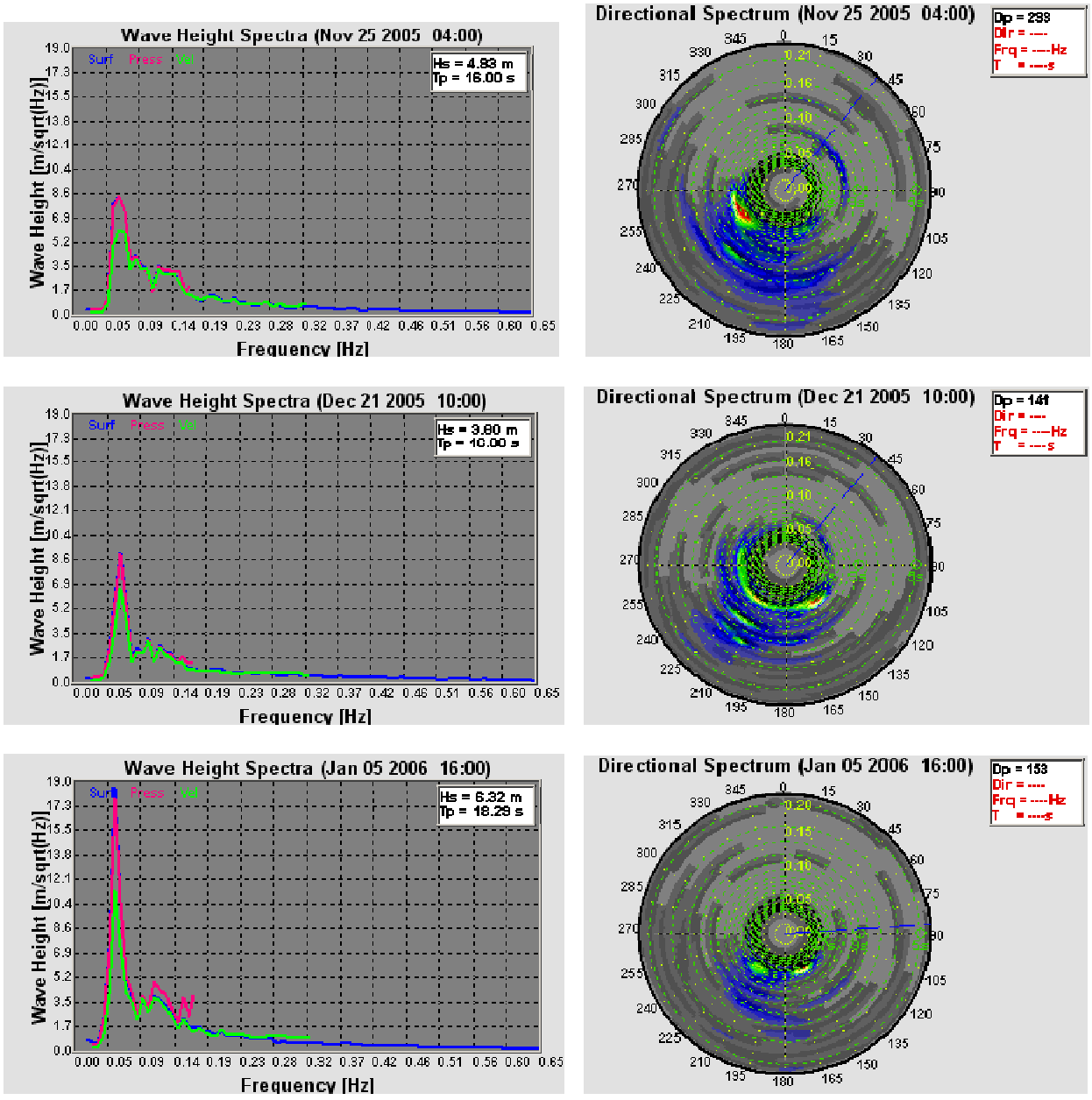

Figure G-13 Non-directional Spectrum and Directional Spectrum (Upper) from 04:00 PDT November 25, 2005 (Middle) 10:00 PDT December 21, 2005 (Lower) 16:00 PDT January 5, 2006, in Caamaño Sound

The upper panel in Figure G-14 shows a case where the dominant waves are the swell; however, the overall significant wave height is only about half a meter. The sawtooth nature of the peak period for this September 16 period (see Figure G-11) also indicates the possibility of forerunners in the study area as the first waves in a forerunner event to arrive in an area will be the longest wavelengths and will have the lowest frequencies.

The November 25, 2006 directional spectrum in Figure G-13 shows a strong directionality in the waves, with most of the waves arriving from the southwest. The December 21 directional spectrum indicates less directionality with some waves arriving from the southwest and southeast. In this second example, the higher-frequency waves arriving from the southwest also become apparent. In the January 5, 2006 event (see lower panel of Figure G-13), waves are observed coming from two narrow regions in the southwest and southeast. Winds Jan 4-5 were initially from the southeast and then strengthened from the south (see Figure G-15 Bonilla Island winds Jan 4-6).

On September 16, the wave spectrum (see Figure G-14, upper panel) is used to derive a significant wave height of just 0.5 m made up of swell waves with periods as long as 25 s as well as small local sea waves. The swell waves originate from the south and the local waves are from the west to northwest. In the lower panel of Figure G-14, a reasonably well-defined wave event with H_s of 2.8 m (T_p=7.5 s) is shown. The long-frequency, swell-wave contributions are absent, but the directional spectra still show waves arriving primarily from the southwest and south-southeast as five or six discrete wave directional spectral peaks.

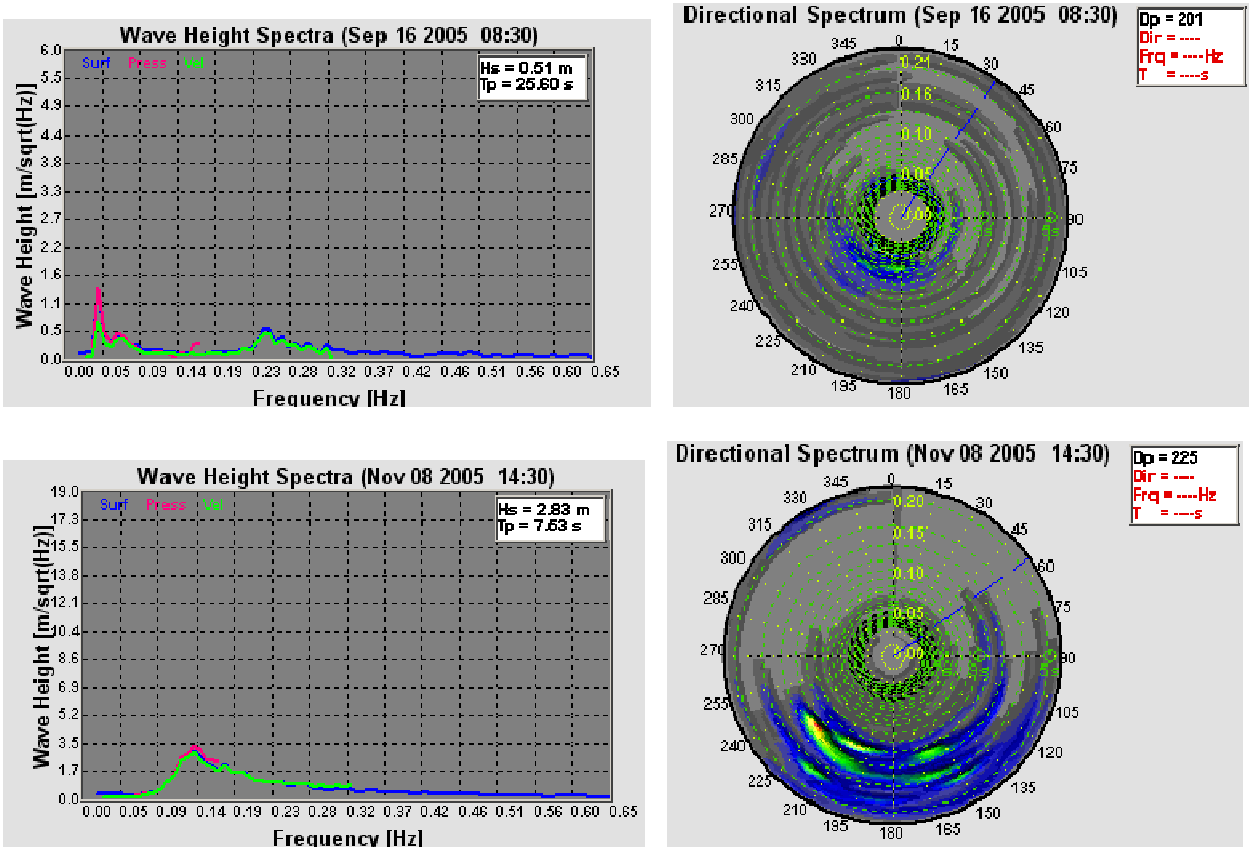

Figure G-14 Non-directional Spectrum and Directional Spectrum from (Upper) 08:30 PDT September 16, 2005 and (Lower) 14:30 PDT November 8, 2005, Caamaño Sound

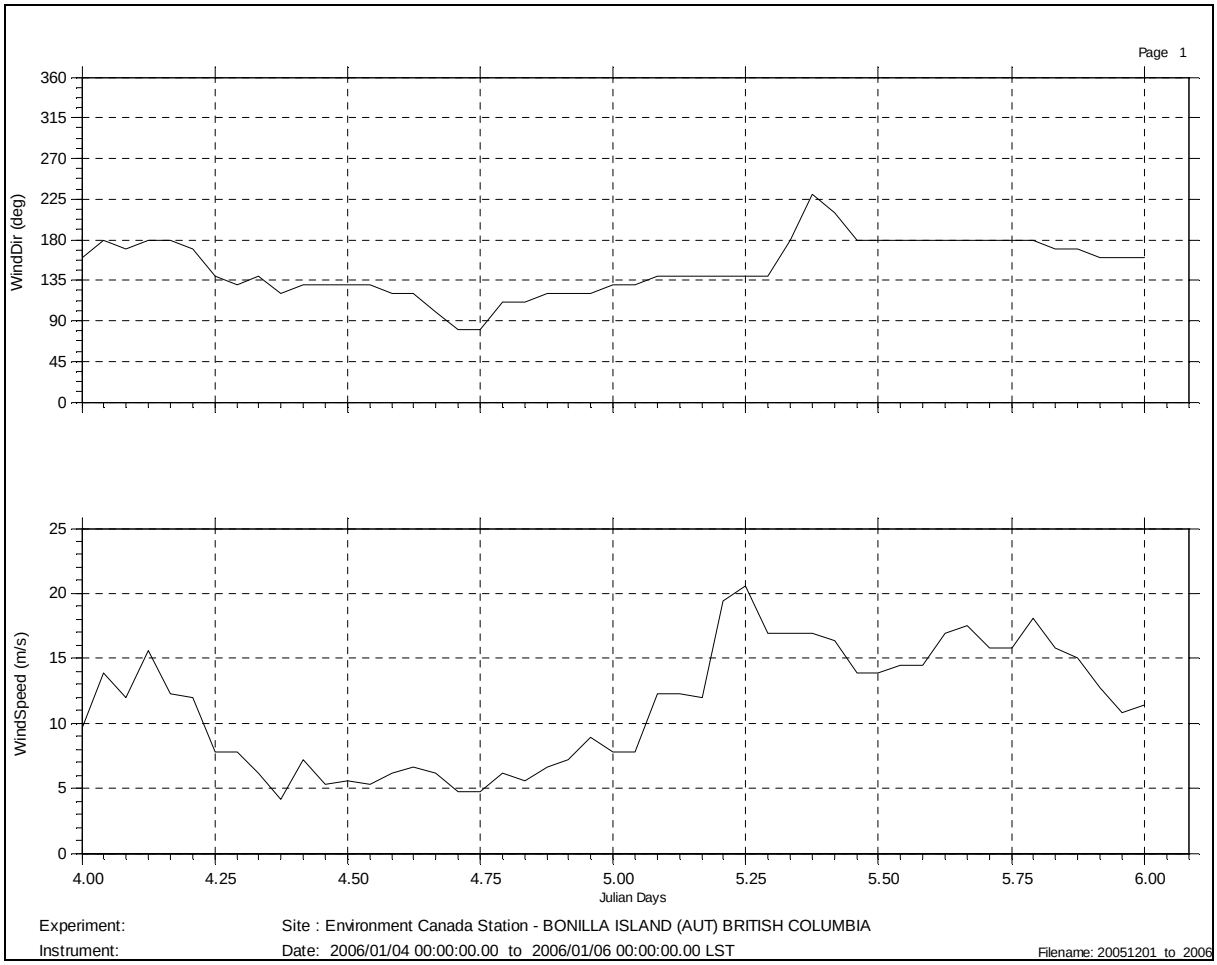

Figure G-15 The Bonilla Island Winds January 4-6, 2006

G.3.4.1 Temperature-Salinity Distributions Derived from CTD Observations in September and January

From a total of 15 CTD profile measurements carried out during both the September 2005 and January 2006 scientific cruises, the temperature and salinity distributions in the CCAA are described. For an example of a temperature and salinity profile in Kitimat Arm near the marine terminal, see Figure G-16. In September, a very strong gradient at 7- to 8-m water depth separates the warm, low-salinity surface water from more saline, colder water at greater depths. Smaller but pronounced vertical gradients in salinity occur to water depths of nearly 80 m, whereas the temperature gradients occur to depths of about 20 m, below which the water temperatures are nearly uniform, with depth at about 7°C. By January, the upper surface layer extends to about the same 7 to 8-m depth and is more saline and markedly colder. The gradient beneath the surface layer is much reduced in intensity. At greater depths, the water temperatures are up to 1°C warmer than they were in September and the salinity values are considerably reduced by about 0.75 to 1.5 psu.

For the distribution of temperature and salinity along the CCAA waterway from Caamaño Sound to Kitimat Arm, see Figure G-17. See Figure G-for the September 2005 CTD observations and the January 2006 CTD observations along Principe Channel. Observations at standard measurement depths are tabulated in Attachment G3.

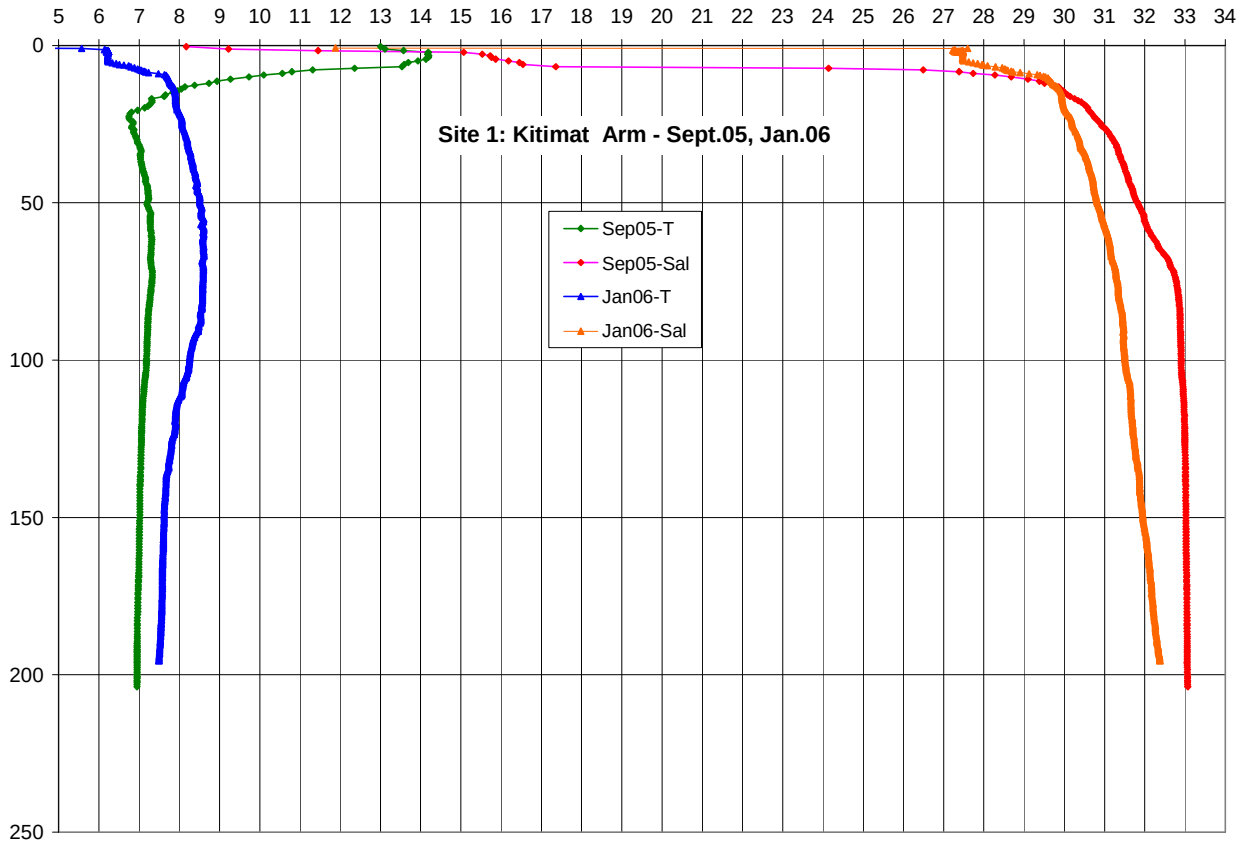

Figure G-16 Temperature (°C) and Salinity Profiles (psu) in Kitimat Arm Measured on September 14, 2005 and January 17, 2006 (Depth in m)

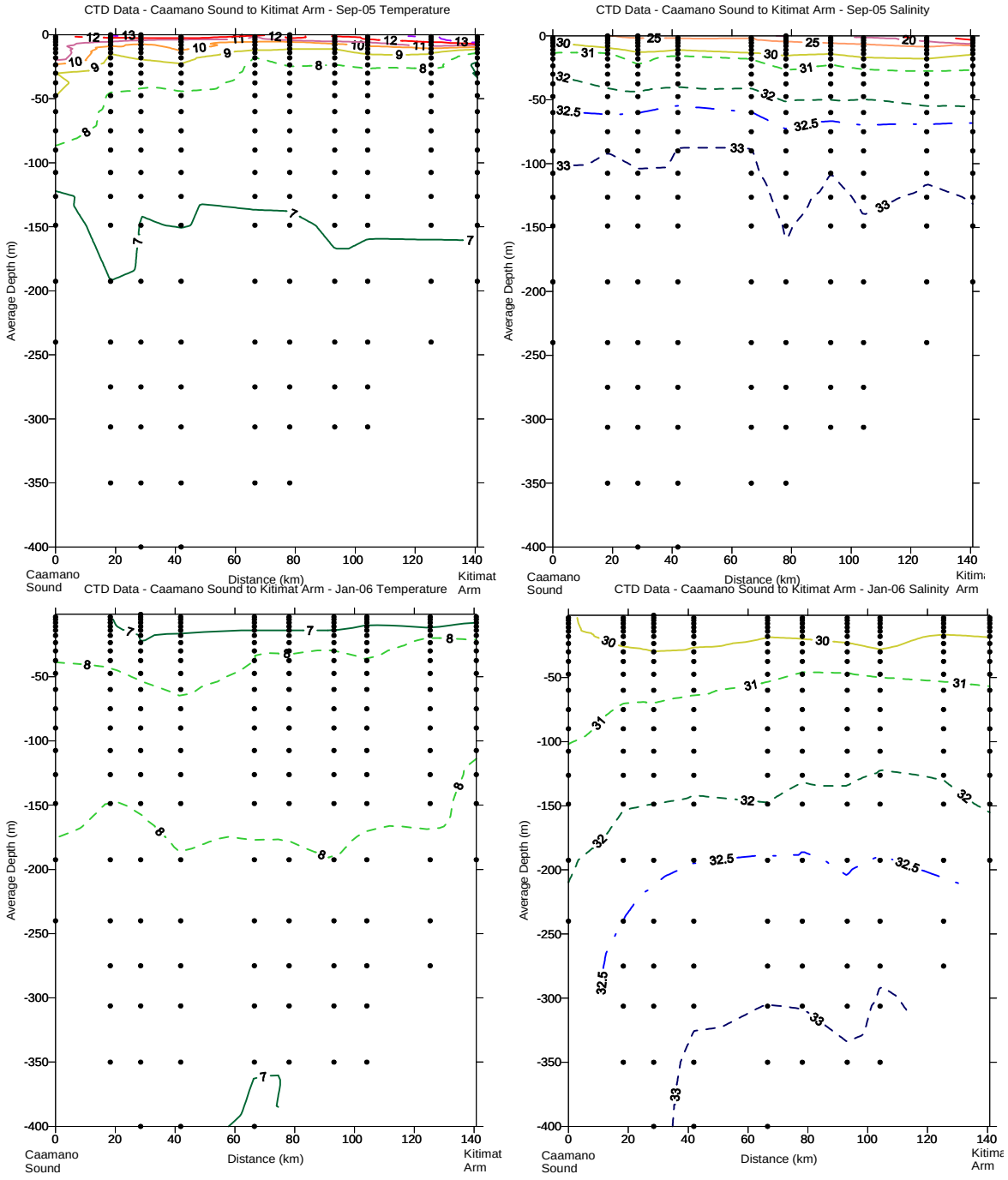

Figure G-17 Temperature and Salinity Distribution through the Main CCAA Waterway from Caamaño Sound to Kitimat Arm from CTD Observations in September 2005 and January 2006

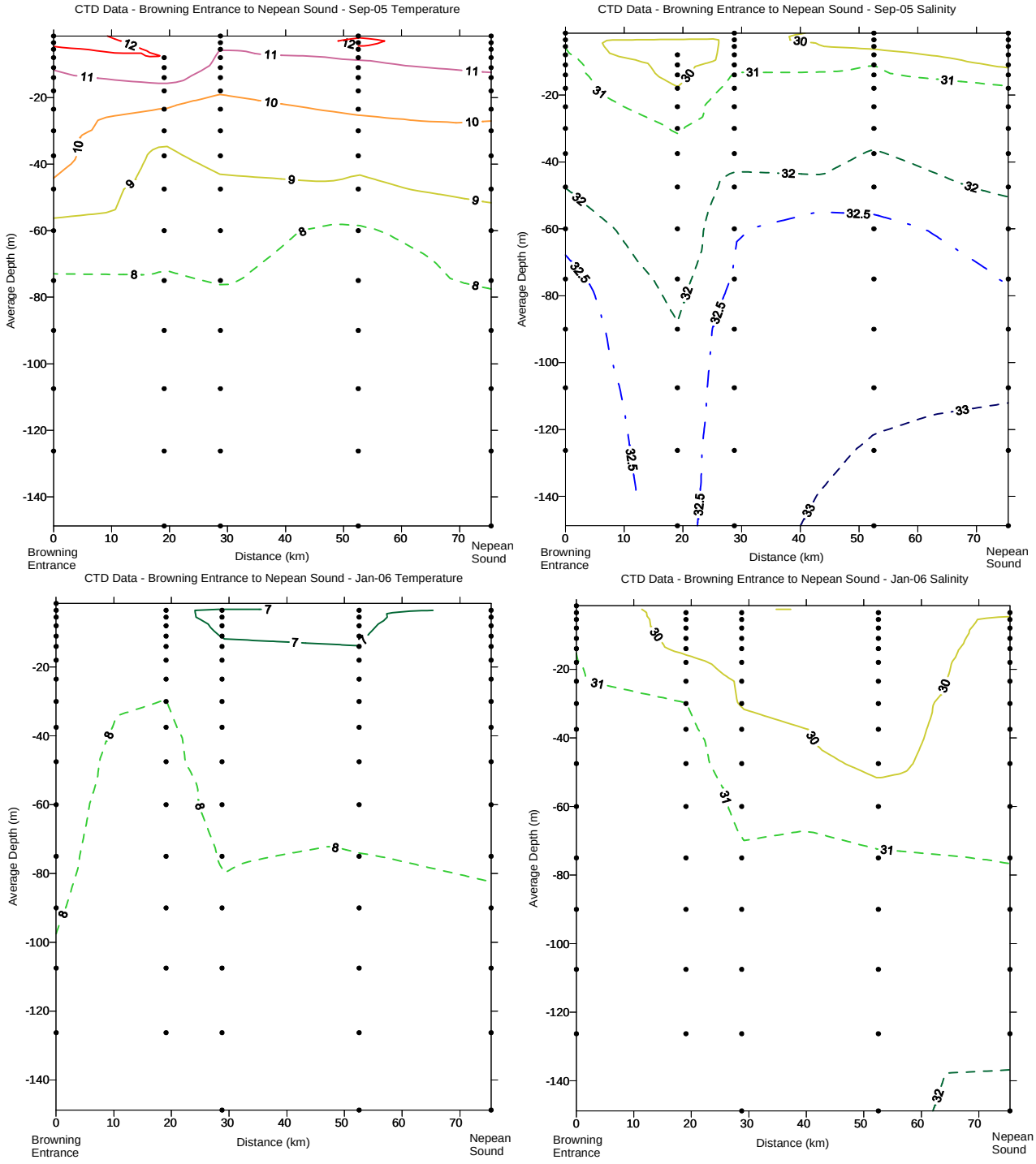

Figure G-18 Temperature and Salinity Distribution through the Principe Channel Waterway from Browning Entrance to Nepean Sound from CTD Observations in September 2005 and January 2006

The temperature and salinity distributions along the CCAA (see Figure G-17) reveal that the warm, less saline upper layer is confined to depths less than 10 m at all locations. The upper-layer salinities are lower at the northern end of the waterway, towards Kitimat Arm, reflecting the larger freshwater discharges in the more inland sections of the waterway, as discussed in Appendix C. Upper-layer temperatures exhibit less consistent spatial variability and are in the range of 11°C to 13°C in September, decreasing sharply to 6.4°C to 7°C in January. The temperature and salinity profile values at the Caamaño Sound site exhibit smaller vertical gradients with generally higher temperatures and higher salinities to 100-m depth in September 2005 and to 40-m depth in January 2006.

Figure G-16 shows the temperature and salinity profiles measured in Kitimat Arm on September 14, 2005 and on January 17, 2006, both under calm to light winds on a flood tide. Like those profiles, the observations at all measurement sites along the main waterway (see Figure G-17) show that the temperatures increase at depth from September to January and the salinities are reduced and exhibit a consistent vertical gradient. This seasonal pattern of reduced salinities in the deeper waters has been observed in the historical data (see Appendix C) in comparing late summer to winter measurements. The changes are likely due to the effects of vertical mixing of the water column in the fall and winter associated with the stronger winds and somewhat reduced freshwater discharges. These activities allow the warmer, less saline upper-layer characteristics to be mixed downwards into the main water column, combined possibly with up-inlet flow at depth (reflected in the vector mean current direction of 278° at 165 m in Kitimat Arm (see Table G-4), which advects more saline water into the inland waterways.

The temperature and salinity distributions along Principe Channel (see Figure G-18) exhibit more similarity to the observations at Caamaño Sound than sites in the inland sections of the study area, reflecting the influence of the waters of northern Hecate Strait in these outer portions of the CCAA. The seasonal trend in the deeper waters from high, relatively uniform salinities in September to lower salinity that increases with depth in January is also evident in this channel as it is in the main waterway. Upper layer salinities tend to be higher in Principe Channel because of its greater distance from large river discharges. The along-channel salinities increase from east to west in January, perhaps indicative of the greater freshwater influence within the main Kitimat system versus the more open waters of Hecate Strait. In September, the salinities at depth were notably reduced by 0.5 to 1.5 psu at the Principe Channel current-meter location when compared with the waters to the east and west. This may be a remnant of lower-salinity water from earlier in the season or from waters originating in Petrel Channel to the north.

G.3.4.2 Summary of Key Findings

As was found in the historical data (see Appendix B), the currents are largest at the approaches and in Douglas Channel and smallest within Kitimat Arm. Mean current speeds are 20 to 39 cm/s at the near-surface, except for Kitimat Arm, where mean surface speeds reach only 5 to 10 cm/s. Maximum near-surface current speeds were near 100 cm/s in the approaches and Douglas Channel, reaching 110 cm/s in Principe Channel. The current speeds tend to decrease with depth except in Principe Channel, where there is less variation with depth and the maximum observed speed (for all sites) of 113 cm/s occurred.

In the inner passages of the Kitimat system, the currents tend to be aligned along the channel. The net flow tends to be seaward movement of fresher water at the surface and inland movement of denser seawater at depth.

This influence from freshwater inputs, which causes stratification of the water column, as well as wind forcing, can be just as important or even more important than tidal forcing, as found in Kitimat Arm and Douglas Channel. As was found in the historical data (see Appendix C), the importance of the tidal currents tends to increase with depth and with proximity to the open ocean.

The largest tidal ranges, up to 8 m for the largest tides, were measured in Principe Channel. The smallest tidal ranges in the study area were measured in Caamaño Sound, where the maximum tidal ranges were 5.5 m. Kitimat Arm and Douglas Channel had similar tidal ranges, which were intermediate, with maximum ranges of 6 m. The ranking and size of the tidal ranges are consistent with the historical results described in Appendix D.

Waves were measured at Yates Shoal on the Aranzazu Banks (Caamaño Sound Site 4). The largest wave event had a significant wave height of 6.3 m and occurred on January 5, 2006 (T_p=18 s and D_p=153°). Waves usually arrive from the south to southwest, though an important contribution arrives from the southeast. Waves generated from the south and southeast sectors have the maximum fetch over which to develop and may then undergo refraction to arrive from the south to southwest. The largest waves (significant wave height greater than 4 m) tended to have peak periods between 10 and 20 s. On September 16, 2005, peak periods of 25.6 s were measured. Most wave events had a very low-frequency contribution. Even on days where the local seas are calm, swell activity may have propagated from a distant storm in the northeast Pacific Ocean in the form of forerunners.

Cruises in September 2005 and January 2006 yielded 15 CTD profile measurements from which spatial and temporal patterns in the salinity and temperature could be obtained. The fresher and warmer surface waters were found to be confined to depths of 10 m or less at all locations along the CCAA. As was found in the historical data presented in Appendix C, the upper layer was somewhat fresher farther inland, because of the influence of freshwater discharge in the region. Gradients in temperature and salinity are reduced in the approaches to the Kitimat system.

Between the summer and winter cruises, the surface temperatures cooled significantly, whereas at depth the temperature increased about a degree. Wind events through the fall allowed vertical mixing, and the surface salinities show a large increase concurrent with a small decrease in salinity at depth, consistent with the historical data examined in Appendix C.

Salinities were found to increase along Principe Channel towards Browning Entrance to the west, farther from the freshwater inputs of the Kitimat system. The September measurements indicate particularly fresh water at the Principe Channel measurement site compared to other locations in the channel. This fresh water may be due to an event that occurred earlier in the season, or it may be due to inputs from Petrel Channel to the north. The effects of vertical mixing and cooling observed in the Kitimat waterway were also observed in Principe Channel between the two cruises.

G.4 References

G.4.1 Literature Cited

Foreman M.G.G. 1978. *Manual for Tidal Currents Analysis and Prediction.* Pacific Marine Science Report, Vol. 78-6. Fisheries and Oceans Canada. Institute of Ocean Sciences. Sidney, British Columbia.

Attachment G1 Specifications of Oceanographic Instruments Used in This Study

Specifications for the 600 kHz ADCP

600 kHz INSTRUMENT

Principles of Operation:

Acoustic pulses are transmitted along four beams. Echoes are returned by scatterers in the water column. The frequency shift of each echo is directly proportional to the component of flow along the beam axis. This is the Doppler effect. Horizontal and vertical flow components are then computed from the axial velocities. Echo returns are time-gated to allow flow resolution into vertical bins (in this case 1.0 m). Flow homogeneity over the four-beam footprint is assumed. Due to side lobe returns, data are usually not available within 6% (20° beam angle) of the vertical distance to strong reflectors, such as the ocean surface or sea bottom. The ADCP was upgraded to include a pressure sensor and includes the WAVES upgrade.

Internal Sensors	**Accuracy**	**Resolution**
Heading	±1°	±0.2°
Tilt (max. 20□)	±2°	±0.01°
Temperature	±0.4°	±0.01°

Power Specification: Internal: 48VDC battery pack (expandable w/ external battery pack). External: 20-60 VDC

Dimensions: 22.8 cm by 36.1 cm

Weight: 13 kg in air; 4.5 kg in water (with battery pack)

Beam Angle: 20°

Maximum Range: Water velocity profile to 47 m (nominal at 2 m bin size)

Accuracy: Water velocity accuracy is 1 cm/sec, based on the sampling parameters chosen (2-m bins, 10 pings per ensemble).

Memory: Expanded to 896 MB

NORTEK

"Aquadopp" 3D Current Meter

Sensors	*Water Velocity*	*3D vector-averaging doppler (2.0 MHz)* Range: ±10 m/s Accuracy: ± 0.5% or ±0.25 cm/s Resolution: cm/s Threshold: cm/s; Noise: cm/s Internal ping rate: 25 Hz Bin size: 150 cm; range: 35-185 cm, or more
	Pressure	*Strain gauge* Range: 600 psi (400 m of water) Accuracy: equiv. to ± 1 m water Resolution: equiv. to ± 4 cm water
	Temperature	*Thermistor* Range: -5 to 40 °C; Accuracy: ± 0.1 °C; Resolution: ± °C
	Direction	*Flux-gate Compass* Range: 0 to 360 degrees Accuracy: ± 2 degrees; Resolution: ± degrees Allowable Tilt: 20 degrees
Electronics	*Controls:*	RS232/RS422 interface; control via PC
	Data Storage	2 MB
	Power	alkaline battery pack (18 AA cells); 13.5VDC
Pr Case	*Material*	plastic w/ titanium hardware
	Size	7.5 cm (3") diameter case by 50 cm (19.7") length
	Weight	3.5kg (air); neutral (water)

Applied Microsystems

STD12+ CTD

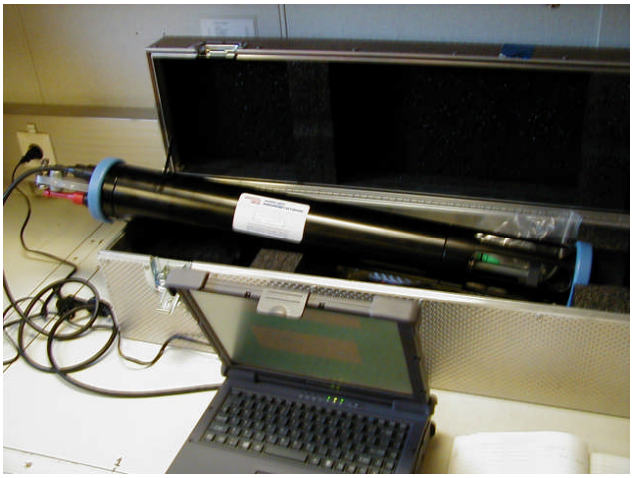

Sensor		Response	Accuracy	Resolution
Temperature ^{o}C	Thermistor	85ms	± 0.005°C	0.001 °C
Conductivity S/m	Four electrode glass cell	5 to 25 ms	±0.001 S/m	0.0003S/m
Pressure dbar (1000 m)	Strain gauge	10ms	± 1.5 dbar	0.05 dbar

Sampling rate: up to 11 scans per second; or by time/pressure increment

Memory: 128 MB RAM

Batteries: Nine Alkaline D-cells

Weight: 9.0 kg in air; 3.5kg in water

Dimensions: 675mm by 102mm

Manufacturer: **Applied Microsystems Ltd.**
2071 Malaview Ave.W. Sidney, BC, Canada V8L 5X6
Contact: Tel:+1-250-656-0771 Fax:+1-250-655-3655
sales@AppliedMicrosystems.com

Attachment G2 Time Series Plots of Ocean Currents at Selected Measurement Depths

G2.1 Kitimat Arm: 9-m, 15-m, 41-m, 81-m and 165-m depths

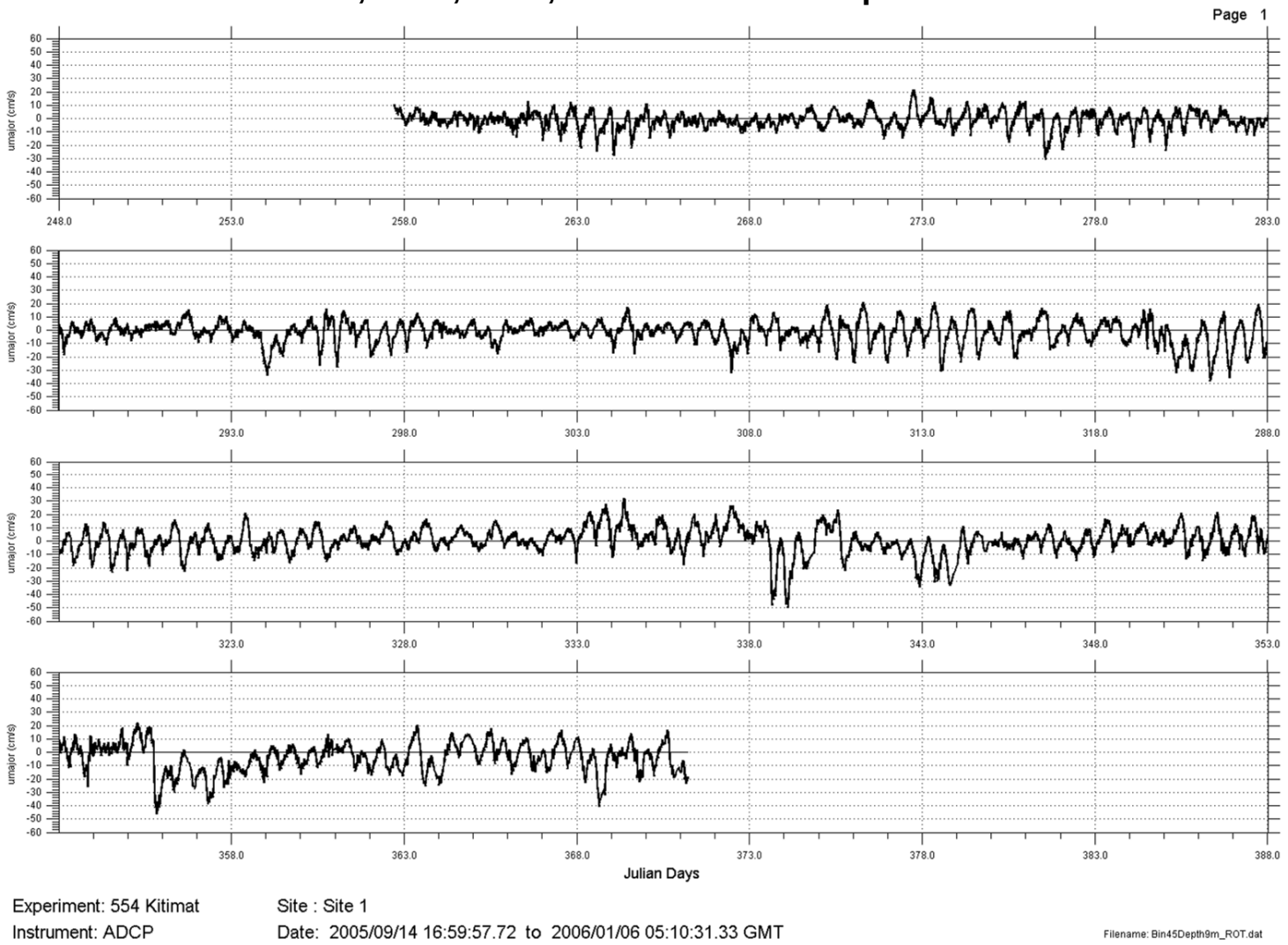

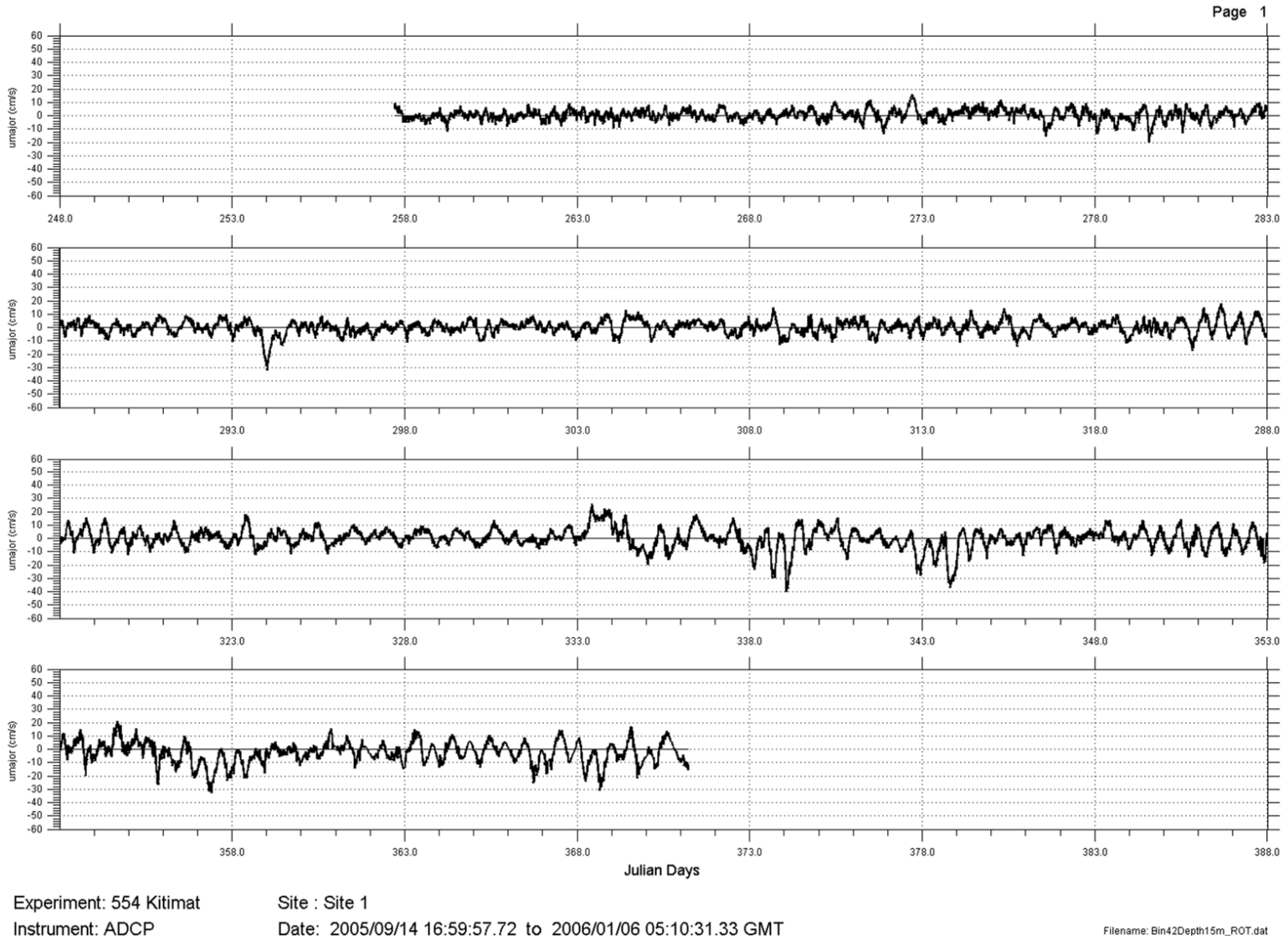
Page 1
umajor (cm/s)
Julian Days
Experiment: 554 Kitimat
Instrument: ADCP
Site : Site 1
Date: 2005/09/14 16:59:57.72 to 2006/01/06 05:10:31.33 GMT
Filename: Bin42Depth15m_ROT.dat

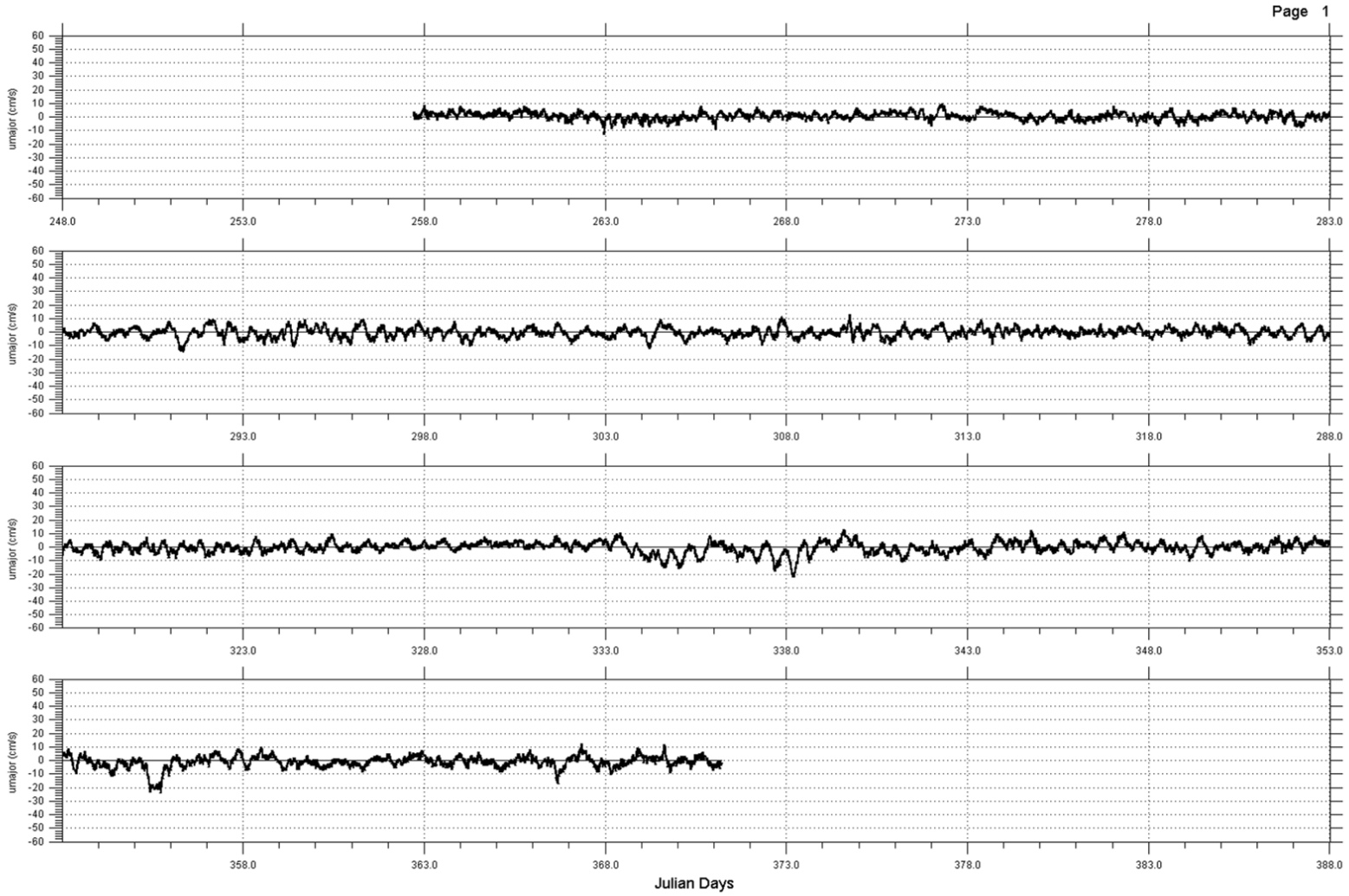
Page 1
umajor (cm/s)
Julian Days
Experiment: 554 Kitimat
Instrument: ADCP
Site : Site 1
Date: 2005/09/14 16:59:57.72 to 2006/01/06 05:10:31.33 GMT
Filename: Bin29Depth41m_rot.dat

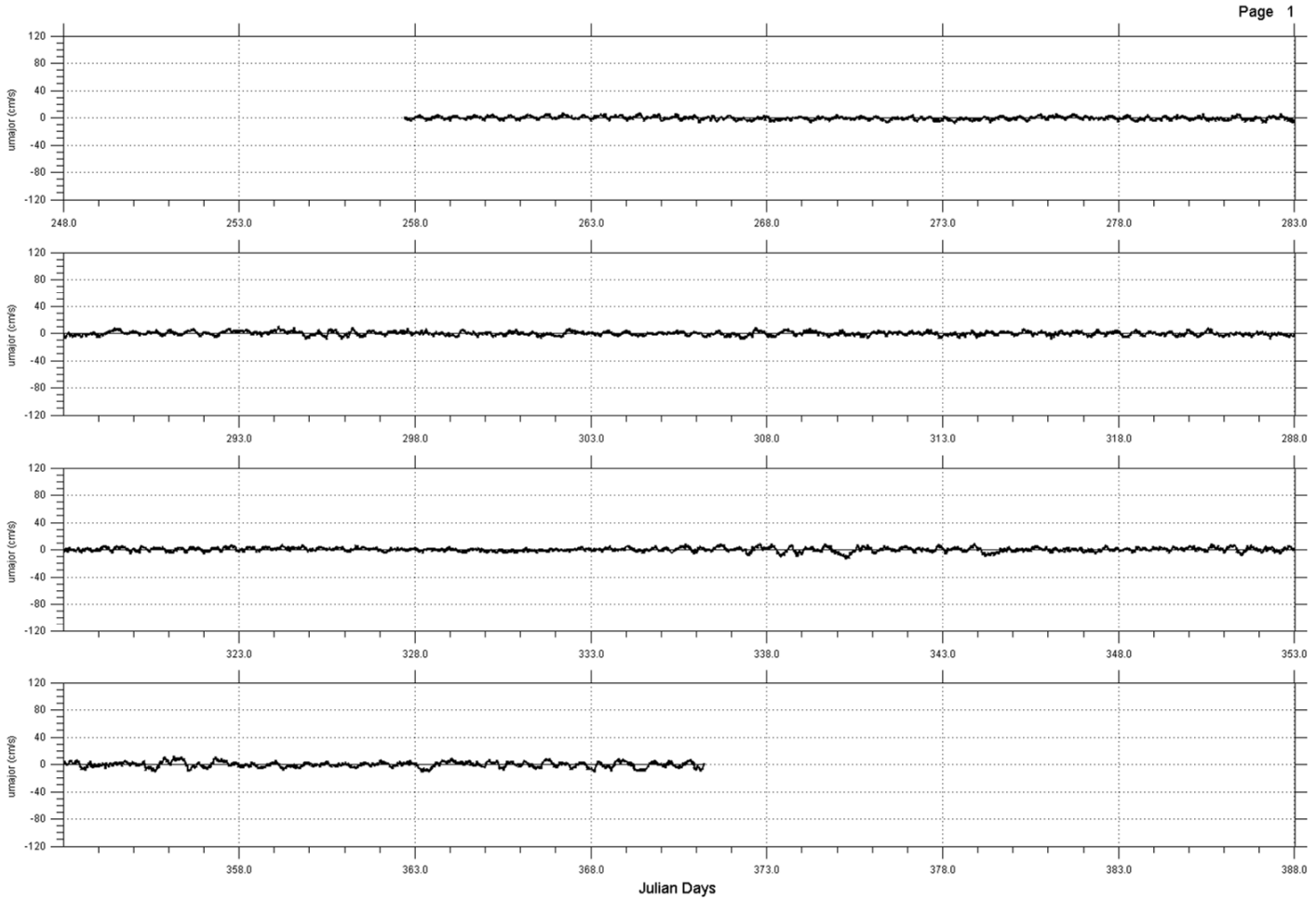
Page 1
umajor (cm/s)
120
80
40
0
-40
-80
-120
248.0
253.0
258.0
263.0
268.0
273.0
278.0
283.0
293.0
298.0
303.0
308.0
313.0
318.0
288.0
323.0
328.0
333.0
338.0
343.0
348.0
353.0
358.0
363.0
368.0
373.0
378.0
383.0
388.0
Julian Days
Experiment: 554 Kitimat
Instrument: ADCP
Site : Site 1
Date: 2005/09/14 16:59:57.72 to 2006/01/06 05:10:31.33 GMT
Filename: Bin9Depth81m_ROT.dat

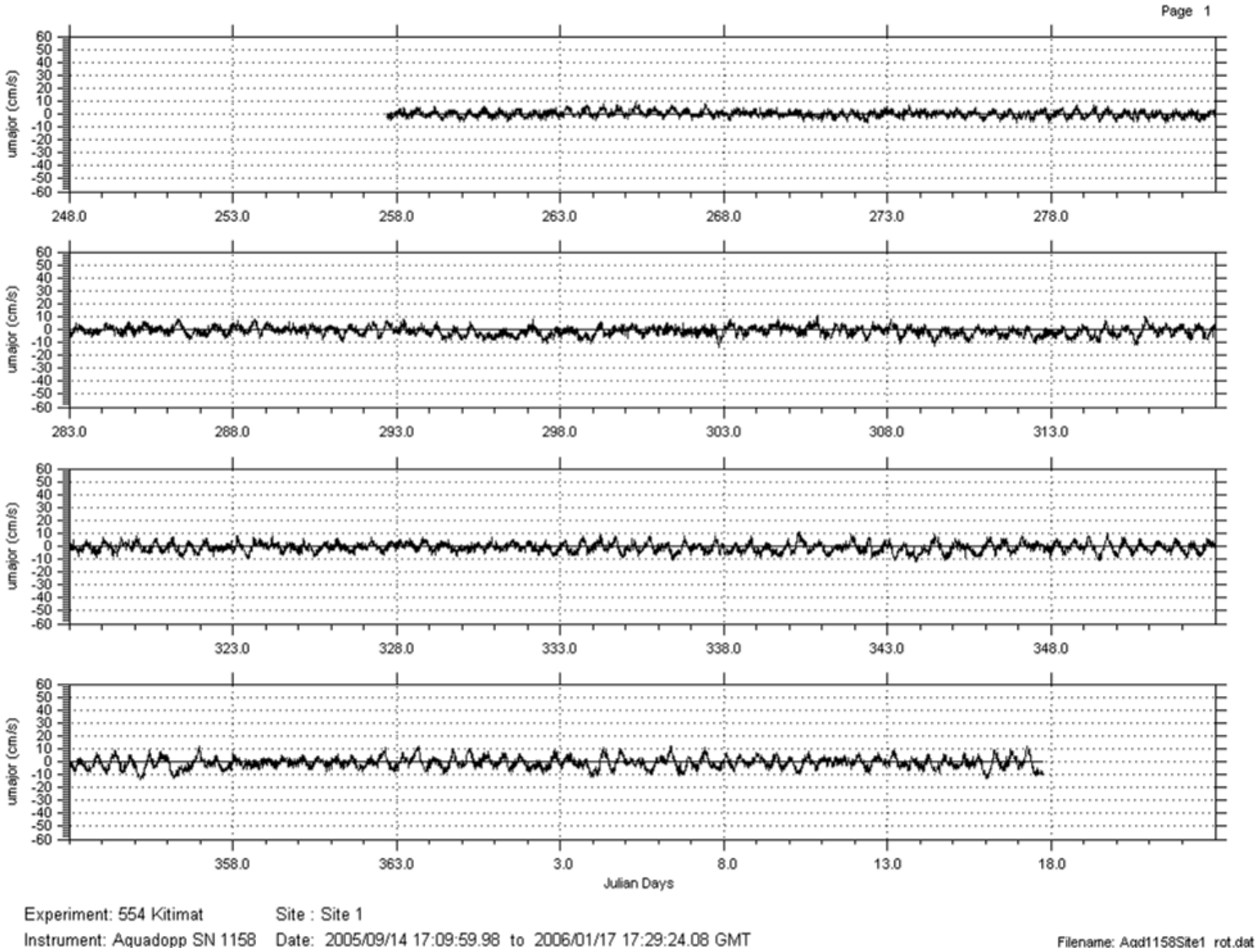
Page 1
umajor (cm/s)
60
50
40
30
20
10
0
-10
-20
-30
-40
-50
-60
248.0
253.0
258.0
263.0
268.0
273.0
278.0
283.0
288.0
293.0
298.0
303.0
308.0
313.0
323.0
328.0
333.0
338.0
343.0
348.0
358.0
363.0
3.0
8.0
13.0
18.0
Julian Days
Experiment: 554 Kitimat
Site : Site 1
Instrument: Aquadopp SN 1158
Date: 2005/09/14 17:09:59.98 to 2006/01/17 17:29:24.08 GMT
Filename: Aqd1158Site1 rot.dat

G2.2 Douglas Channel: 7-m, 15-m, 41-m, 67-m, 91-m, 121-m, 151-m, 194-m and 350-m depths

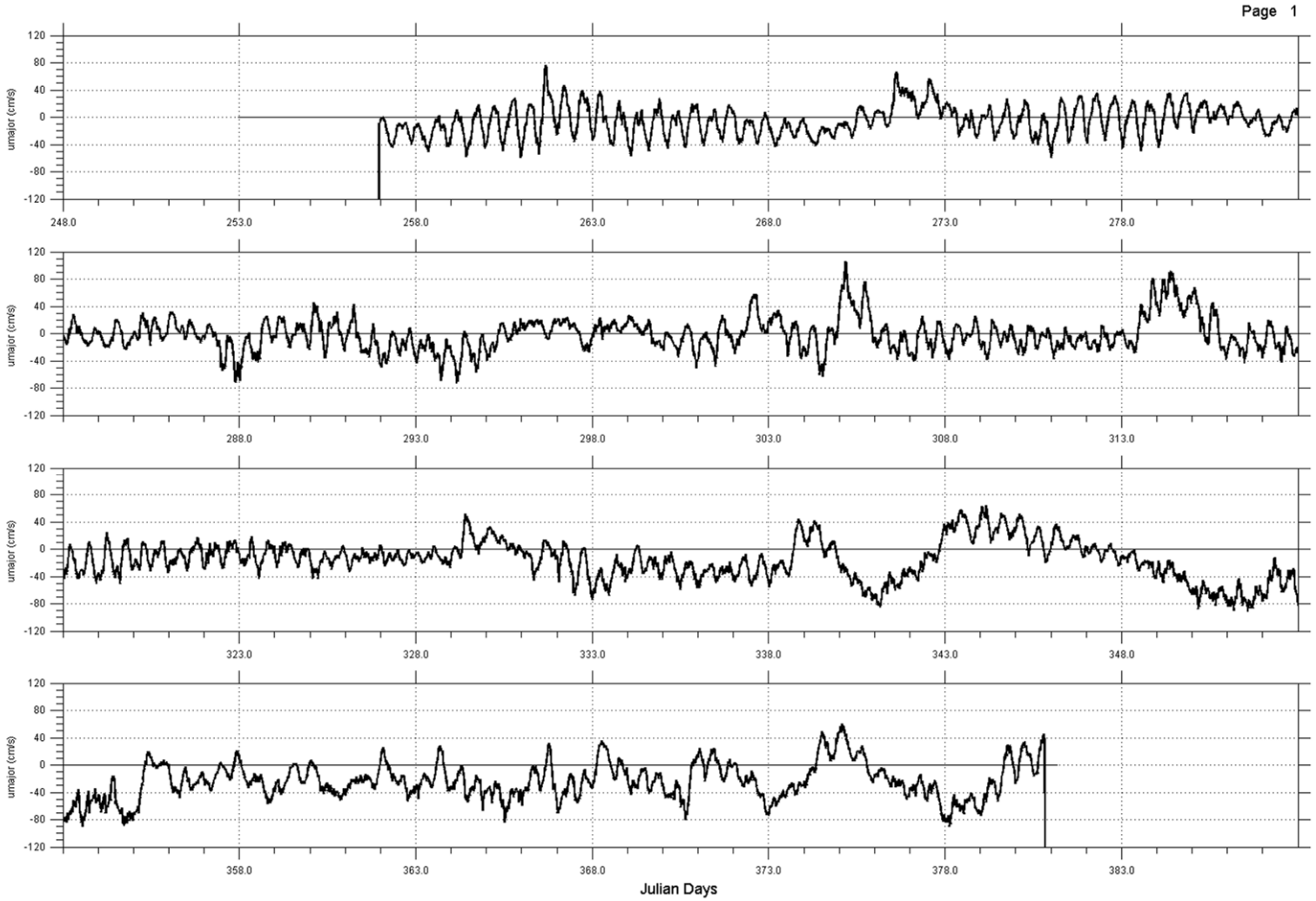

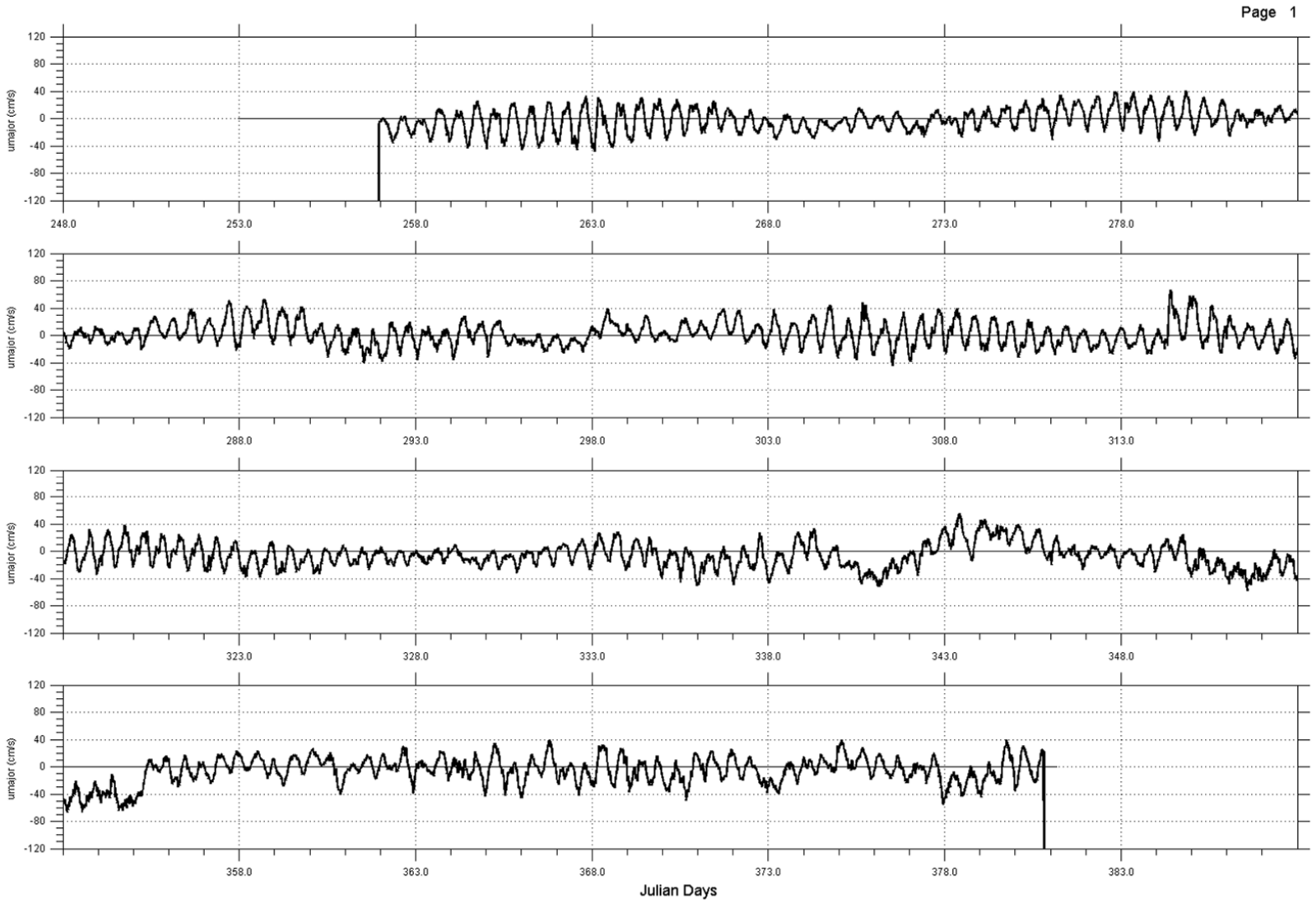
Page 1
umajor (cm/s)
120
80
40
0
-40
-80
-120
248.0
253.0
258.0
263.0
268.0
273.0
278.0
288.0
293.0
298.0
303.0
308.0
313.0
323.0
328.0
333.0
338.0
343.0
348.0
358.0
363.0
368.0
373.0
378.0
383.0
Julian Days
Experiment: 554 Kitimat
Instrument: ADCP
Site : Site 2 Upward Looking
Date: 2005/09/09 23:29:52.65 to 2006/01/16 04:18:43.65 GMT
Filename: Bin22Depth15m_ROT.dat

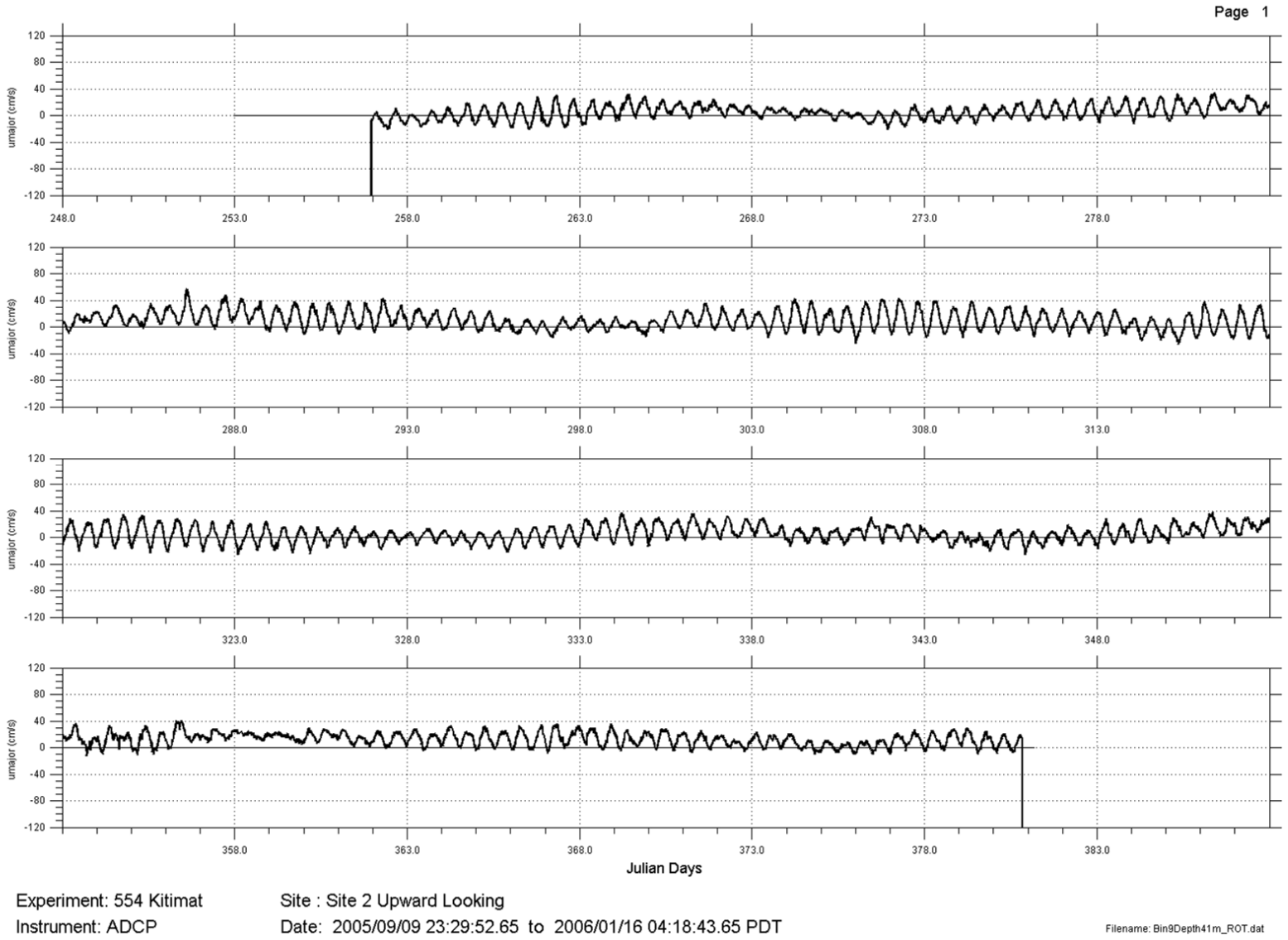
Page 1
umajor (cm/s)
120
80
40
0
-40
-80
-120
248.0
253.0
258.0
263.0
268.0
273.0
278.0
288.0
293.0
298.0
303.0
308.0
313.0
323.0
328.0
333.0
338.0
343.0
348.0
358.0
363.0
368.0
373.0
378.0
383.0
Julian Days
Experiment: 554 Kitimat
Instrument: ADCP
Site : Site 2 Upward Looking
Date: 2005/09/09 23:29:52.65 to 2006/01/16 04:18:43.65 PDT
Filename: Bin9Depth41m_ROT.dat

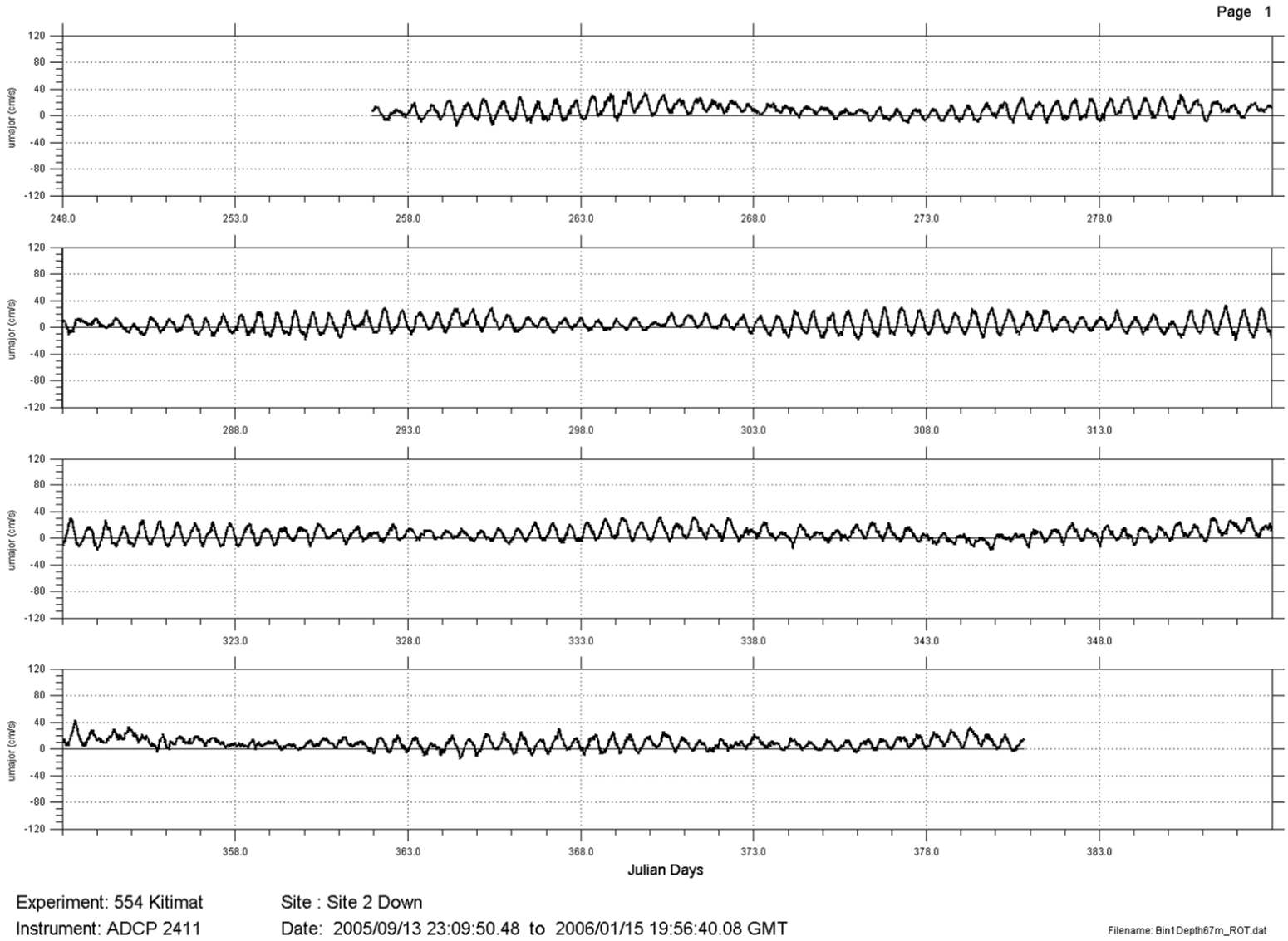
Page 1
umajor (cm/s)
120
80
40
0
-40
-80
-120
248.0
253.0
258.0
263.0
268.0
273.0
278.0
288.0
293.0
298.0
303.0
308.0
313.0
323.0
328.0
333.0
338.0
343.0
348.0
358.0
363.0
368.0
373.0
378.0
383.0
Julian Days
Experiment: 554 Kitimat
Instrument: ADCP 2411
Site : Site 2 Down
Date: 2005/09/13 23:09:50.48 to 2006/01/15 19:56:40.08 GMT
Filename: Bin1Depth67m_ROT.dat

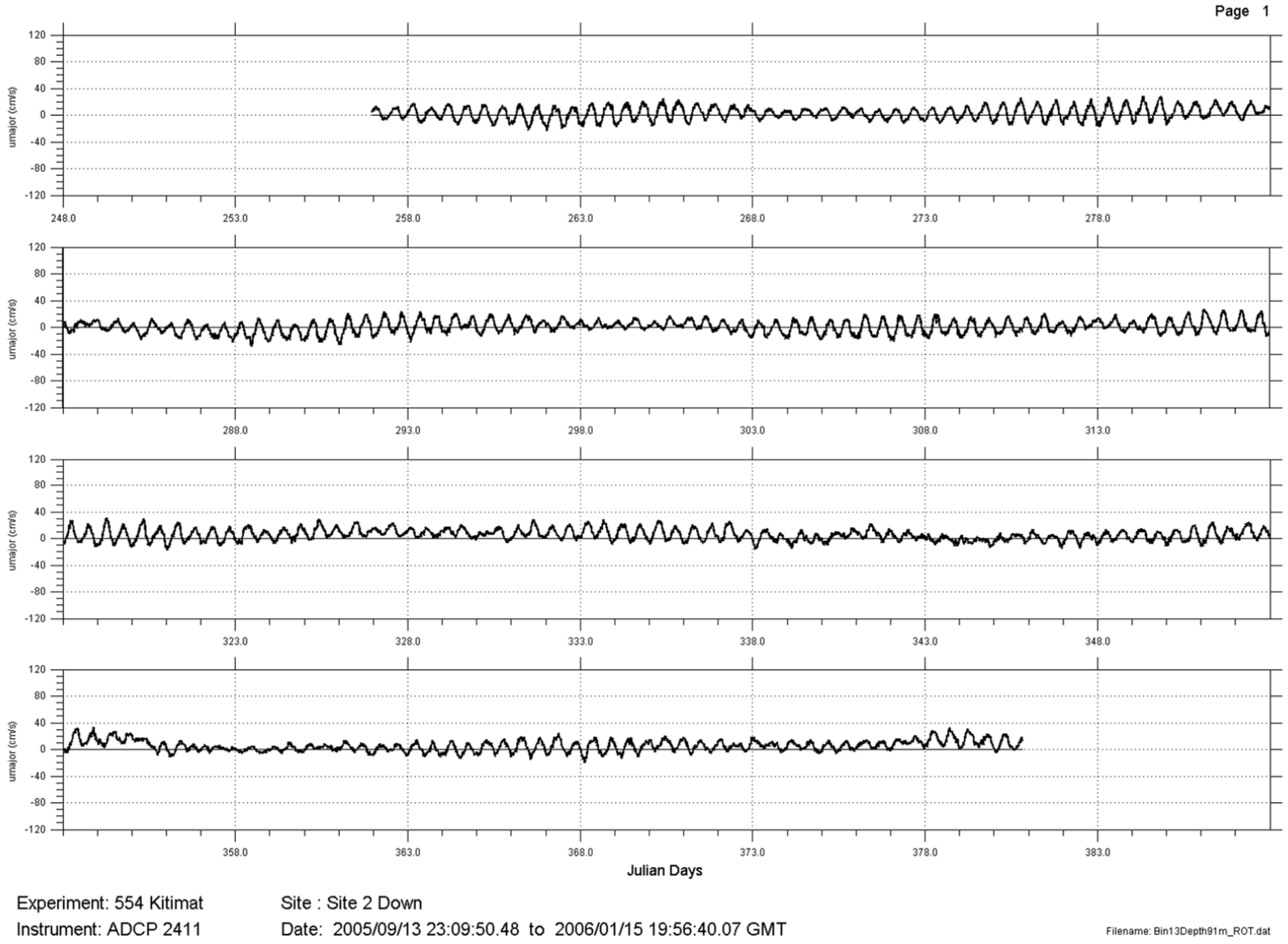
Page 1
umajor (cm/s)
120
80
40
0
-40
-80
-120
248.0
253.0
258.0
263.0
268.0
273.0
278.0
288.0
293.0
298.0
303.0
308.0
313.0
323.0
328.0
333.0
338.0
343.0
348.0
358.0
363.0
368.0
373.0
378.0
383.0
Julian Days
Experiment: 554 Kitimat
Instrument: ADCP 2411
Site : Site 2 Down
Date: 2005/09/13 23:09:50.48 to 2006/01/15 19:56:40.07 GMT
Filename: Bin13Depth91m_ROT.dat

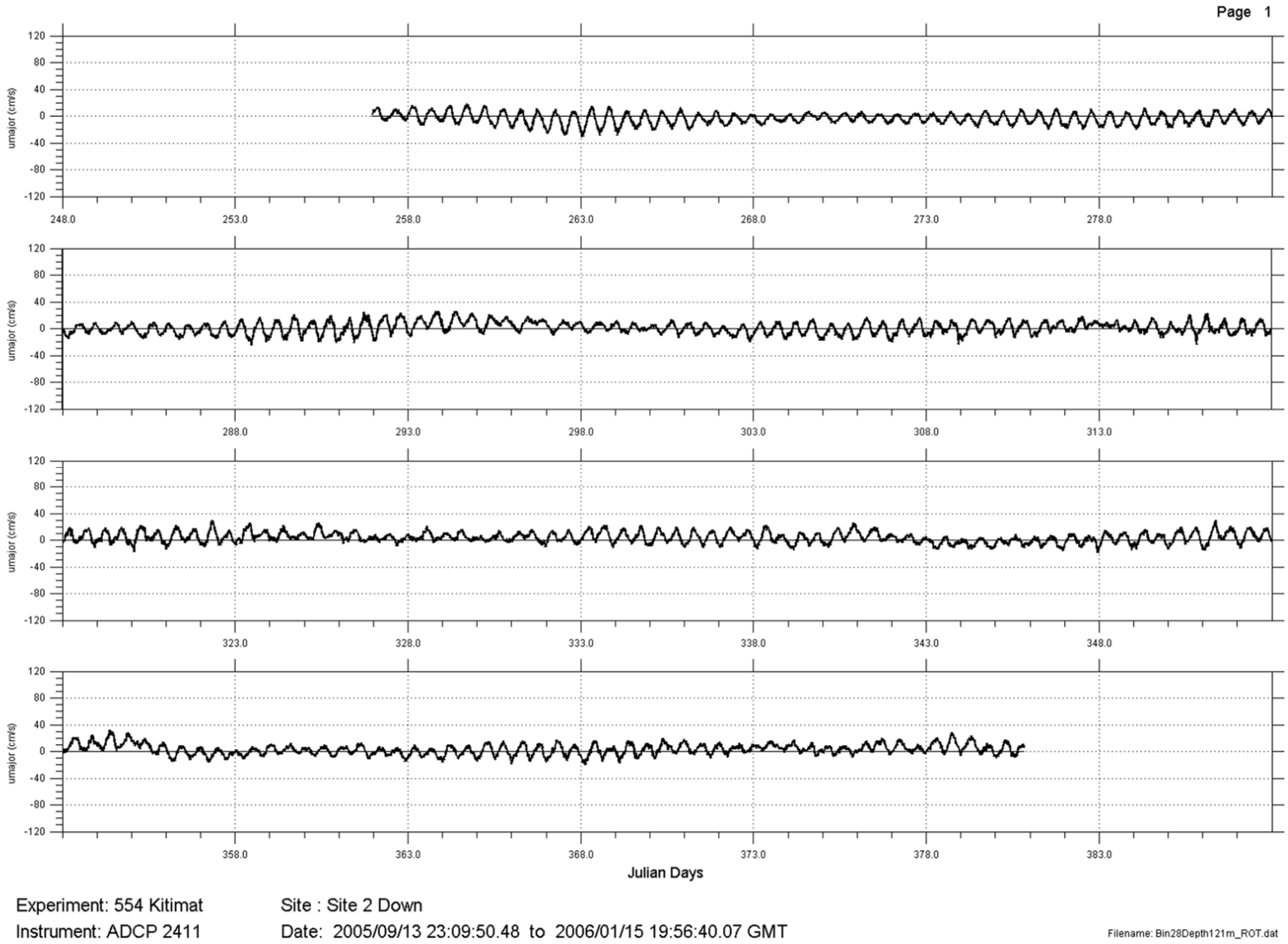
Page 1
umajor (cm/s)
120
80
40
0
-40
-80
-120
248.0
253.0
258.0
263.0
268.0
273.0
278.0
288.0
293.0
298.0
303.0
308.0
313.0
323.0
328.0
333.0
338.0
343.0
348.0
358.0
363.0
368.0
373.0
378.0
383.0
Julian Days
Experiment: 554 Kitimat
Instrument: ADCP 2411
Site : Site 2 Down
Date: 2005/09/13 23:09:50.48 to 2006/01/15 19:56:40.07 GMT
Filename: Bin28Depth121m_ROT.dat

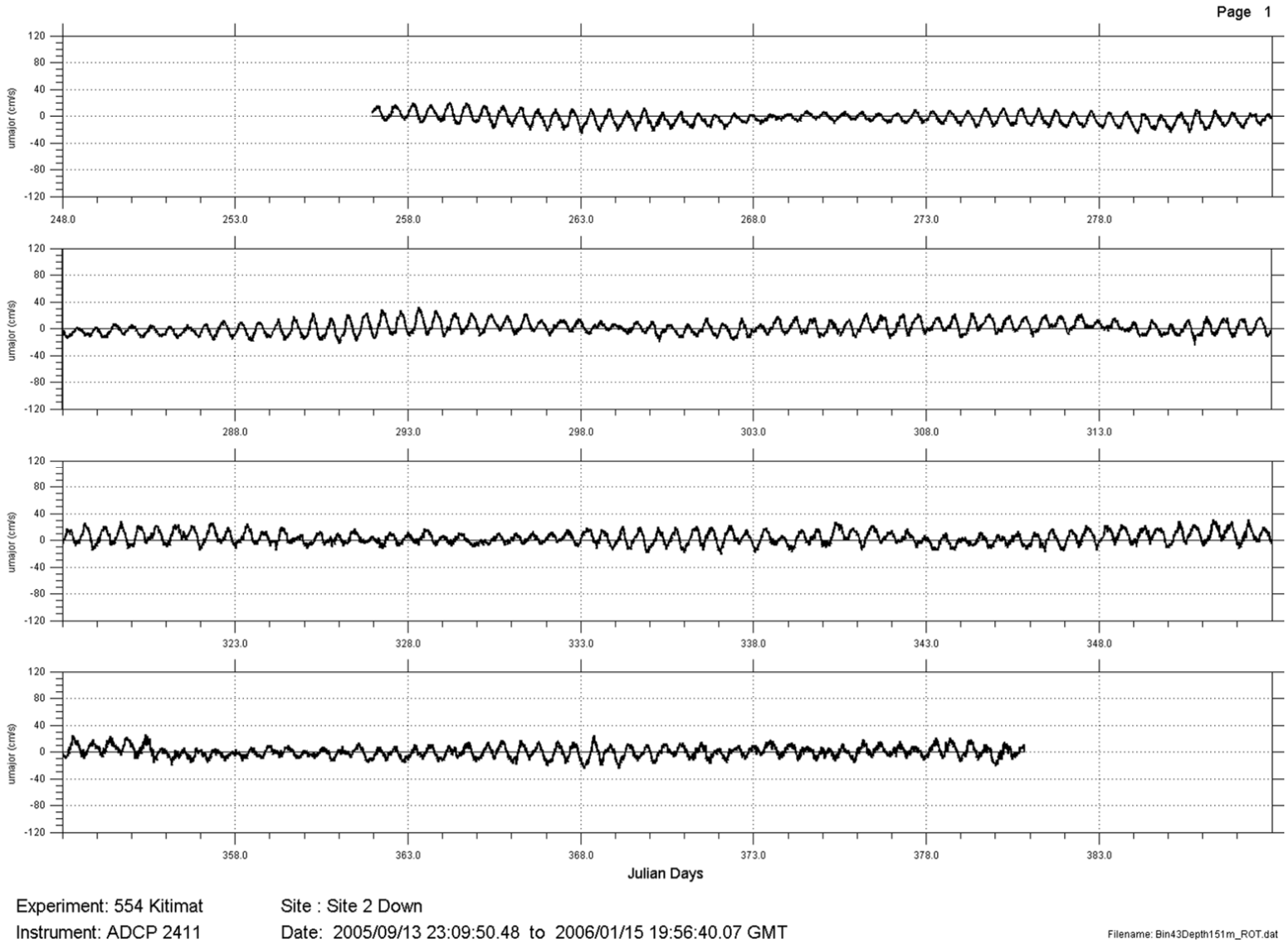
Page 1
umajor (cm/s)
120
80
40
0
-40
-80
-120
248.0
253.0
258.0
263.0
268.0
273.0
278.0
288.0
293.0
298.0
303.0
308.0
313.0
323.0
328.0
333.0
338.0
343.0
348.0
358.0
363.0
368.0
373.0
378.0
383.0
Julian Days
Experiment: 554 Kitimat
Instrument: ADCP 2411
Site : Site 2 Down
Date: 2005/09/13 23:09:50.48 to 2006/01/15 19:56:40.07 GMT
Filename: Bin43Depth151m_ROT.dat

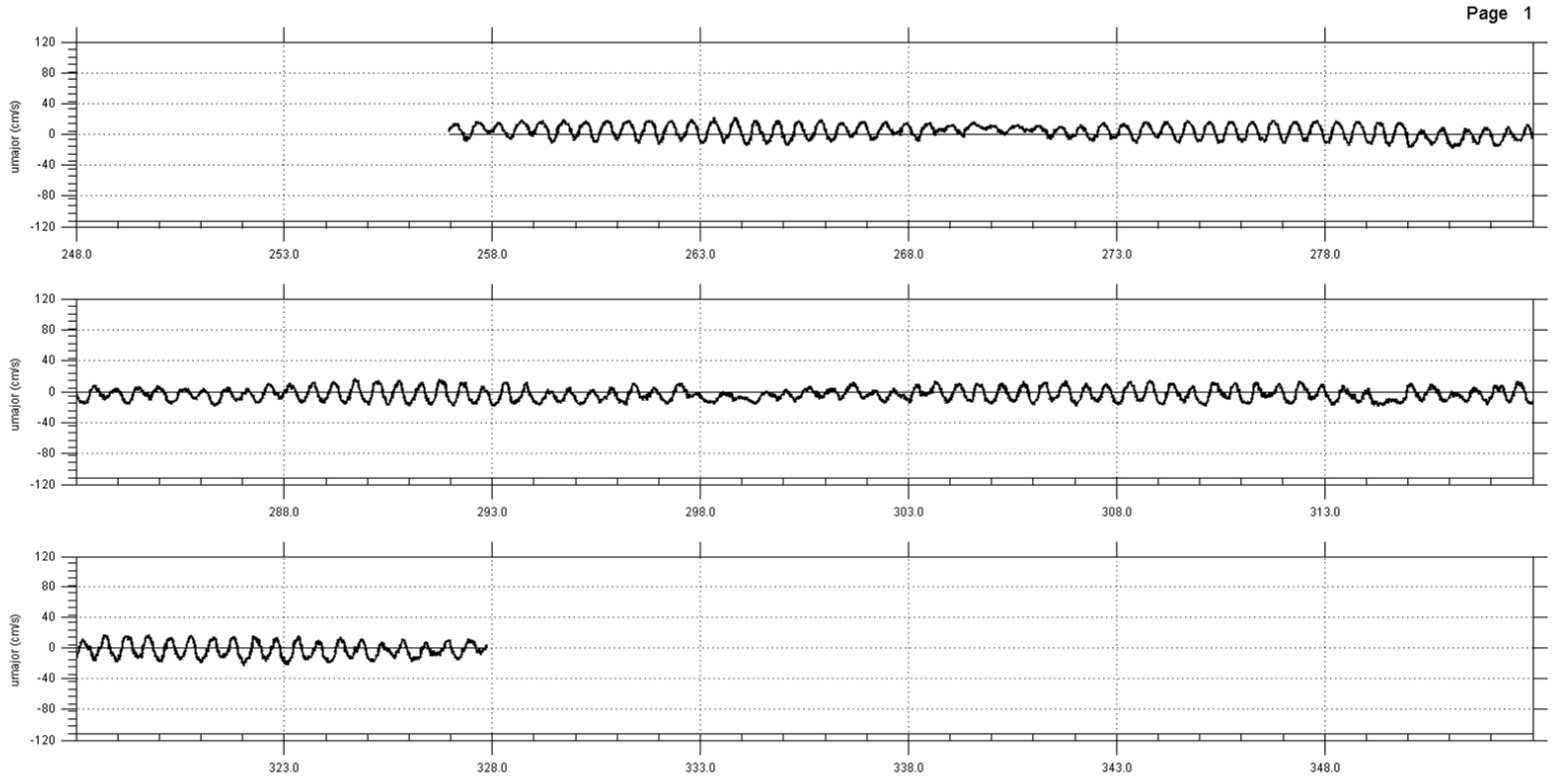

Experiment: 554 Kitimat
Instrument: Aquadopp SN 194

Site : Douglas Channel 250mj Deep
Date: 2005/09/13 23:09:59.88 to 2005/11/23 21:09:06.01 GMT

Filename: DougChann250Msn194_rot.dat

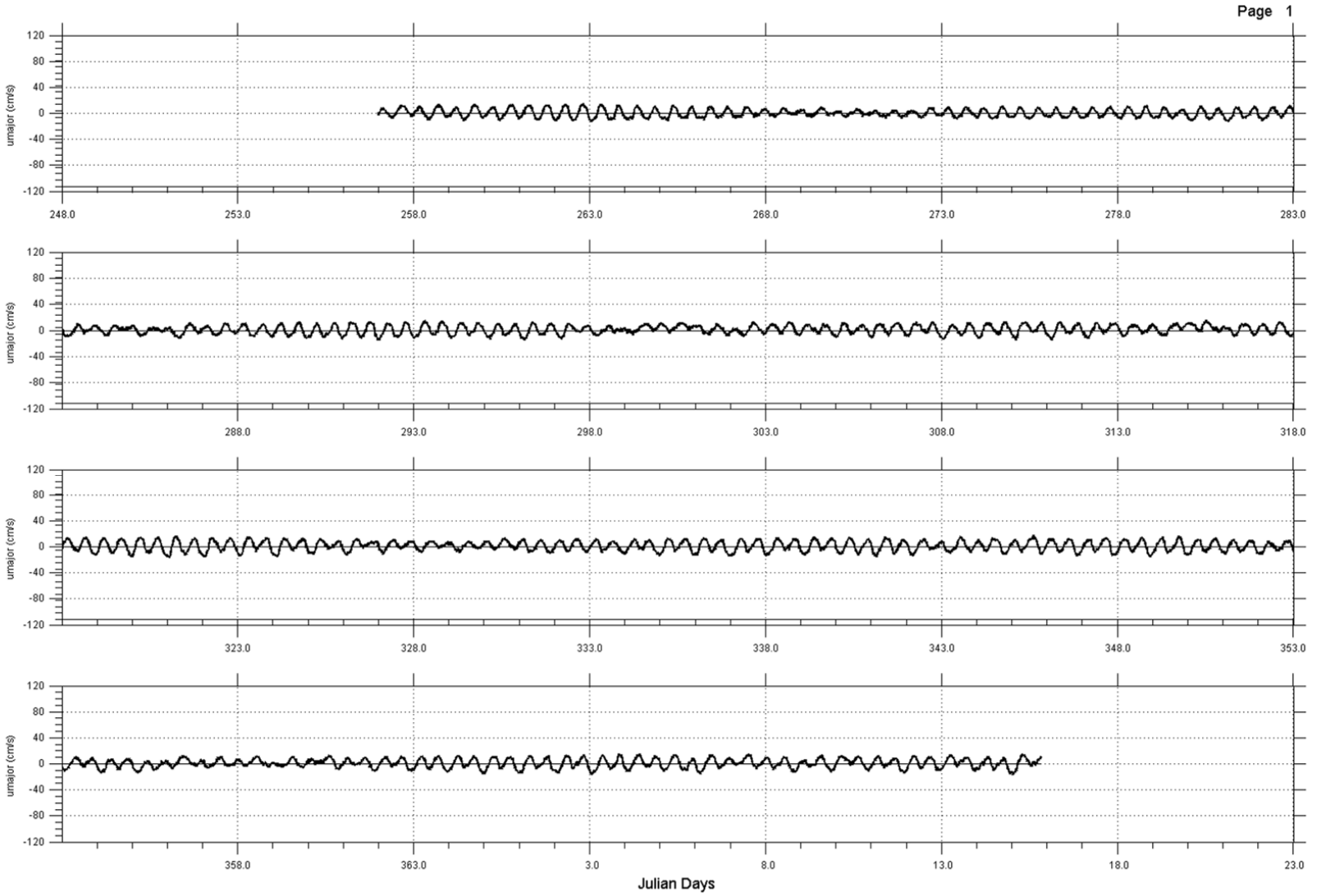

Experiment: 554 Kitimat
Instrument: Aquadopp SN 115

Site : Douglas Channel 350m deep
Date: 2005/09/13 23:20:00.28 to 2006/01/15 20:03:31.69 GMT

Filename: DougChann350Msn115_rot.dat

G2.3 Principe Channel: 20-m, 80-m, 125-m Depths

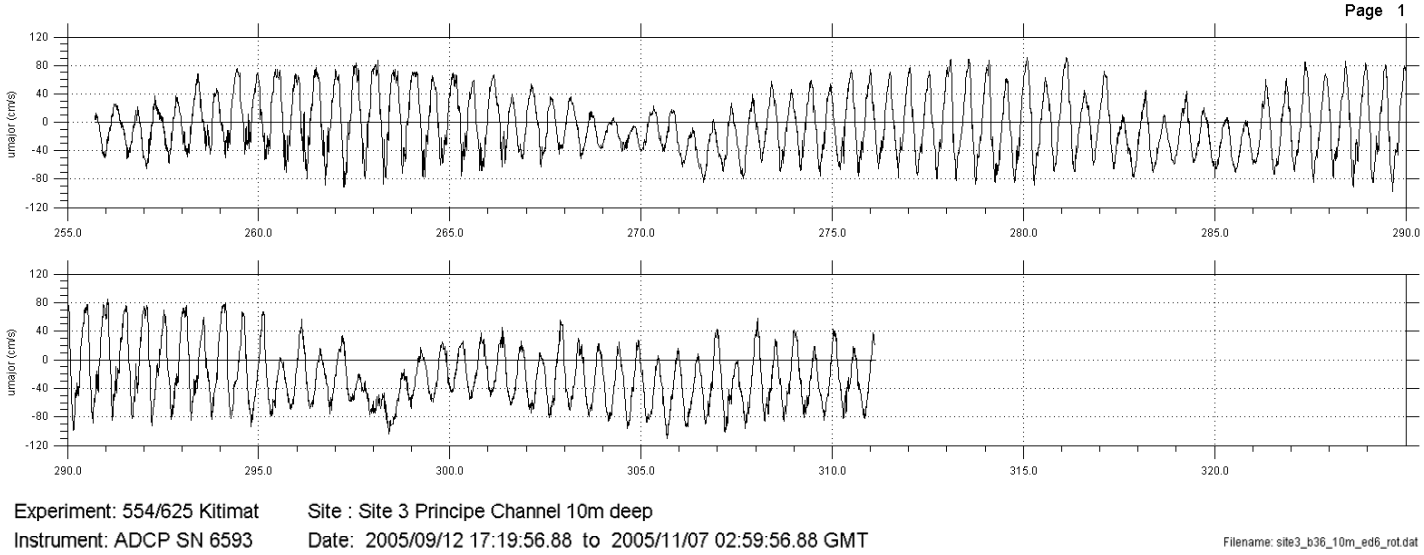

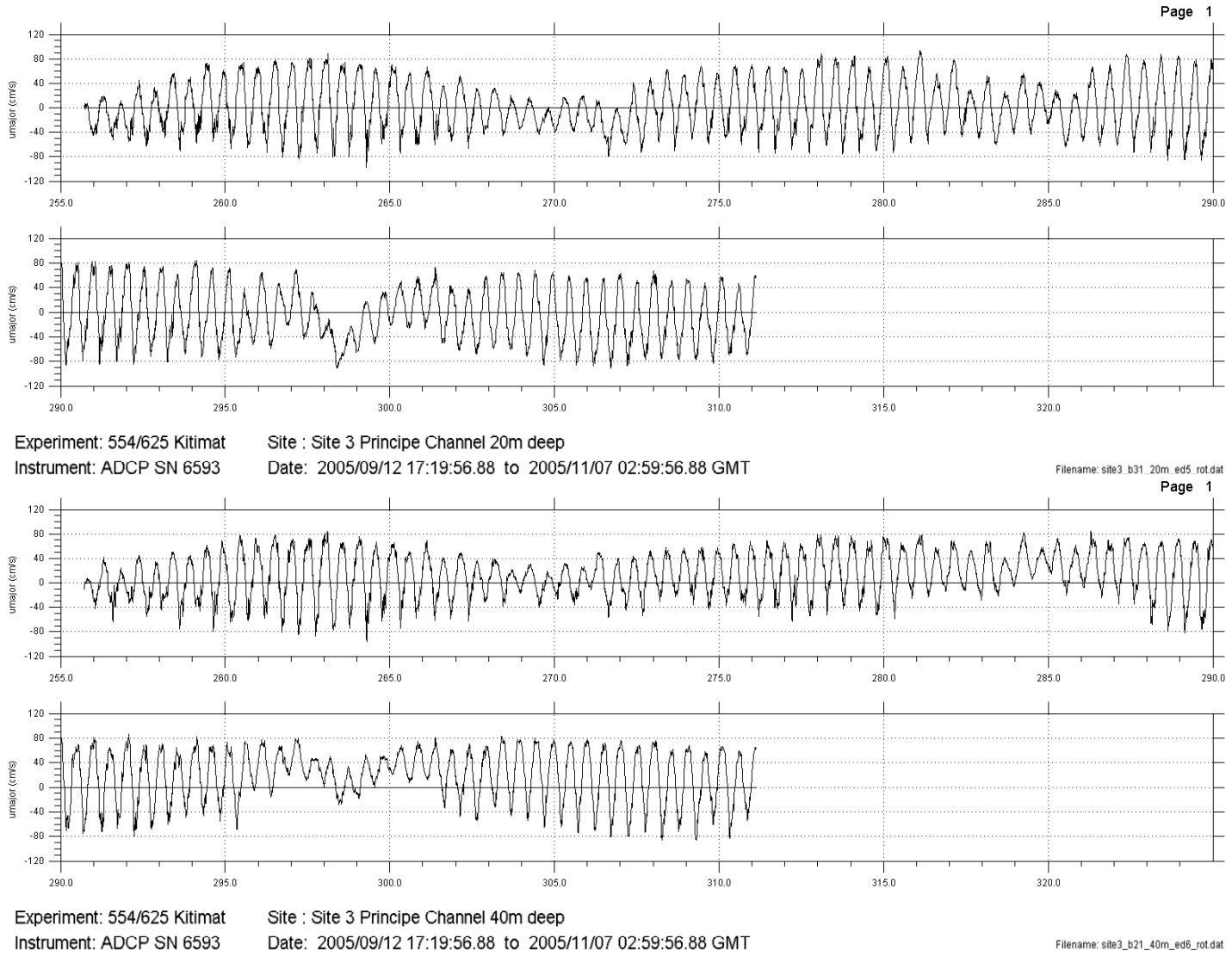
Page 1
umajor (cm/s)
120
80
40
0
-40
-80
-120
255.0
260.0
265.0
270.0
275.0
280.0
285.0
290.0
290.0
295.0
300.0
305.0
310.0
315.0
320.0
Experiment: 554/625 Kitimat
Site : Site 3 Principe Channel 20m deep
Instrument: ADCP SN 6593
Date: 2005/09/12 17:19:56.88 to 2005/11/07 02:59:56.88 GMT
Filename: site3_b31_20m_ed5_rot.dat
Page 1
Experiment: 554/625 Kitimat
Site : Site 3 Principe Channel 40m deep
Instrument: ADCP SN 6593
Date: 2005/09/12 17:19:56.88 to 2005/11/07 02:59:56.88 GMT
Filename: site3_b21_40m_ed6_rot.dat

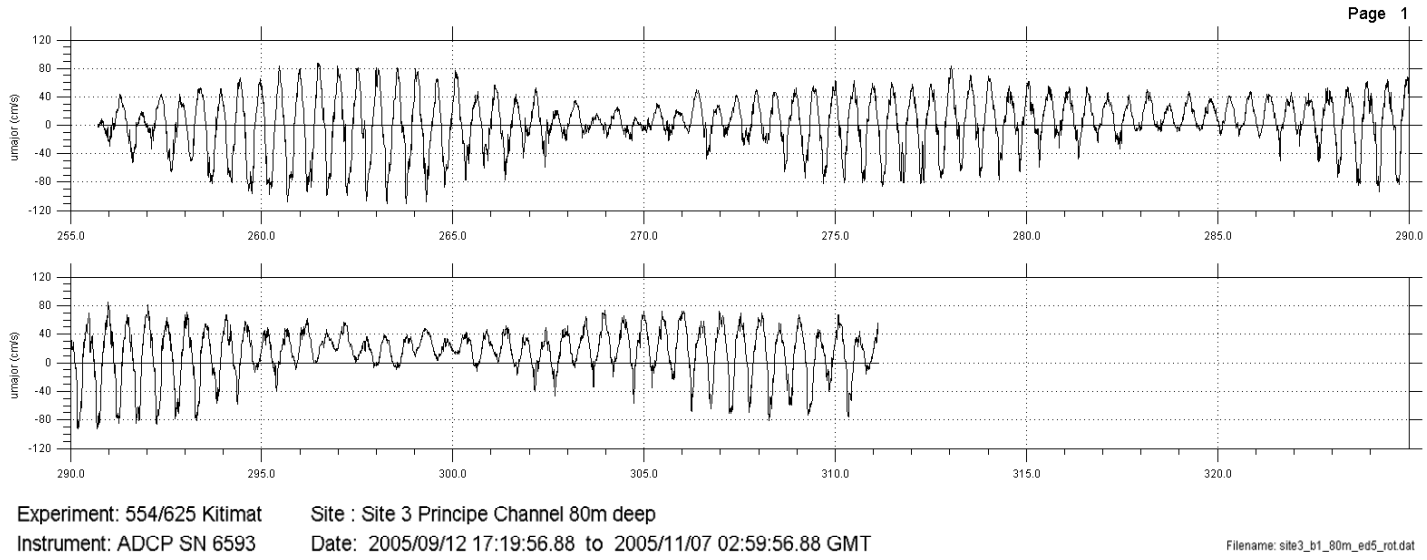
Page 1
umajor (cm/s)
120
80
40
0
-40
-80
-120
255.0
260.0
265.0
270.0
275.0
280.0
285.0
290.0
295.0
300.0
305.0
310.0
315.0
320.0
Experiment: 554/625 Kitimat
Instrument: ADCP SN 6593
Site : Site 3 Principe Channel 80m deep
Date: 2005/09/12 17:19:56.88 to 2005/11/07 02:59:56.88 GMT
Filename: site3_b1_80m_ed5_rot.dat

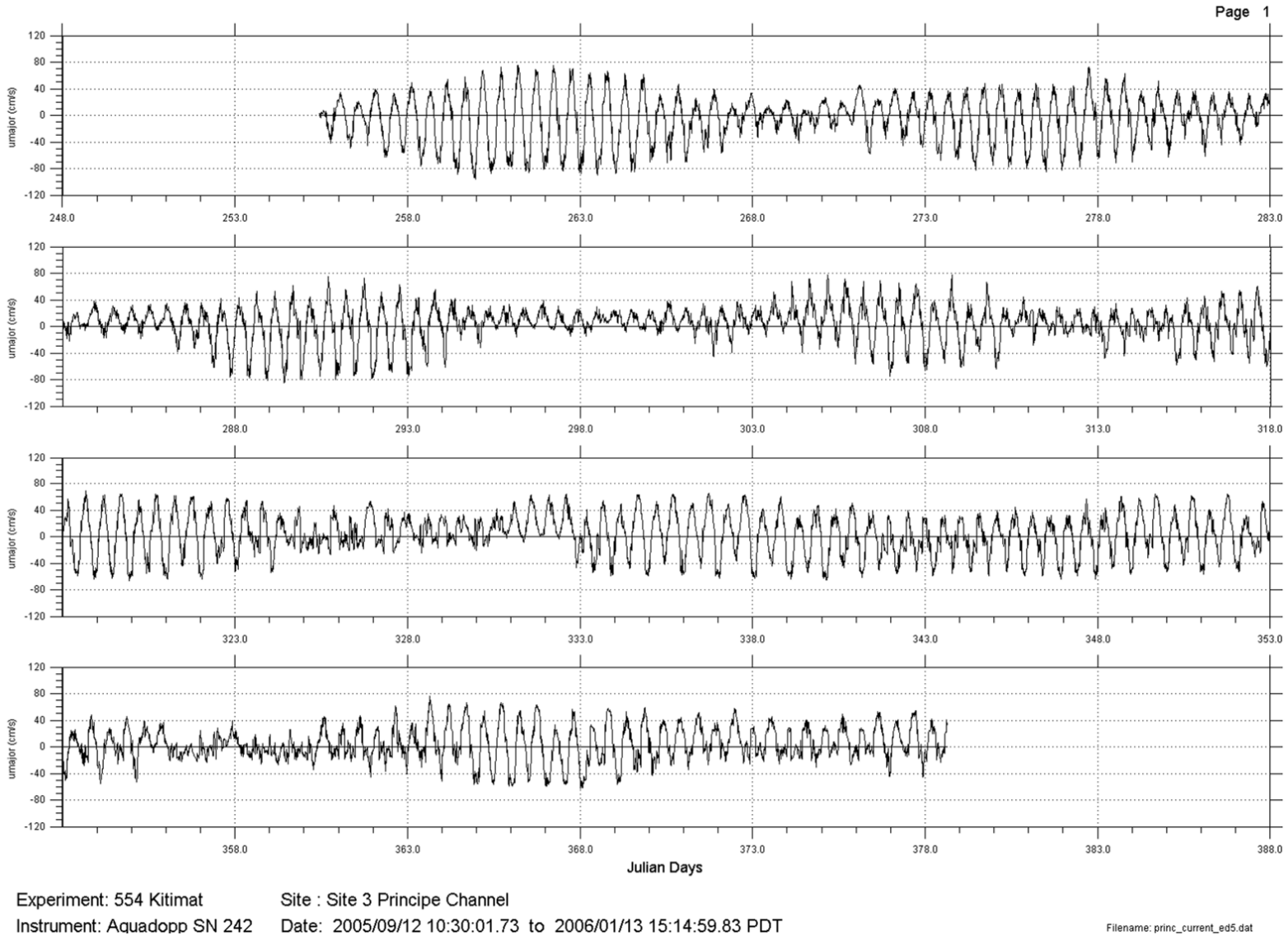
Page 1
umajor (cm/s)
120
80
40
0
-40
-80
-120
248.0
253.0
258.0
263.0
268.0
273.0
278.0
283.0
288.0
293.0
298.0
303.0
308.0
313.0
318.0
323.0
328.0
333.0
338.0
343.0
348.0
353.0
358.0
363.0
368.0
373.0
378.0
383.0
388.0
Julian Days
Experiment: 554 Kitimat
Site : Site 3 Principe Channel
Instrument: Aquadopp SN 242
Date: 2005/09/12 10:30:01.73 to 2006/01/13 15:14:59.83 PDT
Filename: princ_current_ed5.dat

G2.4 Caamaño Sound: 6-m, 10-m, 19-m, 33-m depths.

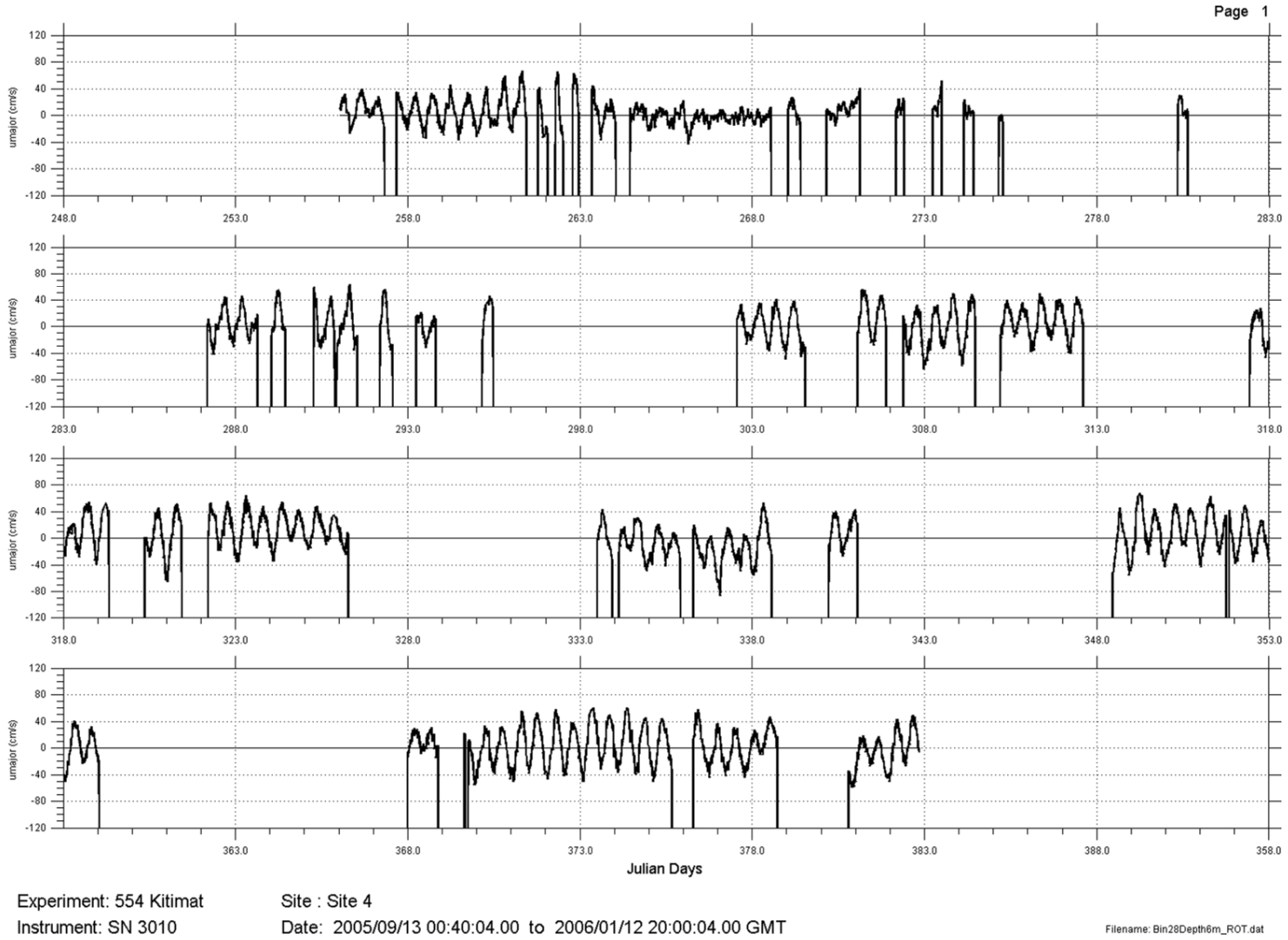

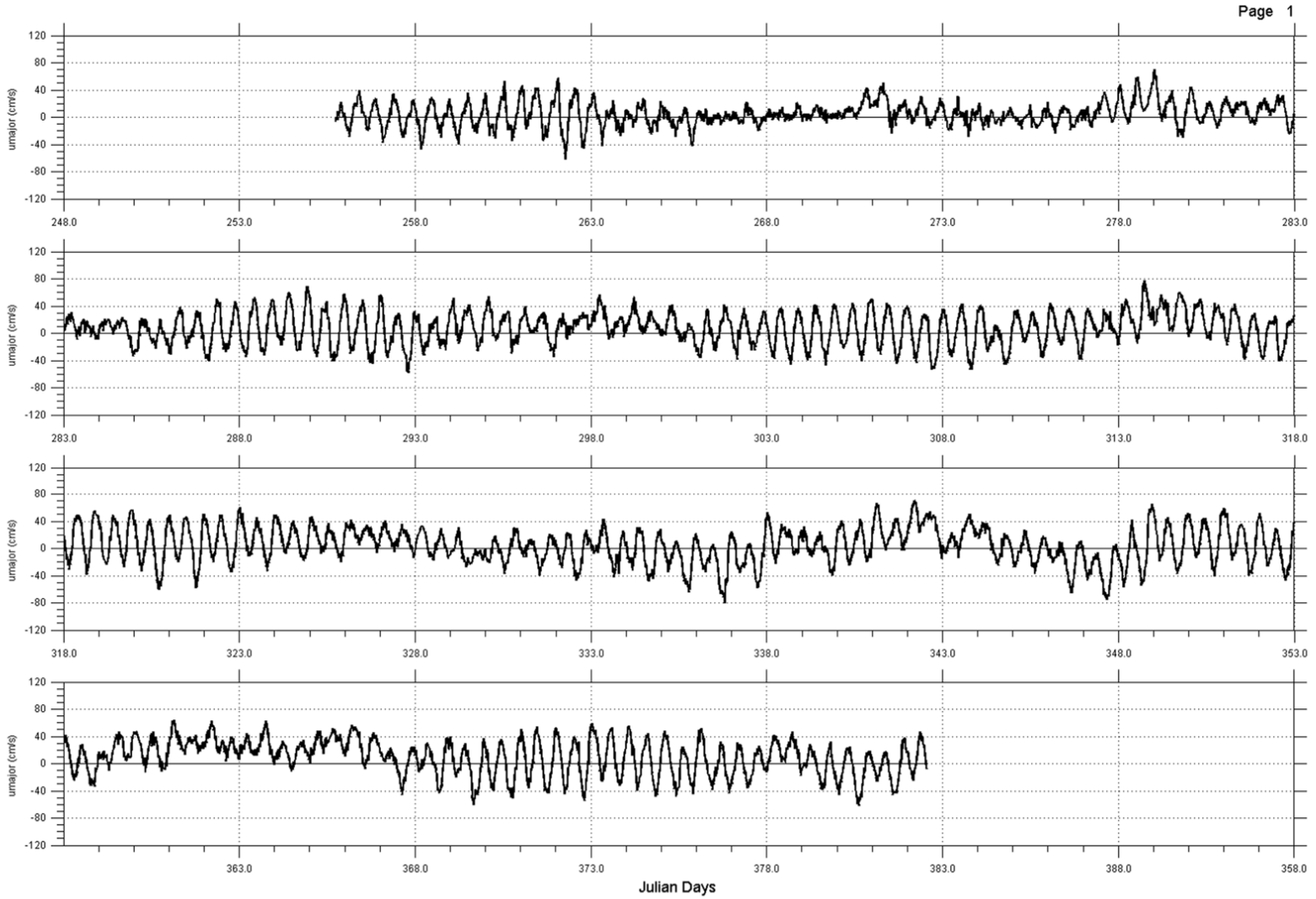

Experiment: 554 Kitimat
Instrument: SN 3010

Site : Site 4
Date: 2005/09/12 17:40:04.00 to 2006/01/12 13:00:04.00 PDT

Filename: Bin24Depth10m_ROT.dat

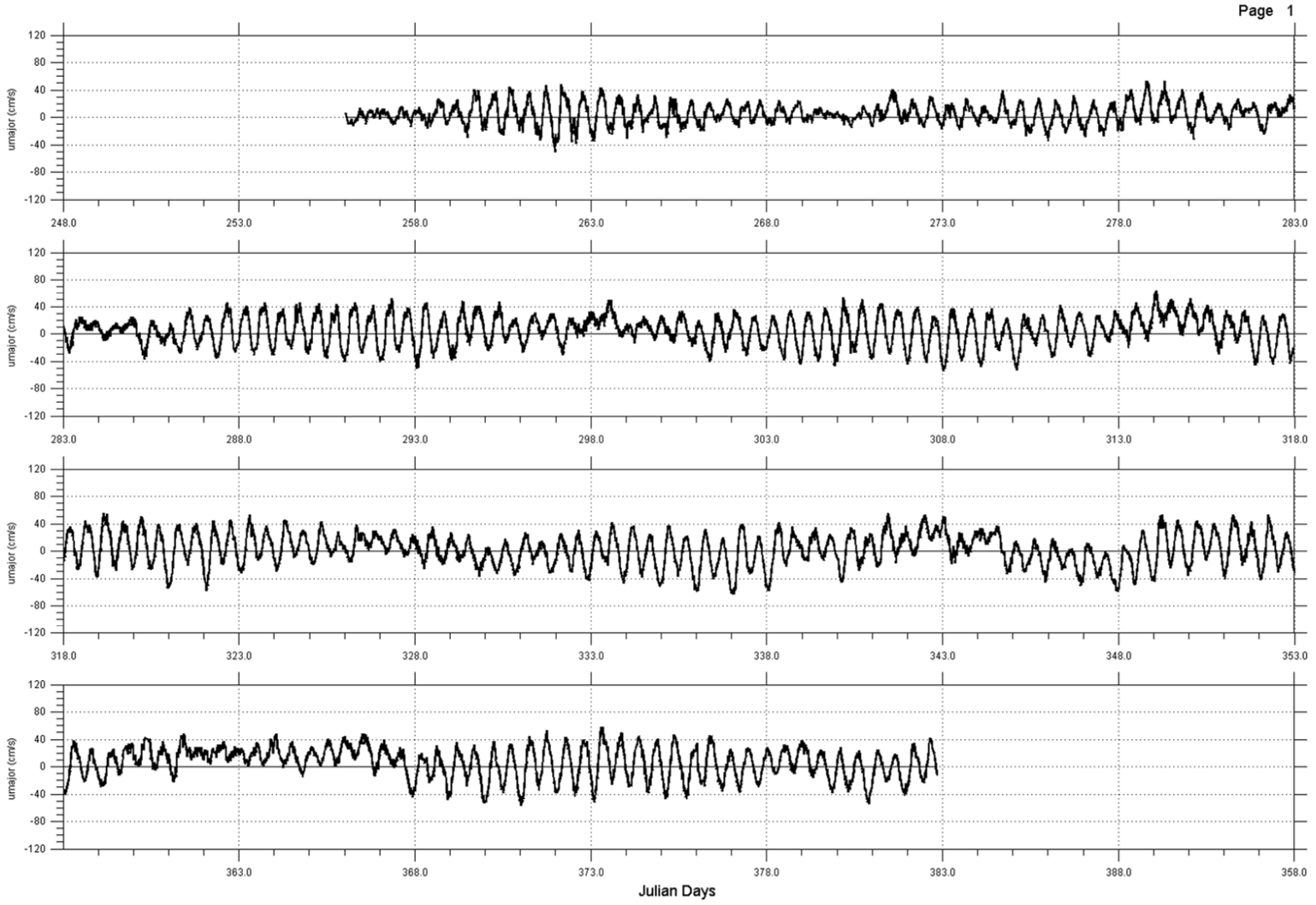

Experiment: 554 Kitimat
Instrument: SN 3010

Site : Site 4
Date: 2005/09/13 00:40:04.00 to 2006/01/12 20:00:04.00 GMT

Filename: Bin15Depth19m_ROT.dat

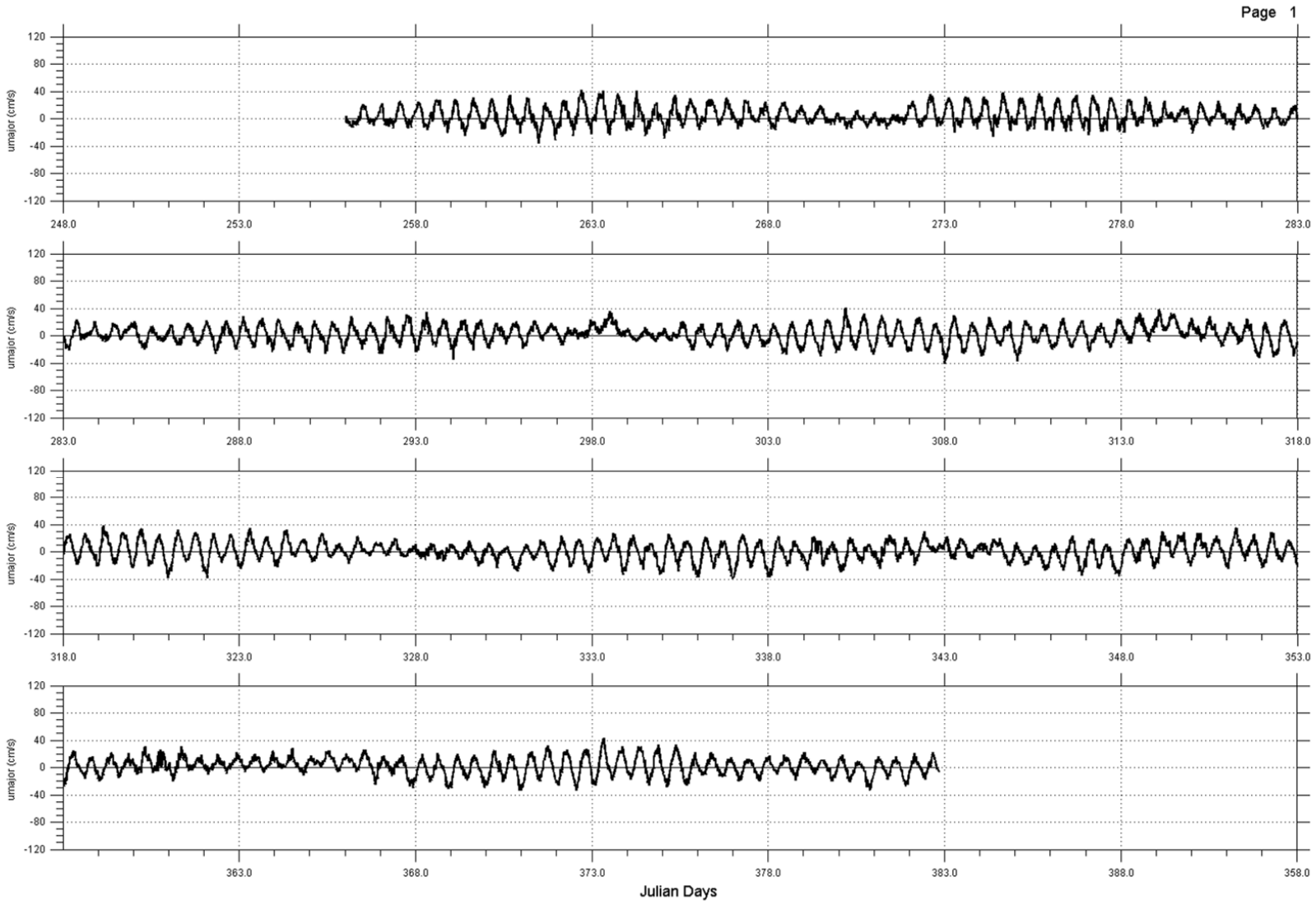
Page 1
umajor (cm/s)
120
80
40
0
-40
-80
-120
248.0
253.0
258.0
263.0
268.0
273.0
278.0
283.0
288.0
293.0
298.0
303.0
308.0
313.0
318.0
323.0
328.0
333.0
338.0
343.0
348.0
353.0
358.0
363.0
368.0
373.0
378.0
383.0
388.0
Julian Days
Experiment: 554 Kitimat
Instrument: ADCP SN 3010
Site : Site 4
Date: 2005/09/13 00:40:04.00 to 2006/01/12 20:00:04.00 GMT
Filename: Bin1Depth33m_ROT.dat

Attachment G3 Tabulations of Temperature and Salinity from CTD Observations

G3.1 Caamaño Sound to Kitimat Arm

Table G3-1 September 2005 – Temperature

Avg. Depth	Caam	d09	d10	d06	d01	s2	d27	c100	c101	s1
0.00		13.5	12.97			12.31				
1.50	11.64	12.49	12.85	11.08	10.74	12.32	11.42	12.19	12.76	13.51
3.50	11.32	11.42	11.25	11.08	10.74	11.71	11.43	12.11	12.64	14.20
5.50	11.46	10.99	10.65	10.28	9.93	9.88	10.89	11.12	12.05	13.67
8.00	11.36	10.28	9.71	10.55	9.43	9.24	9.45	10.19	11.52	11.08
11.00	11.70	9.42	9.59	10.10	9.20	9.03	9.57	9.57	9.79	9.11
14.00	11.82	9.04	9.41	9.90	8.55	8.63	8.70	9.18	9.08	8.02
18.00	11.57	8.84	9.09	9.27	7.98	8.43	8.24	8.59	8.78	7.32
23.50	9.89	8.59	8.68	8.94	7.86	8.04	7.99	8.21	8.41	6.77
30.00	9.01	8.57	8.40	8.69	7.81	7.82	7.84	7.73	7.53	6.95
37.50	9.26	8.23	8.10	8.37	7.73	7.80	7.73	7.72	7.46	7.06
47.50	9.01	7.92	7.87	7.82	7.59	7.63	7.73	7.70	7.50	7.23
60.00	8.64	7.83	7.63	7.51	7.57	7.56	7.57	7.57	7.50	7.30
75.00	8.33	7.78	7.53	7.33	7.26	7.41	7.31	7.35	7.32	7.32
90.00	7.91	7.48	7.41	7.24	7.16	7.24	7.21	7.26	7.26	7.22
107.50	7.32	7.27	7.28	7.06	7.11	7.18	7.14	7.17	7.15	7.13
126.25	6.91	7.18	7.02	7.02	7.04	7.05	7.09	7.10	7.10	7.06
148.75	6.76	7.19	6.99	7.01	6.95	6.96	7.03	7.02	7.02	7.02
192.50	6.77	7.00	6.95	6.84	6.82	6.84	6.95	6.95	6.95	6.95
240.00	6.69	6.81	6.91	6.82	6.74	6.74	6.88	6.91	6.92	
275.00		6.79	6.87	6.81	6.72	6.73	6.84	6.88		
306.25		6.78	6.80	6.70	6.70	6.71	6.83	6.86		
350.00		6.68	6.79	6.66	6.67	6.67				
400.00			6.79	6.65						
500.00										

Table G3-2 January 2006 – Temperature

Avg. Depth	Caam	d09	d10	d06	d01	s2	d27	c100	d25	s1
0.00										
1.50			6.77							
3.50	7.98	6.98	6.78	6.53	6.36	6.31	6.33	6.68	6.15	6.22
5.50	7.98	7.00	6.79	6.59	6.39	6.37	6.36	6.85	6.15	6.32
8.00	7.99	7.01	6.81	6.60	6.42	6.38	6.46	6.96	6.15	7.09
11.00	7.99	7.03	6.85	6.73	6.58	6.54	6.85	7.01	6.92	7.74
14.00	7.99	7.09	6.90	6.75	6.96	6.97	6.98	7.27	7.39	7.88
18.00	7.99	7.57	6.95	7.10	7.63	7.59	7.56	7.59	7.98	7.91
23.50	7.99	7.74	6.96	7.35	7.78	7.88	7.72	7.68	8.13	8.06
30.00	7.99	7.84	7.67	7.65	8.00	7.97	8.02	7.86	8.30	8.20
37.50	7.99	7.94	7.76	7.58	8.00	8.05	8.12	8.03	8.33	8.34
47.50	8.04	8.06	7.93	7.75	8.10	8.10	8.16	8.15	8.33	8.51
60.00	8.12	8.15	8.08	7.95	8.24	8.17	8.23	8.19	8.61	8.61
75.00	8.25	8.21	8.18	8.09	8.21	8.21	8.19	8.27	8.62	8.59
90.00	8.32	8.24	8.27	8.25	8.25	8.23	8.24	8.36	8.58	8.48
107.50	8.45	8.28	8.26	8.22	8.27	8.33	8.34	8.46	8.54	8.10
126.25	8.44	8.16	8.24	8.23	8.29	8.38	8.46	8.48	8.49	7.81
148.75	8.29	7.97	8.04	8.30	8.39	8.46	8.44	8.25	8.34	7.63
192.50	7.82	7.64	7.84	7.96	7.79	7.77	8.01	7.72	7.60	7.51
240.00	7.58	7.47	7.46	7.68	7.44	7.43	7.62	7.33	7.37	
275.00		7.18	7.29	7.49	7.31	7.26	7.33	7.15	7.20	
306.25		7.07	7.25	7.36	7.14	7.11	7.22	7.10		
350.00		7.02	7.10	7.15	7.01	7.01	7.09	7.05		
400.00			7.07	7.06	6.97					
500.00										

Table G3-3 September 2005 – Salinity

Avg. Depth	Caam	d09	d10	d06	d01	s2	d27	c100	c101	s1
0.00		25.08	24.02			19.72				
1.50	27.31	26.01	24.60	24.56	25.05	20.39	22.54	21.28	18.44	11.15
3.50	29.85	27.28	26.52	27.21	25.62	22.56	22.83	21.51	19.08	15.74
5.50	30.23	27.98	28.66	28.23	27.59	27.51	24.65	23.93	22.03	16.46
8.00	30.82	29.51	29.17	29.15	28.56	28.80	28.51	26.53	24.13	26.89
11.00	30.89	30.68	29.39	30.00	29.13	29.13	29.26	28.33	28.46	29.23
14.00	31.04	31.06	30.45	30.72	30.25	29.76	29.97	29.23	29.49	29.92
18.00	31.45	31.35	30.74	31.38	30.98	30.34	30.76	30.27	30.01	30.42
23.50	31.85	31.49	31.09	31.60	31.30	30.81	31.06	30.72	30.71	30.80
30.00	31.99	31.78	31.45	31.77	31.65	31.21	31.33	31.41	31.18	31.21
37.50	32.99	31.85	31.83	31.91	31.94	31.54	31.62	31.62	31.54	31.47
47.50	32.39	32.29	32.11	32.26	32.12	32.92	31.93	31.96	31.79	31.73
60.00	32.53	32.46	32.49	32.68	32.51	32.16	32.28	32.19	32.15	32.15
75.00	32.62	32.86	32.78	32.95	32.89	32.55	32.78	32.66	32.71	32.78
90.00	32.80	32.99	32.83	33.01	33.01	32.74	32.92	32.80	32.90	32.88
107.50	33.09	33.12	33.04	33.06	33.06	32.82	33.00	32.91	32.98	32.94
126.25	33.26	33.14	33.23	33.10	33.10	32.92	33.06	32.97	33.03	32.99
148.75	33.31	33.16	33.25	33.16	33.16	32.98	33.09	33.02	33.07	33.02
192.50	33.31	33.27	33.26	33.24	33.24	33.04	33.15	33.05	33.10	33.05
240.00	33.33	33.38	33.30	33.29	33.27	33.09	33.19	33.08	33.12	
275.00		33.38	33.33	33.31	33.29	33.11	33.22	33.09		
306.25		33.38	33.37	33.31	33.30	33.12	33.22	33.10		
350.00		33.47	33.39	33.32	33.31	33.14				
400.00			33.40	33.34						
500.00										

Table G3-4 January 2006 – Salinity

Avg. Depth	Caam	d09	d10	d06	d01	s2	d27	c100	d25	s1
0.00										
1.50			28.63							
3.50	30.25	28.66	28.66	28.35	27.85	27.87	27.83	28.36	27.33	27.47
5.50	30.27	28.69	28.69	28.40	27.89	27.95	27.90	28.58	27.33	27.73
8.00	30.29	28.72	28.74	28.44	27.93	27.97	28.22	28.69	27.33	28.63
11.00	30.34	28.75	28.81	28.80	28.14	28.20	28.56	28.82	28.58	29.63
14.00	30.36	28.85	28.88	28.91	29.00	29.07	28.85	29.17	29.66	29.88
18.00	30.39	29.56	29.00	29.33	29.96	29.82	29.77	29.54	30.18	29.96
23.50	30.40	29.90	29.08	29.76	30.23	30.35	30.04	29.75	30.42	30.18
30.00	30.43	30.16	30.06	30.27	30.46	30.61	30.67	30.10	30.63	30.37
37.50	30.47	30.44	30.27	30.35	30.68	30.87	30.90	30.56	30.80	30.60
47.50	30.52	30.63	30.62	30.63	30.88	31.03	31.01	30.94	30.86	30.78
60.00	30.60	30.89	30.86	30.94	31.13	31.27	31.24	31.22	31.16	31.08
75.00	30.75	31.05	31.07	31.17	31.25	31.39	31.29	31.51	31.39	31.32
90.00	30.84	31.19	31.32	31.53	31.32	31.50	31.49	31.62	31.60	31.47
107.50	31.08	31.36	31.54	31.59	31.54	31.74	31.62	31.86	31.82	31.63
126.25	31.23	31.72	31.60	31.79	31.73	31.93	31.93	32.04	31.98	31.74
148.75	31.42	31.96	32.00	32.09	32.02	32.23	32.13	32.28	32.12	31.94
192.50	31.93	32.34	32.41	32.49	32.54	32.55	32.45	32.52	32.41	32.34
240.00	32.13	32.51	32.62	32.76	32.78	32.79	32.66	32.81	32.71	
275.00		32.67	32.73	32.88	32.89	32.90	32.83	32.97	32.92	
306.25		32.73	32.78	32.95	33.00	33.00	32.92	33.03		
350.00		32.77	32.88	33.06	33.08	33.08	33.04	33.08		
400.00			32.90	33.11	33.12					
500.00										

G3.2 Principe Channel Waterway – Browning Entrance to Nepean Sound

Table G3-5 September 2005 – Temperature

Avg. Depth	princ_C	site3ctd_2	princ_B	princ_A	dob07
0.00					
1.50	12.39		11.17	11.94	11.65
3.50	12.33		11.13	12.17	11.60
5.50	11.74		11.00	11.84	11.58
8.00	11.23	12.01	10.88	11.04	11.54
11.00	11.05	11.75	10.77	10.79	11.25
14.00	10.86	11.40	10.44	10.72	10.73
18.00	10.64	10.54	10.11	10.58	10.39
23.50	10.50	9.97	9.53	10.21	10.14
30.00	10.37	9.29	9.51	9.44	9.89
37.50	10.33	8.76	9.46	9.15	9.50
47.50	9.84	8.52	8.65	8.89	9.19
60.00	8.64	8.31	8.18	7.87	8.61
75.00	7.90	7.92	8.04	7.74	8.11
90.00	7.70	7.56	7.56	7.49	7.48
107.50	7.46	7.42	7.43	7.27	7.14
126.25	7.35	7.38	7.32	7.17	7.06
148.75		7.29	7.27	7.11	7.03
192.50					

Table G3-6 January 2006 – Temperature

Avg. Depth	princ_C	site3ctd_2	princ_B	princ_A	dob07
0.00					
1.50	7.76				
3.50	7.75	7.16	6.85	6.86	7.10
5.50	7.76	7.16	6.86	6.86	7.52
8.00	7.76	7.17	6.95	6.92	7.54
11.00	7.82	7.19	6.99	9.97	7.54
14.00	7.86	7.22	7.02	7.00	7.56
18.00	7.86	7.59	7.08	7.05	7.58
23.50	7.86	7.87	7.33	7.06	7.57
30.00	7.88	8.01	7.36	7.12	7.59
37.50	7.89	8.10	7.58	7.15	7.60
47.50	7.92	8.13	7.75	7.22	7.66
60.00	7.94	8.14	7.90	7.63	7.73
75.00	7.96	8.15	7.98	8.03	7.87
90.00	7.98	8.16	8.03	8.09	8.14
107.50	8.02	8.21	8.16	8.12	8.14
126.25	8.22	8.23	8.16	8.13	8.15
148.75			8.16	8.14	8.05
192.50					

Table G3-7 September 2005 – Salinity

Avg. Depth	princ_C	site3ctd_2	princ_B	princ_A	dob07
0.00					
1.50	30.78		30.61	29.41	26.62
3.50	30.82		30.63	29.05	27.05
5.50	30.96		30.66	29.63	28.41
8.00	31.13	28.35	30.74	30.77	28.94
11.00	31.28	29.57	30.83	31.00	29.76
14.00	31.30	29.68	31.06	31.06	30.63
18.00	31.28	30.04	31.30	31.19	31.07
23.50	31.64	30.41	31.69	31.47	31.38
30.00	31.74	30.93	31.70	31.88	31.60
37.50	31.80	31.28	31.73	32.02	31.77
47.50	31.99	31.42	32.23	32.16	31.94
60.00	32.33	31.59	32.48	32.68	32.20
75.00	32.66	31.82	32.55	32.73	32.48
90.00	32.76	32.03	32.80	32.86	32.74
107.50	32.88	32.10	32.86	32.96	32.98
126.25	32.94	32.18	32.92	33.01	33.05
148.75		32.26	32.95	33.06	33.07
192.50					

Table G3-8 January 2006 – Salinity

Avg. Depth	princ_C	site3ctd_2	princ_B	princ_A	dob07
0.00					
1.50	30.50				
3.50	30.66	29.63	29.29	29.14	29.63
5.50	30.72	29.64	29.31	29.16	30.27
8.00	30.75	29.65	29.42	29.27	30.32
11.00	30.91	29.72	29.49	29.34	30.34
14.00	30.99	29.78	29.53	29.43	30.36
18.00	31.01	30.27	29.64	29.50	30.40
23.50	31.03	30.75	29.88	29.55	30.43
30.00	31.05	31.01	29.93	29.66	30.47
37.50	31.08	31.21	30.26	29.72	30.49
47.50	31.11	31.29	20.61	29.80	30.55
60.00	31.14	31.34	20.89	30.37	30.76
75.00	31.18	31.36	31.05	31.13	30.96
90.00	31.20	31.38	31.16	31.31	31.34
107.50	31.24	31.45	31.53	31.48	31.48
126.25	31.42	31.47	31.57	31.68	31.72
148.75			31.66	31.78	32.31
192.50					

Appendix H GEM Oceanography Program, January to April 2006

H.1 Introduction

H.1.1 Objectives

The purpose of this document is to describe baseline conditions with respect to oceanographic measurements taken from January to April 2006 within the CCAA to support the environmental assessment for the Project. Oceanographic measurements were taken for the Project from January to April 2006. These measurements are a continuation of a program that ran from September 2005 to January 2006 (see Appendix G). The measurements are specific to one of the four CCAA measurement locations from the 2005 program: the Kitimat Arm location—at a site closer to shore than during 2005—near the proposed marine terminal. Following the recovery of the data that is analyzed here, the instrument was redeployed for further measurements. This report presents the results of the Winter 2006 measurement program, including:

- subsurface currents
- water levels
- CTD profiles

Comparisons are made with historical knowledge, as compiled in Appendices B through D of this volume.

H.2 Methods

H.2.1 Study Area for Field Surveys

In January 2006, one of the current meters was redeployed near site CMI of 2005, in the immediate vicinity of the marine terminal location for ongoing data collection. This report presents the analysis results for near-surface, mid-depth and near-bottom currents at this site, as well as temperature and salinity profile measurements from this site at the recovery on April 22, 2006.

H.2.2 Methodology and Instruments

H.2.2.1 Acoustic Doppler Current Meters

For the location of the Doppler current meters, see Figure H-1. The locations are illustrated in the detailed view of Figure H-1, where “Jan” indicates the January to April site, “Sept” indicates the September to January site and “Kit” indicates the historical summer/fall measurement site from 1977 to facilitate comparisons with the older data. For the location of the September 2005 to April 2006 measurement sites relative to the location of the marine terminal, see Figure H-2. The ADCP was a 600-kHz Sentinel Workhorse model manufactured by RD Instruments. It was deployed on a taut line mooring, and measurements of currents were selected from the near-surface, mid-depth and near-bottom for further analysis. The RD Instruments ADCPs also measure pressure, water temperature and acoustic backscatter return as well as internal parameters.

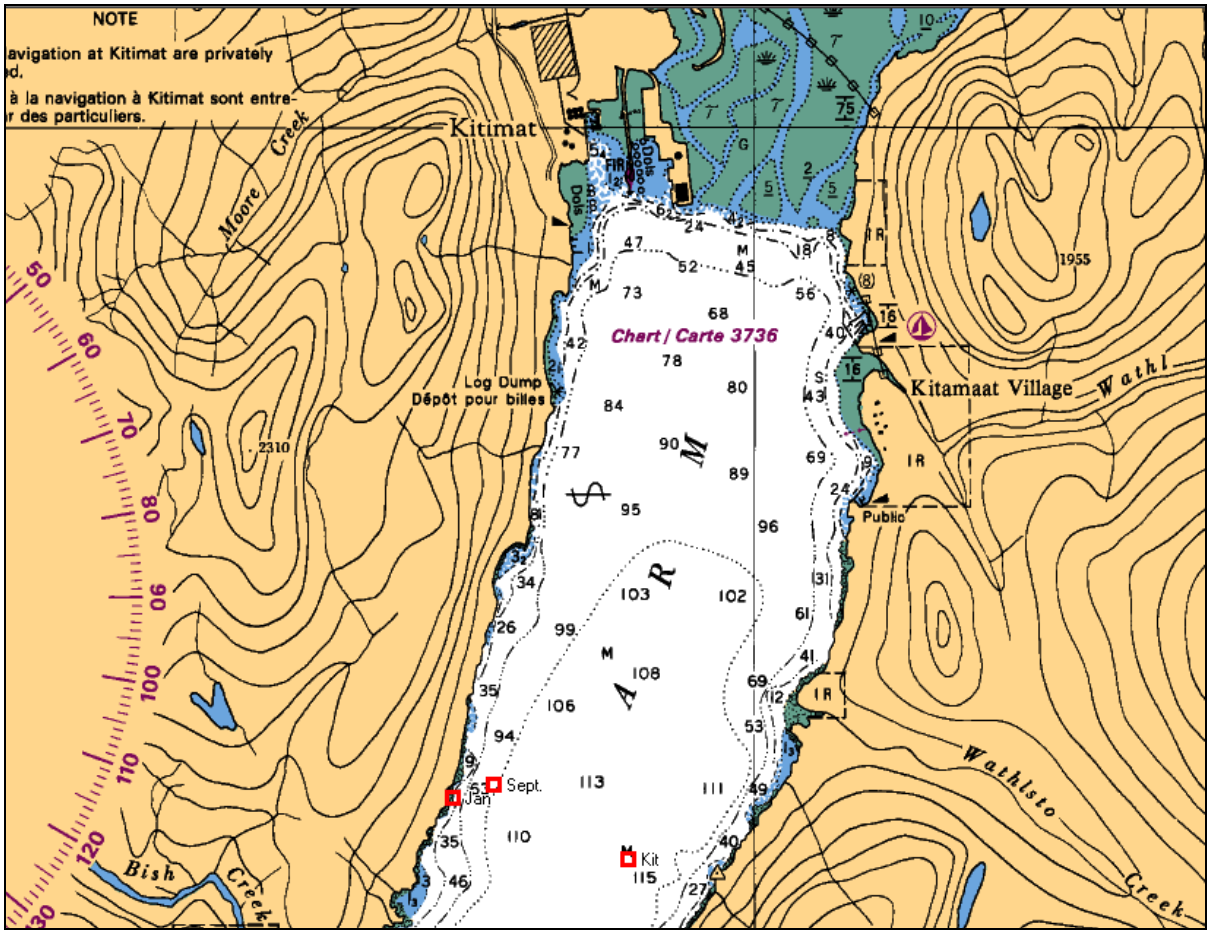

NOTE: The two mooring locations at Site 1 are shown by the red squares labelled “Jan” and “Sept.” Also shown is location of a current meter mooring “Kit” operated in this area in the summer and fall of 1977.

Figure H-1 Location of the GEM Marine Current Mooring at Site CM1 during September 2005 and January 2006 in Kitimat Arm

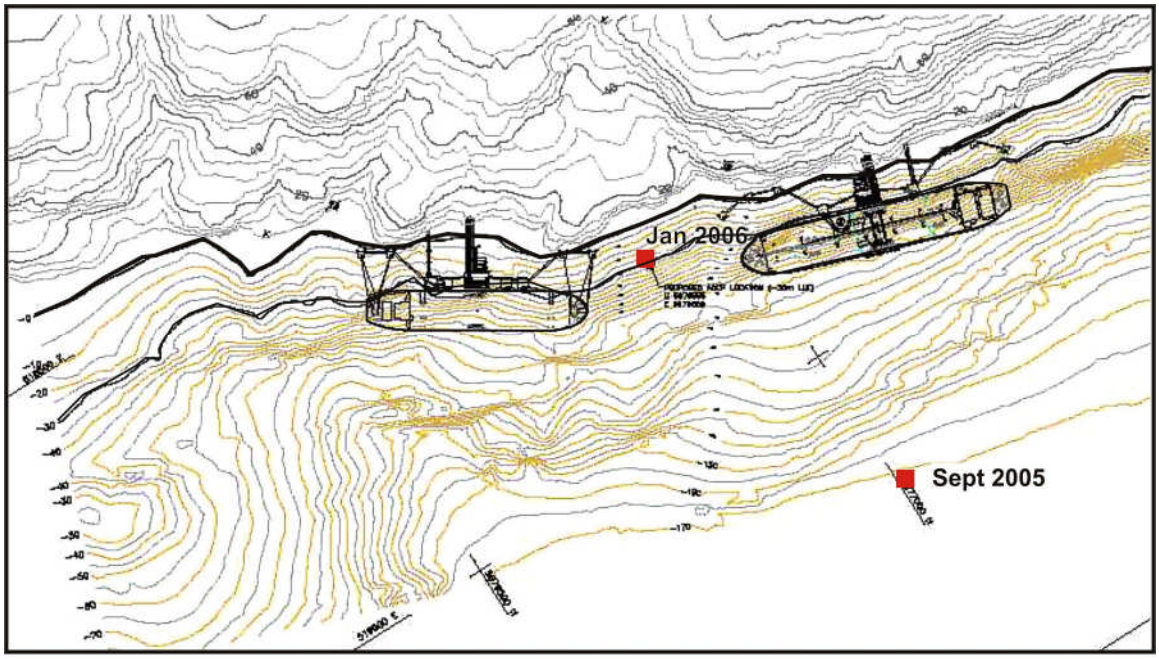

Figure H-2 Location of the September 2005 and January 2006 Kitimat Arm Measurement Sites with Respect to Marine Terminal

H.2.2.2 CTD Profile Measurements in April 2006

As part of the recovery cruise, CTD profile data were obtained near the current meter location (see Table H-1).

Table H-1 List of CTD Stations Occupied in April 2006

Area	Comments	Time Date (PDT)	Lat, Long (WGS84)	Deepest CTD Measurement (m)	CTD File Name
Terminal Area	First of two casts in the area.	22 Apr 06 12:18	53 56.418 128 42.823	33	009658Apr22 .dat
Terminal Area	Second of two casts in the area	22 Apr 06 12:58	53 56.315 128 41.799	148	009658Apr22 .dat

NOTES:
PDT = Pacific Daylight Time
WGS84 = World Geodetic System 1984

H.3 Results of GEM Marine Data Collection, January to April 2006

The CCAA (see Figure 1-1) consists of the Kitimat fjord system (Macdonald 1983), Caamaño Sound and Principe Channel. The Kitimat system has four entrances: Grenville Channel to the west and Princess Royal Channel to the east, as well as two entrances on the south, Campania Sound and Otter Channel. The main CCAA follows the wider western passage through the Kitimat fjord system from Squally Channel through Wright Sound, Douglas Channel and Kitimat Arm. Water exchanged between Kitimat Arm and Campania Sound can also move through the eastern passage of the fjord system via Devastation Channel, Verney Passage (or Ursula Channel and McKay Reach), Wright Sound and Whale Channel. Many inlets and fjords adjoin the Kitimat fjord system, including Gardner Canal, which is by far the largest, and Kildala Arm.

The entrance to the Camaaño Sound-to-Kitimat Arm portion of the CCAA is through Campania Sound for vessels transiting through Caamaño Sound from the south and through Otter Channel for vessels transiting through Principe Channel from the west (see Figure 1-1).

Statistical Summaries

The current statistics are given by depth for the marine terminal. The measurements have been classified as near-surface (5 m), mid-depth (9, 15 and 17 m) and near-bottom (29 m), (depths relative to mean sea level). Maximum speeds were 66 cm/s at the near-surface, reducing to 21 cm/s at the near-bottom (see Table H-2). Comparing these results to those from the measurements at the same depths as reported in Appendix G for the site situated farther from shore between September and January indicates similar statistics. The mean (maximum) current speeds are 8.9 cm/s (49.9 cm/s) and 6.6 cm/s (33.7 cm/s) at 9- and 15-m depths, respectively. In the fall, from September 2005 to January 2006, the mean (maximum) currents were found to be 7.5 cm/s (50.8 cm/s) and 5.3 cm/s (39.9 cm/s). The maximum current speeds are reduced in the January-to-April period, but the mean values are larger. These results do not indicate a seasonal variation in speeds, but the new measurement available at 5-m depth indicates shear in the water column, and the continuation of the progression toward higher speeds as the surface is approached (see Figure H-3). This shear also allows for the possibility of even faster surface currents than estimated for the September 2005 to January 2006 period and a better agreement with the driftpole study presented in Appendix B.

The vector-average magnitude (net flow speed over the measurement period) is typically about 5 cm/s in the near-surface layer, dropping to 1.0 cm/s at the near-bottom. These speeds are substantially larger than the maximum rate of 1.6 cm/s at the near-surface during the Fall 2005. The Winter 2006 flow direction was southward (179^{o} to 184^{o}) at all depths, as also occurred in the fall.

Table H-2 Current Speed Statistics and Vector-Average Currents for the Near-Surface, Mid-Depth and Near-Bottom at Kitimat Arm Site during Winter of 2006

Site	Depth	Speed (cm/s)			Vector-Average		
		Min.	Mean	Max.	Mag.	Dir.	Std. Dev.
1	5	0	10.4	65.7	5.3	183.9	12.3
	9	0	8.9	49.9	3.8	184.3	10.8
	15	0	6.6	33.7	2.6	183.7	7.8
	17	0	5.9	32.0	2.2	183.6	7.0
	29	0	3.3	21.0	1.0	178.6	3.9

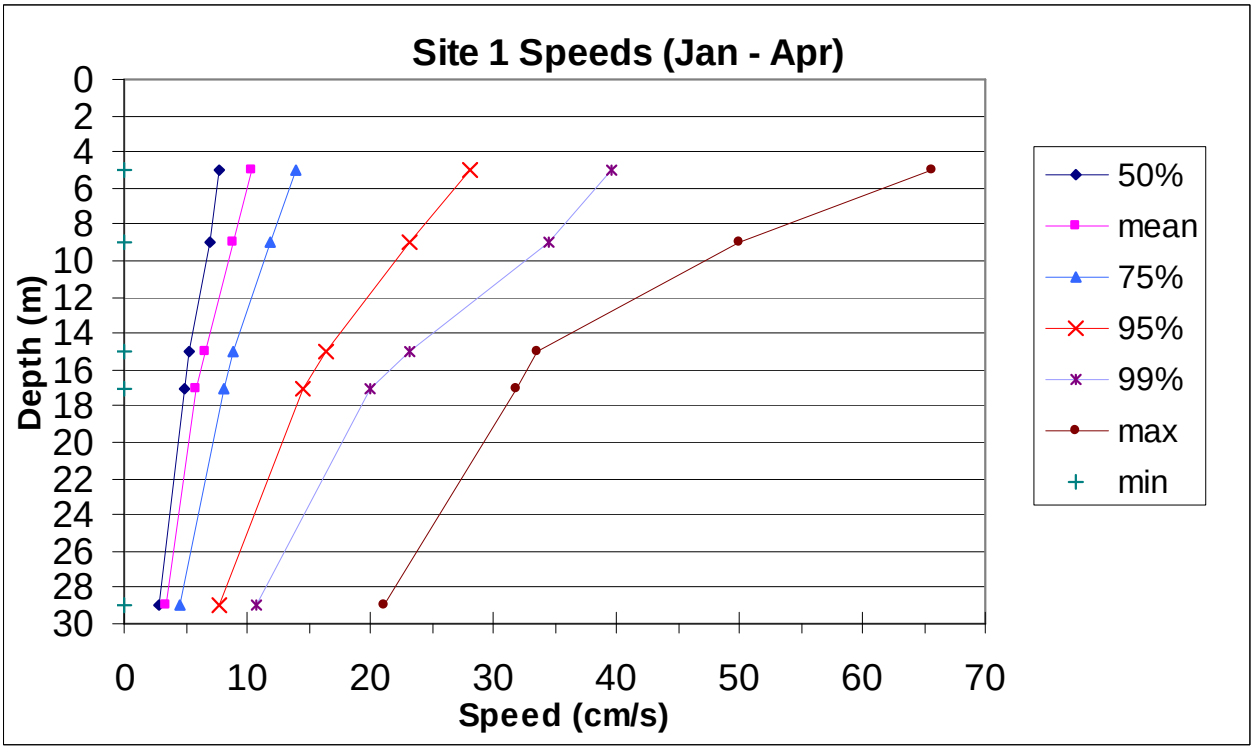

Figure H-3 Current Speed versus Depth for Kitimat Arm Site during Winter of 2006

Distribution of Current Speeds and Directions

Directional distributions of currents are presented as spoke plots in Figure H-4. Each spoke represents the percentage of currents heading toward the indicated direction, and each spoke is segmented according to the speed distribution within that directional segment.

The current direction distribution reflects the along-channel (north-south) flow, with a bias toward down-channel flow. The Fall 2005 measurements (farther from shore in greater water depths) did not show as strong a bias for down-channel flows, and the currents were aligned more NNE-SSW. This alignment is consistent with the rotation in bathymetry shown in Figure H-2 when the currents are moving from the inshore to the offshore measurement site.

a

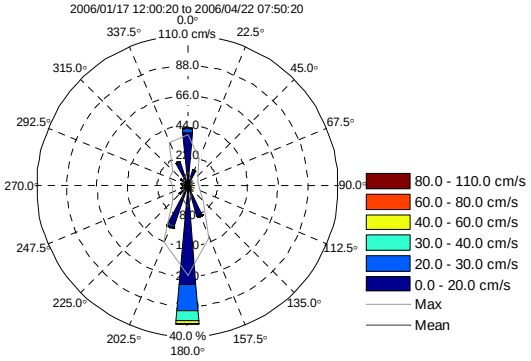

b

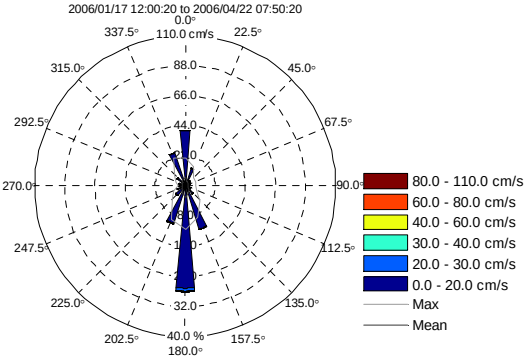

c

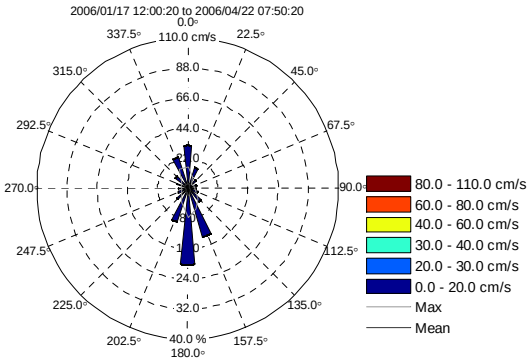

NOTES: (a) 5-m depth (b) 17-m depth and (c) 29-m depth

Figure H-4 Current Speed Direction Joint Frequency Plot at Kitimat Arm Site – Winter of 2006

Variability of Currents by Frequency Band and Tidal Analysis

The distribution of variance in the major current component is examined in this section. The currents were digitally filtered to compute time series for low frequencies (less than 1 cycle per day), high frequencies (greater than 2 cycles per day) and band passed (1 to 2 cycles per day; mainly tidal). The band-passed currents were analyzed by using Foreman's (1978) tidal analysis and prediction programs

and then subtracting the predicted tidal currents from the original band-passed currents to compute the non-tidal mid-band variance. For the energy (variance) distribution for the marine terminal as measured between January and April 2006, see Figure H-5. In the major current component, the detided frequencies dominate at all depths. At the near-surface and mid-depth, the low-frequency contributions, possibly related to the wind, are the second-most dominant frequency band; however, the relative importance drops significantly between the near-surface and mid-depth. Note that the detided variance is considerably larger than the tidally predicted variance. Compared to the distribution obtained from September 2005 to January 2006, the proportion of variance in the tidal frequency band that is tidally predictable drops from January to April. Whether this is due primarily to a change in location or seasonal variation is unclear. The variance distributions in Douglas Channel and Principe Channel (see Appendix B) were found to vary with season. The magnitude of the detided currents indicates that internal tidal activity (which is not simply related to or predicted by the surface tide) is very important at this location.

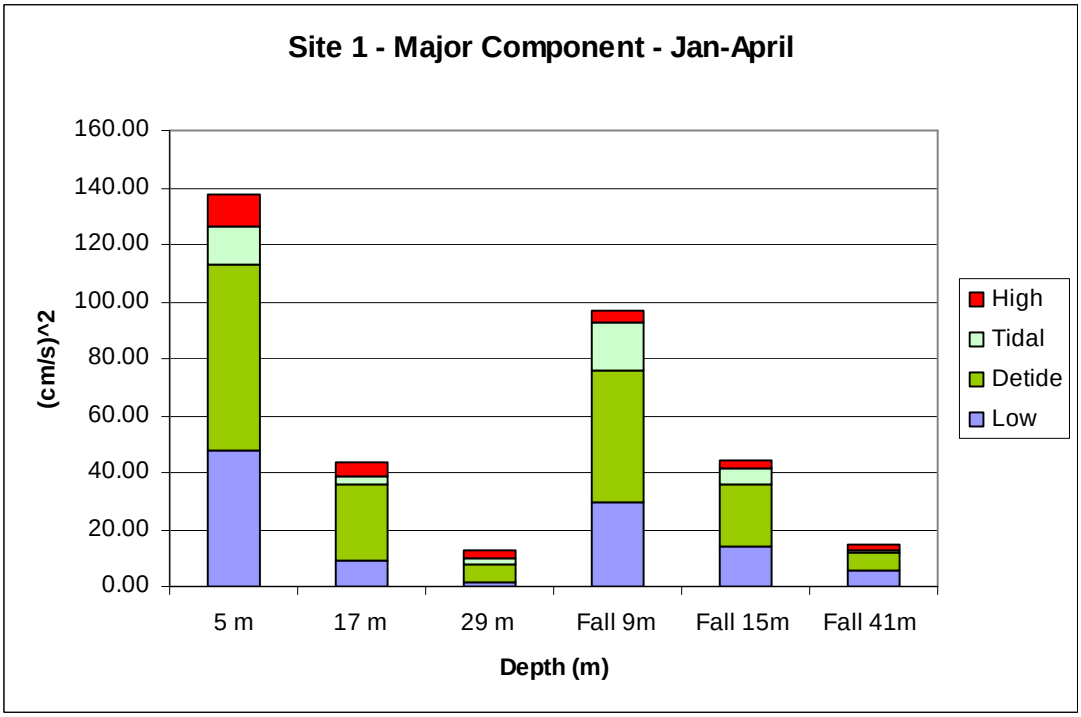

Figure H-5 Variance Distribution between High-Frequency, Astronomical Tides, Detided and Low-Frequency Bins in Kitimat Arm between January and April 2006 and September 2005 and January 2006 (Designated by "Fall")

H.3.1 Response of Currents to Tidal Forcing

Tidal currents driven by astronomical forces are uniform with depth in the absence of friction or other physical mechanisms. In the presence of density gradients within the water column, internal tidal currents can develop. Internal tidal currents are characterized by large depth-dependent variations in the tidal

current amplitudes and phases as well as marked changes in amplitude and phase at a single measurement level. The effect of internal modes of tidal currents can be seen as changes in the fitted tidal constituents as well as significant residual variance or energy in the semi-diurnal to diurnal band-passed currents. As may be seen in the variance distribution plot of Figure H-5 and the discussion above, the detided current variances and changes in tidal current variances indicate that internal tides are important at the marine terminal.

To further examine internal tides, a tabulation of the tidal analysis of the measured current meter data was prepared for the largest tidal constituent (M2) for values of magnitude, phase, sense of rotation and a parameter that will be denoted as R (see Table H-3). The parameter R is the ratio of the magnitude of the minor (cross-channel) to major (along-channel) current components for the M2 tidal current. The amplitude and phase of the M2 tidal constituent exhibits large changes with depth, which may result from excitation of internal tidal modes in the flow field and variations in the currents associated with the river plume.

Table H-3 Summary of the M2 Tidal Current Constituent by Depth in Kitimat Arm between January and April 2006

Site	Time	Depth (m)	M2 Major	M2 Minor	R (min/maj)	Rotation Dir	Phase
Site 1	Jan. – April	5	4.03	0.09	0.02	ccw	271.6
		17	1.06	0.02	0.02	ccw	162.4
		29	1.27	-0.04	-0.03	cw	106.5

H.3.2 Water Levels

For the water-level statistics with respect to mean sea level, see Table H-4. These water-level statistics do not include corrections for variations in atmospheric pressure over the deployment, which tend to be tens of centimetres, up to 30 cm (10% of the measured amplitude) on rare occasions. The tidal ranges at Site 1 in Kitimat Arm are about 6.2 m from maximum to minimum and 4.3 m from the 5% exceedance level to the 95% exceedance level.

Table H-4 Summary of the Water-Level (m) Statistics in Kitimat Arm between January and April 2006

	Min	1%	5%	25%	50%	Mean	75%	99%	Std	Max	Valid	Total
Jan 17 – Apr 22, 2006	-3.32	-2.76	-2.14	-1.04	0.05	0.00	1.05	2.02	1.31	2.90	13,658	13,658

H.3.3 Temperature-Salinity Distributions Derived from CTD Observations in April

Two temperature/salinity profile measurements were made near the marine terminal during the April 2006 recovery and redeployment of the terminal current meter (see Figure H-6). The first profile was made in approximately 26 m of water, and the second profile was made farther from shore in about 150 m of water. The temperature profiles show continuing warming at depth (more than 90 m), warming

followed by cooling at mid-depth (20 to 90 m) and substantial warming at the near-surface from September 2005 through April 2006. At the near-surface level (less than 8 m), the April salinities are less than the January salinities, likely due to earlier synoptic precipitation events. The April salinities are greater than the September salinities, due to a secondary September peak in the annual freshwater discharge. Without the fall 2005 storms acting to mix the fresher surface water, the April salinities are from 10 to 60 m greater than in any of the other measurements. The April densities are greater than the January values at all depths.

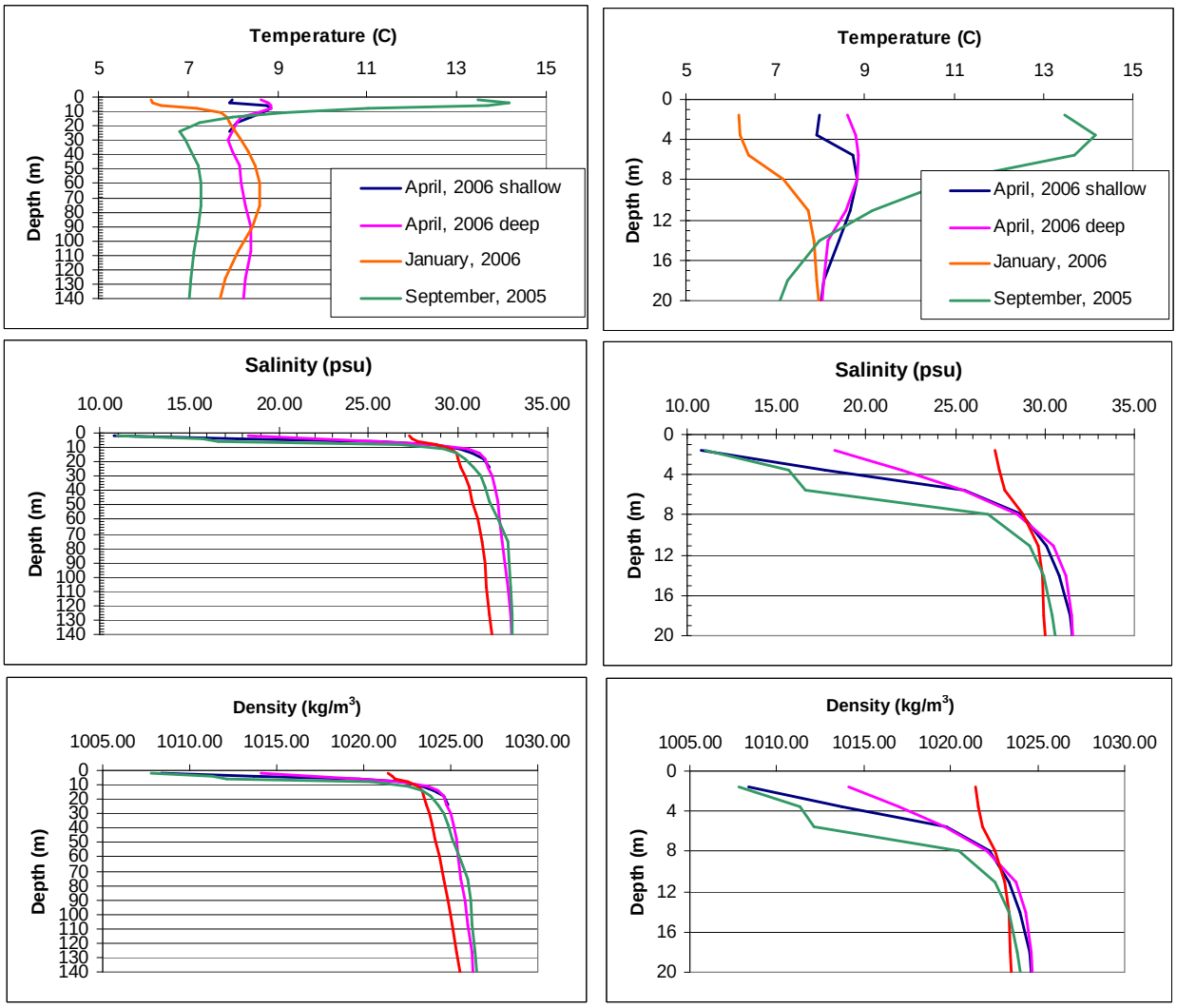

Figure H-6 Temperature, Salinity and Density Profiles at Site 1 in Kitimat Arm on April 22, 2006 over 140-m (Deep) and 20-m (Shallow) Depth Scale

H.3.4 Summary of Key Findings

Measurements were carried out from January to April 2006 at a site closer to shore than the preceding measurements during September 2005 to January 2006. The current speeds were similar in magnitude, while the shallower deployment depth allowed measurements even closer to the surface. The increased proximity to the surface allowed somewhat larger currents to be measured than in the fall. In the fall, the mean (maximum) current speeds were 7.5 cm/s (50.8 cm/s) and 5.3 cm/s (39.9 cm/s) at the near-surface and mid-depth. At the near-shore location, the mean (maximum) were 8.9 cm/s (49.9 cm/s) and 6.6 cm/s (33.7 cm/s) at the near-surface and mid-depth. The largest currents were at 5 m depth where the mean (maximum) speeds were 10.4 cm/s (65.6 cm/s). This measurement was largest likely because it was 4 m closer to the surface than any other previous measurements at this site.

The net flow over the measurement period was about 5 cm/s at the near-surface, decreasing to 1 cm/s at 29 m, with a direction to the south at all depths. These net flow rates are considerably larger than the near-surface flow rates of 1.6 cm/s measured in the fall.

The currents were found to be aligned more along the north-south axis than along the NNE-SSW axis found in the fall. This rotation is consistent with the change in the direction of the bathymetry between the two sites. In Winter 2006, the measurements also indicated a bias toward down-channel flow, which was not observed in the Fall 2005 measurements.

The water levels were found to have a maximum tidal range of 6.2 m, with a range of 4.3 m on the 5% to 95% exceedance level. These values are similar to the values found in the fall where the maximum was 6.2 m (4.3 m, 5% to 95%).

Both freshwater inputs, which cause stratification of the water column, and wind forcing are likely more important than the tidal forcing at in Kitimat Arm. CTD profiles indicate that the near-surface temperatures were intermediate between the warm September values and the cold January values. At mid-depth, between 20 and 90 m, the water is cooler than in January, but below this depth interval the water is warmer than in January.

The near-surface salinities are largest in January 2006, likely due to mixing of the water column, but at depth this mixing has resulted in the least saline measurements. In April 2006, when there has been the least mixing, the 10- to 60-m salinities are the largest measured values. The secondary peak in freshwater discharge during early fall 2005 makes September salinities at the near-surface the lowest measured values. Overall, the density profiles are very similar between measurements.

H.4 References

H.4.1 Literature Cited

Foreman, M.G.G. 1978. *Manual for Tidal Currents Analysis and Prediction.* Pacific Marine Science Report, Vol. 78-6. Department of Fisheries and Oceans. Institute of Ocean Sciences. Sidney, British Columbia.

Macdonald, R.W. 1983. *Proceedings of a Workshop on the Kitimat Marine Environment*. Canadian Technical Report of Hydrography and Ocean Sciences, 18. Department of Fisheries and Oceans. Institute of Ocean Sciences. Sidney, British Columbia.

Attachment H1 Time Series Plots of Ocean Currents

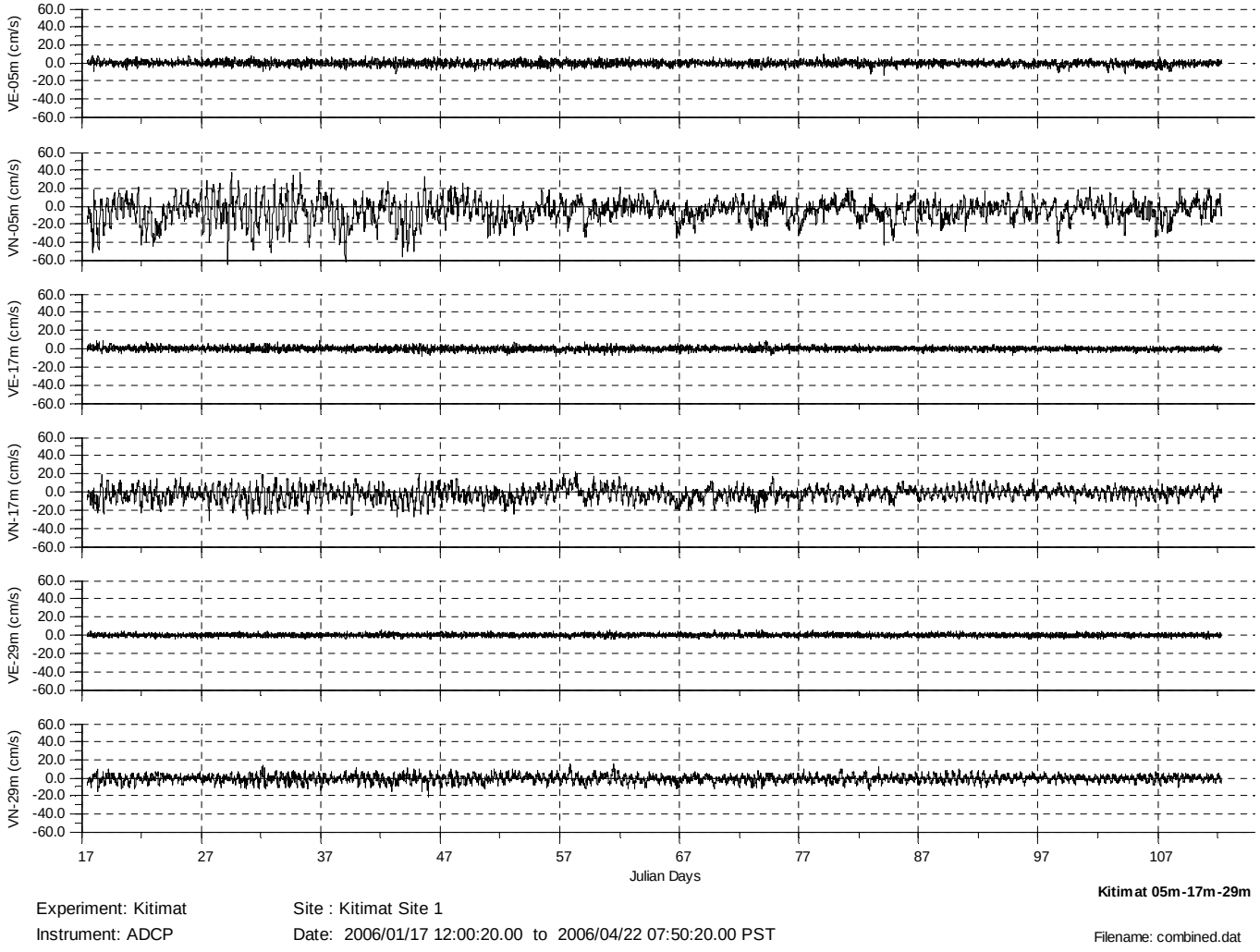
VE-05m (cm/s)
VN-05m (cm/s)
VE-17m (cm/s)
VN-17m (cm/s)
VE-29m (cm/s)
VN-29m (cm/s)
60.0
40.0
20.0
0.0
-20.0
-40.0
-60.0
17
27
37
47
57
67
77
87
97
107
Julian Days
Kitimat 05m-17m-29m
Experiment: Kitimat
Site : Kitimat Site 1
Instrument: ADCP
Date: 2006/01/17 12:00:20.00 to 2006/04/22 07:50:20.00 PST
Filename: combined.dat

Appendix I GEM Oceanography Program, April to December 2006

I.1 Introduction

I.1.1 Objectives

The purpose of this document is to describe baseline conditions with respect to oceanographic measurements taken from April to December 2006 within the CCAA to support the environmental assessment for the Project. Information has been generated and synthesized from an oceanographic study carried out for the Project from April to December 2006. These measurements are a continuation of a program that ran from September 2005 to April 2006. Following the recovery of the data analyzed here, the instrument was redeployed for further measurements. This report presents the results of the measurement program, including:

- subsurface currents
- water levels
- CTD profiles

I.2 Methods

I.2.1 Study Area for Field Surveys

In September 2005, an array of nine current meters was deployed at four locations in the CCAA (see Figure I-1). These instruments were operated until January 2006, at which time eight of the nine instruments were recovered. Temperature and salinity measurements were also made at 15 locations during the deployment and recovery of these instruments. An analysis of these measurements is presented in Appendix G.

One of the current meters was redeployed in near the proposed marine terminal, from January to April 2006 for ongoing data collection (see Appendix H). As part of a one-year study, this mooring was refurbished and redeployed in April 2006. In December 2006, the data was downloaded, and the instrument was once again refurbished. This report presents the analysis results for near-surface, mid-depth and near-bottom currents at this site, as well as temperature and salinity profile measurements made during the recovery on December 13, 2006 using the MV Zodiac Light based in Kitimat.

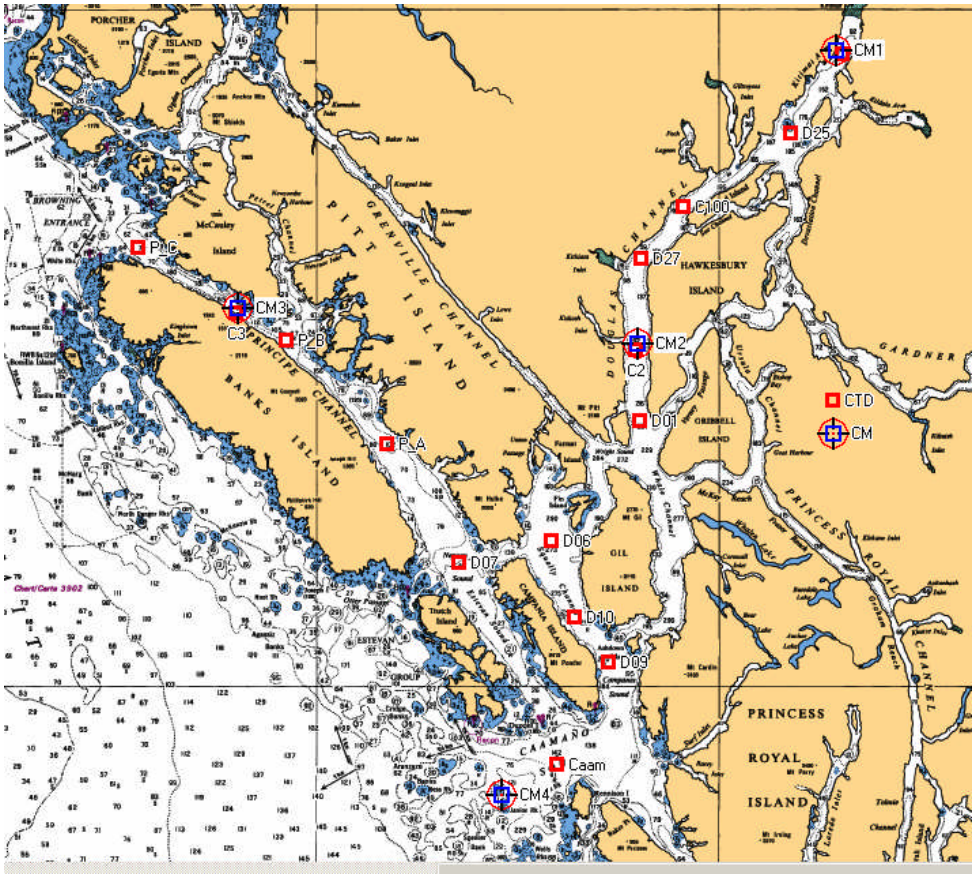

Figure I-1 Locations of Current Meter Measurement Sites from September 2005 to January 2006 (Blue Squares) and CTD (Conductivity, Temperature, Depth) Profiling Sites (Red Squares) of September 2005 and January 2006

I.2.2 Methodology and Instruments

I.2.2.1 Acoustic Doppler Current Meters

One ADCP was deployed (see Table I-1 for the location and time). The location is inshore of the CM1 location shown in overview Figure I-1. The location is also illustrated in the detailed view of Figure I-2, where "Jan" indicates the January to April 2006 site, "Sept" indicates the September 2005 to January 2006 site and "Kit" indicates the historical summer/fall measurement site from 1977. Figure I-3 shows the location of the January to April 2006 measurement sites relative to the marine terminal. The ADCP was a 600-kHz Sentinel Workhorse model manufactured by RD Instruments (see Attachment I1 for specifications). It was deployed on a taut line mooring, and measurements of currents were selected from the near-surface, mid-depth and near-bottom for further analysis. The RDI ADCPs also measure pressure, water temperature and acoustic backscatter return as well as internal parameters. The mooring appeared to be dragged into about 1-m deeper water at the end of May 24.

Table I-1 Location, Deployment Time and Water Depth for the Terminal Current Meter

Site	Area	Deployment Time Date (PDT)	Lat, Long (WGS84)	Water Depth (m)	Recovery Time Date (PDT)	Comments
1	Offshore of Bish Creek Terminal	22 Apr 2006 11:07	53 56.400 128 42.834	41	13 Dec 2006 13:40	RDI ADCP 600kHz: 1 m bins

NOTES:
PDT = Pacific Daylight Time
WGS84 = World Geodetic System 1984

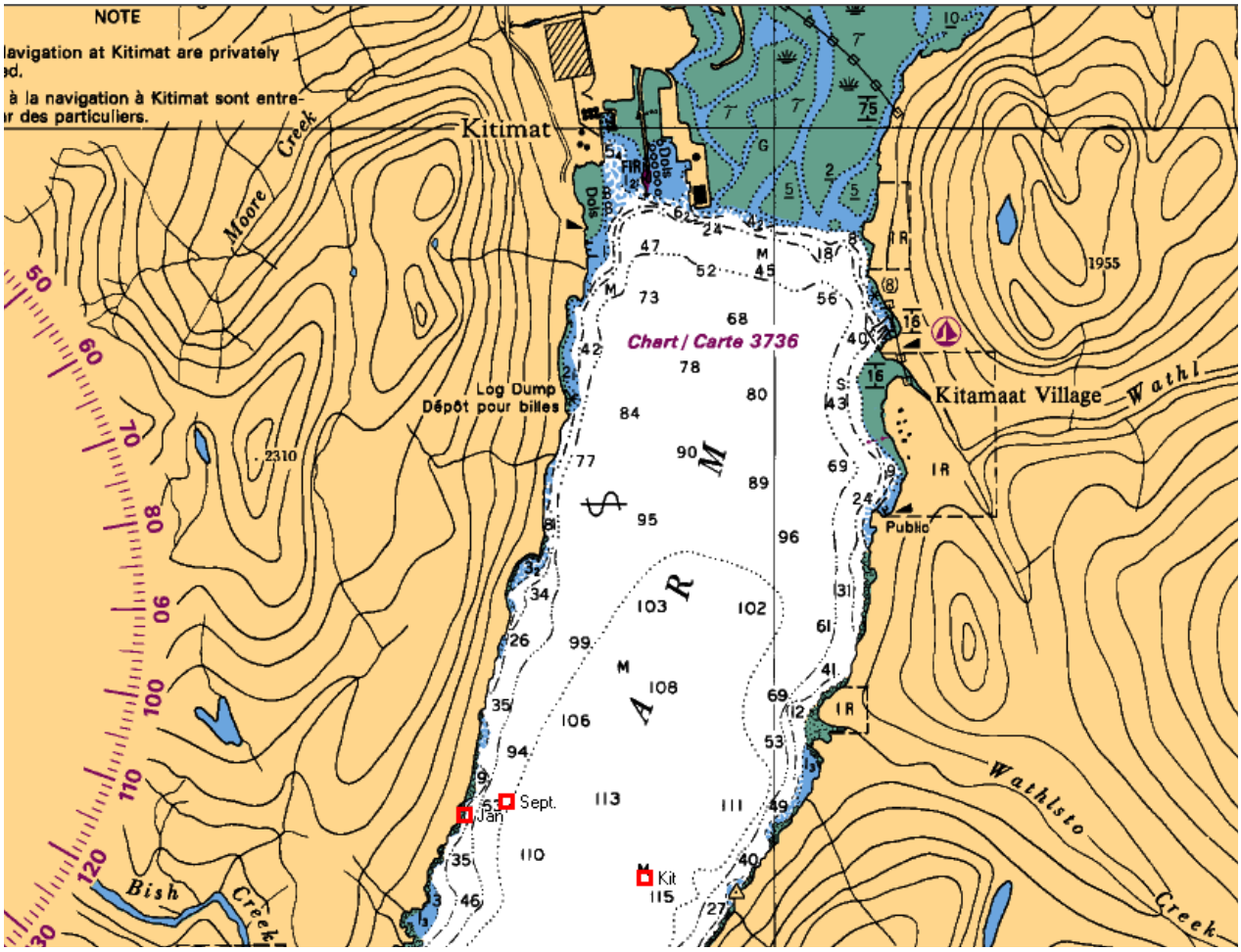

Figure I-2 The Location of the GEM Marine Current Mooring at Site 1

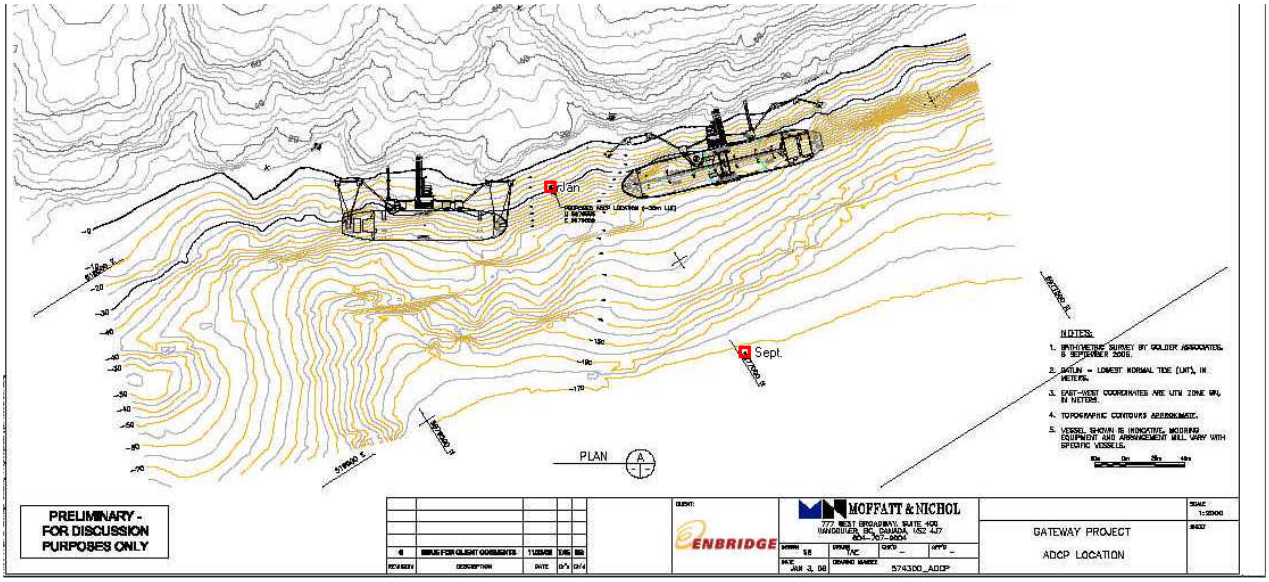

Figure I-3 Location of the September 2005–January 2006 and January–December 2006 Measurements with Respect to the Proposed Marine Terminal

I.2.2.2 CTD Profile Measurements in April 2006

As part of the recovery cruise, CTD profile data were obtained near the current meter location (see Table I-2).

The CTD data were collected during this deployment using an Applied Microsystems STD12+ CTD. The specification sheet for this instrument is given in Attachment I1.

Table I-2 List of CTD Stations Occupied in December 2006

Area	Comments	Time Date (PDT)	Lat, Long (WGS84)	Wire Out (m)	CTD File Name
Terminal Area	Single cast.	13 Dec '06 14:26	53 56.468 128 42.461	33	Site1_Dec2006.dat
NOTES: PDT = Pacific Daylight Time WGS84 = World Geodetic System 1984					

I.3 Results of GEM Marine Data Collection, April to December 2006

I.3.1 Subsurface Current Meter Data Sets

I.3.1.1 Topography and Bathymetry of the CCAA

The CCAA (see Figure I-4) consists of the Kitimat fjord system (Macdonald et al. 1983), Caamaño Sound and Principe Channel. The Kitimat system has four entrances: Grenville Channel to the west and Princess Royal Channel to the east, as well as two entrances on the south, Campania Sound and Otter Channel. Water exchanged between Kitimat Arm and Campania Sound can also move through the eastern passage of the fjord system via Devastation Channel, Verney Passage (or Ursula Channel and McKay Reach), Wright Sound and Whale Channel. There are many adjoining inlets and fjords to the Kitimat fjord system, including Gardner Canal, which is by far the largest, and Kildala Arm. Water depths along the potential project marine corridors are plotted in Figure I-4.

I.3.1.2 Statistical Summaries

The current statistics are given by depth for the marine terminal. The measurements have been classified as near-surface (4 m), mid-depth (22 m) and near-bottom (39 m), where the depths are with respect to mean water level.

Maximum speeds of 66 cm/s were at the near-surface, ramping down to 21 cm/s at the near-bottom (see Table I-3). Comparing these results to those from the measurements at the same depths as reported in Appendix G for the site situated farther from shore between September and January results in similar statistics. The mean (maximum) current speeds are 8.8 cm/s (61.1 cm/s) and 2.8 cm/s (24.8 cm/s) at 4 and 22-m depth, respectively from April to December 2006. The corresponding values from the January to April 2006 measurement period were 10.4 cm/s (65.7 cm/s) and 5.9 cm/s (32.0 cm/s) at 5 and 19-m depth, respectively. In the fall of 2005, from September 2005 to January 2006, the mean (maximum) currents were found to be 7.5 cm/s (50.8 cm/s) and 5.3 cm/s (39.9 cm/s) at 9 and 15-m depth.

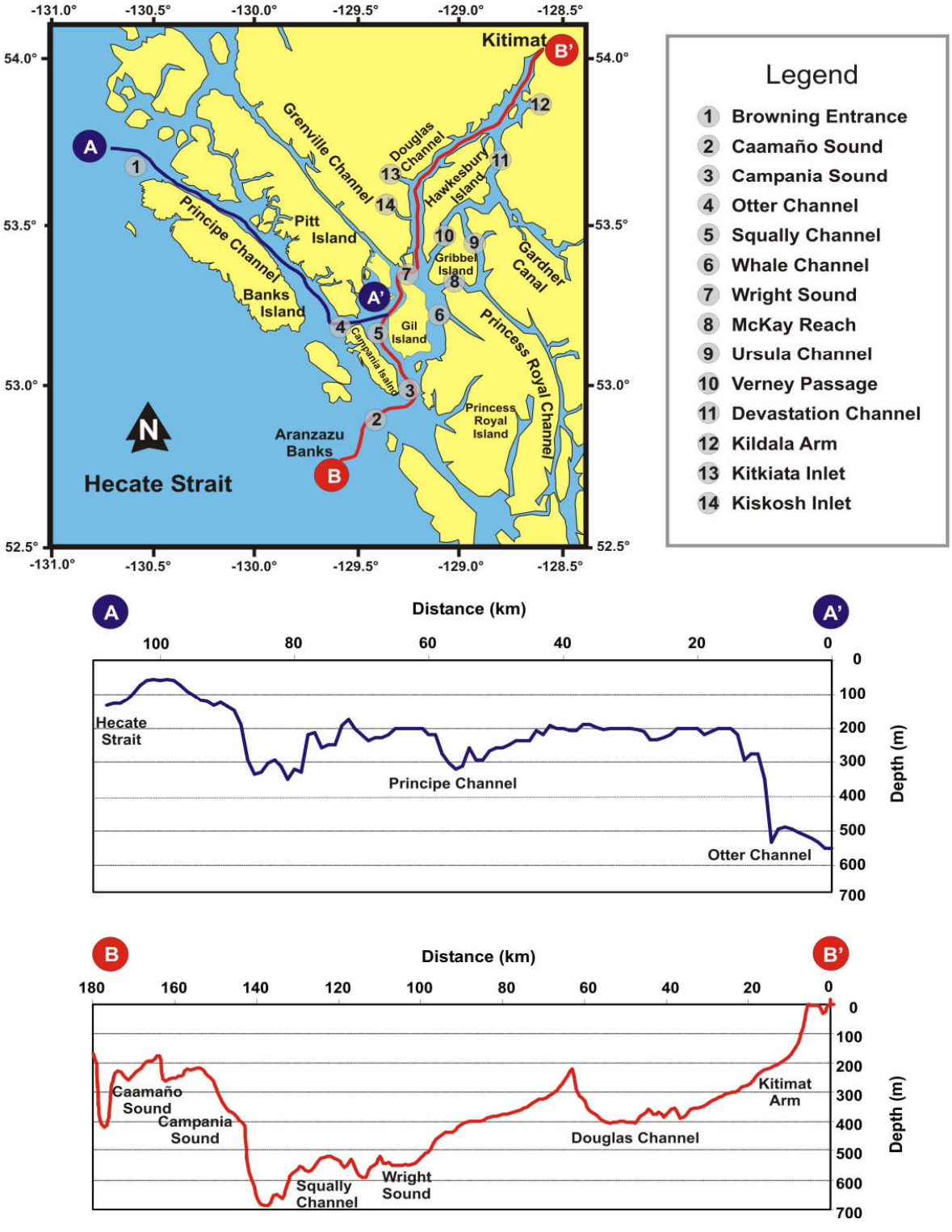

Figure I-4 **The Topography and Bathymetry of the Kitimat Fjord System, Caamaño Sound and Principe Channel.**

Table I-3 Statistics for the Near-Surface, Mid-Depth and Near-Bottom Over the Entire Deployment Period

Depth (m)		Min	1%	5%	25%	50%	Mean	75%	95%	99%	Std	Max	Total
		(cm/s)											
4	Uminor	-13.9	-6.0	-3.7	-1.5	-0.2	-0.3	1.0	3.1	4.8	2.1	17.7	33,856
	Umajor	-61.1	-36.1	-24.0	-9.7	-2.9	-4.2	2.9	11.0	16.2	10.7	31.4	
	Speed	0.0	0.5	1.3	3.5	6.6	8.8	11.7	24.3	36.3	7.6	61.1	
22	Uminor	-9.7	-3.6	-2.5	-1.0	-0.1	-0.2	0.8	2.1	3.1	1.4	7.0	33,856
	Umajor	-24.4	-11.0	-7.1	-2.8	-0.5	-0.5	1.9	5.7	9.3	4.0	22.9	
	Speed	0.0	0.3	0.7	1.6	2.8	3.4	4.5	8.3	12.2	2.5	24.8	
39	Uminor	-6.7	-3.1	-2.1	-0.9	0.0	0.0	0.8	2.0	2.9	1.3	6.1	33,856
	Umajor	-15.4	-5.8	-3.9	-1.7	-0.4	-0.4	1.0	3.1	5.0	2.2	16.8	
	Speed	0.0	0.2	0.5	1.2	1.9	2.2	2.9	4.7	6.6	1.4	17.1	

To better understand the variability over the more than eight months of the deployment, see Tables I-4 to I-6 for the monthly current speed statistics for the near-surface, mid-depth and near-bottom. Overall, there is no trend in the maximum or mean near-surface current speeds, though it peaks around 61 cm/s in August and November. The largest overall current speed was measured in November. There is an overall down channel (seaward) drift at the near-surface, with speeds of 4.4 to 4.5 cm/s until September and then decreasing to 2.3 cm/s in November.

At mid-depth, the mean (maximum) current speed decreases from 3 (14.6) cm/s to 2 (10.3) cm/s from May to June. Starting in August, the mean (maximum) current speeds ramp up again until they reach 4.7 (23.9) cm/s in November. Except for August, there is a small seaward flow at mid-depth.

At near-bottom, the mean current speed is about 2 cm/s, and the maximum current speed is about 8 to 10 cm/s. November is distinct in that the mean (maximum) current speeds go as high as 2.6 (17.1) cm/s. There tends to be a net seaward drift in all months.

The vector average current (net flow considered over the measurement period) was typically about 5 cm/s in the near-surface layer, progressing to 1.0 cm/s at the near-bottom. These speeds were substantially larger than the maximum rate of 1.6 cm/s at the near-surface during the fall. The flow direction was down-inlet (179 to 184 degrees) at all depths, as had also occurred in the fall.

Table I-4 Monthly Statistics for the Near-Surface (4 m)

Month		Min	0.01	0.05	0.25	0.5	Mean	0.75	0.95	0.99	Std	Max	#Pts
						cm/s							
May	Uminor	-12.4	-7.4	-4.9	-2.0	-0.5	-0.7	0.8	2.8	4.4	2.4	9.4	4,464
	Umajor	-49.6	-34.9	-23.5	-9.3	-3.3	-4.7	1.6	9.2	14.5	9.8	23.3	4,464
	Speed	0.0	0.5	1.2	3.1	5.8	8.3	11.2	23.9	35.0	7.4	49.6	4,464
June	Uminor	-8.0	-4.6	-3.0	-1.2	-0.1	-0.1	1.0	2.9	4.6	1.8	11.4	4,320
	Umajor	-45.5	-32.6	-25.0	-10.0	-2.4	-3.9	3.3	11.2	17.7	10.7	31.4	4,320
	Speed	0.0	0.5	1.2	3.4	6.5	8.9	12.0	25.4	32.4	7.5	45.7	4,320
July	Uminor	-8.0	-5.0	-3.5	-1.5	-0.2	-0.2	1.0	3.2	5.2	2.0	11.2	4,464
	Umajor	-50.1	-35.0	-26.0	-11.8	-2.7	-4.4	3.9	12.3	17.8	11.6	30.4	4,464
	Speed	0.0	0.5	1.3	3.9	7.6	9.8	13.8	26.3	35.0	7.9	50.1	4,464
Aug.	Uminor	-9.3	-5.6	-3.6	-1.5	-0.2	-0.2	1.2	3.2	4.8	2.1	7.9	4,464
	Umajor	-60.8	-41.9	-27.1	-11.1	-3.9	-5.5	2.2	10.0	14.1	11.4	20.8	4,464
	Speed	0.1	0.5	1.4	3.8	7.1	9.6	12.5	27.1	41.8	8.5	60.8	4,464
Sept.	Uminor	-13.1	-4.8	-3.2	-1.3	-0.1	-0.1	1.1	3.1	4.6	1.9	10.7	4,320
	Umajor	-46.1	-35.2	-22.4	-9.1	-3.0	-4.4	1.9	8.7	12.8	9.5	16.8	4,320
	Speed	0.1	0.6	1.2	3.1	5.8	7.9	10.2	22.4	35.1	7.0	46.1	4,320
Oct.	Uminor	-8.2	-4.9	-3.2	-1.4	-0.2	-0.2	1.0	2.8	4.3	1.8	9.6	4,464
	Umajor	-40.3	-26.3	-18.7	-8.2	-2.4	-2.9	2.9	10.8	14.9	8.8	19.3	4,464
	Speed	0.1	0.5	1.2	3.2	6.1	7.5	10.3	18.9	26.2	5.7	40.4	4,464
Nov.	Uminor	-11.5	-5.7	-3.7	-1.4	-0.1	-0.1	1.2	3.4	6.2	2.3	17.7	4,320
	Umajor	-61.1	-42.2	-23.4	-7.4	-0.8	-2.3	4.8	13.3	19.6	11.5	27.0	4,320
	Speed	0.0	0.6	1.4	3.6	6.4	8.9	11.5	23.9	42.2	8.1	61.1	4,320

Table I-5 Monthly Statistics for the Mid-Depth (22 m)

Month		Min	0.01	0.05	0.25	0.5	Mean	0.75	0.95	0.99	Std	Max	#Pts
						cm/s							
May	Uminor	-5.9	-3.6	-2.5	-1.2	-0.3	-0.3	0.6	1.9	2.9	1.4	4.6	4,464
	Umajor	-14.2	-10.0	-7.1	-3.3	-0.6	-0.7	2.0	5.4	8.0	3.8	11.7	4,464
	Speed	0.0	0.3	0.7	1.8	3.0	3.4	4.6	8.0	10.4	2.2	14.6	4,464
June	Uminor	-4.7	-3.1	-2.2	-0.9	-0.1	-0.1	0.7	2.0	2.9	1.2	4.3	4,320
	Umajor	-10.3	-6.5	-4.6	-1.9	-0.4	-0.4	1.2	3.6	5.2	2.5	8.4	4,320
	Speed	0.0	0.2	0.5	1.3	2.1	2.4	3.2	5.2	6.7	1.5	10.3	4,320

Table I-5 Monthly Statistics for the Mid-Depth (22 m) (cont'd)

Month		Min	0.01	0.05	0.25	0.5	Mean	0.75	0.95	0.99	Std	Max	#Pts
cm/s													
July	Uminor	-4.9	-3.2	-2.3	-1.0	-0.1	-0.1	0.8	2.0	3.0	1.3	4.8	4,464
	Umajor	-10.0	-6.8	-5.0	-2.3	-0.4	-0.4	1.5	4.3	6.0	2.8	8.8	4,464
	Speed	0.1	0.3	0.6	1.5	2.4	2.7	3.6	5.8	7.3	1.6	10.0	4,464
Aug.	Uminor	-5.1	-3.3	-2.3	-1.0	-0.1	-0.1	0.7	2.0	2.9	1.3	4.7	4,464
	Umajor	-11.1	-6.3	-4.2	-1.6	0.2	0.3	2.1	5.1	7.2	2.9	10.8	4,464
	Speed	0.0	0.3	0.6	1.4	2.3	2.7	3.6	6.0	7.9	1.7	11.1	4,464
Sept.	Uminor	-6.5	-3.4	-2.4	-1.0	-0.1	-0.1	0.7	2.1	3.0	1.3	4.7	4,320
	Umajor	-17.2	-10.0	-6.9	-2.7	-0.4	-0.3	2.2	6.1	8.5	3.9	11.3	4,320
	Speed	0.0	0.3	0.6	1.7	2.9	3.4	4.7	8.1	10.5	2.3	17.5	4,320
Oct.	Uminor	-6.0	-3.6	-2.5	-1.1	-0.1	-0.2	0.8	2.2	3.2	1.4	6.2	4,464
	Umajor	-18.2	-11.5	-7.4	-3.0	-0.5	-0.5	2.2	6.1	8.9	4.1	13.4	4,464
	Speed	0.1	0.3	0.7	1.8	3.0	3.6	4.9	8.4	11.8	2.5	18.5	4,464
Nov.	Uminor	-9.7	-4.6	-3.1	-1.2	-0.1	-0.2	0.9	2.4	3.9	1.7	7.0	4,320
	Umajor	-23.9	-13.2	-9.2	-4.1	-0.9	-0.6	2.5	9.0	15.7	5.6	22.9	4,320
	Speed	0.0	0.4	0.9	2.1	3.8	4.7	6.3	11.7	16.8	3.5	23.9	4,320

Table I-6 Monthly Statistics for the Near-Bottom (39 m)

Month		Min	0.01	0.05	0.25	0.5	Mean	0.75	0.95	0.99	Std	Max	#Pts
cm/s													
May	Uminor	-4.7	-2.9	-2.0	-0.8	0.0	0.0	0.8	1.9	2.7	1.2	4.2	4,464
	Umajor	-9.0	-5.6	-3.7	-1.6	-0.2	-0.2	1.3	3.4	5.1	2.2	8.0	4,464
	Speed	0.0	0.2	0.5	1.2	1.9	2.1	2.8	4.6	6.2	1.3	9.3	4,464
June	Uminor	-5.1	-2.9	-2.0	-0.9	-0.1	-0.1	0.7	1.8	2.7	1.2	4.0	4,320
	Umajor	-7.9	-4.5	-3.3	-1.5	-0.3	-0.3	0.9	2.6	3.9	1.8	7.2	4,320
	Speed	0.0	0.2	0.5	1.1	1.7	1.9	2.5	3.9	5.1	1.1	8.0	4,320
July	Uminor	-4.2	-3.0	-2.1	-0.9	0.0	0.0	0.8	2.1	2.9	1.2	4.7	4,464
	Umajor	-7.6	-4.8	-3.4	-1.5	-0.3	-0.3	1.0	2.8	4.4	1.9	8.8	4,464
	Speed	0.0	0.2	0.5	1.1	1.8	2.0	2.7	4.2	5.3	1.2	9.0	4,464
Aug.	Uminor	-5.7	-3.0	-2.0	-0.8	0.0	0.0	0.8	2.0	2.9	1.2	4.6	4,464
	Umajor	-6.9	-4.8	-3.4	-1.6	-0.4	-0.4	0.8	2.8	4.2	1.9	7.2	4,464
	Speed	0.0	0.2	0.5	1.1	1.8	2.0	2.6	4.1	5.3	1.1	7.2	4,464

Table I-6 Monthly Statistics for the Near-Bottom (39 m) (cont'd)

Month		Min	0.01	0.05	0.25	0.5	Mean	0.75	0.95	0.99	Std	Max	#Pts
cm/s													
Sept.	Uminor	-5.0	-3.1	-2.3	-0.9	0.0	0.0	0.9	2.1	3.0	1.3	5.1	4,320
	Umajor	-9.0	-5.6	-4.0	-1.9	-0.6	-0.6	0.8	3.0	4.6	2.1	8.0	4,320
	Speed	0.0	0.2	0.5	1.3	2.0	2.2	2.9	4.7	6.4	1.3	9.1	4,320
Oct.	Uminor	-4.6	-3.3	-2.3	-0.9	-0.1	-0.1	0.8	2.2	3.1	1.3	4.6	4,464
	Umajor	-10.5	-5.9	-3.8	-1.7	-0.3	-0.2	1.2	3.5	5.4	2.3	9.7	4,464
	Speed	0.0	0.2	0.5	1.3	2.0	2.3	3.0	4.8	6.8	1.4	10.8	4,464
Nov.	Uminor	-6.7	-3.5	-2.3	-1.0	-0.1	-0.1	0.8	2.2	3.1	1.4	6.1	4,320
	Umajor	-10.6	-7.7	-5.0	-2.0	-0.5	-0.5	1.1	3.8	7.1	2.8	16.8	4,320
	Speed	0.0	0.3	0.5	1.3	2.1	2.6	3.3	6.0	8.9	1.8	17.1	4,320

I.3.2 Water Levels

Table I-7 shows the water-level statistics with respect to mean sea level. To account for the dragging of the mooring into deeper water at the end of May 24, this data was offset by 0.9 m before demeaning the water levels. These water-level statistics do not include corrections for variations in atmospheric pressure over the deployment, which are typically equivalent to several cm of water-level variation, up to 30 cm (10% of the measured amplitude) on rare occasions. The tidal ranges at Site 1 in Kitimat Arm are about 6.3 m from maximum to minimum and 4.2 m from the 5% exceedance level to the 95% exceedance level.

Table I-7 Summary of the Water-Level Statistics between April and December 2006

	Min	1%	5%	25%	50%	Mean	75%	95%	99%	Std	Max	Total
m												
Water Level	-3.11	-2.72	-2.19	-1.01	0.03	0.00	1.06	2.02	2.61	1.32	3.19	33,855

I.3.3 Temperature-Salinity Distributions Derived from CTD Observations in December 2006

One temperature/salinity profile measurement was made in the vicinity of the marine terminal during the December 2006 recovery and redeployment of the terminal current meter (see Figure I-5). The near-surface salinities are the second-highest after the January 2006 measurements, as are the densities.

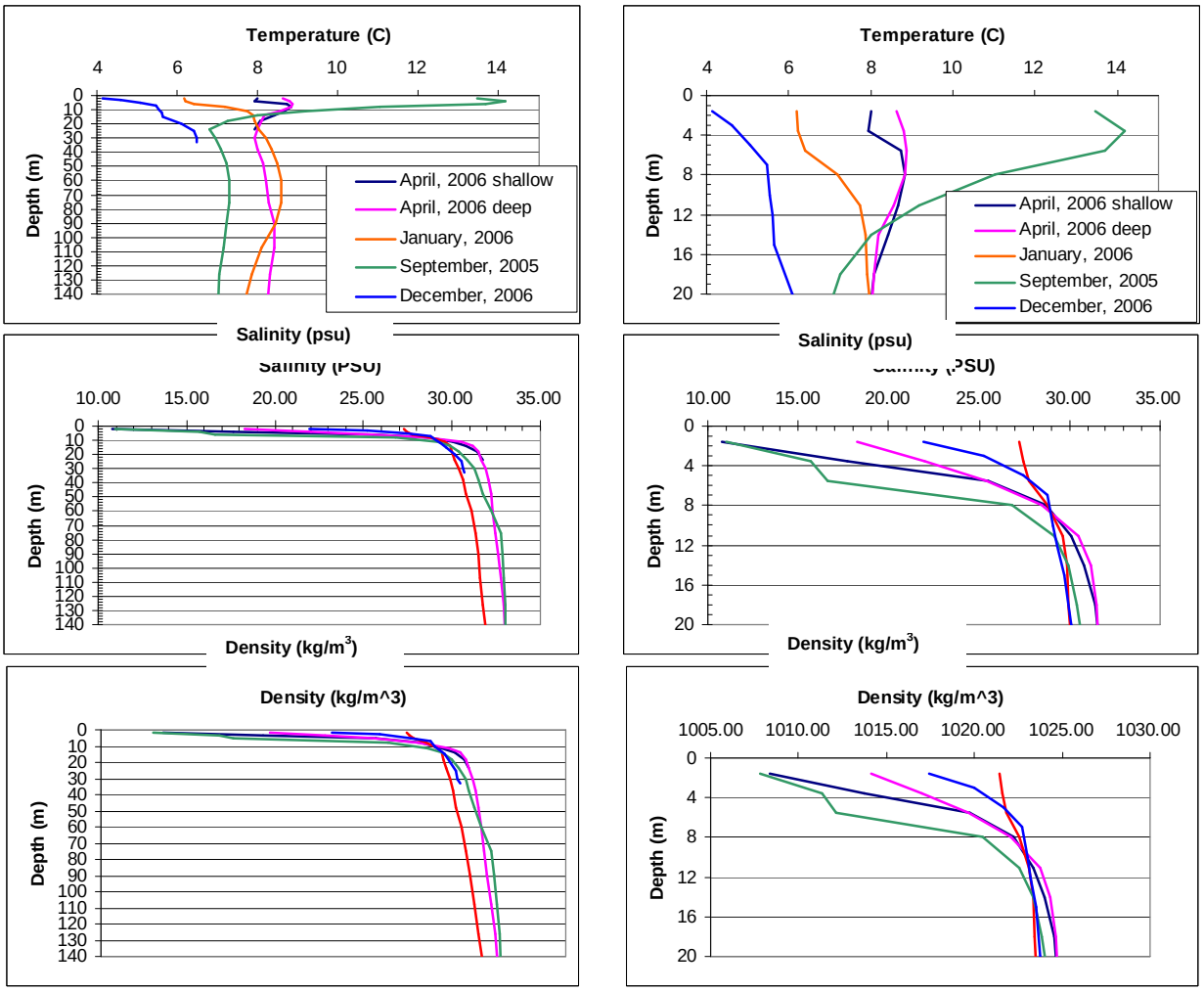

Figure I-5 Temperature, Salinity and Density Profiles at Site 1 in Kitimat Arm

I.3.4 Summary of Key Findings

Ocean current measurements were carried out from April to December 2006 as a continuation of measurements from January to April 2006 in the vicinity of the proposed marine terminal. Previously, measurements from September 2005 to January 2006 were made at a nearby site in deeper waters. The maximum current speeds of 61.6 cm/s were measured in November 2006. Net seaward drift was measured at all depths during the deployment. Mean current speeds varied from 9 cm/s at the near-surface to 2 cm/s at the near-bottom.

The CTD profile indicated the coldest water-column measurements to date in the program. The near-surface salinity and density profiles were the second-highest after the January measurements.

The measured water levels' range is about 6.3 m from maximum to minimum and 4.2 m from the 5% exceedance level to the 95% exceedance level.

I.4 References

I.4.1 Literature Cited

Macdonald, R.W. 1983. *Proceedings of a Workshop on the Kitimat Marine Environment*. Canadian Technical Report of Hydrography and Ocean Sciences, 18, Department of Fisheries and Oceans. Institute of Ocean Sciences, Sidney, British Columbia.

Attachment I1 Specifications of Oceanographic Instruments Used in This Study

600 kHz SENTINEL WORKHORSE

Principles of Operation:

Acoustic pulses are transmitted along four beams. Echoes are returned by scatterers in the water column. The frequency shift of each echo is directly proportional to the component of flow along the beam axis. This is the Doppler Effect. Horizontal and vertical flow components are then computed from the axial velocities. Echo returns are time gated to allow flow resolution into vertical bins (in this case 1.0 m). Flow homogeneity over the four-beam footprint is assumed. Due to side lobe returns, data are usually not available within 6% (20° beam angle) of the vertical distance to strong reflectors, such as the ocean surface or sea bottom. The ADCP was upgraded to include a pressure sensor and includes the WAVES upgrade.

Internal Sensors	Accuracy	Resolution
Heading	±1°	±0.2°
Tilt (max. 20□)	±2°	±0.01°
Temperature	±0.4°	±0.01°

Power Specification: Internal: 48VDC battery pack (expandable w/ external battery pack)

External: 20-60 VDC

Dimensions: 22.8 cm by 36.1 cm

Weight: 13 kg in air; 4.5 kg in water (with battery pack)

Beam Angle: 20°

Maximum Range: Water velocity profile to 47 m (nominal at 2-m bin size)

Accuracy: Water velocity accuracy is 1 cm/sec, based on the sampling parameters chosen (2-m bins, 10 pings per ensemble).

Memory: Expanded to 896 MB

ASL Environmental Sciences Inc

05/03/04

Applied Microsystems

STD12+ CTD

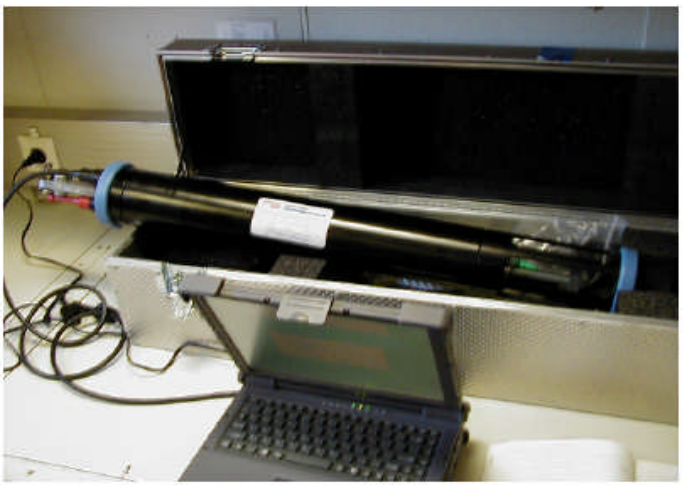

Sensor		Response	Accuracy	Resolution
Temperature °C	Thermistor	85ms	± 0.005°C	0.001 °C
Conductivity S/m	Four electrode glass cell	5 to 25 ms	±0.001 S/m	0.0003S/m
Pressure dbar (1000 m)	Strain gauge	10ms	± 1.5 dbar	0.05 dbar

Sampling rate: up to 11 scans per second; or by time/pressure increment

Memory: 128 MB RAM

Batteries: Nine Alkaline D-cells

Weight: 9.0 kg in air; 3.5kg in water

Dimensions: 675mm by 102mm

Manufacturer: **Applied Microsystems Ltd.**
2071 Malaview Ave.W. Sidney, BC, Canada V8L 5X6
Contact: Tel:+1-250-656-0771 Fax:+1-250-655-3655
sales@AppliedMicrosystems.com

ASL Environmental Sciences Equipment Leasing
1986 Mills Rd, Sidney BC Canada V8L 5Y3 Phone 250-656-0177 Fax 250-656-2162
Contact Rick Birch rbirch@aslenv.com or denglish@aslenv.com

Appendix J GEM Oceanography Program, December 2006 to July 2007

J.1 Introduction

J.1.1 Objectives

The purpose of this document is to describe baseline conditions with respect to oceanographic measurements taken from December 2006 to July 2007 within the CCAA to support the environmental assessment for the Project. Information has been generated and synthesized from an oceanographic study carried out for the Project from December 2006 to July 2007. These measurements are a continuation of a program that ran from September 2005 to December 2006. This appendix presents the results of the most recent measurement program, including:

- subsurface currents
- water levels
- CTD profiles

J.2 Methods

J.2.1 Study Area for Field Surveys

In September 2005, an array of nine current meters was deployed at four locations in the CCAA (see Figure J-1). These instruments were operated until January 2006, at which time eight of the nine instruments were recovered. Temperature and salinity measurements were also made at 15 locations during the deployment and recovery of these instruments. An analysis of these measurements is presented in Appendix G.

One of the current meters was redeployed in near the proposed marine terminal, from January to April 2006 for ongoing data collection (see Appendix H). As part of an extended study, this mooring was refurbished and redeployed in April 2006. In December 2006, the data were downloaded and analyzed, and the instrument was once again refurbished (see Appendix I). Further measurements were made near the proposed marine terminal from December 2006 to July 2007. This report presents the analysis results for near-surface, mid-depth and near-bottom currents at this site, as well as temperature and salinity profile measurements made during the recovery on July 10, 2007 using the MV Zodiac Light based in Kitimat.

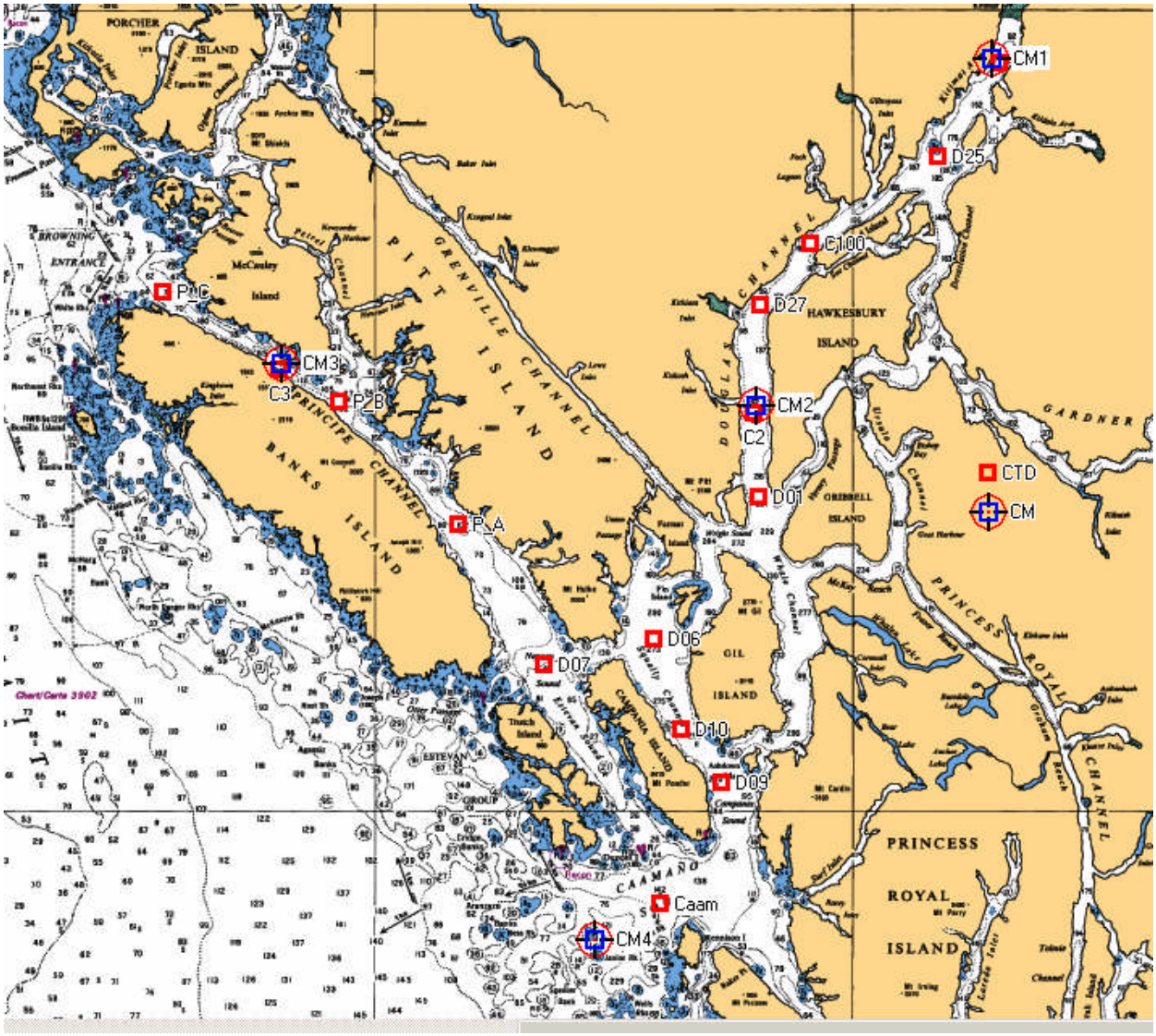

Figure J-1 **Locations of Current Meter Measurement Sites from September 2005 to January 2006 (Blue Squares) and CTD (Red Squares)**

J.2.2 Methodology and Instruments

Acoustic Doppler Current Meters

One ADCP was deployed (see Table J-1 for the location and time). Due to boat drift during the deployment, the location is inshore of the CM1 location shown in Figure J-1. The location is also illustrated in the detailed view of Figure J-2, where "CM1A" indicates the January to April 2006 site, "CM1B" indicates the September 2005 to January 2006 site and "Kit" indicates the historical summer/fall measurement site from 1977.

For the location of the January to April 2006 measurement sites relative to the marine terminal, see Figure J-3. The ADCP was a 600-kHz Sentinel Workhorse model manufactured by RD Instruments (see Attachment J1 for specifications). It was deployed on a taut line mooring, and measurements of currents were selected from the near-surface, mid-depth and near-bottom for further analysis. The RDI ADCPs also measure pressure, water temperature and acoustic backscatter return as well as internal parameters.

Table J-1 Location, Deployment Time and Water Depth for the Terminal Current Meter

Site	Area	Deployment Time Date (PST)	Nominal Lat, Long (WGS84)	Water Depth (m)	Recovery Time Date (PDT)	Comments
1	Offshore of Bish Creek Terminal	13 Dec. 2006 14:00	53 56.400 128 42.834	26	10 Jul, 2007 11:13	RDI ADCP 600kHz: 1 m bins

NOTES:
PDT = Pacific Daylight Time
WGS84 = World Geodetic System 1984

CTD Profile Measurements in July 2007

As part of the recovery cruise, CTD (Conductivity–Temperature–Depth) profile data was obtained near the current meter location (see Table J-2). The CTD data collected during this deployment were collected using an RBR CTD. For the specification sheet for this instrument, see Attachment J1.

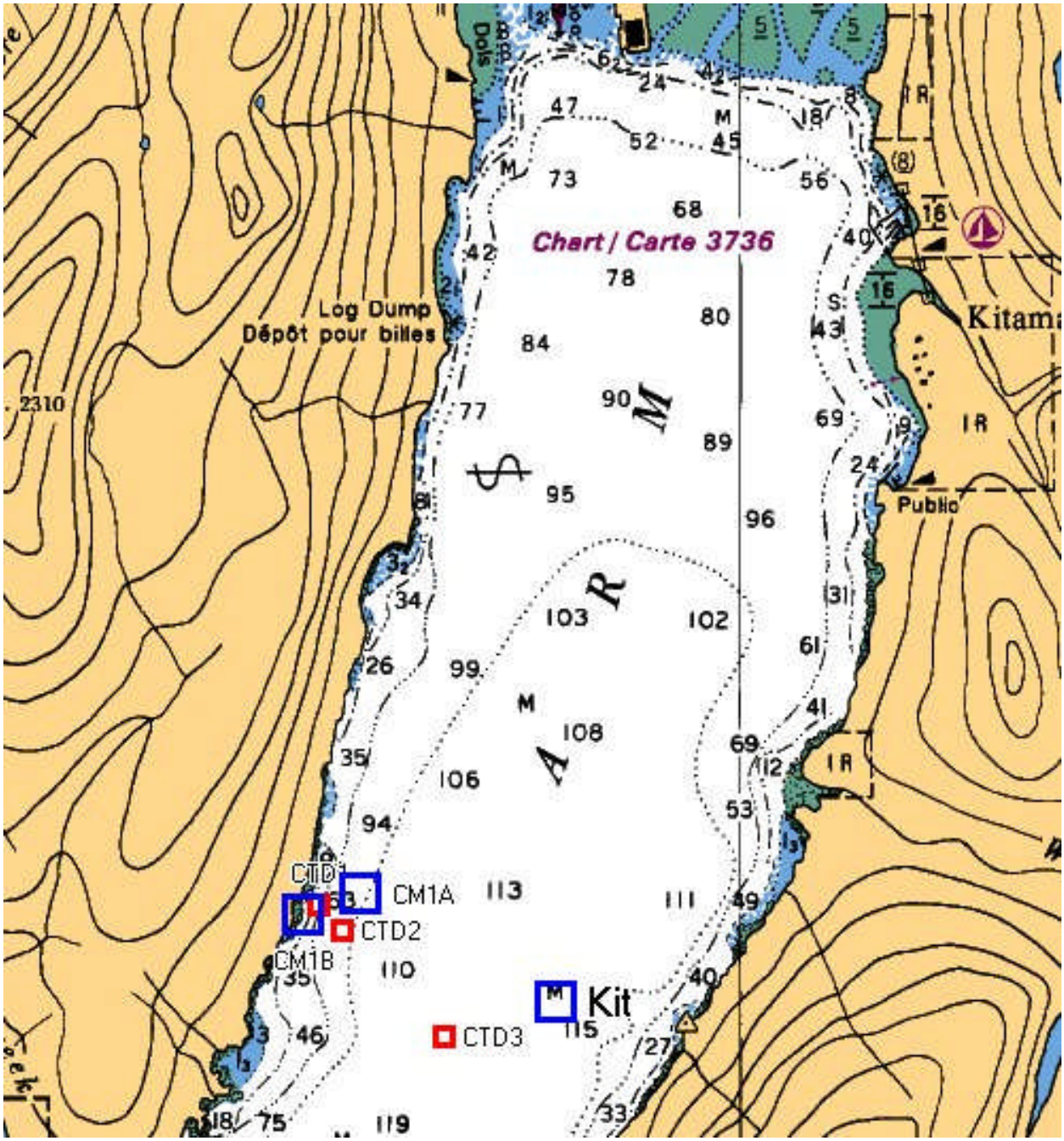

NOTE: The December 2006 to July 2007 deployment was inshore of CM1B. Also shown is the location of a current meter mooring "Kit" operated in this area in the summer and fall of 1977. The locations of the 3 CTD casts are shown using red squares.

Figure J-2 Location of the GEM Marine Current Mooring at Site 1 from September to January ("CM1A") and from January to December 2006 ("CM1B") in Kitimat Arm

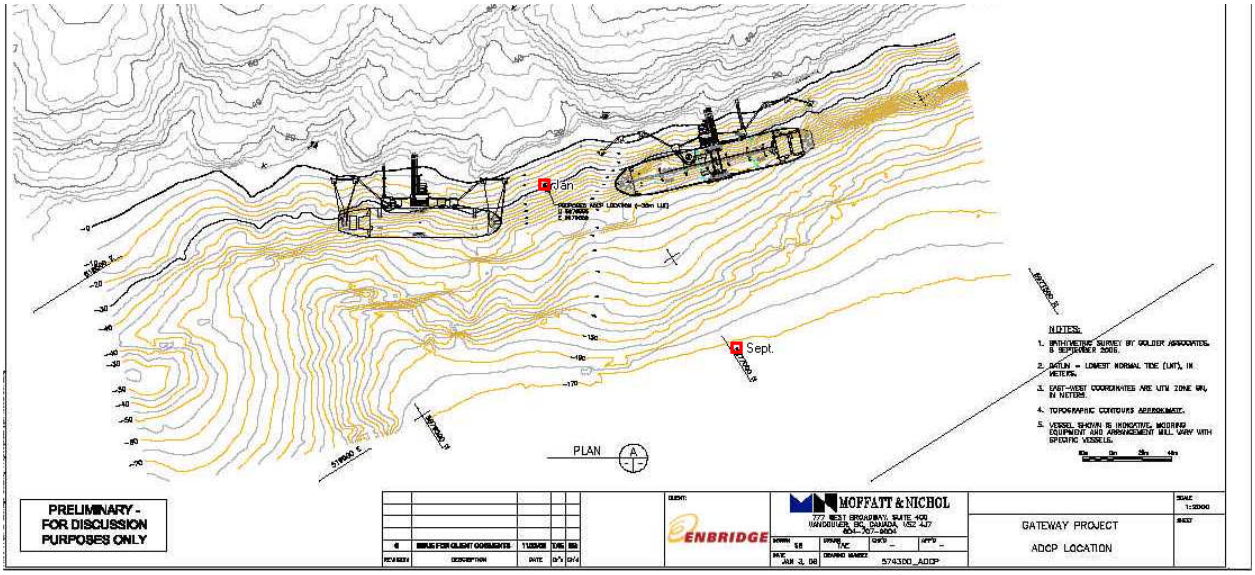

NOTE: The December 2006 to July 2007 measurements are located inshore of the January - December 2006 measurements

Figure J-3 Location of the September 2005 – January 2006 and January - December 2006 Measurements with Respect to the Proposed Marine Terminal

Table J-2 List of CTD Stations Occupied in July 2007

Area	Comments	Time Date (PDT)	Lat, Long (WGS84)
Terminal Area	Near-mooring	10 Jul, 2007 12:52	53° 56.430' N 128° 42.713' W
Terminal Area	Midway shore to mid-channel	10 Jul, 2007 13:02	53° 56.338' N 128° 42.593' W
Terminal Area	Mid-channel	10 Jul, 2007 13:15	53° 55.950'N 128° 41.946'W

NOTES:
PDT = Pacific Daylight Time
WGS84 = World Geodetic System 1984

J.3 Results of GEM Marine Data Collection, December 2006 to July 2007

J.3.1 Subsurface Current Meter Data Sets

Topography and Bathymetry of the CCAA

The CCAA (see Figure 1-1) consists of the Kitimat fjord system (Macdonald et al. 1983), Caamaño Sound and Principe Channel. The Kitimat system has four entrances: Grenville Channel to the west and Princess Royal Channel to the east, as well as two entrances on the south, Campania Sound and Otter Channel. The inner part of the CCAA follows the wider western passage through the Kitimat fjord system from Squally Channel through Wright Sound, Douglas Channel and Kitimat Arm. Water exchanged between Kitimat Arm and Campania Sound can also move through the eastern passage of the fjord system via Devastation Channel, Verney Passage (or Ursula Channel and McKay Reach), Wright Sound and Whale Channel. There are many adjoining inlets and fjords to the Kitimat fjord system, including Gardner Canal, which is by far the largest, and Kildala Arm. Water depths are plotted in Figure J-4.

Statistical Summaries

The current statistics are given by depth for the marine terminal. The measurements have been classified as near-surface (3 m), mid-depth (14 m) and near-bottom (24 m), where the depths are with respect to mean water level. (The current statistics are given at each depth for the speed, the component parallel to the shore, U_{major}, and the component perpendicular to the shore, U_{minor}.) The nominal location had been started during the deployment in December, but comparing the deepest measurement of 24 m in this deployment with the 39-m depth in the previous deployment, it was apparent that the boat had drifted inshore during deployment.

Table J-3 shows maximum (mean) speeds of 81.6 (14.2) cm/s at the near-surface, ramping down to 24.6 (3.7) cm/s at the near-bottom (24 m depth). The near-surface maximum (mean) is much larger than in the previous deployment in this area, but the 22–24 m depth current speeds are similar.

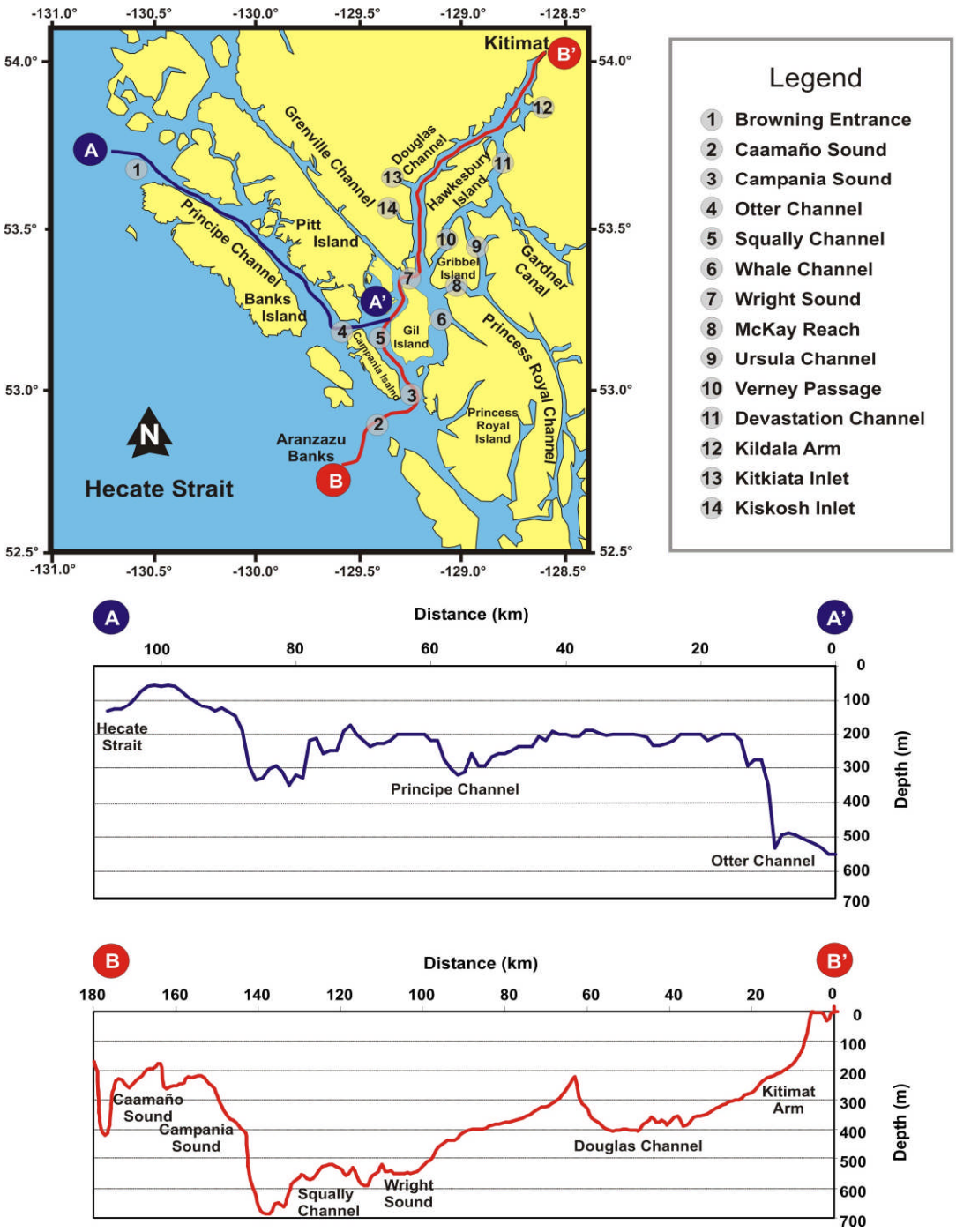

NOTE: Also shown are the water depths along two of the project marine corridors (A-A') from Browning Entrance in Hecate Strait through to Otter Channel and (B-B') from Caamaño Sound to Kitimat Arm.

Figure J-4 Topography and Bathymetry of the Kitimat Fjord System, Caamaño Sound and Principe Channel

Table J-3 Statistics for the Near-surface, Mid-depth and Near-bottom over the Entire Deployment Period

Depth (m)		Min	1%	5%	25%	50%	Mean	75%	95%	99%	Std	Max	Total
		(cm/s)											
3	U_{minor}	-16.9	-5.5	-3.5	-1.3	0.0	0.0	1.3	3.5	5.4	2.2	12.4	30,079
	U_{major}	-81.4	-48.7	-35.1	-17.4	-6.1	-6.9	4.3	18.9	26.9	16.4	45.8	
	Speed	0.0	0.7	1.8	5.7	11.7	14.2	20.0	35.6	48.8	10.9	81.6	
14	U_{minor}	-10.4	-3.7	-2.4	-0.9	0.0	0.1	1.0	2.6	3.9	1.6	10.3	30,079
	U_{major}	-36.0	-21.5	-14.7	-5.9	-1.4	-1.9	2.7	9.2	14.3	7.2	30.2	
	Speed	0.0	0.4	0.9	2.5	4.6	5.9	8.0	15.6	21.9	4.7	36.4	
24	U_{minor}	-6.9	-2.8	-1.9	-0.7	0.1	0.1	0.9	2.2	3.1	1.2	7.3	30,079
	U_{major}	-24.3	-12.2	-8.4	-3.8	-1.1	-1.3	1.4	5.3	8.2	4.1	16.6	
	Speed	0.0	0.3	0.7	1.7	3.0	3.7	4.9	8.9	12.4	2.7	24.6	
SOURCE: Statistics for December 13, 2006–July 10, 2007													

Previously, the maximum (mean) current speeds were 61.1 (8.9) cm/s and 24.8 (2.8) cm/s at 4 and 22-m depth, respectively, from April to December 2006. The corresponding values from the January to April 2006 measurement period were 65.7 (10.4) cm/s and 32.0 (5.9) cm/s at 5 and 19-m depth, respectively. In the fall of 2005, from September 2005 to January 2006, the maximum (mean) currents were found to be 50.8 (7.5) cm/s and 39.9 (5.3) cm/s at 9 and 15-m depth. The 14-m depth currents during this deployment had maximum (mean) current speeds of 36.4 (5.9) cm/s.

To better understand the variability over the seven months of the deployment, monthly current speed statistics are presented in Table J-4 through Table J-6 for the near-surface, mid-depth and near-bottom. Overall, there is no trend in the maximum or mean near-surface current speeds, though it peaks around 81 cm/s in January and then again in March. The largest overall current speed was measured in January. There is an overall down-channel (seaward) drift at all depths, with speeds of 5 to 8 cm/s at the near-surface and 1 to 3 cm/s at the other depths. The mean current speeds tend to ramp down from January through June at the mid- and near-bottom levels, but there is no clear trend at the near-surface.

Table J-4 Monthly Statistics for the Near-surface (3 m)

Depth (m)	Month		Min	0.01	0.05	0.25	0.5	Mean	0.75	0.95	0.99	Std	Max	#Pts
			cm/s											
3	Jan	U_{minor}	-10.8	-5.7	-3.8	-1.4	0.0	0.0	1.4	3.9	5.7	2.3	9.0	4,464
		U_{major}	-81.4	-53.4	-40.8	-18.5	-5.6	-6.1	7.6	24.1	31.6	19.2	39.6	
		Speed	0.0	0.9	2.0	6.8	14.1	16.3	22.6	40.8	53.4	12.0	81.6	
	Feb	U_{minor}	-13.7	-5.6	-3.8	-1.6	-0.1	-0.1	1.2	3.5	5.4	2.2	9.7	4,032
		U_{major}	-67.6	-47.1	-34.9	-16.0	-6.3	-7.4	2.1	15.5	23.5	14.7	32.9	
		Speed	0.1	0.7	1.6	5.0	10.2	12.9	17.6	35.0	47.0	10.5	67.7	

Table J-4 Monthly Statistics for the Near-surface (3 m) (cont'd)

Depth (m)	Month		Min	0.01	0.05	0.25	0.5	Mean	0.75	0.95	0.99	Std	Max	#Pts
			cm/s											
3 (cont'd)	Mar	U_{minor}	-12.3	-6.2	-4.1	-1.7	-0.2	-0.2	1.3	3.7	5.8	2.4	12.4	4,464
		U_{major}	-80.7	-51.1	-38.6	-21.7	-9.5	-8.1	7.0	22.4	30.8	19.1	45.8	
		Speed	0.2	0.9	2.4	8.7	15.9	17.4	23.9	39.0	50.7	11.6	80.7	
	Apr	U_{minor}	-16.4	-5.5	-3.4	-1.2	0.0	0.0	1.3	3.4	4.8	2.1	8.7	4,320
		U_{major}	-63.2	-44.8	-30.8	-13.8	-4.9	-5.5	4.4	16.5	23.4	14.2	31.7	
		Speed	0.1	0.7	1.7	5.1	10.0	12.1	16.3	30.9	44.5	9.5	63.2	
	May	U_{minor}	-16.9	-5.4	-3.2	-1.1	0.0	-0.1	1.1	3.0	4.8	2.0	10.5	4,464
		U_{major}	-69.3	-46.9	-33.9	-15.8	-4.9	-7.1	2.9	13.9	20.0	14.4	25.1	
		Speed	0.0	0.5	1.4	4.2	9.0	12.2	17.5	33.9	46.9	10.6	69.4	
	Jun	U_{minor}	-7.8	-3.9	-2.5	-0.8	0.3	0.4	1.4	3.4	4.8	1.8	9.6	4,320
		U_{major}	-54.6	-40.8	-30.3	-18.9	-7.4	-7.1	4.8	16.6	22.9	14.9	30.2	
		Speed	0.1	0.7	2.0	6.4	12.4	13.8	20.0	30.3	40.8	9.2	54.7	

Table J-5 Monthly Statistics for the Mid-depth (14 m)

Depth (m)	Month		Min	0.01	0.05	0.25	0.5	Mean	0.75	0.95	0.99	Std	Max	#Pts
			cm/s											
14	Jan	U_{minor}	-7.9	-4.1	-2.6	-0.9	0.1	0.1	1.1	2.7	4.0	1.6	7.7	4,464
		U_{major}	-31.2	-22.7	-17.0	-8.6	-2.9	-2.9	2.8	10.7	15.5	8.4	24.7	
		Speed	0.1	0.5	1.1	3.2	6.2	7.3	10.3	17.4	22.9	5.2	31.5	
	Feb	U_{minor}	-6.1	-4.2	-2.8	-1.1	-0.1	0.0	1.0	2.8	4.0	1.7	8.7	4,032
		U_{major}	-32.5	-23.8	-17.0	-8.5	-2.7	-2.4	3.9	12.3	16.1	8.9	23.2	
		Speed	0.1	0.5	1.3	3.8	6.7	7.8	10.9	17.6	23.8	5.3	32.7	
	Mar	U_{minor}	-10.4	-3.9	-2.6	-0.9	0.2	0.2	1.2	2.9	4.4	1.7	10.3	4,464
		U_{major}	-36.0	-21.5	-16.2	-7.5	-2.8	-3.2	1.7	7.9	12.9	7.3	25.5	
		Speed	0.1	0.5	1.1	2.9	5.1	6.5	8.8	16.4	21.6	4.9	36.4	
	Apr	U_{minor}	-7.7	-3.6	-2.4	-0.8	0.1	0.2	1.2	2.8	4.2	1.6	7.3	4,320
		U_{major}	-27.4	-17.3	-11.9	-5.4	-1.5	-1.5	2.4	9.0	14.1	6.3	19.1	
		Speed	0.1	0.4	0.9	2.4	4.5	5.4	7.3	13.2	17.7	3.9	27.4	
	May	U_{minor}	-5.3	-3.0	-2.1	-0.8	0.0	0.0	0.9	2.2	3.0	1.3	6.2	4,464
		U_{major}	-23.2	-12.2	-8.3	-3.4	-0.6	-0.6	2.3	7.2	10.8	4.7	13.8	
		Speed	0.0	0.3	0.7	1.8	3.2	4.0	5.4	9.6	13.0	2.9	23.2	
	Jun	U_{minor}	-4.2	-3.0	-2.1	-0.9	0.0	0.0	0.8	2.1	3.1	1.3	4.7	4,320
		U_{major}	-14.7	-10.2	-7.2	-2.5	0.3	0.2	3.1	7.1	9.4	4.3	15.0	
		Speed	0.1	0.3	0.7	1.8	3.1	3.7	5.1	8.6	11.1	2.5	15.0	

Table J-6 Monthly Statistics for the Near-bottom (24 m)

Depth (m)	Month		Min	0.01	0.05	0.25	0.5	Mean	0.75	0.95	0.99	Std	Max	#Pts
			cm/s											
24	Jan	U_{minor}	-4.0	-2.8	-1.9	-0.8	0.1	0.1	0.9	2.2	3.1	1.2	6.2	4,464
		U_{major}	-17.1	-12.1	-9.0	-4.2	-1.2	-1.2	1.9	6.1	8.3	4.5	12.0	
		Speed	0.0	0.4	0.8	2.0	3.4	4.0	5.5	9.2	12.2	2.7	17.1	
	Feb	U_{minor}	-5.5	-3.0	-2.0	-0.8	0.1	0.1	1.0	2.3	3.3	1.3	4.8	4,032
		U_{major}	-21.7	-14.5	-10.8	-5.2	-1.7	-1.9	1.7	6.3	9.4	5.1	16.6	
		Speed	0.0	0.4	0.9	2.1	3.9	4.6	6.4	11.1	14.8	3.2	21.8	
	Mar	U_{minor}	-6.9	-2.9	-2.0	-0.8	0.0	0.1	0.9	2.3	3.1	1.3	5.3	4,464
		U_{major}	-17.0	-11.2	-8.4	-4.1	-1.1	-1.1	1.7	6.1	9.1	4.4	14.6	
		Speed	0.0	0.3	0.7	1.8	3.3	3.9	5.3	9.0	11.9	2.6	17.0	
	Apr	U_{minor}	-4.8	-2.9	-2.0	-0.7	0.1	0.1	0.9	2.2	3.2	1.3	7.3	4,320
		U_{major}	-21.3	-11.8	-8.0	-3.9	-1.2	-1.3	1.3	5.0	8.7	4.0	15.3	
		Speed	0.0	0.3	0.7	1.7	2.9	3.6	4.8	8.7	12.4	2.6	21.8	
	May	U_{minor}	-5.5	-2.8	-1.8	-0.7	0.1	0.1	0.9	2.1	3.0	1.2	5.2	4,464
		U_{major}	-12.2	-8.7	-5.9	-2.8	-0.9	-0.9	1.1	4.3	6.8	3.1	10.7	
		Speed	0.1	0.2	0.6	1.5	2.4	2.9	3.8	6.6	9.2	1.9	12.3	
	Jun	U_{minor}	-3.9	-2.6	-1.8	-0.7	0.1	0.1	0.9	2.0	2.8	1.2	5.3	4,320
		U_{major}	-11.6	-8.0	-6.0	-2.8	-0.8	-0.9	1.2	3.8	5.4	3.0	9.3	
		Speed	0.0	0.2	0.5	1.4	2.4	2.8	3.7	6.3	8.2	1.8	11.7	

The vector average current (net flow considered over the measurement period), was typically about 7 cm/s in the near-surface layer, reducing to 1.0 cm/s at the near-bottom, with the flow being down-inlet at all depths. These near-surface speeds were substantially larger than found in the preceding measurements, which had a maximum vector average speed of about 5 cm/s.

J.3.2 Water Levels

Table J-7 shows the water-level statistics with respect to mean sea level. These water-level statistics do not include corrections for variations in atmospheric pressure over the deployment, which are typically equivalent to several cm of water-level variation, up to 30 cm (10% of the measured amplitude) on rare occasions. The tidal ranges at Site 1 in Kitimat Arm are about 6.3 m from maximum to minimum and 4.2 m from the 5% exceedance level to the 95% exceedance level.

Table J-7 Summary of the Water-Level Statistics between December 2006 and July 2007

	Min	1%	5%	25%	50%	Mean	75%	95%	99%	Std	Max	Total
	m											
Water Level	-3.11	-2.72	-2.19	-1.01	0.03	0.00	1.06	2.02	2.61	1.32	3.19	33,855

J.3.2.1 Temperature–Salinity Distributions Derived from CTD Observations in July

Three temperature/salinity profiles were obtained near the marine terminal during the July 2007 recovery of the terminal current meter. The temperature and salinity profiles, along with the derived density profile, are illustrated in Figure J-5 for a shallow- and deep-water cast. This figure also gives these profiles in the context of previous measurements.

The near-surface salinities are the freshest measured in this program and are most likely related to the spring freshet when river discharge rates increase due to melting snow in the mountains. The salinities were from 1.3 to 2.0 psu at the near-surface, but if the measurements had been made about a month earlier in the peak of the freshet, perhaps the salinities would have been even smaller. The temperatures showed warming at the surface but not as much as the measurements that were taken in September 2005.

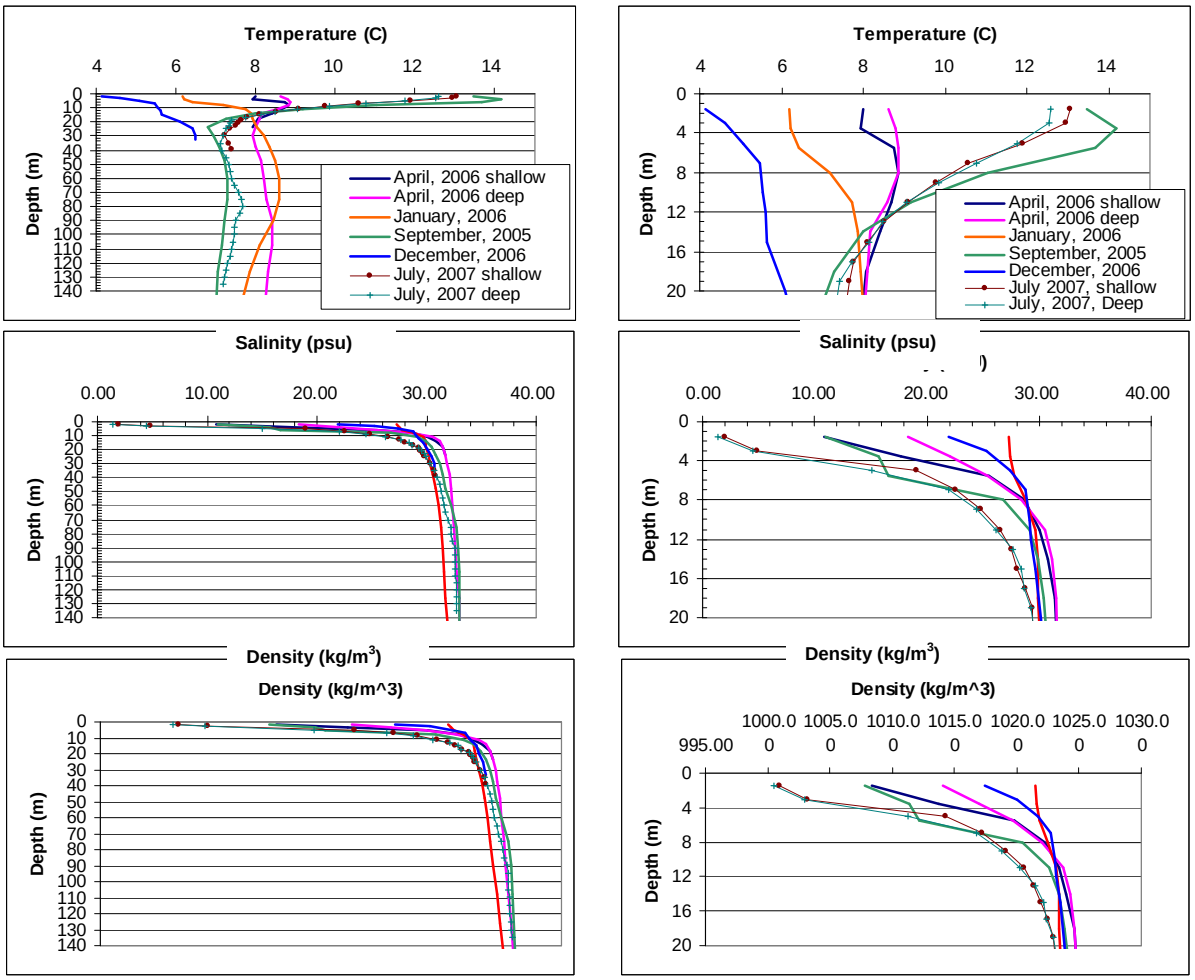

Figure J-5 Temperature, Salinity and Density Profiles at Site 1 in Kitimat Arm, as Measured on July 10, 2007 (Curves with Symbols) Overlaid on Previous Measurements, Over a 140-m and 20-m Depth Scale

J.3.3 Summary of Key Findings

Ocean current measurements were carried out from December 2006 to July 2007 as a continuation of measurements in 2006 near the proposed marine terminal. Previously, measurements from September 2005 to January 2006 were made at nearby sites in deeper waters. The maximum current speeds of 81.6 cm/s were measured in January 2007. Net seaward drift was measured at all depths during the deployment. Mean current speeds varied from 14 cm/s at the near-surface to 4 cm/s at the near-bottom.

The CTD profile indicated a warming near-surface, but not as warm as the September 2005 measurements. The near-surface salinities were the freshest measured in the program at 1.3 to 2.0 psu.

The measured water levels range is about 6.3 m from maximum to minimum and 4.2 m from the 5% exceedance level to the 95% exceedance level.

J.4 References

J.4.1 Literature Cited

Macdonald, R.W. 1983. *Proceedings of a Workshop on the Kitimat Marine Environment*. Canadian Technical Report of Hydrography and Ocean Sciences, 18, Department of Fisheries and Oceans. Institute of Ocean Sciences, Sidney, BC.

Attachment J1 Specifications of Oceanographic Instruments Used in This Study

Specifications for the RD Instruments 600 kHz Workhorse ADCP

600 kHz SENTINEL WORKHORSE

Principles of Operation:

Acoustic pulses are transmitted along four beams. Echoes are returned by scatterers in the water column. The frequency shift of each echo is directly proportional to the component of flow along the beam axis. This is the Doppler Effect. Horizontal and vertical flow components are then computed from the axial velocities. Echo returns are time gated to allow flow resolution into vertical bins (in this case 1.0 m). Flow homogeneity over the four-beam footprint is assumed. Due to side lobe returns, data are usually not available within 6% (20° beam angle) of the vertical distance to strong reflectors, such as the ocean surface or sea bottom. The ADCP was upgraded to include a pressure sensor and includes the WAVES upgrade.

Internal Sensors	Accuracy	Resolution
Heading	±1°	±0.2°
Tilt (max. 20□)	±2°	±0.01°
Temperature	±0.4°	±0.01°

Power Specification: Internal: 48VDC battery pack (expandable w/ external battery pack)
External: 20-60 VDC

Dimensions: 22.8 cm by 36.1 cm

Weight: 13 kg in air; 4.5 kg in water (with battery pack)

Beam Angle: 20°

Maximum Range: Water velocity profile to 47 m (nominal at 2 m bin size)

Accuracy: Water velocity accuracy is 1 cm/sec, based on the sampling parameters chosen (2 m bins, 10 pings per ensemble)

Memory: Expanded to 896 MB

Specifications for the RBR XR-420 CTD

RBR Precision Instruments for over 25 years

Submersible Conductivity, Temperature and Depth Logger — Model XR-420CTD

XR-420 CTD

Conductivity, Temperature and Depth Logger

The XR-420 CTD Marine is a small, autonomous data logger designed to monitor conductivity, temperature and depth. High accuracy Speed of Sound and Salinity may be derived from the data.

The normal marine conductivity range of 0 to 70 mS/cm is measured by an inductive cell. RBR uses a three-coil system with a closed loop feedback for superior temperature compensation. The titanium housing provides a depth rating for the cell of 6,600m which can be axial to the logger. It also provides shielding and stable cell geometry. The response time of the inductive cell is better than 0.095 seconds, which, along with a large hole diameter, allows for long-term operation without an additional flow pump.

Features:

- High Accuracy
- Large Memory
- Low Power
- High-speed Data Download

8MB of nonvolatile flash memory provides sufficient memory for 2,400,000 readings, which can be logged on one set of high-powered 3V lithium batteries. The batteries are common camera batteries (CR123A), which are readily available. Power consumption can vary significantly depending on the sampling rate, and operating temperature. A fresh set of batteries will usually permit collection of a full complement of readings over periods exceeding one year.

For more details, please visit our website: www.rbr-global.com

Software

The XR-420 use fully integrated RBR Windows® software, which is compatible with Windows® 95/98/NT/2000/XP. Please see the "RBR Logger Software" datasheet, or visit the RBR website (www.rbr-global.com) for more information.

Technical

Base Logger

Power:	QTY 4, 3V CR123A cells
Communications:	RS-232/485; logged, cable, or telemetry
Download Speed:	~115,000 samples/minute
Clock Accuracy:	± 32 seconds/year
Size:	400mm x 64mm
Weight (plastic):	1259g (in air); 389g (in water)
Memory:	8Mbyte Flash (2,400,000 samples)
Sample Rate:	1Hz* to 24 hours (programmable)
Calibration:	NIST traceable standards

* see RBR XR-620CTD Profiler for faster sampling rate

Temperature

Range:	-5 °C to 35 °C; extended range to -40 °C
Accuracy:	± 0.002 °C
Resolution:	<0.00005 °C
Time Constant:	depends on probe construction

Conductivity

Range:	0 to 70 mS/cm
Accuracy:	± 0.003 mS/cm
Resolution:	<0.0001 mS/cm
Time Constant:	< 95msec

Depth

Range:	10/25/60/150/250/740/1000/2000/3000/4000/6600 m (dBar)
Accuracy:	± 0.05% full scale
Resolution:	<0.001% full scale

RBR Ltd. 27 Monk Street Ottawa, ON Canada K1S 3Y7
ph: (613) 233-1621 fax: (613) 233-4100 info@rbr-global.com
www.rbr-global.com

05/05